Mechanisms involved in the recognition of apoptotic cells by B lymphocytes

Marzena Ciechomska

Thesis submitted in partial fulfilment of the requirements
of the regulations for the degree of Doctor of Philosophy

Newcastle University

Faculty of Medical Sciences

Institute of Cellular Medicine

March 2010

Acknowledgements

My PhD studies have been an amazing experience. They would not have been possible without the help from many people whom I would like to thank for their support and believe during this scientific journey.

Most importantly, I would like to thank my supervisor, Dr. Andrew Knight, who spent his time and shared his knowledge helping me to complete my thesis. I am very grateful for motivation and support he has provided throughout the years of my project and for being not only a mentor but also a friend, giving me a learning environment so that I could develop personally as well as professionally.

Further thanks go to my second supervisor, Prof. John Kirby, for his assistance in proof reading of this thesis and for his bright ideas during our meetings.

I wish also not to forget about all the support received from my colleagues from the lab and the office. I thank them for being kind and very helpful during these three years.

I am forever indebted to my parents for their understanding and encouragement when it was most required. I am also very grateful to my sister Iwona who inspires me every day to be a good scientist as she is.

And last but not least, I would like to thank Maciej for his endless patience during this stressful time, his love, help and much more…

Table of contents

Index of Figures and Tables

Abstract:

As many tumours are poorly immunogenic, one approach for cancer therapy aims to improve natural anti-tumour immunity. Recently it has been shown that anthracycline-induced apoptosis in tumour cells results in the relocation of the ER resident chaperone calreticulin to the cell surface. Interestingly, this relocation directly stimulates T cell-mediated anti-tumour immunity following tumour cell phagocytosis by dendritic cells. In addition, evidence from medullary carcinoma of the breast patients shows a correlation between tumour-infiltrating B cells and a more favourable prognosis. Surprisingly, many of these infiltrating B cells recognise proteins relocated from their normal intracellular distribution to the tumour cell surface, also as a result of apoptosis.

As B cells have recently been shown to be an important population of antigen presenting cells capable of extracting membrane antigens from target cells, these findings raise the possibility that tumour infiltrating B cells may be capable of presenting tumour antigens promoting the generation of anti-tumour immunity. In particularly, this thesis envisages that following apoptosis induction in tumour cells, antigen specific B cells will be able to acquire relocated tumour antigens, therefore directly promoting antigen-specific T cells.

To provide a proof of principle I have characterized the processes involved in the extraction of membrane-tethered antigens by B cells from target cells using flow cytometry and a novel proliferation bio-assay. Unexpectedly, surface antigen acquisition by B cells has been demonstrated to be rapid, proceeding in times as short as 1 min. Furthermore, I have also characterised the processes involved in the relocation of antigens to the cell surface of dying target cells from various intracellular locations using anthracyclines and UVC as immunogenic apoptotic agents. This has allowed me to demonstrate that antigens from several intracellular compartments following apoptosis induction are acquired by antigen-specific B cells. Importantly, this antigen acquisition was sufficient to induce CD4+ T cell activation as confirmed by proliferation assay.

These *in vitro* findings demonstrate that B cells are capable of activating CD4+ T cells following interaction with apoptotic target cells. Therefore, further investigations concerning the role of B cells in natural anti-tumour immunity may improve current anti-cancer therapies.

Abbreviations:

ADCC – Antibody Dependent Cellular Cytotoxicity

APC – Antigen Presenting Cell

BCR – B Cell Receptor

bp – base pair

cpm – counts per minute

CRT – Calreticulin

CTL – Cytotoxic T Lymphocytes

Cy – Cyclophosphamide

Da – Dalton

DC – Dendritic Cells

DNA – Deoxyribonucleic Acid

DX – Doxorubicin

EGFP – Enhanced Green Fluorescent Protein

E/T – EGFP-TTCF fusion protein

FACS – Fluorescence Activated Cell Sorting

FDC – Follicular Dendritic Cell

HEL – Hen Egg Lysozyme

HLA – Human Leukocyte Antigen

HMGB1 – High Mobility Group Box 1

HRP – Horseradish Peroxide

IDO – Idoleamine 2,3-dioxygenase

Ig – Immunoglobulin

IFN-γ – Interferon-γ

IL – Interleukin

ILT – immunoglobulin-like inhibitory receptor

LSM – Laser Scanning Microscopy

IS – Immunologic synapse

MHC – Major Histocompatibility Complex

MTT – 3-(4,5-Dimethylthiazol -2-yl)-2,5-diphenyl Tetrazolium Bromide

MX – Mitoxantrone

NK – Natural Killer

NO – Nitric Oxide

PCR – Polymerase Chain Reaction

PS – Phosphatidyl Serine

ROS - Reactive Oxygen Species

SDS-PAGE – Sodium Dodecyl Sulfate Polyacrylamide Gel Electrophoresis

SS – Signal Sequence

STS – Staurosporine

TAA – Tumour Associated Antigen

TAM – Tumour Associated Macrophage

TIB – Tumour Infiltrating B Cell

TID – Tumour Infiltrating Dendritic Cell

TIL – Tumour Infiltrating Lymphocyte

TLR – Toll-Like Receptor

TNF-α – Tumour Necrosis Factor-α

TTCF – Tetanus Toxin C Fragment

UVC – Ultraviolet C

VEGF – Vascular Endothelial Growth Factor

WGA – Wheat Germ Agglutinin

- 1. Introduction -

1.1. The role of immune system in tumour control

1.1.1. Cancer as a global problem

Until the late twentieth century, little progress had been made in understanding the mechanisms involved in the development of cancer. The death rate for cancer dropped by only 5% between 1950 and 2005. In contrast, the death rate for heart disease dropped 64% at the same time, and for flu and pneumonia it fell by 58%. The World Health Organization predicts that by 2010 more than 12 million people will die due to cancer. Such a negative prognosis for patients is the result of the multi-complexity of cancer in comparison to other diseases. In particular, cancer is characterised by three malignant properties which change during the time of cancer growth.

The first property is pro-tumourogenic alteration that starts to occur in a healthy tissue. This step can include the uncontrolled growth of cells due to various mutations in growth factor receptors or in signalling pathways and unresponsiveness for inhibitory signals. The second property of tumour development is characterised by the invasion of nearby tissue which results in tissue damage. Finally, tumour metastasis allows cancer to spread to other organs via lymph or blood.

Therefore, there is a great need for better understanding of the complexity of cancer biology which will help to improve current anti-cancer therapies. This includes clinical treatment such as gene therapy, chemotherapy or surgery. The multiplicity of the biology of most cancers along with many deficiencies of current clinical practices still prevents this disease from being cured, although great improvements have been made by introducing many prevention screening programs.

More recently, scientists have tried to understand the natural mechanisms by which the immune system can modulate tumour growth and have attempted to use these approaches to cure cancer. These methods are based on the natural function of the immune system to protect the body against invading pathogens. Importantly, such approaches are based on the fact that the immune system is also capable of recognising unhealthy or abnormal mammalian cells such as tumour cells leading to their elimination. Therefore, many recent studies have focused largely on how to improve natural mechanisms involved in anti-tumour immunity which hopefully will prove less harmful and more effective than current treatment.

1.1.2. The tumour microenvironment

The microenvironment of a developing tumour is comprised of proliferating cells, the tumour stroma, blood vessels, infiltrating inflammatory cells and a variety of associated tissues. It is created and shaped by the tumour, but also by cellular events which take place in the surrounding tissues (Micalizzi and Ford, 2009).

Immune cells that infiltrate the tumour site include effector cells of innate immunity such as dendritic cells (DC), macrophages, natural killer (NK) cells along with B and T lymphocytes. Inflammatory cells present in the tumour microenvironment can either contribute to tumour rejection or may paradoxically promote tumour growth. Specifically, many of these tumour-promoting cells are directly modified by the tumour itself creating a tumour-favourable microenvironment. For example, tumour-associated macrophages or DC can either secrete special immunosuppressive reagents that inhibit T cell function or produce growth factors that promote tumour survival (Melief, 2008). These observations have clearly convinced scientists that tumours do not represent simple passive targets for host immunity. Instead, cancer cells actively downregulate or suppress many phases of anti-tumour immunity using a spectrum of different strategies consequently leading to poor immunogenicity and immunesurveillance of many tumours that will be discussed in **Section 1.2**.

Another important aspect for understanding the biology of tumour development is the interaction between cancer cells and the surrounding stroma. There is a cross-talk between the tumour cells, the extracellular matrix, fibroblasts and other mesenchymal cells in the supporting stroma. This contact results in formation of a scaffold-supporting environment which is conducive with tumour expansion. Subsequently, tumours become vascularised as a result of secretion of angiogenesis growth factors such as fibroblast growth factor, vascular endothelial growth factor or platelet-derived growth factor by tumour-associated cells (Zhang et al., 2009b) (van Zijl et al., 2009). These factors also activate bystander endothelial cells to proliferate and to build channels further supporting tumour growth. Also, the proteolytic enzymes, which are present in this microenvironment, allow the degradation of components of the extracellular matrix (fibronectin, laminin or collagens) essential for tumour metastasis. For example, it has been shown in several types of tumour (skin, breast, lung and colon cancers) that the level of expression of various proteases such as plasminogen activator, cathepsin, collagenase, stromelysin is upregulated. In most of these cases, the upregulation of these enzymes correlates with a higher tumour grade to metastasis and invasion (De Wever and Mareel, 2003).

1.1.3. The immune recognition of tumour cells

The mammalian immune system has evolved to protect against invading organisms ranging from viruses to multi-cellular organisms. However, it has been suggested that tumours have also played a role in defining immune recognition strategies (Seymour et al., 1999) (Pettit et al., 2000). As a consequence of adapted changes, immunological responses are mainly based on the identification and neutralisation of specific pathogen-encoded molecules and the destruction of malignant cells.

In general, immune recognition is now known to consist of two distinct responses: innate and adaptive immunity based on antigen specificity and timing, which are discussed below.

- **Innate immunity**

Innate immunity is rapidly activated when pathogens try to invade the body. This non-specific response is the first line of defence that blocks the entry and spread of disease-causing agents. Innate immunity involves the release of soluble mediators such as cytokines, chemokines and reactive oxygen species (ROS). These bioactive mediators are produced mainly by DC, NK cells, macrophages, neutrophils, eosinophils, basophils and masts cells. In particular, when tissue homeostasis is perturbed or undergoes neoplasmatic modifications, tissue-resident macrophages and mast cells secrete cytokines, chemokinases that recruit leukocytes from the circulation into the affected tissue (de Visser and Coussens, 2006). In addition, recruited NK cells directly kill tumour cells *in situ*. They can eliminate tumour cells using two mechanisms that require direct cellular contact. Firstly, NK cells secrete granules that contain perforins - membrane disrupting molecules and granzymes - pro-apoptotic serine caspases involved in DNA fragmentation of target tumour cell (Chan and Housseau, 2008). The second pathway is mediated through pro-apoptotic members of the tumour necrosis factor (TNF) family. This family includes FasL and TNF-related apoptosis inducing ligand (TRAIL/Apo2L). The mechanism by which TRAIL and FasL induce cell death involves the recruitment of their receptors, TNFR and Fas respectively. Following binding to these receptors, downstream serine caspases are activated. Caspases (cysteine proteases) are involved in DNA fragmentation and participate in apoptotic cell death (Ames et al., 2009). This process will be described in more detail in **Section 1.5**.

Simultaneously, macrophages and DC, which are termed antigen-presenting cells (APC), are involved in the uptake of available antigen or the engulfment of apoptotic cells for presentation to T lymphocytes. Several subsets of DC have been defined, including myeloid-

DC, plasmacytoid-DC and Langerhans cells. Not surprisingly, DC can also infiltrate several types of tumours and function as scavenger cells that contain tumour associated antigens (TAA). Following antigen encounter, DC migrate to specific sites within lymphoid organs where they interact with naive T cells providing the initial activation stimuli that leads to the induction of full anti-tumour immunity (Miller et al., 2004).

It has been shown that tumour infiltration by DC results in a more favourable prognosis for brain and lung cancer patients via the activation of cytotoxic T cells (CTL) which then directly kill tumour cells. (Palamara et al., 2004). In particular, stimulation of Toll-like receptors (TLR) on DC by agonists leads to the upregulation of costimulatory molecules and to the production of anti-tumour cytokines such as interferon-γ (IFN-γ) and interleukin-12 (IL-12). Such pro-inflammatory cytokines induce CTL activity leading to effective killing of tumour cells. Therefore, cytokines produced by TLR-activated DC stimulate effector cells and may represent a useful approach to developing a more effective immunotherapy (Mitchell and Sampson, 2009). Furthermore, recent studies have demonstrated that following irradiation or anthracycline-treatment, dying tumour cells induce the maturation of DC and enhance antigen presentation to tumour-specific CTL. This mechanism will be described in more detail in **Sections 1.3.4.** and **1.3.5**. Nevertheless, the role of DC is controversial because of their bivalent nature of DC in many tumour microenvironments. Although, DC can mediate efficient anti-tumour immunity, there are many examples where DC actively promote tumour survival (Fricke and Gabrilovich, 2006). Therefore, more studies focusing on the role of DC in anti-tumour immunity need to be carried out.

- **Adaptive immunity**

Upon exposure to a pathogen, the innate arm of the immune system is engaged non-specifically. This is an important initial step in clearing the pathogen; however adaptive immunity is required to generate a more specific and efficient response that eliminates the pathogen. In particular, adaptive immunity has the capacity to recognise unique components of individual pathogens. This is achieved by expression of an array of unique antigen receptors on the surface of specialised immune cells termed lymphocytes. These receptors are generated by random gene rearrangements and allow a diverse flexible response to invading pathogens. In addition to the specific recognition of pathogen-derived antigens, these receptors are also capable of recognising antigens expressed by both normal mammalian cells as well as cells undergoing tumorogenesis which may result in the synthesises of novel or 'neo' antigens. Therefore, in healthy individuals there are several processes that ensure

lymphocytes expressing antigen receptors reactive with proteins expressed by normal healthy cell are either physically removed or inactivated. Furthermore, another defining feature of adaptive immunity is the generation of pathogen-specific memory lymphocytes. Following pathogen re-exposure, the presence of these cells allows a more robust and rapid immune response to take place. Lymphocytes are divided into two subsets (B and T lymphocytes) which differ in their response to antigen. Following antigen encounter and subsequent activation, B cells secrete their antigen-specific receptor as antibodies (immunoglobulin-Ig) that circulate in blood and lymph leading to antigen neutralisation or elimination. The role of B cells in anti-tumour immunity will be described in **Section 1.4.**

In contrast, following antigen encounter the receptor expressed by T cells mediates their cellular differentiation into various subsets that play a central role in cell-mediated immunity. By responding to fragments or small peptides derived from antigens which have either entered mammalian cells or are synthesised by intracellular pathogens, T cells provide homeostatic immunosurveillance. Also in contrast to antigen recognition by B cells, these antigenic fragments are recognised in the context of molecules encoded by the major histocompatibility complex (MHC). Based on which class of MHC molecule is recognised, T cells can be divided into two subsets consisting of CD8+ CTL and CD4+ T helper (Th) cells.

CD8+ T cells are the major effector cells which recognise altered cells including those infected with intracellular parasites, stressed cells producing altered proteins or tumour cells expressing neo antigens. MHC class I molecules are expressed on every nucleated cell and bind and present peptides of 8–10 amino acid residues in length, which are largely derived from the degradation of cytosolic proteins to CD8+ T cells. Recognition of these antigenic peptide-MHC complexes provides activation signals for the differentiation of these cells into CTL that consequently kill the peptide/MHC expressing target cells. For this reason, CTL are not limited to detection of abnormal protein synthesized in the cell, but can be greatly expanded for the range of tumour antigens expressed intact on the cell surface. Therefore, numerous reports have described the beneficial role of cytotoxic CD8+ T cells that induce anti-tumour immunity. For example, in many types of tumours including melanomas (Hirohashi et al., 2009), lung carcinomas (Mami-Chouaib et al., 2002), primary breast tumours (Liu et al., 2009) or prostate cancers (Kiessling et al., 2008), the occurrence of infiltrating CTLs was directly related to tumour shrinkage in patients. Furthermore, *in vivo* animal studies have shown that adoptive transfer of CTL to SCID/NOD mice, which were previously challenged with lung cancer cell lines, significantly reduced tumour growth, in comparison to those mice which did not receive CTL (Mami-Chouaib et al., 2002). The mechanism of CTL-mediated anti-tumour killing is largely

due to release of perforin and granzymes and the surface expression of FasL. These cytotoxic molecules induce cancer cell death via caspase activation. In addition, IFN-γ secretion by activated CTL at the tumour site promotes NK cells activity and increases tumour antigen presenting function of DC and macrophages. Moreover, IFN-γ also stimulates CD4+ T cells to clonal expansion (Mata-Espinosa and Hernandez-Pando, 2008).

CD4+ T cells generally have a role of helper T cells (Th) for other types of cells. This is predominantly by the production of cytokines that affect other populations of cells. CD4+ T cells recognise MHC class II molecules displaying the peptides of approximately 20 amino acids long, which are derived from extracellular proteins, in contrast to the cytosolic proteins presented by MHC class I molecules. Therefore, MHC class II-dependent antigen presentation is termed endocytic or exogenous pathway. Th cells have been further divided into several subsets based on the cytokines that they secrete (pro- or anti-inflammatory) (Borghaei et al., 2009). One major subset (Th1) is characterised by the secretion of pro-inflammatory cytokines such as IFN-γ, TNF-α which function to activate and generate memory CTL. In addition, Th1 cells activate APC maturation and enhance antigen uptake and presentation. CD4+ T cells also promote DC maturation through CD40 ligation which results in surface stabilisation of MHC I-peptide complexes, upregulation of costimulatory molecules required in signal transduction and production of IL-12. Indeed, this advance interaction between CD4+ T cells and DC is required for maximal clonal expansion of effector CD8+ T cells, induction of primary responses and most memory responses (Wang and Livingstone, 2003). Therefore, cognate interaction between CD4+ T cells and DC has the capacity to drive the specific CD8+ T cell-response. This interaction determines whether CD8+ T cells move into a state of activation or tolerance. Several studies have shown that in the presence of pro-inflammatory cytokines stimulated CD4+ T cells are responsible for the delivery of a third signal essential to full activation of CTL cells, thereby increasing the efficiency of CTL-mediated anti-tumour immunity (Cools et al., 2007).

Th cells can also directly kill tumour cells via the release of cytokines that activate death receptors on the tumour cell surface. In particular, Th cells are able to induce the apoptosis of tumour cells through Fas/FasL pathway. This mechanism is induced by ligation of Th cell CD40L to CD40 expressed on the lymphoma cell surface and subsequently resulted in upregulation of Fas on tumour cells (Knutson and Disis, 2005). Furthermore, Nguyen et al. has shown that Th cells also mediate tumour killing via mechanisms involving TRAIL and granzyme–perforin-dependent pathways (Nguyen et al., 2000).

These mechanisms demonstrate that as well as the previously described indirect effect of Th cells on the modulation of tumour cell death (CTL via activation), these cells are also capable of directly triggering multiple death pathways in cancer cells. In addition, Th cells play an important role in the generation of long-lived immunity and enhanced CTL-mediated response. Therefore, an effective anti-tumour response requires cooperation between APC, Th and CD8+ T cells.

- **Antigen cross-presentation**

As described, most cells, including tumour cells, express MHC class I molecules and present antigens allowing the monitoring of the endogenously synthesised antigens to CD8+ T cells. APC (DC, macrophages and B cells) also express MHC class II and have the ability to present exogenous antigens via the MHC class II pathway for the priming of CD4+ T cell-mediated immunity. In addition, many APC types also have the ability to prime CD8+ T cells by a process termed cross-presentation. This was first described in 1976 by M.J. Bevan. His experiments showed that mice immunized with cells expressing exogenous antigen, generated specific CTL-responses as a consequence of antigen presentation by MHC class I molecule (Bevan, 1976). Groh at el., has also shown using an *in vitro* system that DC were able to cross-present tumour antigens to CD8+ T cells through MHC class I path resulting in their clonal expansion. Such cross-primed CD8+ T cells produced IFN-γ, which led to growth inhibition of several tumour cells including breast, melanoma, or ovarian cell lines (Groh et al., 2005).

It is now known that cross-presented antigens do not always trigger an inflammatory immune response (cross-priming) but may also induce tolerance to self-antigens (cross-tolerance). Recently, experiments performed by Dudziak and co-workers revealed that differences in the cytokine environment may lead to the generation of either tolerance or immunity. They showed that the presence of inflammatory cytokines and costimulatory signals, results in cross-presentation leading to priming of an inflammatory response. It has also been shown that murine CD8α+ DC subset efficiently cross-present antigens for CD8+ T cell priming and also directly stimulate CD4+ T cells via MHC class II molecules (Dudziak et al., 2007).

- **Non-classical antigen recognition**

As well as tumour antigen presentation via classical MHC molecules, some tumour antigens are also presented by non-classical molecules representing a third lineage of antigen presenting molecules, including MHC class I-related chain A (MICA) and chain B (MICB) surface proteins. These unconventional MHC molecules interact with C-lectin activatory receptor

(NKG2D) expressed by NK cells, γδ and αβ CD8+ T cells. Fiona et al. demonstrated that using HSP-90 inhibitors in myeloma cells, the upregulation of MICA and MICB was observed, leading to NKG2D ligation that triggered NK cells degranulation and tumour killing (Fionda et al., 2009). Also Zhang reported that HeLa and HepG2 tumour cell lines treated with sodium butyrate upregulated the expression of MICA and MICB on the surface. This resulted in an enhanced susceptibility of tumour cells to NK cell lysis (Zhang et al., 2009a). In addition, other molecules such as CD1 proteins also belong to the family of non-MHC-encoded proteins specialized in the presentation of hydrophobic antigens including lipids and glicolipid to γδ T cells or NKT cells. It has been shown that CD1 plays an important role in the presentation of tumour ganglioside 3 (GD 3) expressed by melanoma and small-cell lung carcinoma to NKT cells, resulting in better anti-tumour immunity (Wu et al., 2003). In contrast, the increased expression of another non-classical MHC molecule, HLA-G, on the surface of T-cell lymphomas, renal carcinomas (Ibrahim et al., 2001) and melanomas (Seliger et al., 2003a) favour their escape from anti-tumour immunity. In particular, binding of HLA-G with immunoglobulin-like inhibitory receptors such as ILT2, ILT4 and KIR2DL4 resulted in the inhibition of the cytotoxic activity of NK cells and T lymphocytes bearing these receptors. In addition, the HLA-G5 soluble protein has been shown to trigger apoptosis in activated CD8+ T lymphocytes (Fournel et al., 2000). Similarly to HLA-G, also HLA-E expressed on the surface of melanoma cells is correlated with a negative prognosis for patients. Because of their capacity to bind the inhibitory receptor NKG2A, expressed by NK cells and CTL, HLA-E molecules might favor tumor cell escape from CTL and NK immunosurveillance (Derre et al., 2006).

1.2.The mechanisms leading to tumour escape from immune recognition

Despite the ability of the immune system to recognise, target and destroy abnormal cells, tumours frequently acquire mutations that allow them to avoid immuno-recognition. It is estimated that tumours typically accumulate 10 000 or more mutations due to genomic instability (Tomlinson et al., 2002). In addition, tumour cells are able to manipulate immune responses leading to either self-tolerance or to the local secretion of immunosuppressive cytokines. Paradoxically, the immune system can also promote tumour survival. The combination of these effects generally leads to poor anti-tumour immunity and prognosis. In particular, the poor immunogenicity of many tumours directly corresponds with:

1. downregulation of tumour cell MHC I and costimulatory molecules
2. alteration of DC and macrophage function in tumour tissue
3. induction of regulatory T cells
4. tumour-mediated immune cell death

These mechanisms are described in more detail in subsequent sections.

1.2.1. Downregulation of tumour cell MHC I and costimulatory molecules

As described previously, CTL represent a major component of anti-tumour immunity by recognising antigenic peptides expressed by altered cells in the context of MHC class I molecules. However, one of the primary mechanisms underlying the failure of the immune system to control tumour progression is a general downregulation of many proteins involved in antigen processing and presentation by tumour cells. For example, reduced levels of MHC class I molecules has repeatedly been described in melanoma cells where approximately 50% of neoplasmatic human melanocytes have reduced class I expression as a result of various defects in the antigen-presenting machinery (Rees and Mian, 1999).

Likewise, the loss of expression of large multifunctional proteases, such as LMP2 and LMP7 reduces the generation of many tumour antigen derived peptides. In addition, the lack of peptide-transporter proteins: TAP-1 and TAP-2 lead to block a transport of peptide epitopes from the cytoplasmic compartment into the endoplasmic reticulum in many tumours (Ogino et al., 2007). Seliger and co-workers showed that murine tumour cell lines derived from spontaneous or chemical-induced tumours have a coordinated downregulation of expression of TAP-1 and LMP subunits, which led to reduced surface MHC class I molecule expression

(Seliger et al., 2003b). These observations strongly support the concept that tumours escape from immune surveillance as a result of sequential antigen loss and down-regulation of antigen-processing mechanisms over time. Similarly, Lou et al. have shown that mice challenged with murine lung carcinoma cell line (CMT.64) are characterized by a down-regulation of surface MHC class I expression as a result of a deficiency in antigen-processing components such as tapasin (Tpn), growth of tumour was observed. In contrast, CMT.64-bearing animals, which were additionally transfected with an adenovirus encoding human Tpn to restore surface MHC class I, showed increased tumor cell killing by antigen-specific CTL and a significant reduction in tumor growth was observed. These findings demonstate that Tpn can enhance survival and immunity against tumors and also suggests that Tpn may be used as a component of immunotherapeutic vaccine protocols to eradicate tumors (Lou et al., 2008)

1.2.2. Alteration of DC and macrophages function

- **Dendritic cells**

A growing body of evidence reveals an ambivalent role for tumour-infiltrating DC (TID) that may participate in the regulation of either tumour regression or growth. It is becoming clear that modifications of DC, which are central regulators of immune responses, can induce anti-tumour immunity or, in some cases, even promote tumour survival (Frumento et al., 2006). Chaux (Chaux et al., 1997) has reported that when compared to splenic DC, TID are poor stimulators of primary allogeneic T-cell proliferation and cytokine secretion (e.g. IL-2 and IFN-γ). Indeed, when the cytokines secreted by TID were examined, they were shown to be similar to those previously tolerogenic DC (e.g. IL-10, transforming growth factor (TGF-β) and vascular endothelial growth factor (VEGF)) along with reduced levels of costimulatory molecule expression (Ryan and Evavold, 1998).

Some studies have also revealed that human TID, obtained from both melanomas and breast cancer have reduced expression of costimulatory molecules (Frumento et al., 2006). This failure of TID to effectively activate T cells may explain why in many cases tumour-infiltrating lymphocytes (TIL) fail to eliminate tumour cells. It is also possible that TID cells can promote the expansion of regulatory T cells (Treg), described in **Section 1.2.3.**, in tumour environments. Another study, showing a pro-tumourogenic role for DC has been presented by Battaglia et al. They demonstrated that metastatic tumour cells produce VEGF, a natural ligand for Nrp1 expressed by pDC, which induces a tolerogenic phenotype (Battaglia et al., 2009). Such tumour associated DC show decreased costimulatory molecule expression and produce

immunosuppressive cytokines including IL-10 or TGF-β. Consequently, the uptake of tumour cells by DC in the presence of immune-suppressive cytokines tends to induce T cell differentiation into Treg leading to a lack of anti-tumour immunity.

- **Macrophages**

Similar to their specialised phenotypes (once located in many healthy tissues) macrophages present in many tumour environments (tumour associated macrophages (TAM)) appear to specifically inhibit T cell functions through the release of suppressive cytokines, including TGF-β, IL-10, and prostaglandins (Sica et al., 2007). Prostaglandins such as PGE_2 can stimulate cell proliferation, induce angiogenesis and inhibit apoptosis of tumours by increasing expression of the anti-apoptotic Bcl-2 protein. Furthermore, secretion of TGF-β and IL-10 has a negative impact on cytotoxic CD8+ T cells that infiltrate the tumour site again leading to immunosuppresion. In addition, TAM and tumour associated neutrophils produce reactive oxygen species (ROS) and nitric oxide (NO) that participate in the carcinogenic effect of a chronic inflammatory reaction. These reactive species directly induce DNA damage and are responsible for neoplastic transformation (Osinsky et al., 2009). In particular, oxidative products induce single or double-stranded breaks and DNA modifications such as alkylation adducts formation leading to increased mutations. It has also been shown that ROS activate the NFκ-B signaling pathway in infiltrating leukocytes leading to secretion of TNF-α and other pro-inflammatory cytokines. NFκ-B activation results in expression of pro-inflammatory cytokines in stromal cells. These cells produce a variety of soluble mediators affecting both the matrix and blood vessel growth promoting tumour progression (Tobar et al., 2008). Furthermore, many tumours directly produce factors such as IL-10, VEGF, GM-CSF that promote the recruitment of macrophages and DC to the tumour site. Consequently, these infiltrating cells exhibit an immature phenotype leading to inhibition of tumour antigen presentation.

1.2.3. Induction of regulatory T cells

Treg are a subset of CD4+ T cells that are generated either intra or extra-thymically expressing high levels of the receptor for the T cell growth factor, IL-2 (CD25) and the transcription factor FoxP3 (Beyer and Schultze, 2009; Itoh et al., 1999). They inhibit the activity of other T cell populations by limiting the availability of IL-2 or by the secretion of anti-inflammatory cytokines such as IL-10 or TGF-β. Thereby, Treg maintain immune system homeostasis and

tolerance. Paradoxically, Treg can also lead to tumour-antigen unresponsiveness and induce state of Immunosupression for tumour (**Fig. 1.1.**).

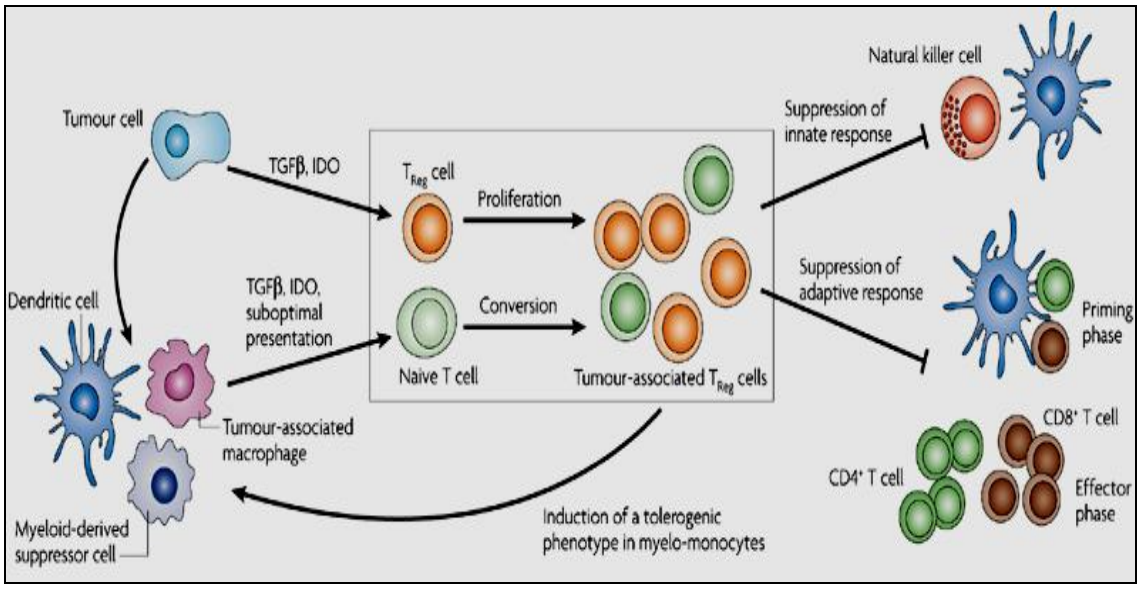

Fig. 1.1. Induction of Treg cells within the tumour site. Tumour cells produce suppressive factors that directly act on Treg or license TAM and DC to expand Treg. Such expansion occurs through the proliferation of pre-existing Treg and the conversion of naive precursors into *de novo* inducible Treg. Tumour-associated Treg suppress both the innate and the adaptive immune response, including the priming and effector phase of both CD4 (green) and CD8 (brown) T cells. Adapted from *Nature Reviews Cancer* 7, 880-887 (November 2007).

Bergman et al., revealed that there is a 5-15% increase in the proportion of Treg present in infiltrating neck and head carcinoma when compared to the frequency present in the blood (Bergmann et al., 2007). To address this high frequency of Treg present within the tumour environment, Borhaeti et al., proposed that Treg acquire their regulatory phenotype and suppressive function *in situ*. The authors also revealed that TGF-β, produced by tumour cells and by Treg, is an important factor that drives conversion and clonal expansion of tumour infiltrating Treg (Borghaei et al., 2009). In addition, expression of the enzyme idoleamine 2,3-dioxygenase (IDO), that participates in degradation of the essential amino acid tryptophan, by either tumour cells or tumour-altered-APC, also modulates conventional T cells into Treg within the tumour microenvironment. Furthermore, it has been shown that IDO expressed by DC also inhibits effector T-cell proliferation and survival through consumption of tryptophan leading to tolerance induction (Mellor and Munn, 2004).

The impact on increased tumour survival as a result of Treg activity was confirmed by an *in vivo* model used by Tanaka and co-workers. They showed that depletion of Treg by the

administration of an anti-CD25 monoclonal antibody, led to the prolonged survival of animals previously administered the B16 melanoma or the methylcholanthrene (MCA)-induced fibrosarcoma (Tanaka et al., 2002). Furthermore, when Treg-depleted mice were repeatedly challenged with tumour cells, the animals still maintained long-lasting protective anti-tumour immunity. It has also been observed that elimination of Treg in mice enhances the cytotoxic function of tumour-specific CD8+ T cells resulting in delayed tumour growth (Steitz et al., 2001). Therefore, elimination or inhibition of Treg function can help to induce potential cancer immunotherapy.

1.2.4. Tumour-mediated cell death

In addition to the mechanisms by which tumour cells avoid inducing immunity, experiments conducted by Esche et al. have shown that some tumours can upregulate Fas ligand (FasL/CD95L) expression, directly leading to the induction of immune effector cell apoptosis (Esche et al., 2001). They demonstrated that tumour cells can induce TID to undergo apoptosis *in vitro* and *in vivo* after contact with different types of tumours. In addition, studies performed by Debatin and co-worker also described that TIL are dysfunctional or significantly apoptotic in many types of cancer such as neuroblastoma, melanoma, breast carcinoma, head and neck cancers (Debatin and Krammer, 2004).

Tumour-induced death of DC was confirmed by the activation of caspase-3 along with an increased expression of pro-apoptotic Bax and the formation of apoptotic bodies. Furthermore, other studies have shown that NK cells also undergo apoptosis via the activation of natural cytotoxicity triggering receptor upon interaction with tumour cells (Zwirner et al., 2007). Again, these mechanisms lead to poor, local immunogenicity of tumour-tissue as a result of the induction of apoptosis in infiltrating T, DC and NK cells.

Due to the diverse mechanisms described above that allow cancer cells to avoid immune recognition, the induction of anti-tumour immunity in many animal models and patients is limited. Understanding these mechanisms, in particular the role of APC, may allow future strategies for the re-establishment of anti-tumour immunity.

1.3. Immunotherapeutic treatment of cancer cells

1.3.1 Cytokine therapy

Cytokines are proteins or glycoproteins secreted by immune cells which, by binding specific receptors, regulate both the adaptive and innate immune system. They have autocrine and paracrine functions, leading to either local or distal effects which may enhance or suppress immune responses. As well as their characterised role in the control of anti-pathogen immunity, cytokines are also involved either directly in the control of tumour growth or indirectly in regulation of anti-tumour immunity.

In the early 1980's, many promising results of various cytokine therapies in numerous animal tumour models were reported. In particular, IFN-γ, TNF-α, IL-2, IL-3, IL-4 IL-6, IL-12 GM-CSF were studied with great expectation. Simultaneously, after the cloning of many cytokine genes large-scale clinical testing of the anti-tumour properties of many cytokines became achievable. Some of the most promising anti-tumour cytokines therapies are described below.

IL-1: This interleukin has many functional activities as a costimulatory agent for T cells and has also been implicated as an inflammatory adjuvant. In particular, IL-1 administration was shown to mediate an adjuvant effect in mice vaccinated with lung cancer (McCune and Marquis, 1990). IL-1 administration resulted in better infiltration of activated T cells into the vaccination site. In addition, experimental data have shown that mice injected with fibrosarcoma cells that were transfected with an IL-1 expressing plasmid, rapidly rejected the transfectants when compared to mice injected with un-transfected tumour cells. This experiment clearly indicates that recruitment of anti-tumour immunity results from the secretion of IL-1 by tumour cells (Douvdevani et al., 1991).

IL-2: Since the early 1980's, IL-2 has been used to treat a variety of cancers including renal cell carcinoma, leukaemia and lymphoma. Degrate et al., have shown that patients with pancreatic adenocarcinoma who receive recombinant IL-2 have an improved prognosis. Following IL-2 administration higher levels of NK cells and eosinophils have been observed in these patients. This indicates that IL-2 administration stimulates innate anti-tumour immunity (Degrate et al., 2009). Numerous studies have also shown that IL-2 treatment increase anti-tumour CTL-mediated immunity (Hawkins, 1993) (Ge et al., 2002). Although interleukins have moderate

success in some types of tumours, significant toxicity and side effect in patients are also apparent. Therefore other mediators are also currently used in the clinic as described below.

IFN: The anti-proliferative actions of the three major types of interferons on tumour growth have been well documented for over the last thirty years. The role of IFN-α, -b and –γ was first described by Priestman showing anti-tumour activity in patients with advanced melanoma (Priestman, 1979). This treatment resulted in anti-proliferative and immunomodulatory effects and is still in limited use today in clinics treating hematologic malignancies and solid tumours. In particular, IFN-γ have been approved for the treatment of renal and kidney carcinoma and chronic myelogenus leukaemia. This class of cytokine has highly pleiotropic effects acting on tumour cells both in a direct and indirect manner. It has been shown both *in vivo* and *in vitro* models that anti-neoplastic functions of IFNs can be mediated by direct cytostatic activity (characterised by reduced proliferation), modulation of oncogenes expression and also in cell lysis. In addition, IFNs have many anti-tumour effects including the induction of anti-tumour antibody responses and the enhancement of tumour cytotoxcity by macrophages, NK cells or CTL. For example, genetically modified mice lacking the interferon-receptor show enhanced development of many types of tumours (Kaplan et al., 1998). Also, it has been shown that the introduction of tumour cells that were transfected with the IFN-γ gene into animals generated enhanced anti-tumour immunity (Viret and Lindemann, 1997). Another study has demonstrated that the upregulation of a tumour antigen expression by IFN-γ leads to enhanced anti-tumour monoclonal antibody production. Santini et al. have also demonstrated that IFN-α and IFN-β can promote the differentiation of *ex vivo* human DC towards an immunosuppressive phenotype that lead to the priming and expansion of protective anti-tumour immune responses. (Santini et al., 2009).

In animal models it has been observed that IFN-β in combination with IL-12 can activate NK cells and CTL. Unfortunately, there is limited use of IFN-β in the clinic due to its modest therapeutic benefits and cytotoxic side effects that include fever, hypotension and multi-organ malfunction (Eriksen et al., 2009) (Santini et al., 2009).

TNF-α: Tumour necrosis factor-alpha was originally identified in the late 1970's as a mediator of necrosis for various murine and human tumours and cell lines. TNF-α is a potent pro-inflammatory, pleiotropic cytokine that is produced by macrophages, neutrophils, fibroblasts, keratinocytes, NK, T, B cells and also by tumour cells themselves. TNF-α binds to the receptors TNF-RI and TNF-RII, which are expressed on most mammalian cells. There is evidence that the

binding of TNF-α to these receptors induces a cytolytic cascade of events characterised by generation of ROS, DNA fragmentation and apoptosis (Kirkwood, 2002). Therefore, a significant effort has been made to efficiently deliver TNF to many tumour sites. In 1995 liposome-encapsulated recombinant human TNF-α was reported to be anti-tumorogenic in patients with sarcomas or melanomas whilst showing reduced cytotoxic side effects. This reagent is currently still used to treat patients with stage IIB/III melanoma (Kirkwood et al., 2001). Unexpectedly, some evidence suggests that endogenously secreted TNF-α by tumour cells has a different effect on tumour pathophysiology. Paradoxically, TNF-α may also act as a tumour promoting factor by the induction of immunosuppressive macrophages. Such tolerogenic TAM secrete angiogenic factors including VEGF and SDF-1α which are important in tumour invasion and metastasis (Green et al., 2009a). In contrast, exogenous high levels of TNF-α induce the recruitment and activation of cytotoxic NK and T cells, subsequently leading to tumour killing. Li et al., have also shown that soluble TNF-α significantly promotes lymphocyte infiltration attracting both CD4+ and CD8+ T cells to the tumour site in murine cell line H22-induced hepatic carcinoma. In addition to a secreted form, TNF-α can also be expressed as a trans-membrane variant (TM-TNF-α). Expression of TM-TNF-α stimulates induction of Fas expression on tumour cells surface implying that the involvement of Fas/FasL signaling pathway in TM-TNF-α –induced death of H22 tumour cells. These results suggest that secreted and trans-membrane forms of TNF induce killing of cancer cells *in vivo* through different mechanisms (Li et al., 2006). Thus the pharmacological administration of TNF-α has both promising anti-tumour effects, as well as severe cytotoxicity which will limit its use as an anti-tumour therapeutic (Leist and Jaattela, 2002).

1.3.2. Adoptive immunotherapy

In addition to the non specific immune-based therapies previously described, another major focus in current anti-tumour immunity is the generation of specific immune responses targeted towards distinct tumour antigens. This can involve either the adoptive transfer of *ex vivo* tumour-specific effector cells or active immunisation strategies (cancer vaccination).
Encouragingly, initial clinical trials following administration of adoptive therapy are beginning to show some promising results in several types of cancer (Zhang and Herlyn, 2009). This type of therapy involves the removal of lymphocytes from individual patients followed by their *ex vivo* manipulation before re-introduction. In particular, T cells isolated from fresh tumour biopsies or PBMC are cultured with IL-2 and both anti-CD3 and CD28 leading to progressive

selection and clonal explanation of various subsets of T cells. Currently, adoptive therapy focuses not only on TIL, but also on transfer of *ex vivo* manipulated APC (**Fig. 1.2.**).

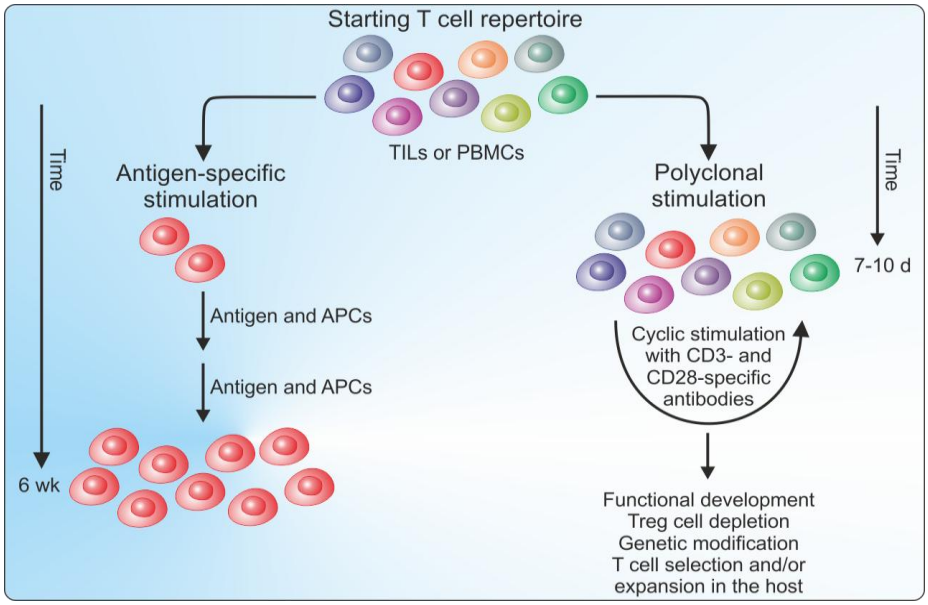

Fig. 1.2. General approaches for *ex vivo* generated tumour-specific T cells. Following lymphocytes isolation from either peripheral blood (PBMC) or the tumour itself (TIL), antigen-specific CTL can be selected and expanded by repeated stimulation with antigen pulsed APC or inactivated tumour cells. This process requires several rounds of stimulation (left). Alternatively, the T cell population can be numerically expanded by polyclonal stimulation by cyclic stimulation with anti-CD3 and CD28 antibodies leading to depletion Treg and selection CTL which maintaining the tumour specific TCR (right). Adapted from the *J. Clin, Invest*. 117:1204-1212 (2007).

Several studies have shown that T cells isolated from tumour-draining lymph nodes (TDLN), followed by *ex vivo* activation and then re-infusion into tumour bearing mice led to tumour rejection. According to Cohen, T cells from TDLN were able to inhibit tumour growth due to interaction with APC. Host APC constantly migrate from tumour site to draining lymph nodes where they present tumour antigens to T cells (Cohen et al., 2001). In addition to the studies described that have focused on *ex vivo* activation and expansion of the effector T cell populations, a few recent reports have also demonstrated that down regulation of Treg function prior to adoptive therapy treatment has beneficial results (Muranski and Restifo, 2009) (Antony et al., 2005; Gattinoni et al., 2005). It has been shown that Treg appear to be more sensitive to a common chemotherapeutic agent cyclophosphamide (Cy). Apart from its antineoplastic properties in the treatment of Hodgkin's disease, lymphoma and breast cancer, Cy may also have immunostimulatory function when used in low doses. In particular, it has been shown that a low dose of Cy leads to decreased expression of GITR and FoxP3 resulting in

attenuation of suppressive activity of Treg (Motoyoshi et al., 2006). This allowed more effective killing of B16/F10 melanoma cells by *ex vivo* generated TIL.

Therefore, more advanced studies on drugs which selectively depletes Treg, may lead to reduced Treg-mediated suppression. This will improve the efficiency of adoptively transferred effector cells in tumour elimination.

Another approach for cancer immunotherapy is the 'cancer vaccination' strategy. Currently, many studies have been made in identification of tumour antigens. These peptides can become the targets of tumour-specific T cell response because they are not displayed on the surface of normal/healthy cells or can be displayed in an abnormal manner. In general, tumour antigens can be broadly categorized into six types – unique, differentiation, over-expressed, cancer-testis, universal and oncoviral antigens. The examples of each group of tumour antigens are given in **Table 1**.

The first category consists of unique antigens that are the result of point mutations or gene rearrangements leading to ontogenesis. Typical examples include proto-oncogenes (e.g. ras, β-raf) that are involved in cell division and differentiation. Mutations of these proto-oncogenes have been seen in 15% of patients with colorectal or pancreatic cancer. Furthermore, mutations resulted in inactivation of tumour suppressor genes such as CDK4, p53 observed in 50% of human malignancies are also part of this group. In addition, mutated form of α-actinin-4 causing uncontrolled actin binding is also classified as a unique tumour antigen. Accumulation of α-actinin-4 in the cytoplasm induces cellular motility and contributes to metastasis in patients with breast cancer (Honda et al., 1998).

The second category comprises of peptides encoded by genes normally expressed only in particular types of tissue. The best examples of differentiation tumour antigens are peptides expressed in melanocytes and melanoma tumour cells such as tyrosine (gp75) which participate in melanin biosynthesis. The strong correlation between the level of IgG antibodies against the gp75 present in serum and cancer progression has been seen in melanoma patients. Also gangliosides (GM2, GM3, GD2, GD3) belong to the group of differentiation antigen. In particular, it has been shown that mice vaccinated with GM2 and then challenged with lung or breast cancer cells induce strong NK cells activation leading to anti-tumour immunity and consequently tumour rejection. In contrast, unvaccinated mice developed previously injected tumour and died (Labrada et al.).

The third group of tumour antigens is over-expressed antigens which are stronger expressed in neoplasmatic cells than normal cells. The example is Human Epidermal growth factor Receptor 2 (HER2), the glycoprotein which is over-expressed in 30% of breast cancer patients and

correlated with poor prognosis. The antibody against HER2 is currently a valuable tool in ADCC-mediated tumour cells death. Also epidermal growth factor (EGFR) and CD20 belong to this class of tumour antigen as they significantly over-expressed on colorectal and lymphomas, respectively.

Cancer-testis is a group of antigens that have been originally found on healthy male germ cells as silent antigens, but many types of tumorus including melanomas (Fratta et al.), lung cancer (Kim et al., 2009c) and brain tumour (Jacobs et al., 2008) also express these antigens. Due to their presence in various cancers and their limited expression in normal tissues, cancer-testis antigens, therefore, are ideal vaccine targets for tumor immunotherapy. Indeed, newly detected, NY-ESO-1 antigen is regarded as one of the most immunogenic antigens ever isolated, inducing spontaneous host immune responses in 50% of patients with NY-ESO-1-expressing in various neoplasms.

The fifth class, which is universal antigens, is comprised of proteins which are expressed in most neoplasmatic cells, but not in normal, differentiated tissues such as survivin and telomerase. Anderson et. al. has shown that survivin (regulator and cell death inhibitor) may be an important and widely applicable target for anti-cancer immunotherapeutic strategies (Andersen and thor, 2002).

The final group of tumour antigens comprises of proteins encoded by viral oncogenes which are involved in ontogenesis such as E6 and E7 proteins expressed by the human papilloma virus type 16 (HPV16). As oncoviral proteins have foreign origins they are able to be unrecognisably by immune-effector cell. However, Yan et. al., showed that mice vaccinated with HPV16-E6E7-DNA, construct expressing in mammalian cells, were able to induce HPV-16-specific antibody production and CTL response in tumour bearing animals (Yan et al., 2007).

Table 1. General classification of tumour antigens. Adapted and modified from Journal of Translational Medicine 2004, 2:12.

ANTIGEN	EXAMPLES	TYPE OF TUMOUR
unique	b-raf, ras, CDK4, p53, α actinin-4	colorectal, pancreatic, breast
differentiation	tyrosinase/gp75, gangliosides,	melanoma, lung, breast
over-expressed	HER2, EGFR, CD20	breast, colorectal, lymphoma
cancer-testis	MAGE, NY-ESO-1	melanoma, lung, brain
universal	telomerase, survivin	many types
oncoviral	HPV type 16, E6, E7	cervical

Based on these findings, it was possible to generate protein-based-vaccines that were able to treat many types of cancers, however some promising results have been also observed in patients who received *ex vivo* loaded autologous DC with tumour apoptotic bodies, tumour lysates or tumour mRNA/DNA as an alternative approach to induce tumour-antigen recognition.

Although the identification of various tumour antigens has significantly advanced our understanding of anti-tumour immunity (Rosenberg, 2001), the discovery that many cancers do not express MHC class II molecules on their surface, experiments have focused on the modulation of antigen processing and presentation pathways, as a valuable tool for cancer immunotherapy. In particular, genes that encode molecules enhancing the immune response are introduced into tumour cells. Furthermore, $CD8^+$ cytotoxic T cells are able to induce lysis of tumour cells exclusively upon recognition of tumours antigen presented in context of MHC class I. It has been shown that even one round of *in vitro* stimulated CTL cells allows inhibition of tumour growth. Also, using pulsed DC cells with MHC class I restricted peptides enhanced CTL cells anti-tumour function in melanoma patients (Oh et al., 2006) (Santin et al., 2002).

Overall, clinical trials using MHC class I restricted antigens elicited only modest or transient immune response in most immunised patients (Bonehill et al., 2005). The reason of explaining the partial failure of this therapy is the lack of tumour specific CD4+ T cells that help to expand an effective CTL response. Since the 1980's, the importance of CD4+ T cells in protection against tumour growth has been widely reported. However, insufficient progress has been made to understand the role of CD4+ T cells recognising MHC class II-restricted tumour antigens, mostly due to technical difficulties.

1.3.3. Chemotherapy

Chemotherapy is one of the principal approaches for the treatment for cancer patients by causing damage to rapidly dividing tumour cells. There are more than 90 different drugs available to the clinic, which have vastly improved since middle 1940's when Louis S. Goodman for the first time treated lymphoma-bearing mice using mustine.

The choice of specific chemotherapies depends on tumour type, histologic grade (how aggressive the tumour is) but also on tolerance to side effects resulting from the chemotherapeutic agent. It has been shown that cytotoxic drugs that can lead to complete remissions of some form of cancers such as lymphoma, are also effective in decreasing tumour size, and may prolong life even in metastatic cancers, such as osteosarcoma. Unfortunately,

chemotherapeutic multidrug resistance of many tumours is still a major obstacle in cancer therapy. Therefore, the different chemical structures and mechanisms of intracellular activity of chemotherapeutic agents need to be constantly developed. Interestingly, many studies have shown that a combination of chemotherapy and adoptive immunotherapy give better results than either therapy administrated separately. For example Dudley et al., have shown that patients with refractory metastatic (stage IV) melanoma given chemotherapeutic lymphodepletion with Cy administration, fludsrabine and 12 Gy irradiation, who were subsequently infused with lymphocytes previously isolated from their tumour site, had a high clinical response rate reaching 70%. However, patients who were administrated only one type of treatment (adoptive or chemotherapy) showed moderate anti-tumour responses (between 10% and 34% clinical rates) (Dudley et al., 2005) (Dudley et al., 2008). Therefore, a combination of different strategies for anti-tumour immunity helps to minimise the side effects of chemotherapy including nephrotoxicity, hair loss, vomiting or nerve damage resulting in improved quality of life for patients.

1.3.3.1. Anthracycline treatment and immunogenic cell death

Anthracyclines including Aclarubicin, Daunorubicin, Doxorubicin and Mitoxantrone are an effective anti-neoplastic group of drugs derived from *Streptomyces* bacteria widely used in clinics. Although they are active against a variety of solid tumours such as sarcomas, breast and prostate cancers and haematological malignancie including leukemias or Hodgkin's disease, their clinical use is not ideal due to tumour resistance and toxicity to healthy adjacent tissue. In particular, myocardial tissue is susceptible to free radical damage, therefore anthracycline-treatment might be an important risk factor resulting in cardiomyopathy (Lebrecht et al., 2009). Currently, scientists are focusing on the modification of the general anthracycline ring structure that allows reduction of the side effect but maintains a strong anti-tumour profile.

The biological activity of anthracyclines is related to topoisomerase II inhibition (which is involved in DNA repair mechanisms), intercalation between DNA base pairs causing double and single strand break, inhibition of DNA/RNA synthesis and cell cycle arrest at the G(2)/M phase (Kim et al., 2009b). Production of hydroxyl free radicals and damage to the plasma membrane is also associated with the anti-tumour effects of anthracyclines (Mizutani, 2007). Furthermore, it has been described that doxorubicin treatment induces disruption of inner mitochondrial membrane potential resulting in apoptotic cell death (Kohler et al., 2008).

Recently another important aspect of anthracycline-therapy has been investigated by the Kroemer laboratory group (Panaretakis et al., 2009). They demonstrated that chemotherapeutic agents such as anthracyclines not only participate in selective killing of tumour cells but additionally stimulate anti-tumour immunity leading to more vigorous elimination of neoplasmatic tissue. This was shown in several mouse cancer cell lines including CT26 colon cancer, EL4 thymoma, GOS osteosarcoma, MCA-induced fibrosarcoma or the TS/A mammary tumour cell line. Following anthracycline treatment or γ-irradiation, tumours were shown to undergo apoptosis and to induce anti-tumour responses. Other classical apoptotic stimuli such as staurosporine or mitomycin C failed to induce anti-tumour immunity (Obeid et al., 2007b) (Apetoh et al., 2007b), (Casares et al., 2005). This 'immunogenic' cell death following anthracycline treatment was shown to be dependent on the surface exposure of the chaperone proteins calreticulin and ERp57. These proteins are relocated from the ER lumen to the plasma membrane and constitute an 'eat me signal' which is required for the phagocytosis of the dying tumour cells by DC. Antigens released from engulfed immunogenic tumour cells are then processed via the cross-presentation pathway for the activation of MHC class I-restricted CTL. Thus anthracycline-treatment not only induces cell death, but also stimulates tumour antigen-specific immune responses.

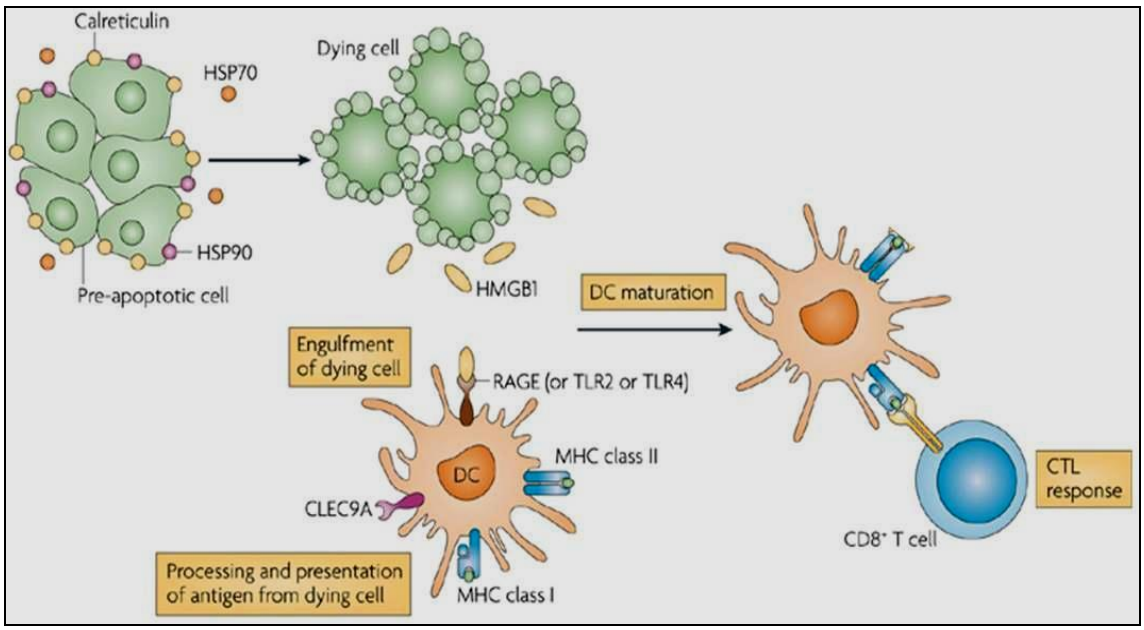

Fig. 1.4. A schematic representation of immunogenic cell death. Following anthracycline treatment apoptotic tumour cells relocate CRT and chaperone proteins to the cell surface. Additionally, by releasing HMGB1, dying tumour cells activate DC. In particular, CRT and HMGB1 interacting with CD91 and RAGE/TLR4/TLR2, respectively can facilitate the uptake of the dying cells and induce cross-presentation of tumour antigens that consequently elicit anti-tumour immunity. Adapted from Nature Reviews Immunology 9, 353-363 (May 2009).

In particular, Apetoch et al. injected CT26 colon cancer cells that had been treated with anthracyclines, mitomycin C or etoposide into the foot pad of BALB/c mice or CRT negative mice. Following lymph node isolation they assessed IFN-γ production by draining T cells. Only T cells isolated from CRT sufficient mice significantly secreted IFN-γ and rejected the anthracycline-treated tumour cells. In contrast, CRT sufficient mice that were challenged with CT26 tumour cell line previously treated with etoposide or mitomycin, failed to control tumour growth. As etoposide and mitomycin were shown to be non-immunogenic agents which do not trigger CRT relocation, this confirmed the role of CRT in the induction of anti-tumour immunity. Similarly, CRT negative mice challenged with anthracycline-treated CT26 cells had significant tumour growth, again indicating that anti-tumour immunity was CRT mediated.

1.3.4. Radiotherapy

Since the discovery by Roentgen in 1895, the X-ray has played one of the major roles in modern medicine. Radiotherapy (x-ray therapy or irradiation) is the use of a certain type of energy (ionizing radiation) to kill cancer cells and reduce tumour size. Although radiation damages both cancer cells and normal cells, most normal cells can recover from the effects of radiation and regain proper function. Currently radiotherapy has been improved by providing more specific mechanisms delivering energy to neoplastic tissue. In particular, using tumour-specific antibodies conjugated with radioisotopes (Y^{90}-trytium or I^{131}-iodine) nearby healthy tissues receive limited damage (Borghaei et al., 2009).

Many key biochemical processes in irradiated cells including DNA, RNA or protein synthesis, respiration or other metabolic pathways are inhibited or even completely eradicated by irradiation. However, the mechanisms by which irradiation triggers these biochemical changes including the induction of apoptosis in normal and neoplastic cells has not been completely understood until recently.

It is now known that the p53 tumour suppressor gene is key in this process (Therrien et al., 1999). In particular, it has been suggested that the product of the p53 gene is involved in monitoring the integrity of the genome. If DNA is damaged, the p53 product accumulates through a post-translational stabilisation mechanism and arrests the cell cycle at G1 to facilitate DNA repair. If repair fails, p53 then may trigger apoptosis. To address the role of p53 in cell death following irradiation, Kerr et al. has showed that thymocytes lacking p53 are resistant to lethal effects of ionizing radiation. However following exposure to glucocorticoids as an alternative apoptotic stimulus, p53 deficient thymocytes undergo apoptosis (Kerr et al.,

1994). Furthermore, DNA mutations that occur as a result of UV irradiation can lead to cell lethality. It has been shown by Ward that small doses of irradiation causes significant single or double-strand DNA breakage (Ward, 1994). In addition, a moderate dose of UV light induces apoptosis demonstrated in several *in vivo* and *in vitro* studies (Kimura et al., 2009) (Chathoth et al., 2009), (Reich et al., 2009). According to Kim et al., following UVB and UVC irradiation the colorectal cancer cell line (CX-1) exhibited morphological changes characteristic of apoptosis including the appearance of apoptotic bodies, the activation of caspases 8, 3, 1 as well as cytochrome c release (Kim et al., 2008b). Furthermore, whilst the CX-1 cell line was originally resistant to TNF-related apoptosis-inducing ligand (TRAIL) stimuli, following UV exposure CX-1 cells were sensitive for TRAIL induced cell death. These studies may help to improve cancer therapy for certain TRAIL-resistant tumours such as lung, colorectal or prostate cancers by using UVC treatment to increase the sensitivity of these tumours to TRAIL –induce death.

1.3.4.1. γ–irradiation or UVC exposure also leads to immunogenic cancer cell death

In addition to anthracycline-treatment (described in **Section 1.3.3.**) several studies have also shown that UVC and γ-irradiation are capable of inducing immunogenic cancer cell death (Panaretakis et al., 2009), (Tufi et al., 2008). Studies carried out by Brusa and co-workers revealed that UVC treated renal carcinoma cells (RCC) induce an accelerated maturation of TID enabling efficient tumour antigen CTL cross-priming (Brusa et al., 2008). Notably, they showed that post-apoptotic RCC (20 h following UVC exposure) release high mobility group box 1 (HMGB1) protein that activates DC. HMGB1 is a non-histone protein which is bound to DNA and induces maturation and migration of DC via upregulation of costimulatory molecules and the induction of IFN-α production by DC (Dumitriu et al., 2007) (Yang et al., 2007). Consequently, following incubation with apoptotic RCC cells, matured DC were shown to upregulate CD80, CD83 and CD86 along with the chemokine receptor CCR7 as well as increasing production of IL-1β, IL-6 and TNF-α. Pre-treatment of immature DC (iDC) with antibodies blocking the HMGB1 receptor, confirmed that DC maturation was HMGB1-mediated. Furthermore, they also revealed that iDC incubated with UVC-treated RCC had elevated levels of inflammatory cytokine gene expression. More importantly they also showed that incubation with RCC induced an upregulation of molecules involved in the antigen-processing machinery including the TAP subunits as well as inducing increased the expression of MHC class II genes. These findings clearly showed that selective apoptotic stimuli induce the

release of HMGB1 from various carcinomas during the later stages of apoptosis leading to DC activation and improved T cell stimulation.

Similar mechanisms leading to immunogenic cell death following UVC treatment was observed by Brusa et al. They showed that following UVC treatment or exposure to raised temperature ($56^{o}C$) the human prostate cancer cell line (LNCaP) was more effectively engulfed by DC (Brusa et al., 2009). Brusa et at. additionally showed that dying tumour cells also release HMGB1, which interacts with TLR4 or the receptor for advanced glycation end products expressed by DC. Ligation of these receptors was subsequently shown to induce enhanced targeting and processing of engulfed antigens. Indeed, DC from patients with deficient TLR4 alleles were also shown to be inefficient at presenting antigens from dying tumour cells (Apetoh et al., 2007a). Furthermore, using an ELISPOT assay, Brusa also demonstrated that UVC treatment of the tumour cells before DC loading induced MHC I-restricted IFN-γ release by autologus T cells as a result of tumour antigen cross-presentation. In contrast, live LNCaP cells inhibited DC maturation resulting in the attenuation of autologous responses.

Another study demonstrated that DC incubated with γ-irradiated B-cell lymphoma (B-CLL) were 300 times more efficient in their ability to present B-CLL antigens than DC incubated with non-treated B-CLL. Using proliferation assays they revealed that autologus T cells isolated from B-CLL patients, after stimulation with apoptotic B-CLL loaded DC, produced five times more IFN-γ than T cells activated by DC pulsed with live B-CCL leukaemia. It was suggested that apoptotic B-CLL display 'novel' intracellular proteins which induce the anti-tumour response (Kokhaei et al., 2003).

Therefore, there now exist many examples where radiotherapy not only is effective at inducing tumour death, but also induces a type of cell death that directly activates interacting APC leading to efficient T cell stimulation. Thus either γ-irradiation or UVC-treatment along with anthracycline treatment could induce a break in 'classical' apoptotic cell-induced tolerance to novel or 'neo' antigens leading to the initiation of improved anti-tumour immunity.

Concluding remarks for current cancer therapy

Cancer is recognised as a lethal disease that is rarely controlled by host immune responses sometimes even in the presence of high frequencies of tumour-specific T cells. In order to overcome this apparent 'weak immunogenicity' of tumours, scientists have focused on methods that increase anti-tumour immunity including combinations of both specific cytotoxic T cell-mediated responses and humoral immunity. In principle, any therapy that delivers higher levels of presented or cross-presented tumour antigens to the draining lymph nodes could synergize with immunotherapy. Thus, immunogenic apoptotic tumour cell death following anthracycline chemotherapy or UVC radiotherapy treatment could be a valuable approach boosting natural anti-tumour immunity. In addition, inducing this kind of cell death in conjunction with cancer vaccination therapy should prove more efficient in terms of both priming an anti-tumour response and in the generation of tumour antigen-specific memory. Therefore, future treatments will require a multidisciplinary approach integrating surgical, radiation, chemotherapeutic and especially immunotherapy options to improve the quality of life of cancer patients, rather than just focusing on survival endpoints.

1.4. B cells and anti-tumour immunity

1.4.1. Antigen recognition and B cell activation

As previously described, B cells represent an important arm of the adaptive immune response. They specifically neutralize pathogens by production and secretion of antibodies. More recently, it is now known that B cells also play an important role as APC activating CD4+ T cells (Batista and Harwood, 2009; Clark et al., 2003; Rivera et al., 2001). Furthermore, some studies indicate that B cells which infiltrate tumour tissue play an important role as APC in tumour antigen presentation to specific T cells (Kotlan et al., 2005). However, little is known about the origin and specificity of B cells infiltrating the tumour microenvironment. Also anti-tumour recognition and elimination, based on specific antibodies binding to tumour antigens, has not been thoroughly explored and still needs to be developed. Therefore, a better understanding of the role and nature of B cells in anti-tumour immunity might be a powerful approach in further clinical practice for the treatment of many cancer patients.

B cells express a membrane-bound antigen receptor (BCR) that binds and internalizes antigen into the endocytic compartment (Hou et al., 2006). In this environment the antigen-BCR complex forms a substrate for the action of proteolytic enzymes generating peptide fragments which associate with MHC class II molecules and are subsequently displayed on the B cell surface (Shlomchik, 2009). These complexes are consequently recognised by CD4+ T cells. Antigen presentation by B cells was until recently thought to be predominantly responsible for the activation of T cells that would provide helper signals for B cell activation and differentiation leading to the eventual secretion of the BCR as soluble antibody. However, recent data has shown that in several different situations, B cell APC-function is also crucial for full activation of T cell-mediated immunity (Crawford et al., 2006). In particular, Whitmire et al. showed that mice lacking B cells rapidly lost antigen-specific CD4+ T cells, but not CD8+ T cells memory after acute infection by lymphocytic choriomeningitis virus (LCMV). Consequently, the lack of CD4+ T cell memory led to incomplete recovery from chronic virus infection in B cell-deficient mice. These data implicate a B cell function other than antibody production that induces long-term protective immunity (Whitmire et al., 2009). Similarly, Linton et al., demonstrated that mice lacking B cells were able to develop memory T cells, but such animals had significantly lower frequencies of both primary and memory antigen-specific T cells. However, *in vitro* when IL-4 and antigen activated B cells were provided, antigen-specific T cells were completely reconstituted (Linton et al., 2000). These results provide direct evidence

that B cells can have an essential role in determining the T cells expansion in response to antigen and generation the size of the memory antigen-specific T cells. Furthermore, in autoimmune disorders such as rheumatoid arthritis (RA), B cells also play a crucial role as APC. O'Neill showed using a mouse model of RA, proteoglycan (PG)-induced arthritis (PGIA), that B cells were a major source of APC which activated autoreactive PG-specific T cells via CD80/86-CD28 costimulatory signals (O'Neill et al., 2007). In contract, mice with CD80/86 deficient B cells phenotype did not develop PG-specific T cells in this PGIA model, indicating that APC function of B cells in RA is essential. Therefore, understanding the mechanisms involved in the acquisition of antigen by B cells may be the key feature in this unique APC role. It may allow the evaluation of these mechanisms in the development of anti-tumour immunity.

For the initiation of B cell responses peripheral antigens are transported via afferent lymphatics to the secondary lymph organs where they are 'displayed' as native proteins, either complexed with antibody, or complement components on the surface of specialized cells termed follicular dendritic cells (FDC) (Szakal and Tew, 1992). FDC are stromal cells located in specialised areas involved in B cell maturation. By providing native antigen and activation signals, FDC/B cell interactions are essential for B cell survival and consequently induce class switching and differentiation (Szakal et al., 1992). While it was shown more than twenty five years ago that antigen displayed by FDC is subsequently internalised into the B cell endocytic compartment (Schnizlein et al., 1984) the mechanisms involved in B cell antigen acquisition from these cells was only recently described. In pioneering experiments, Batista has shown that B cells can physically extract native antigens which are tethered to non-internalisable surface (Batista and Neuberger, 2000). Subsequently, it was also demonstrated that B cells can acquire tethered antigens displayed by target cells resulting in an immunological synapse (IS) formation.

As well as FDC, both DC and macrophages have also been demonstrated to display antigens for B cell acquisition. Wykes et. al. showed that non-immunized rats, challenged with DC previously pulsed with antigen, could elicit antigen-specific IgM and IgG responses (Wykes et al., 1998). Furthermore *in vivo* studies performed by Bergtold, Desai et al. demonstrated that DC capture naive antigens that subsequently are endocytosed by the Fc receptor. Such FcγR-antigen complexes access a nondegradative intracellular vesicular compartment and recycle to the cell surface of DC allowing interaction of native antigen with the BCR. This interaction consequently leads to B cell activation and class switching (Bergtold et al., 2005). These findings show that DC maintain intact native antigen that is capable of initiating a primary B cell response. Furthermore, more recent studies identified subcapsular sinus CD11b+ CD169+

MHC II+ macrophages in the marginal zones of lymph nodes as a cell type displaying native antigens for B cell acquisition during the first few hours following antigen administration (Carrasco and Batista, 2007) (Junt et al., 2007).

Central to the acquisition of antigen by B cells is the expression of BCR. The BCR is a molecular complex consisting of a membrane anchored pre-cursor of the subsequently secreted antibody along with the Igα/Igβ heterodimer. In addition to BCR/antigen binding, interactions between adhesion molecules expressed by the B and target cell including leukocyte function-associated molecule-1 (LFA-1) and intercellular adhesion molecule-1 (ICAM-1) are essential for antigen acquisition and IS formation (Carrasco and Batista, 2006b). Koopman et. al. have shown that binding between CD49d/CD29 (VLA-4), an integrin expressed on leucocytes and its ligand: vascular adhesion molecule-1 (VCAM-1) which is expressed on FDC facilitates this interaction (Koopman et al., 1994). Carrasco and Batista suggest that B cell antigen acquisition consists of four steps (Carrasco and Batista, 2006b). Firstly, initial interaction between VLA-4 and VCAM-4 promotes adhesion of B cells to the membrane bearing native antigen. Secondly, binding of LFA-1 to ICAM-1 activates signaling pathways that lead to cytoskeletal changes in the B cell. Next a supramolecular structure (cSMAC) is formed consisting of a docking structure with the BCR and antigen at the centre, whilst LFA-1 and VLA-4 remain in the periphery of the SMAC (pSMAC). Finally, the BCR/antigen complex is internalized inside the B cell endocytic pathway completing the process of antigen acquisition.

Furthermore, Arana et. al. demonstrated that prior to IS formation, phosphoinositide 3-kinases (PI3K) and the small GTP-ase protein, Rac2, play a crucial role in the process of antigen recognition. In particular, they showed that Rac2 is involved in both early cytoskeleton rearrangement and in the up-regulation of LFA-1 essential for IS formation (Arana et al., 2008). To confirm the role of Rac2 in the adhesion process, the authors showed that B cells isolated from Rac2 deficient (Rac2-/-) mice had a defect in the adhesion process as a consequence of down-regulation of LFA-1 molecule, compared to wild-type mice. Surprisingly, B cells from Rac1-/- mice did not show any significant differences in adhesion. They also examined the role of PI3K in B cell adhesion and IS formation. In the presence of the PI3K inhibitor, wortmannin, they observed a lack of Rac2 activation which led to reduction of IS formation. This data confirmed the essential role of Rac2 in the promotion of B cell adhesion. Consistent with this they also demonstrated that overexpression of a constitutively active form of Rac2 led to enhanced antigen aggregation and integrin expression. Interestingly, these experiments were performed using an artificial bilayer membrane system, allowing controllable antigen dose availability. Thus, for the first time they demonstrated the complex interplay involved in

antigen mediated intracellular signaling events and cytoskeleton rearrangements results in the IS formation (Treanor et al.).

Following antigen acquisition, B cells are selected in specialised areas of secondary lymphoid tissues termed germinal centres, based on a combination of their efficiency to bind, internalize and present peptide fragments generated from these extracted antigens to CD4+ T cells. This B-T interaction is crucial for the mutual activation of both cells. Contact between B and T cells helps to develop a fully maturated antibody response involving class switching and memory cell formation. Furthermore, B-T interaction also leads to full T cell activation. In some cases, such activation of CD4+ T cells by B cells may also lead to either the generation of functional CTL that directly eliminate tumour cells or to the development of long-term tumour specific-CTL (Ho et al., 2002).

1.4.2. The role of B cells in anti-tumour immunity

According to several reports the role of B cells in anti-tumour immunity is controversial. Indeed, Shah et al. suggests that role of B cells in tumour biology maybe immunosuppressive, resulting in the inhibition of tumour rejection (Shah et al., 2005). It has been shown that B cell depleted mice, (using anti-CD20 antibody) that were vaccinated with adenovirus expressing the virus-E7 gene (Ad.E7) in mice bearing TC1 tumors (murine lung cancer cells expressing human papilloma virus-E7), have enhanced anti-tumour immunity compared to non-depleted mice. Therefore, these studies demonstrate that B cell depletion may be a useful adjunct in anti-tumour treatment (Kim et al., 2008a). In addition, it has been shown that long-term B cell-mediated inflammatory response can influence tumour development. This results in the activation of signaling pathways regulating tumour progression. In particular, chronic production of Th2 cytokines such us IL-10, IL-4 or immunoglobulin complexes may lead to tumour expansion (Howell and Rose-Zerilli, 2006) (Tan and Coussens, 2007). Indeed, increased level of IL-10 in patients with gastric cancer was correlated with poor prognosis as a result of tumour angiogenesis and inhibition of CTL infiltration (Sakamoto et al., 2006). Another study has demonstrated that anti-tumour antibodies were involved in the recruitment of macrophages and granulocytes via FcR into the tumour site. Such activated macrophages and granulocytes produce VEGF which stimulate tumour angiogenesis and promote metastasis (Barbera-Guillem et al., 1999).

Further studies need to be done to determine which type of anti-tumour immunity will be most effective in certain types of human cancers. Although these selected papers demonstrate

pro-tumourogenic function of B cells in tumour sites, the vast majority of studies have shown the beneficial role on B cells in anti-tumour immunity. Some examples of these beneficial roles will be described below.

1.4.2.1. The role of antibodies as adjuvant in cancer therapy

Several mechanisms have been described to explain the anti-tumour activity of tumour-antigen-specific antibodies. In particular, the immunomodulatory mechanisms of antibody-mediated anti-tumour immunity are based on mediation of the cellular cytotoxicity of tumour cells by ADCC mechanism. In addition, by cross-linking FcR expressed on DC or macrophages this also promotes antigen presentation leading to activation adaptive CD4+T cell-mediated immunity.

- **Tumour vaccination enhances antibody production**

Li et al. have highlighted the important role of antibodies in anti-tumour immunity where CTL-mediated response was either difficult to detect or absent (Li et al., 2008). They demonstrated that breast tumour (TUBO)-bearing mice vaccinated with chaperon-rich TUBO-cell lysates (CRCL) induced strong anti-tumour antibody production and delayed tumour growth, in contrast to tumour-bearing mice which were not vaccinated. To prove that vaccination enhanced antibody production and consequently led to improved anti-tumour immunity, they also vaccinated J_H knockout mice lacking B cells and antibodies (Ig-/-). Vaccination of these Ig-/- tumour-bearing mice with CRCL lysates did not lead to protection and tumour growth kinetics was significantly faster than in vaccinated B cell sufficient tumour-bearing mice. This experiment clearly indicates that B cell responses generated by CRCL vaccination plays an important role against tumour growth. In addition, they tested the possibility that anti-tumour immunity could be transferred with immune sera. They pooled sera from mice deficient in T cells but not with B cells and immunised with TUBO-CRCL lysates. Following transfer of sera, mice were challenged with TUBO cells and anti-tumour activity was measured. They showed that in these mice, tumour growth was significantly delayed. Interestingly when TUBO challenged mice received sera raised against lysates from different types of tumour cells, these mice did not induce protection against their tumours. This provides additional evidence that CRCL vaccination induces specific antibody responses which enhance anti-tumour immunity. They proposed that these antibodies functioned in ADCC mediating tumour lysis. In particular, IgG1, IgG2a, IgG3 iso-types were observed in the sera 1 week after the first CRCL-immunization and these antibodies persisted for at least 3 weeks, suggesting that long-term immunity can be

elicited. Also they examined the role of CD4+ and CD8+ T cells in TUBO-bearing mice. Using mice depleted of either CD8+ or CD4+ T cells before and after vaccination they assessed which population of T cells is involved in tumour regression. In this type of cancer, CD8+ T cells did not play a role in anti-tumour immunity in TUBO-bearing mice followed CRCL administration. In contrast, in mice depleted of CD4+ T cells, the tumours grew significantly faster than in control mice with intact CD4+ T cells. This suggests that tumour-reactive CD4+ T cells are crucial for the induction of this antibody-mediated anti-tumour immunity.

- **ADCC in tumour therapy**

The majority of antibodies, which have been used for anti-tumour therapy, act by simultaneously binding to tumour antigens and to FcR stimulating tumour-specific ADCC. This antigen/FcR cross-linking induces the release of cytokines including IFN-γ and also cytotoxic granules by NK cells, CTL and neutrophils. These granules contain perforin and granzymes and actively lyse target tumour cells displaying antigens. In addition, antibody/FcR cross-linking on macrophages stimulates enhanced phagocytosis of antibody-coated tumour cells and simultaneous release of ROS, NO, a variety of proteases and FasL (Iannello and Ahmad, 2005). Due to the relative efficiency of this process, substantial effort in the development of monoclonal antibodies that effectively promote ADCC through improved FcγR interactions has been made. The most common antibody used in clinics is an anti-HER2/neu monoclonal (trastuzumab) that has been approved to treat patients suffering for breast cancer. For example a clinical study performed by Kute and co-workers has shown that administration of trastuzumab leads to significant activation of granulocytes or mononuclear cells in patients with breast cancer (Kute et al., 2009). They revealed that these effector cells showed enhanced tumour killing properties. In addition, *in vitro* experiments confirmed that the natural killer cell line (NK-92) showed enhanced tumour killing in the presence of trastuzumab.

Similar to treatment with trastuzumab, the use of the anti-CD20 monoclonal antibody (rituximab) has been very effective for a number of years in the treatment of various types of B cell lymphoma (Weiner et al., 2009). For example, Weitzman et al. demonstrated the activation of NK cells following treatment with rituximab in patients with chronic lymphocytic leukemia (Weitzman et al., 2009). Interestingly, Jazirehi, Bonavida showed another function of rituximab as an agent that negatively regulates survival pathways in lymphoma cells. In particular, they demonstrated downregulation of the p38MAPK signaling pathway resulting in the inhibition of constitutive STAT-3 activity and subsequent downregulation of pro-apoptotic Bcl-2 expression following rituximab treatment. Furthermore, they showed rituximab is involved in the upregulation of Raf-1 kinase inhibitor protein (RKIP). Activated RKIP leads to

inhibition of pro-survival ERK1/2 and NF-κB pathways and therefore chemosensitizes tumour cells for apoptotic cell death (Jazirehi and Bonavida, 2005).

It is noteworthy that Green et al. have shown the administration of an anti-E-cadherin antibody prior to the administration of pools of various anti-tumour antibodies disrupts multi-cellular tumour aggregates and increases tumour antigen availability and hence increases the efficiency of ADCC (Green et al., 2002).

- **Monoclonal antibodies as adjuvants for DC**

As described previously, monoclonal antibodies are a valuable tool for treatment of many malignant diseases. In the last decade, monoclonal antibodies are the most common classes of new generation drugs for cancer treatment. More than 20 therapeutic antibodies have been approved for clinical use and many others are now at the clinical and preclinical stage of development (Kubota et al., 2009).

Many tumours do not express MHC class I or II molecules and therefore the uptake of opsonised tumour cells by DC via Fcγ receptor leads to cross presentation and efficient generation of both antigen-specific CD4+ and CD8+ T cell-mediated responses. However, during the steady state DC cells exhibit immature phenotype which can promote tolerance. Therefore to induce effective anti-tumour recognition by DC the maturation stimulus need to be applied. Importantly, FcγRIIa and FcγRIIIa receptors not only mediate antigen uptake, but also affect the DC maturation in contrary to inhibitory receptor FcγRIIb. It has been shown that opsonised tumour cells that bind to activating receptors FcγRIIa or FcγRIIIa on DC are engulfed via interferon pathway and therefore antigen uptake and cross-presentation were enhanced. For those reasons, monoclonal antibodies, which selectively bind to activating receptors and block inhibitory, could be a valuable tool delivering maturation stimulus to DC cells. This mechanism might be one of the most potent determinants boosting adaptive immunity.

1.4.2.2. Tumour infiltrating B cells

Recent evidence from medullary carcinoma of the breast (MCB) patients has shown that there is a correlation between TIB and a more favourable prognosis (Kotlan et al., 2005). Moreover some studies have shown increased numbers of plasma cells in patients with different types of breast cancer (Coronella-Wood and Hersh, 2003). One important finding from these studies was the identification of the antigens recognised by many of these B cells. Surprisingly, many B cells recognised antigens normally located in intracellular compartments in healthy cells. In addition these studies also demonstrated that a significant proportion of the tumour cells that

were associated with B cells were undergoing apoptosis. Therefore this study demonstrated that during apoptosis normal protein trafficking is somehow altered in MCB cells leading to the display of novel or 'neo' antigens on the cell surface that could be recognised by B cells.

Similar studies showing the important role of infiltrating B cells that helps to evaluate tumour bio-markers were performed by Shigematsu et al. They revealed that tumour-specific antibodies, mostly IgG class, obtained from B cells infiltrate isolated from malignant mesothelia could be used to serological identify of tumour neo-biomarkers by recombinant expression cloning method (SEREX). In particular, they identified 22 antigens that correlated with the clinical course of patients including mutated p53 and thrombospondin-2 (Shigematsu et al., 2009). These promising results demonstrated that TIB could be used as a valuable tool for tumour diagnosis.

The same correlation between strong lymphoplasmatic infiltration by B cells in tumour site and improved prognosis for patients with MCB was shown by Pavoni and co-workers (Pavoni et al., 2007). They demonstrated that local humoral immune response within the tumour site of breast cancer patients had an oligoclonal character. They found that antibody genes derived from tumour infiltrating B cells are predominantly oligoclonal and specific for neo-antigens expressed within the tumour site. Using phage-display libraries isolated from MCB tumours they tested the functional binding of antibodies from TIB. In particular, they examined reactivity against a common tumour associated antigen CEA (carcinoembryonic antigen) but also against the MUC1 antigen associated with colon cancer or against the Ed-B domain of fibronectin, a marker of angiogenesis in many types of cancers. These results clearly imply that oligoclonal antibody selection (mostly IgG as opposed to IgA seen in healthy individuals) takes place at the tumour site. Using primary tumours as a source of genes encoding anti-tumour antibodies, they described a useful technique for tumour antigen screening that may prove to be a valuable tool for future diagnostic and therapeutic anti-tumour approaches.

It has been also shown that tumour infiltrating human B cells are involved in direct killing of tumour cells. Kemp et al., demonstrated that following CpG-A containing oligodeoxynucleotides (CpG ODN) stimulation of periphery isolated B cells, the level of TRAIL/Apo2 ligand was unregulated. Surprisingly these CD14+, CD19+, and CD56+ B cells were able to kill tumour cells in a TRAIL/Apo-2L-dependent manner (Kemp et al., 2004).

1.4.2.3. Use of B cells as APC in anti-tumour treatment

Since Lanzavecchia in the middle 1980s clearly showed that antigen-specific B cells efficiently present antigen to T cells (Lanzavecchia, 1985) (Lanzavecchia and Bove, 1985), the use of B

cells as APC when designing effective tumour vaccines for weak tumour antigens has been explored. Indeed, Lapointe et al. tested the capacity of human peripheral B cell to simulate T cells against poorly immunogenic tumour melanoma antigens (gp100) or melanoma cell lysates. The authors demonstrated that resting B cells, which were activated via CD40 ligation and IL-4 treatment and then pulsed with tumour antigens, efficiently processed and presented MHC class II restricted peptides to specific CD4+ T cells (Lapointe et al., 2003). This was inhibited by the inclusion of anti-MHC class II antibodies. In addition, they also showed B cell presentation was sensitive to treatment with chloroquine, which inhibits the processing of exogenous antigens by raising the pH of the endocytic pathway. In contrast, CD8+ specific-T cells were able to recognise cross-presented antigen from B cells in the presence of chloroquine. However, cross-presentation of antigens to CD8+ T cells was five times less efficient then canonical MHC class II restricted antigen presentation to CD4+ T cells. Importantly, they also demonstrated that compared to DC, B cells have an additional advantage in that their proliferation was substantial, thus generating increased numbers of effective APC from a reduced volume of patient blood which could also be cryopreserved (Coughlin et al., 2004) (Schultze et al., 1997). Consequently, these authors argue that using primary B cells as APC, following appropriate stimulation and expansion, has a great potential for effective anti-tumour CD4+ T cell generation.

1.4.3. Apoptotic antigens as a trigger for anti-tumour immunity

Substantial evidence supports the concept that antigens displayed on cancer cells upon apoptosis are able to trigger the local immune-response initiated by B cells. Such infiltrating B cells uptake apoptotic antigens from tumour tissue and present to CD4+ T cells, which mediate anti-tumour immunity. This state is atypical where apoptosis is usually poorly immunogenic or even tolerogenic, with only necrosis resulting in immunity. Understanding the mechanism of this process is currently limited and forms the basis of my studies.

For example, it has been shown that the cytoskeletal protein β-actin was exposed on the surface of medullary breast carcinoma (MBC) cells treated by TNF$-\alpha$, cycloheximide (CHX) or granzyme B as an early apoptotic event. Hansen et. al. (Hansen et al., 2002) indicated an 18% increase in actin display on the surface compared with non-treated MBC cells. They also observed that B cells and plasma cells infiltrating MBC are specific for actin and induce an oligoclonal response.

Similar evidence has been provided by Obeid et al. (Obeid et al., 2007b) who have shown that calreticulin, a ER resident chaperon, can be exposed on the surface of cancer cells upon

apoptosis and can stimulate immunogenicity. Furthermore, they classified differences between several apoptotic-inducing stimuli. Most cytotoxic agents that target the ER (brefeldin, tunicamycin), the mitochondria (arsenite, C2 ceramide) or DNA (etoposide, mitomycin C) failed to induce immunogenic cell death. However, treatment with anthracyclins (doxorubicin, idarubicin and mitoxantrone) did lead to specific calreticulin-induced immunogenicity (Obeid et al., 2007b). Another study by Koltan et al. (Kotlan et al., 2005) has described the importance and immunogenic capacity of gangliosides, particularly GD3 in breast carcinomas. The authors postulated that tumour infiltrating B cells have specific tumour-recognizing capacity against GD3. Moreover they indicated that in the other types of cancers like neuroblastoma or melanoma, GD2 is overexpressed and stimulates a local oligoclonal B cell response against this antigen.

Another example of the apoptotic induction of protein relocation resulting in 'neo' antigen recognition by B cells can be seen in the autoimmune disorder primary biliary cirrhosis (PBC). Patients with this disorder are characterized by the presence of high levels of auto-antibodies specific for several components of inner mitochondria membrane proteins. Interestingly, one of these auto-antigens, pyruvate dehydogenase complex (PDC) was shown to be redistributed to the cell surface upon apoptotic induction (Robe et al., 2005) (Jones et al., 2002). Following this relocation, it is therefore possible that the PDC specific auto-reactive B cells can bind, internalize and present this normally intracellular antigen to activate auto-reactive, PDC specific CD4+ T cells and initiate disease.

All together these findings imply that several distinct intracellular proteins such as actin, gangliosides and PDC, can become targets for B cell recognition following relocation induced by apoptosis.

1.5. Changes in intracellular protein organization during apoptosis

1.5.1. Apoptosis as a type of cell death

Apoptosis is a physiological, gene-directed form of cell death causing controlled cell proliferation in several biological conditions and maintenance of tissue homeostasis. It plays a crucial role in modulating tissue growth during embryonic development and cell turnover in adult life. Moreover, apoptosis plays an important role in the immune system and represents a highly efficient mechanism for the destruction of infected cells as well as removing excess lymphocytes both during immune cell development as well as a way of controlling lymphocytes life span following immune responses. Programmed cell death was first described in 1972 by Currie, Kerr and Wyllie. The term was used to describe a common type of programmed cell death that the authors repeatedly observed in various tissues and cell types. The authors noticed that these dying cells shared many morphological features, which were distinct from the features observed in cells undergoing pathological, necrotic cell death. Unregulated necrotic cell death is the result of sudden, massive destruction of organelles such as mitochondria or lysosomes. According to Savill et al., (Savill et al., 2003) a crucial feature of necrosis *in vivo* is that dying cells disintegrate and release cell contents before the debris is ingested by phagocytes. Moreover, necrosis is difficult to prevent, whereas the apoptotic pathway can potentially be modulated to maintain cell viability. These two processes are temporally dislocated and represent two extremes of a continuum: the necrosis process can start only and exclusively when the cell dies and is an irreversible process, a 'no return' way in the cell life, while apoptosis is a 'special' form of cell death with the characteristics of an active process. On the other hand, mild perturbation of different cellular compartments can trigger a coordinated sequence of biochemical events. The culmination of this process is apoptotic cellular demise that is regulated at the organellar or cellular levels. Characteristic features of apoptosis mostly concern: cell shrinkage, chromatin condensation, nucleosomal DNA degradation and fragmentation of the cell into 'apoptotic bodies' (Gozuacik and Kimchi, 2004) which are phagocytosed by neighbour cells.

This chapter has documented many recent findings that the consensus on apoptotic cell death largely result in immunosupression appears no longer valid. Indeed, in the study of anti-tumour immunity the certain cytotoxic agents may have been shown to induce immunostimulatory apoptosis. A key feature of this apoptotic immnunoactivation is intracellular protein relocation to the cell surface from dying cells resulted in effector cells

stimulation. Therefore, understanding how proteins from different cellular compartments are reorganized during apoptosis is of considerable importance. In this way, cellular components might reflect novel markers either as a signal for phagocytosis or for the induction of immune recognition. Moreover, each organelle can sense a stressful and pathogenic alteration, which either leads to adaptation or reaches a critical threshold of damage.

1.5.2. The major pathways of apoptosis

The initiation of apoptosis in mammalian cells is broadly divisible into two separate pathways (Putcha et al., 2002). One pathway known as the intrinsic pathway is initiated by several stimuli, including cell-cycle or metabolic perturbations, oxidative stress, DNA damage or the lack of growth-factor signalling, treatment with corticosteroids or staurosporine. This causes the induction of apoptotic protease activating factor 1 (Apaf-1), cytochrome c and activated proteolytic enzymes termed caspases which are the core of the apoptotic machinery caspases. In particular caspases-9 plays a pivotal role in the intrinsic pathway. Currently, about 14 caspases have been identified and they are synthesized as inactive zymogens containing a pro-domain, a p20 large domain and a p10 small domain (Lamkanfi et al., 2007). These zymogens can be cleaved to their active form following the induction of apoptosis. A characteristic feature of caspases is substrate cleavage at the C-terminal region.

Most physiological cell death in mammals occurs through apoptosis, mainly proceeding via the intrinsic mitochondrial pathway. The metabolic consequences of mitochondrial outer membrane permeabilization (MOMP), as well as the leakage of apoptotic factors normally confined to mitochondria determine the catabolic features of cell death. Regulation of the mitochondrial apoptotic pathway is mainly controlled by B cell lymphoma-2 (Bcl-2) family members located within mitochondria, ER and nucleus (Patel et al., 2009). All isolated Bcl-2 family members (about 20 proteins in mammals) are characterised by one of the four relatively conserved Bcl-2 Homology Domains (BH). Some of the family members (including Bcl-2 and Bcl-X_L) are apoptosis-inhibitory proteins, others (such as Bax, Bad, and Bid) are promoters of apoptosis. Normally, Bax and Bak reside in the cytosol, however upon receipt of the apoptotic signal, these proteins migrate and bind to the mitochondrial membrane in the place called 'permeability transition pore'. This state induces loss of selective ion permeability. The loss of mitochondrial membrane integrity and permeability is the result of releasing many proteins from lumen of mitochondria for example: cytochrome c, Smac/DIABLO (second mitochondrial activator of caspases), HtrA2/Omi (high-temperature requirement serine protease A2),

adenylate kinase 2, AIF (apoptosis-inducing factor), pro-caspases-2, -3, and 9. The consequences of this process are the loss of mitochondrial functions essential for cell survival (Ferri and Kroemer, 2001a). As a result of the membrane changes, there is release into the cytosol of the contents of the intermembrane space, including cytochrome c and AIF. AIF moves directly to the nucleus, where it produces chromatin condensation and nuclear fragmentation. Cytochrome c is the only known activator of the cytoplasmic protein Apaf-1 but binding to Apaf-1 which is necessary for the subsequent activation of procaspase-9. Caspase-9 activates downstream caspases, including procaspase-3, responsible for the cytological changes (Burz et al., 2009).

The second type of apoptotic pathway (the extrinsic pathway) is initiated by the binding of extracellular ligands (e.g. Fas ligand and granzyme B) to tumour necrosis factor (TNF) family receptors such as Fas that finally activate executor caspases that mediate DNA fragmentation (Duiker et al.). Initial activation of the extrinsic pathway requires Fas-associating death domain (FADD), caspase 8. The link in intrinsic and extrinsic mechanism is carried by a Bcl-2 family member (BID). When BID connects the receptor-initiated (extrinsic) and stress-signal (intrinsic) pathways through caspase-8 cleavage of BID into truncated BID (tBID), then tBID translocates to the mitochondria resulted in the release of cytochrome c and activation of Apaf-1 and caspases (Ashkenazi, 2008). The binding of cytochrome c to Apaf-1 causes Apaf-1 to adopt a more open conformation. This state facilitates the further binding of dATP/ATP, allowing Apaf-1 multimerization and association of pro-caspase-9, thus generating the apoptosome. Activated caspase-9 in turn cleaves caspase-3, causing apoptotic cell death.

1.5.3. Apoptosis regulation at the endoplasmic reticulum

The proper functioning of the ER is crucial for numerous aspects of cell physiology. All eukaryotes react rapidly to ER dysfunction through a set of adaptive pathways know as ER stress (ERS). Although ERS has been implicated in numerous types of pathology, the regulation and execution of ERS-induced apoptosis in mammals is still not completely understood. ERS can be triggered by disparate perturbation in normal ER function, such as the accumulation of unfolded, misfolded or excessive proteins or by Ca^{2+} signaling (Ferri and Kroemer, 2001b). Moreover ER lipid or glycolipid imbalances, or changes in the redox or ionic conditions of the ER lumen can lead to ERS (Ferri and Kroemer, 2001b) (Granville et al., 2001). However, when a stress is so strong or persistent that ER dysfunction cannot be corrected, cells can initiate apoptosis, allowing the regulated destruction of cell rather than cause irreparable damage or a

risk to the organism as a whole. The mechanism by which ER stress is induced, results in the activation of caspases-12. According to Nakagawa et al., caspases-12 null mice and cells are partially resistant to apoptosis induced by ER stress but not by other stimuli (Nakagawa et al., 2000). Caspase-12 is specifically located on the cytoplasmic side of ER. During releasing Ca^{2+} ion stores from the ER caspase-12 is proteolytically activated by m-calpain.

1.5.4. Dynamics of nuclear proteins during apoptosis

One of the biochemical hallmarks of apoptosis is genetic DNA fragmentation and disintegration of nuclear envelope that precede the nuclear breakdown phase. Proteins of the nuclear envelope, which support the nuclear architecture, are directly cleaved by the effector caspases. Disintegration of the lamina proteins is a typical feature for cell death because the structural support of the nucleus depends on an intact lamina structure. The lamin B proteins are cleaved by caspase-3, whereas the lamin A/C proteins are cleaved by caspase-6 (Ruchaud et al., 2002). Moreover, it was suggested that chromatin condensation during apoptosis depends on degradation of lamin A (Ruchaud et al., 2002).

According to Croft et al., 2005 (Croft et al., 2005) the cytoskeletal actin-myosin-based contraction is required for disruption of nuclear integrity during apoptosis. Thus, it is possible that activation of apoptosis affects first the cytoskeleton, which subsequently affects lamina organization and the formation of intra-nuclear structures. This process leads to massive degradation of the lamina and causes nuclear breakdown. Degradation of lamina proteins is not specific for caspase-8-induced apoptosis because the intrinsic pathway also triggers degradation of lamina proteins (Broers and Ramaekers, 2004). Thus, lamina degradation is a crucial event before DNA degradation and nuclear breakdown can take place. It has been shown that cleavage of lamin A by caspase-6 is required for chromatin condensation (Ruchaud et al., 2002). During the nuclear breakdown phase, cleavage of the lamina proteins precedes DNA condensation, which is subsequently fragmented. First the genome is cleaved into 50-300 kbp DNA fragments, which possibly reflects structure of chromatin loops and hexametric loops structures.

1.5.5. Protein relocation upon apoptosis

- **from nuclei:**

In the past decade, there have been considerable improvements in the way of characterization auto-antigens in chronic autoimmune diseases. One of autoimmune disorder is Sjogren's syndrome characterized by the abnormal production of antibodies in the blood that are directed against various tissues of the body. This particular autoimmune illness features inflammation in certain glands of the body as a result of recognition by auto-antibodies of nucleic acid or protein complexes relocated to the cell surface. However the mechanism of intracellular antigens relocation is still unclear. According to McArthur et al., one of the possibilities of distribution auto-antigens to the surface is process of apoptosis induced by TNF-α in the salivary gland cells. They demonstrated that nuclear proteins like SS-A (Ro) and SS-B (La) and cytoplasmatic protein fodrin are translocated to the membrane of apoptotic cells leading in local secretion of auto-antibodies and finally tissue injury (McArthur et al., 2002). Using cell fractionation and immunofluorescence techniques they revealed that at increasing time after TNF-α and cycloheximide treatment these proteins were relocated to the cell surface. These findings have been clearly implicated in salivary gland destruction in Sjogren's syndrome as a potential auto-antigens acting autoantibody production that may allow in better understanding the mechanism of autoimmunity.

- **from cytoplasm:**

During the process of apoptosis, cells lose volume due to cytoplasm 'boiling' and plasma membrane blebbing, and form apoptotic bodies that initially remain surrounded by membranes. This increased membrane usage has to be substituted from internal sources. Recently, it has been indicated that ER and Golgi apparatus are candidates for substituting the membrane loss during the process of particle ingestion. Franz et al. (2007) (Franz et al., 2007) revealed that cells undergoing apoptosis change the glycosylation status of their membrane, for example at the surface exposure of the lectin-binding sites. Furthermore, they demonstrated that after shrinkage apoptotic cells displayed increased levels of ER-resident lipids, proteins and immature glycoproteins. They suspected that immature proteins are translocated via the actin network to the cell surface during the late phase of apoptosis. Particularly, it has been shown that ER-resident chaperon calnexin was observed on the surface of PI impermeable cells after shrinkage induced by UVB in Jurkat cells. Moreover, a small fraction of calnexin was also relocated to the surface of various cells such as mastocytoma cells, murine splenocytes, fibroblast cells and human HeLa cells. The same

observation was made using confocal microscopy. Viable and necrotic cells did not show surface staining for calnexin, while PI negative apoptotic cells exclusively displayed plasma membrane fluorescence. To support this hypothesis Franz et al. (2007) (Franz et al., 2007) used a μHC immunoglobulin heavy chain that in viable cells should be retained in the ER and not reach the cell surface. Using fluorescence microscopy, they verified that vital μHC transfected Ag.8 cells (mouse myeloma) did not show surface exposure of μHC. In contrary, after UV-B irradiation, μHC could be detected at the surface of apoptotic Ag.8 cells.

Franz and coworkers (2007) (Franz et al., 2007) also demonstrated that: glycolipid gangliosid (GM1) and ER-Tracker are redistributed to the plasma membrane in late apoptotic cells. These two lipids are normally located in the ER membrane. The location of GM1 and the ER-Tracker showed that both molecules co-located inside viable cells and at the plasma membrane of apoptotic cells. Furthermore, Franz et al. (2007) (Franz et al., 2007) monitored the relocation of internal membranes to the surface using KDEL receptor-GFP transfected HeLa cells. In viable cells the KDEL receptor was located in ER/cis-Golgi compartment as an integral membrane protein. However, after UVB irradiation when the plasma membrane had started blebbing the ER-membranes and KDEL receptor were relocated to the cell surface. These results clearly show that during apoptosis the ER membrane is transported to the cell surface to replace plasma membrane that is lost during the blebbing process.

- **from ER:**

In order to prior belief, apoptotic cell death can be non-immunogenic. However Tufi et al. revealed that cancer cell lines HeLa and neuroblastoma (SH-SY5Y) treated with anthracyclines can elicit anticancer immune response. They show that anthracyclines lead to the exposure of intra-cellular protein calreticulin on the plasma membrane of dying tumour cells and hence stimulate the recognition and engulfment dying cells by DC or macrophages (Tufi et al., 2008).

CRT was identified in 1974 as a soluble protein from the lumen of the ER which buffers Ca^{2+} level and also participates in the folding of newly synthesised glycoproteins, preventing their aggregation. Interestingly, translocation CRT to the surface occurred only when ER Ca^{2+} level was reduced. These results are in contrast to former study where in colon cancer and fibrosarcoma cell lines low level of ER Ca^{2+} did not play crucial role in the relocation CRT to the cell surface. For example, they indicated that only in anthracyclines-treated SH-SY5Y or HeLa cell lines that overexpressed Reticulon-1C (RTN-1C) or treated with thapsigardin, translocation of CRT to the surface is observed. Both RTN-1C and thapsigardin are involved in the decrease of ER Ca^{2+} level. To regulate Ca2+ level by overexpession RTN-1C they used tetracycline-

inducible model in doxycycline pre-treated SH-SY5Y cells (SH-SY5Y$^{RTN\text{-}1C}$). Interestingly, western blot analysis shows that 24h from anthracycline-treating in SH-SY5Y$^{RTN\text{-}1C}$ the total level of CRT was comparable to SH-SY5Y cell. This observation suggests that ecto-CRT occurrence on the cell surface is due to translocation rather than *de novo* synthesis of CRT. *In situ* immunofluorescence images also revealed ecto-CRT surface staining and partially overlapping with ecto-RTN in non-permeabilized cells. Moreover, inhibition SERCA pomp by thapsigardin was also able to induce CRT relocation to the surface in SH-SY5Y cells. To summarize Tufi et al. suggest that ER Ca^{2+} homeostasis plays a major role in the regulation of CRT exposure, however many aspects are still unclear. For example this manipulation does not induce apoptotic features, suggesting that CRT exposure and apoptosis may be independent processes from each other. There is necessity for further investigation to answer this question.

Also Brusa et al. has found that late stage of apoptosis have the ability to stimulate DC to phagocytosis of cancer cells. They demonstrated that renal carcinoma cells (RCC53), followed UVC irradiation undergo apoptotic changes like extracellular exposure of PS, surface relocation of CRT and releasing of HMGB1 (Brusa et al., 2008). In addition DC, incubated with apoptotic tumour cells, more efficiently cross-present tumour antigen to CTL cells. Surprisingly, UVC treated tumour cells are more likely phagocytised by DC cells than γ-irradiated RCC53 cells. According to Brusa et al. 3.6 J/cm^2 of UVC dose within 4 h cause apoptotic changes in RCC53 cells leading to PS externalization, translocation of CRL from the ER to the cell surface and occurrence of other molecules which are involved in the process of apoptotic cell uptake. Therefore, DC during 20 h incubation with apoptotic tumour cells endocytose them and produce pro-inflammatory cytokines such as TNF-α, IL-1β and IL-6. Furthermore, they show that isolated mRNA from DC, previously pulsed with UVC-treated RCC53 cells, expressed a large number of genes encoding IFN-α, in particular IFNA2, IFNA5 but also genes encoding IL-12. In protein level they also revealed upregulation in expression of costimulatory molecule CD80, CD83 and MHC class I complexes. 28 h later such maturated DC cells present tumour antigens in context MHC class I more efficiently to CD8+ T cells than DC cells loaded with untreated tumour cells. Using degranulation assay they demonstrated that expression of CD107α in CD8+ T cells, following stimulation with DC loaded with apoptotic tumour antigens, significantly increases. This experiment clearly indicates that cytolytic phenotype of T cells was correlated with type of tumour antigen presented by DC (Brusa et al., 2008).

1.6. Aim of the project

As discussed in this chapter, there are various anti-tumour therapies including cytokine therapy, adoptive transfer, chemotherapy and radiotherapy. However, neither of these therapies in general results in complete eradication of tumours and has various side effects. Therefore, this project intended to explore a novel approach of anti-tumour immunotherapy. In particular, this thesis has focused on the hypothesis that following the induction of apoptosis by certain agents, intracellular tumour antigens will be relocated to the cell surface. Importantly, I also hypothesised that antigen-specific B cells would be capable of recognising these relocated antigens and directly activate antigen-specific T cells. Understanding novel mechanisms of tumour antigen recognition by B cells may consequently lead to improved tumour elimination and may find potential implementation in the clinics.

In particular, to test this hypothesis I will attempt to:

1. generate a panel of plasmids encoding a model antigen targeted to various subcellular compartments

2. monitor the surface relocation of this intracellular antigen following treatment with different apoptotic stimuli

3. establish an *in vitro* system to allow the detection of surface re-distributed antigen by antigen-specific B cells and its subsequent presentation to cognate T cells

- 2. Hen egg lysozyme as a model antigen to study antigen recognition -

2.1. Introduction

Previous experiments from several laboratories have demonstrated that proteins can relocate to the cell surface following apoptosis from the mitochondria, the ER and from the cytosol (Lane et al., 2005; McArthur et al., 2002; Obeid et al., 2007b; Panaretakis et al., 2008). A number of these antigens can be termed 'silent' tumour antigens that following apoptosis may become immunogenic and consequently promote anti-tumour immunity. Therefore, we decided to establish an assay to allow the measurement of antigen extraction by B cells from the cell surface of a tumour cell line. These intracellular antigens following apoptotic stimuli should be relocated to the tumour cells surface, extracted and presented to T cells (**Fig. 2.1.**). This novel *in vitro* system of tumour antigen recognition by B cells following apoptosis may allow the understanding of the induction of improved anti-tumour immunity that could eventually be translated into the clinic.

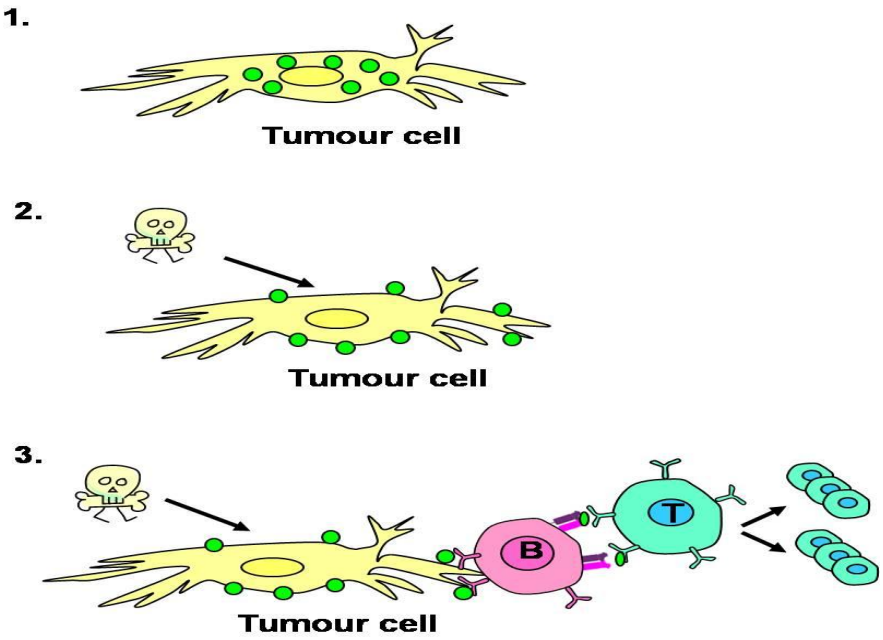

Fig. 2.1. A schematic representation of hypothesis for a novel role of B cells in the induction of anti-tumour immunity. Tumour cell e.g. HeLa cells transfected with intracellular model antigen (1.) undergo apoptotic cell death. This specific type of cell death induces intracellular protein relocation to the surface (2.). B cells can activate T cell-mediated anti-tumour immunity in response to protein relocation from apoptotic tumour cells (3.).

To establish and study protein relocation following apoptosis induction, I decided to use a well defined model antigen - hen egg lysozyme (HEL). HEL is an enzyme with bacteriolytic properties that was first identified and named by Alexander Fleming almost ninety years ago. It is comprised of 129 amino acid residues and its molecular weight is 14.5 kDa.

This antigen has many advantages. Firstly, HEL is a small easy to purify and commercially available soluble protein. The X-ray crystallography of HEL (**Fig. 2.2.**) complexed with several anti-HEL monoclonal antibodies is also well documented. One of these antibodies, HyHEL 10 (Gerwing and Thompson, 1968) (Smith-Gill et al., 1984) can be used to detect HEL expression by immunofluorescence. Additionally, our laboratory has B cells expressing the HyHEL10 antibody as a membrane bound BCR (Smith-Gill et al., 1984). To follow antigen presentation of HEL by these specific-B cells our laboratory also has a panel of HEL-specific T cell hybridomas (Adorini et al., 1993). To this end, T cell hybridomas will be used as a read out of extracted antigen by B cells in this *in vitro* system. Following antigen relocation from various sub-cellular compartments and its subsequent extraction and presentation to HEL-specific CD4+ T cells, it is hoped that this system will allow to understand the role of B cells presenting novel antigen from apoptotic tumour cells.

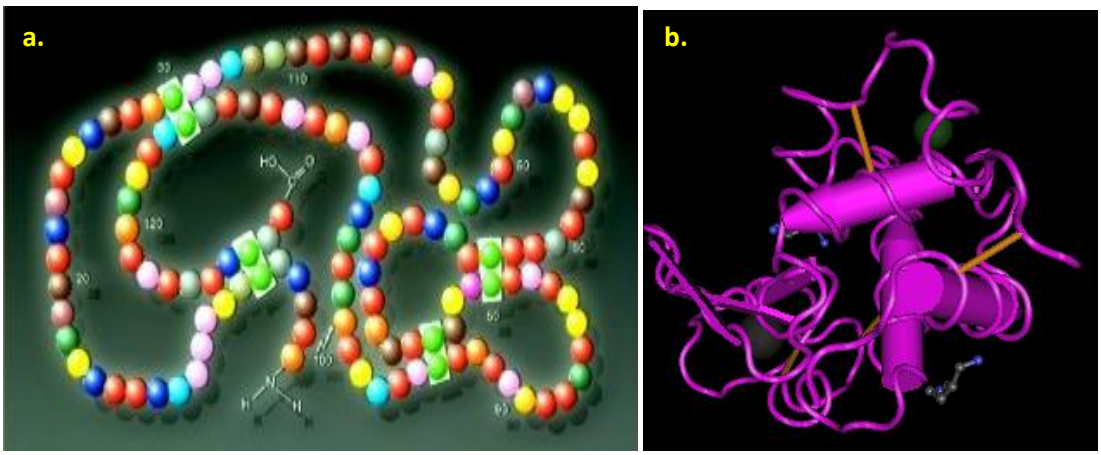

Fig. 2.2. Schematic representation of the structure of HEL (a.) (www.fodras.com). Panel b. shows the X-Ray of 3D structure of HEL with disulphate bonds highlighted on orange http://www.ncbi.nlm.nih.gov/Structure/mmdb/mmdbsrv.cgi?uid=69658.

2.2. Results

2.2.1. Sub-cellular localization of HEL

To localize HEL to a number of discrete sub-cellular compartments, I used a panel of plasmids (**Fig. 2.3.**) received as a kind gift from S. Ostrand-Rosenberg (Qi et al., 2000) and F. Batista (Batista and Neuberger, 2000) (Carrasco and Batista, 2006a).

1. membrane–HEL (**mem-HEL**). This construct encodes a membrane anchored variant of HEL (using the transmembrane domain of the mouse MHC class I molecule, $H2K^b$). The predicted molecular weight of the protein encoded by this construct is 21 kDa.

2. mitochondria-HEL (**mito-HEL**). This construct contains cytochrome c oxidase subunit VIII that is expected to localize HEL within mitochondria. The predicted molecular weight of the protein encoded by this construct is 16 kDa.

3. nucleus-HEL (**nuc-HEL**). This construct contains a triplicate nuclear localization sequence (NLS) from SV40 large T antigen which is expected to direct HEL expression into the nucleus. The predicted molecular weight of the protein encoded by this construct is 19 kDa.

4. cytosol-HEL (**cyto-HEL**). This construct does not contain any targeting sequences and is therefore expected to retain HEL in the cytosol. The predicted molecular weight of the protein encoded by this construct is 15.5 kDa.

Following bi-directional sequencing I transfected HeLa cells (epithelial cell line derived from cervical cancer) (Scherer et al., 1953) with each of the plasmids. I decided to use this type of tumour cells for two reasons. Firstly, HeLa cells are relatively easy to transfect by liposome compounds for the delivery of exogenous nucleic acids commonly used in laboratories. In particular, using Lipofectamine 2000™ (Invitrogen) transfection agent, HeLa cells could be transfected into 70-90%, according to the manufacturer's protocols. Secondly, these adherent cells have a typical mammalian cell morphology which allows easy visualization of sub-cellular compartments. Also, HeLa cells are very easy to maintain in culture.

Initially, I optimised conditions for the most efficient transfection. Then, I tested various time points of plasmid expression between 24 h and 72 h and I also examined different amounts of DNA used during transfection procedure ranging between 0.2 μg to 2 μg of DNA (data not shown). Optimal HeLa transfection was shown to be using 1 μg of DNA with protein expression

being measured 24 h following transfection. Furthermore, transfection efficiency was routinely 60 – 70% using Lipofectamine 2000.

The expression pattern of HEL was characterised with either the HyHEL 10 monoclonal antibody or a polyclonal anti-HEL antibody using a combination of immunofluorescence microscopy and laser scanning microscopy (LSM). To confirm the correct localisation of nuc-HEL, mito-HEL and cyto-HEL expression, the HeLa transfectants were co-stained with antibodies/reagents specific for the appropriate sub-cellular compartments. In particular, I used Hoechst, which binds to nuclei and the mitochondrial-specific dye MitoTracker Red. In addition, I also co-transfected control plasmids expressing either green fluorescent protein (GFP) in mitochondria (mito-GFP) or enhanced green fluorescent protein (EGFP) in the cytosol (cyto-EGFP). As these vectors also contain sequences encoding an additional 10 amino acid c-Myc tag, protein expression was also detected either by polyclonal anti-HEL antibody or by anti-c-Myc (9E10) antibody using Western blotting. (Note: plasmid encoding mem-HEL did not contain c-Myc epitope and expression was detected only with a polyclonal anti-HEL antibody).

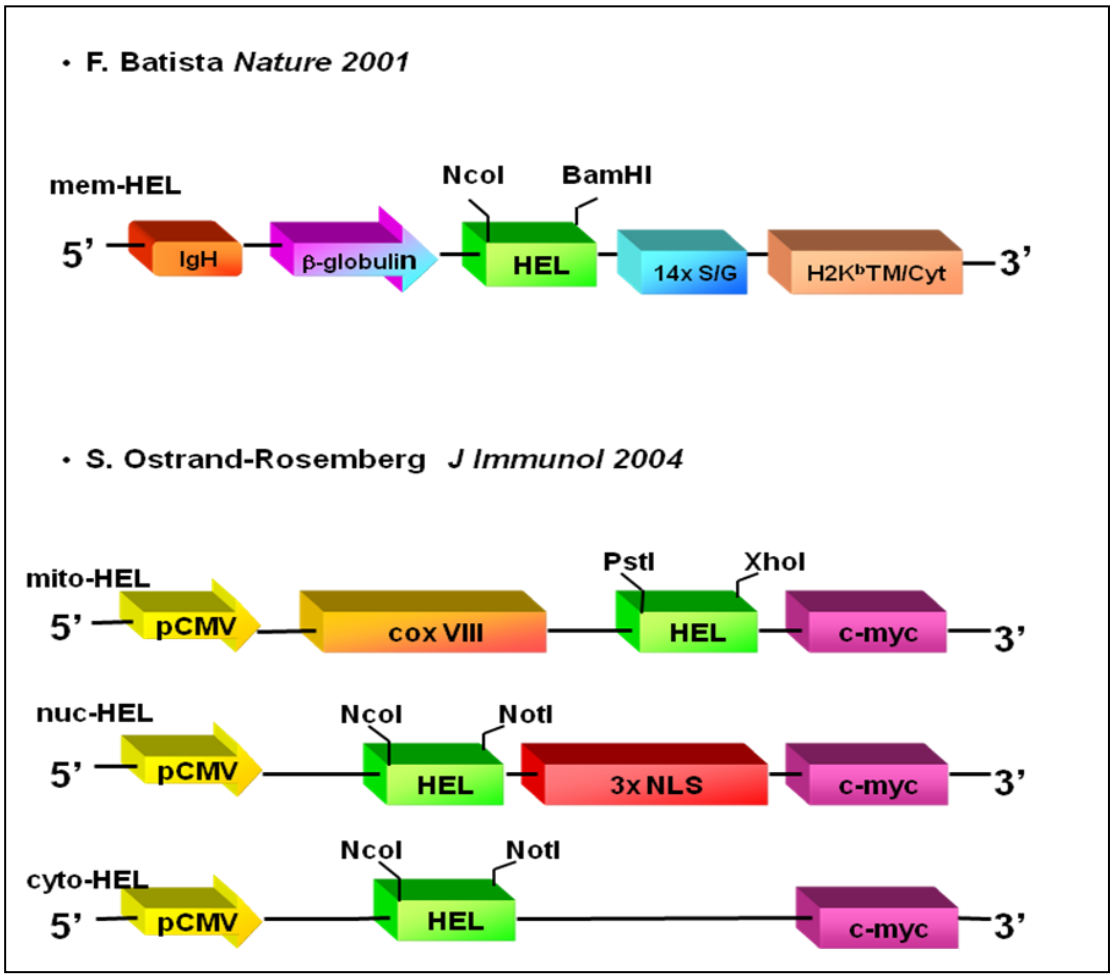

Fig. 2.3. A schematic representation of the panel of HEL cDNA constructs used in this study.

2.2.2. Mem-HEL expression

Initially, to confirm correct mem-HEL expression in HeLa transfectants, I performed Western blotting. **Fig. 2.4.** shows that the lysates from mem-HEL transfectants contain a protein which is reactive with a polyclonal anti-HEL antibody of the expected molecular weight (21kDa).

Furthermore, as this plasmid represents a control for HEL expression on the cell surface my first aim was to confirm surface detection using fluorescence and confocal microscopy (**Fig. 2.5.**). Following transfection, HeLa cells were stained with HyHEL 10 (anti-HEL) primary antibody and then an anti-mouse FITC labelled secondary antibody. After fixation, cells were either stained directly (**Fig. 2.5.**, **Fig. 2.6.**) or permeabilized prior to staining (**Fig. 2.7.**). Direct staining with primary and secondary antibodies without permeabilization prevented intracellular binding of HEL and surface staining was able to be distinguished from intracellular staining (**Fig. 2.5.**). Using confocal microscopy single cells were also analysed in both vertical and horizontal planes to produce images such as those shown in **Fig. 2.5. panel c**., where the expression of HEL can be clearly seen as a circle around the edge of cell. Furthermore, results from immunofluorescence microscopy also revealed membrane staining as a diffused fluorescence without any discrete intracellular staining. When the transfectants were permeabilized prior to staining, both a diffused pattern and accumulation of HEL surrounding the nuclei was observed consistent with normal protein synthesis and exit from the ER (**Fig. 2.7.**).

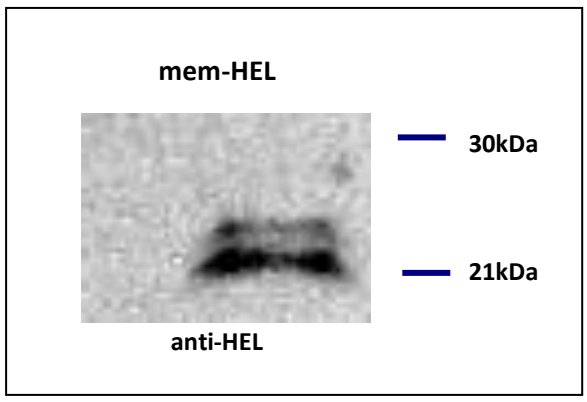

Fig. 2.4. Western blot analysis of transiently transfected mem-HEL HeLa cells. Lysates form 0.8x10^{5}cells per lane were separated on 14 % gel and following transfer were stained with primary anti-HEL and anti-rabbit-HRP. Numbers to the right represent the migration of standard molecular weight markers (kDa) (ProSieve). The western blot analysis is representative of 2 separate experiments.

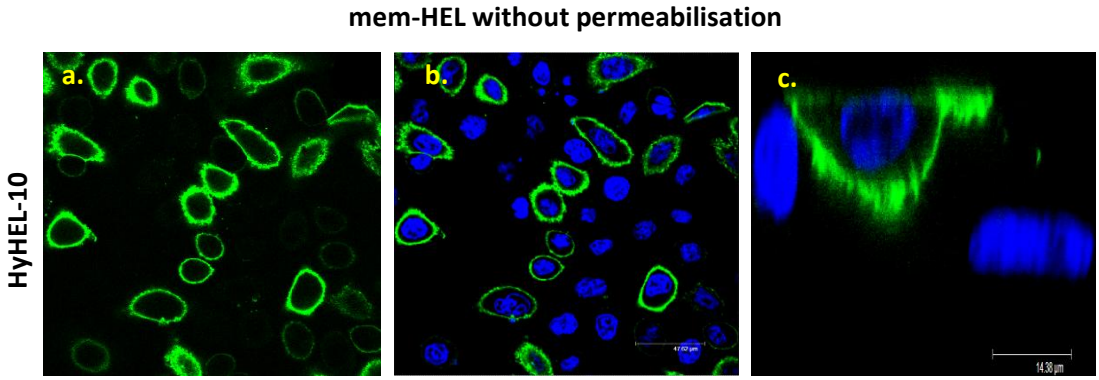

Fig. 2.5. Immunofluorescence analysis of mem-HEL expression in transiently transfected HeLa using confocal microscopy. After fixation cells were stained with anti-HEL mouse primary antibody (HyHEL 10) and anti-mouse-FITC (panel a., b., c.). Panel b. and c. show cells incubated with Hoechst 33342 dye to visualise nuclear staining. Panel c. shows a 3D projection of single HeLa cell which was sectioned in vertical and horizontal plane to directly visualise cell membrane. The images are representative of 6 separate experiments.

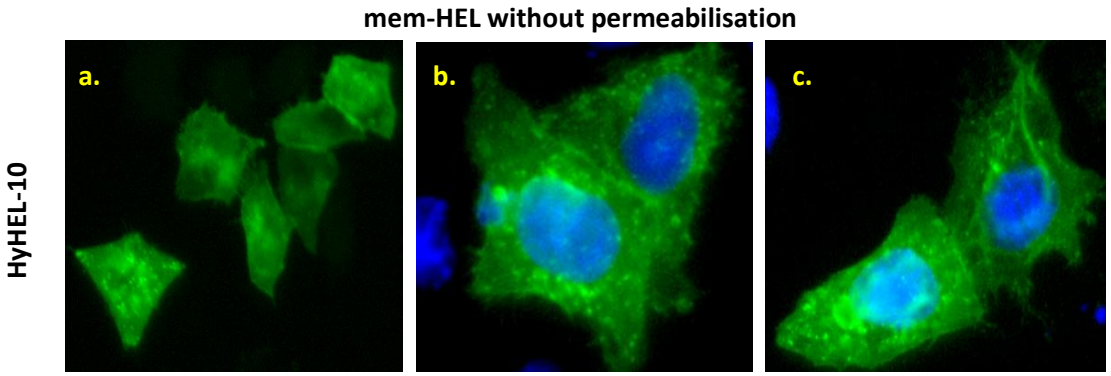

Fig. 2.6. Immunofluorescence analysis of mem-HEL expression in transiently transfected HeLa using fluorescence microscopy. After fixation cells were stained with anti-HEL mouse primary antibody (HyHEL 10) and anti-mouse-FITC (panel a.). Then cells were incubated with Hoechst 33342 dye (panel b. and c.) to visualise nuclei. The images are representative of 6 separate experiments.

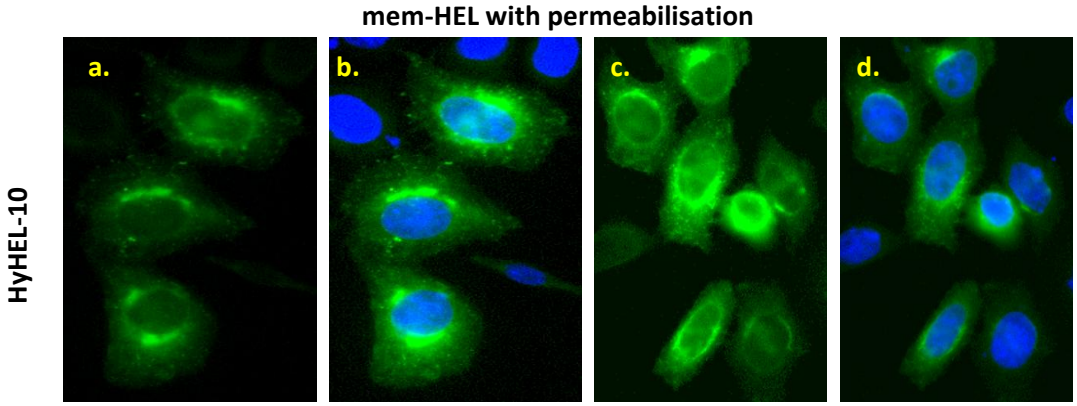

Fig. 2.7. Immunofluorescence analysis of mem-HEL expression in transiently transfected HeLa using fluorescence microscopy. After fixation and permeabilisation cells were stained with anti-HEL mouse primary antibody (HyHEL 10) and anti-mouse-FITC (panel a. and c.). Panel b. and d. are representation of the same images from panel a. and c. respectively, but additionally including nuclei visualised by Hoechst 33342 dye. The images are representative of 6 separate experiments.

2.2.3. Mito-HEL expression

The first plasmid designed to target intracellular antigen localisation contained a mitochondrial targeting sequence (mito-HEL). As previously, HeLa transfectants were analysed using a combination of Western blotting and fluorescence/confocal microscopy. Lysates from transfectants were separasted on SDS-PAGE gels and transferred to nitrocellulose. As the mito-HEL plasmid contains the c-Myc tag, following transfer the membranes were incubated with the anti-c-Myc monoclonal antibody 9E10. In **Fig. 2.8.**, it can be seen that 9E10 antibody recognises endogenous c-Myc seen in lysates from both untransfected and as well HeLa transfectants (upper band on the level of 32 kDa) (Ferre et al., 1986). In addition, it can be seen a band of approximately 16 kDa, that is consistent with the expected size of mito-HEL that also contains a c-Myc epitope.

Furthermore, to establish that the mito-HEL plasmid was targeting HEL to the correct sub-cellular compartment, I analysed transfectants using fluorescence and confocal microscopy. To identify mitochondrial staining, I co-transfected the cells with a control plasmid: mito-GFP (pShooter commercial plasmid from Invitrogen) and also incubated them with a mitochondrial specific dye MitoTracker Red. This dye passively diffuses across the plasma membrane and accumulates in the active mitochondria (**see Material and Methods**). Importantly, MitoTracker contains a mildly thiol-reactive chloromethyl moiety that maintains the dye associated with the mitochondria following fixation. Indeed, in **Fig. 2.9.** it can be clearly seen that the mito-GFP expression and the MitoTracker Red staining overlap and localise to many punctuate vesicles surrounding the nuclei. Furthermore, it was also confirmed using colocalisation analysis software that these two staining patterns show significant overlap (data not shown). These initial findings allowed the subsequent analysis of mito-HEL localisation to be examined. When I transfected HeLa cells with the pCMV-mito-HEL construct, punctuate vesicles surrounding the nuclei were also observed following staining with the HyHEL 10 antibody (**Fig. 2.10.**). However, this staining pattern was identical neither to that seen in cells transfected with the mito-GFP construct nor to these labelled with MitoTrackerRed. Therefore, I co-transfected HeLa cells with mito-HEL and mito-GFP to analyse colocalization. **Fig. 2.11. panel b.** (colocalisation chart) represents dual colour analysis of mito-GFP and mito-HEL expression that indicates that HEL and GFP proteins did not colocalise. It can be seen that both green and red fluorochromes are still distinct. If colocalisation was observed, orange should be seen in the middle of chart due to overlay red (mito-HEL) and green (mito-GFP) fluorochromes. Based on this and the data illustrated in **Fig. 2.11.**, it appears that mito-HEL was not expressed in mitochondria.

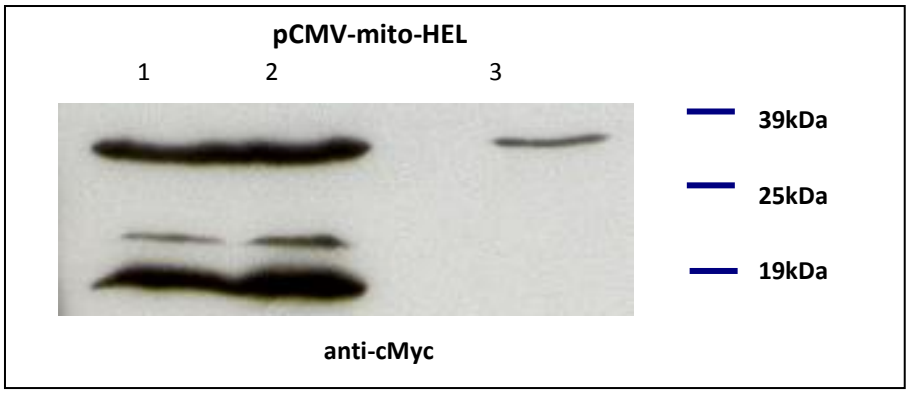

Fig. 2.8. Western blot analysis of transiently transfected mito-HEL HeLa cells. Cells lysates from different numbers of mito-HEL HeLa transfectants (lane 1: $1.6x10^5$ of cells, lane 2: $3.2x10^5$ of cells and lane 3: $0.8x10^5$ of untransfected cells) were separated on 14 % SDS-PAGE gel and following transfer were stained with primary anti-cMyc (mouse 9E10) antibody and anti-mouse-HRP. Numbers to the right represent the migration of standard molecular weight markers (kDa) (ProSieve). The western blot analysis is representative of 2 separate experiments.

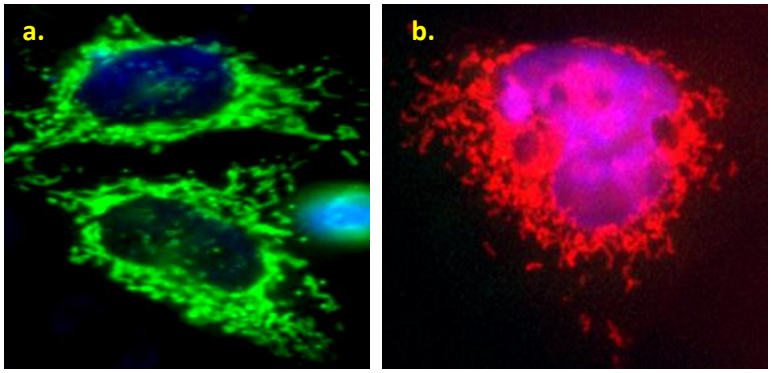

Fig. 2.9. Fluorescence microscopy of HeLa cells transiently transfected with mito-GFP (panel a.). Panel b. represents HeLa cells stained with MitoTracker Red to visualise mitochondria. Additionally, both panels show Hoechst nuclear staining (blue). The images are representative of 6 separate experiments.

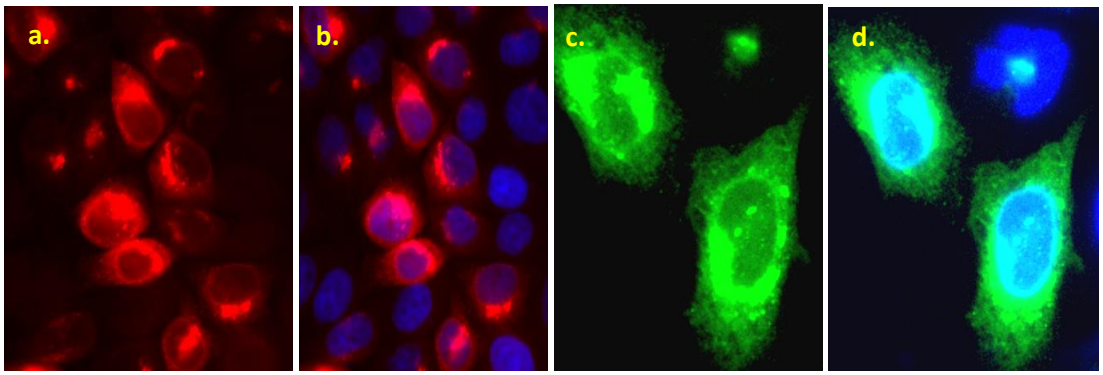

Fig. 2.10. Fluorescence microscopy of HeLa cells transiently transfected with mito-HEL (panel a., b., c. and d.) to visualise mitochondria. Additionally, panel b. and d. show Hoechst nuclear staining (blue). These experiments used anti-HEL mouse antibody (HyHEL 10) and anti-mouse conjugated with TRITC (panel a. and b.) or FITC (panel c. and d). The images are representative of 6 separate experiments.

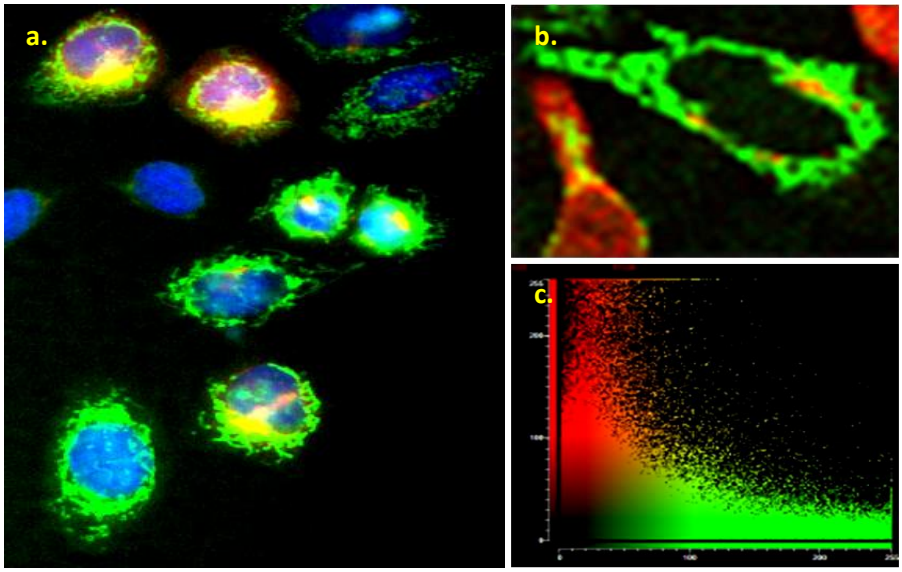

Fig. 2.11. Transient co-transfection of HeLa cells with mito-HEL (red) and mito-GFP (green). Panel a. represents images captured from fluorescence microscopy, while panel b. represents images using confocal microscopy. Panel c. is a colocalization chart demonstrating the intensities of measured red (mito-HEL) and green (mito-GFP) pixels (on the y and x axes respectively) corresponding to the randomly selected field of 2 individual HeLa cells shown in panel b. Cells were stained with anti-HEL antibodies (HyHEL 10) and secondary anti-mouse-TRITC and Hoechst (blue). The images are representative of 6 separate experiments.

2.2.4. Mito-GFP-HEL expression

Consequently, as mito-HEL did not appear to localise to mitochondria, I constructed a new plasmid. This construct (mito-GFP-HEL) was engineered as a fusion protein to express both HEL and GFP in mitochondria. Having N'terminal inserted GFP as a marker of expression it was easy to detect whether the fusion protein is correctly translated and directed into mitochondria.

Dual colour analysis from confocal microscopy shows (**Fig. 2.12. panel b.**) that the pattern of GFP expression was similar to that seen with mito-GFP construct (**Fig. 2.9. panel a. and b.**). However, this figure also shows (**Fig. 2.12. panel c.**) that no HEL expression can be detected by the HyHEL10 antibody. Thus, it appears that the failure to detect HEL in the mitochondria maybe as a result of incorrect HEL folding/structure. To test that this fusion construct is synthesised, I also examined lysates from mito-GFP-HEL transfectants. Protein extracts from transfectants were run on gels and transferred to nitrocellulose and probed with anti-c-Myc, anti-HEL and anti-GFP antibodies (**Fig. 2.13. panel a. and b.**). This confirmed that both anti-HEL antibodies as well as the C-terminal c-Myc tag antibody 9E10 were not reactive with this HEL fusion protein.

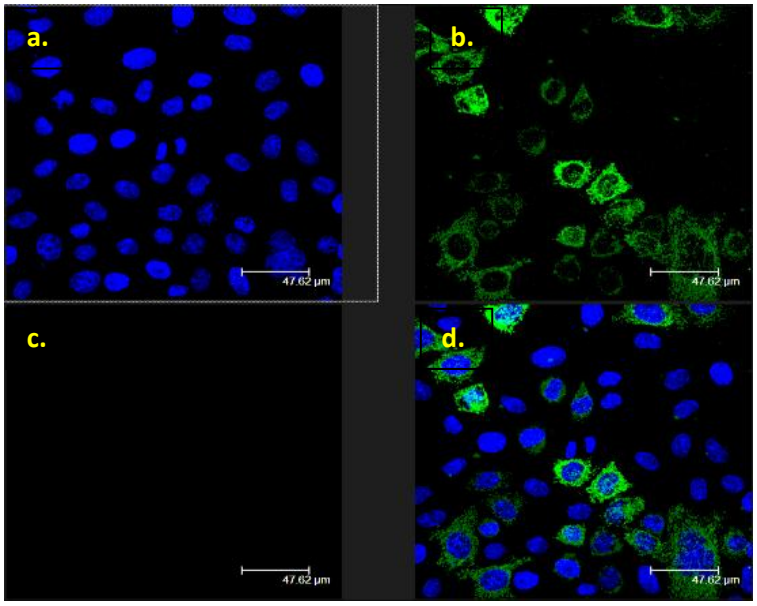

Fig. 2.12. Visualisation of mitochondria in transiently transfected mito-GFP-HEL HeLa cells performed using confocal microscopy. In these experiments were used anti-HEL mouse antibody (HyHEL 10) and anti-mouse conjugated with TRITC (panel c.). Panel a. shows Hoechst nuclear staining, panel b. indicates GFP expression and panel d. represents overlap image from these three colours. The images are representative of 6 separate experiments.

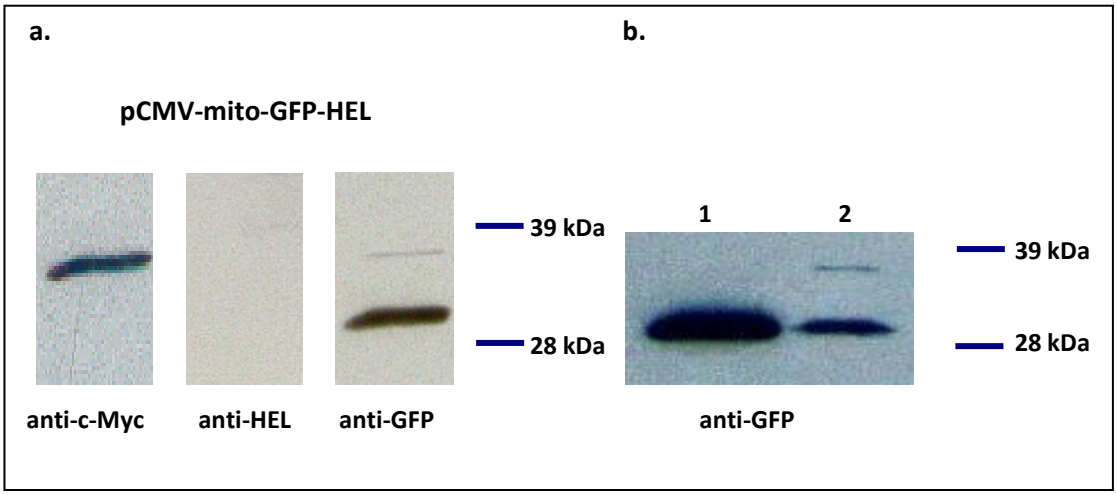

Fig. 2.13. Western blot analysis of transiently transfected (a.: pCMV-mito-GFP-HEL and b.: pCMV-mito-GFP (lane 1), mito-GFP-HEL (lane 2)) HeLa cells. Cell lysates from 0.8x10^5 cells were separated on 14% SDS-PAGE gel and following transfer were stained with primary (a.) anti-c-Myc (mouse 9E10), anti-HEL and rabbit anti-GFP antibodies (followed by secondary anti-mouse-HRP, anti-rabbit-HRP, anti-rabbit-HRR respectively), (b.) with primary anti-GFP (rabbit) antibody and secondary anti-rabbit-HRP. Numbers to the right represent the migration of standard molecular weight markers (kDa) (ProSieve). The western blot analysis is representative of 2 separate experiments.

2.2.5. Nuc-HEL expression

To characterise the expression of the nuc-HEL construct, I performed Western blotting with lysates from pCMV-nuc-HEL transiently transfected HeLa cells following separation on SDS-PAGE and transfer to nitrocellulose membrane. Using either anti-c-Myc or anti-HEL antibodies to detect HEL expression, it can be seen in **Fig. 2.14. panel a.** and **b.** that bands of the predicted molecular weight (19 kDa) were detected.

As before, immunofluorescence analysis was used to visualise the expression pattern of HeLa cells transfected with nuc-HEL. HEL was visualised using HyHEL10 and anti-mouse-FITC antibodies. Immunofluorescence microscopy indicated that the pattern of nuc-HEL expression was heterogeneous (**Fig. 2.15. panel a.** and **b.**). It can be seen that HEL expression demonstrated either strong inter-nuclear staining (red arrows) or an atypical peri-nuclear pattern (blue arrows).

To formally assess whether nuc-HEL expression is directed into the nucleus I performed co-localisation studies with the DNA staining dye Hoechst using confocal microscopy. As can be seen in **Fig. 2.15. panel c.**, the dual colour analysis chart generated from nuc-HEL transfectants shows that even though there is some co-localisation between Hoechst and nuc-HEL, the vast majority of nuc-HEL is localised extra-nuclear.

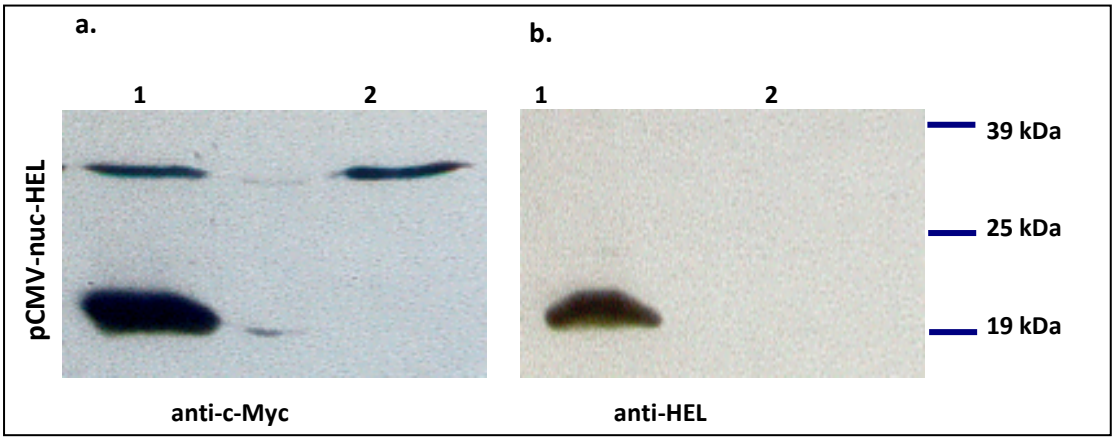

Fig. 2.14. Western blot analysis of transiently transfected nuc-HEL HeLa cells. Cell lysates from $0.8x10^5$ cells (lane 1: HeLa cells transfected with nuc-HEL and lane 2: untransfected HeLa cells) were separated on 14% gel and following transfer were stained with (a.) primary anti-c-Myc (mouse 9E10), and (b.) anti-HEL antibody (followed by secondary anti-mouse-HRP and anti-rabbit-HRP antibodies respectively). Numbers to the right represent the migration of standard molecular weight markers (kDa) (ProSieve). The western blot analysis is representative of 2 separate experiments.

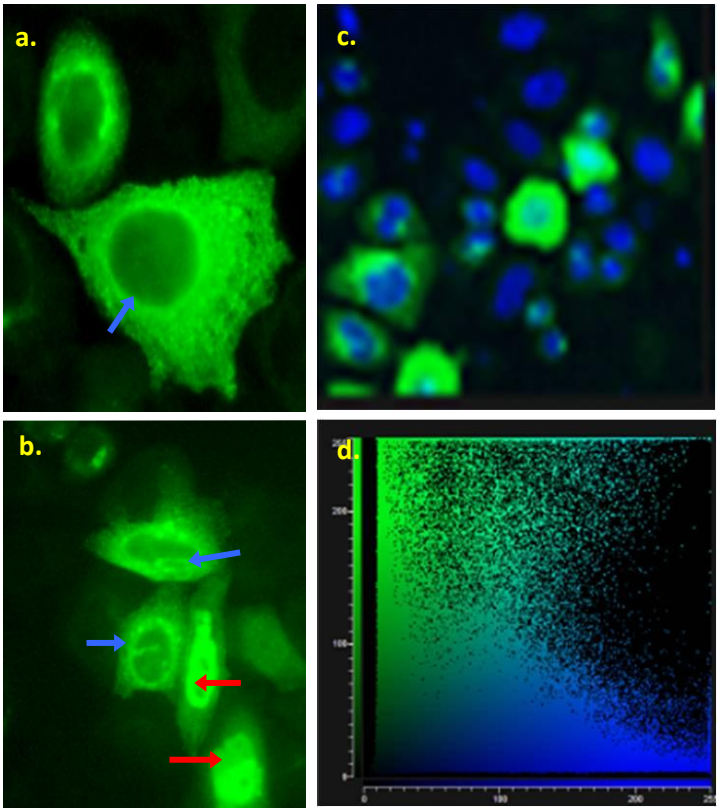

Fig. 2.15. Fluorescence (panel a., b.) and confocal microscopy analysis (panel c.) of HeLa cells transiently transfected with mito-GFP-HEL (all panel) to visualise nuclei. Red arrow represents inter-nuclear staining, blue arrows indicate an atypical peri-nuclear pattern of nuc-HEL expression. In these experiments were used anti-HEL mouse antibody (HyHEL 10) and anti-mouse conjugated with FITC (all panel). Panel c. represents overlap image from Hoechst staining (blue) and nuc-HEL. Panel d. is a colocalization chart demonstrating the intensities of measured green (nuc-HEL) and blue (Hoechst) pixels (on the y and x axes respectively) corresponding to the randomly selected field of 20 individual HeLa cells shown in panel c. The images are representative of 6 separate experiments.

2.2.6. Cyto-HEL expression

I also analysed HEL expression targeted to the cytosol. To this end, I have transfected a positive control cyto-EGFP plasmid (Clontech) to visualise the green cytoplasm. In **Fig. 2.16. panel a.**, cyto-GFP expression can be seen as an evenly diffused pattern of fluorescence with a slightly stronger distribution in the nucleus. To analyse the expression of cyto-HEL, I therefore either compared the expression pattern of cyto-HEL to that of cyto-EGFP (**Fig. 2.16. panel b.** and **c.**) in co-transfected HeLa cells. In **Fig. 2.16. panel b.**, clearly shows that the expression cyto-HEL was different to that seen with cyto-EGFP. The dual colour analysis chart generated from co-transfectants confirmed this diversion (**Fig. 2.16. panel c.**).

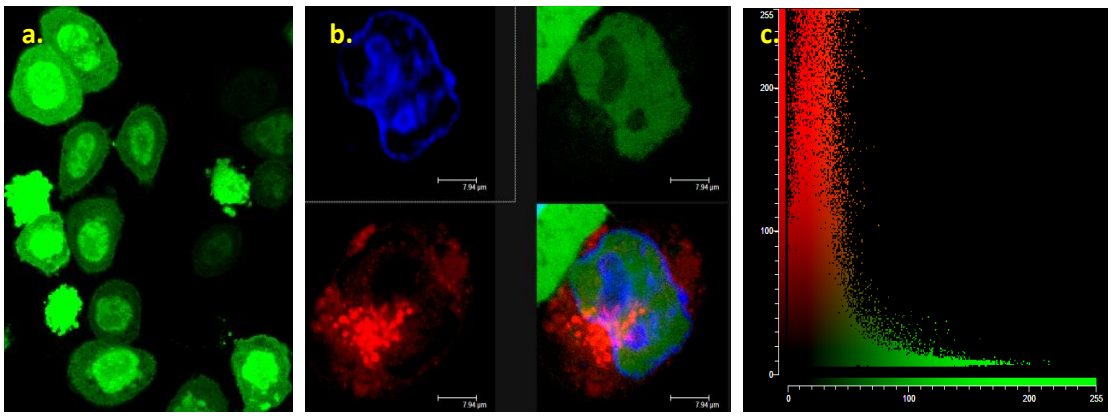

Fig. 2.16. Confocal microscopy analysis representing the expression pattern of cyto-EGFP HeLa transfectants. HeLa cells were transfected by cyto-EGFP plasmid (panel a.). Panel b. shows the transiently co-transfected HeLa cells with cyto-HEL (red) and cyto-EGFP (green). Cells were stained with anti-HEL antibodies (HyHEL10) and secondary anti-mouse-TRITC and nuclei were stained by Hoechst 33342 (5 μg/ml). Panel c. is a colocalization chart demonstrating the intensities of measured red (cyto-HEL) and green (cyto-GFP) pixels (on the y and x axes respectively) corresponding to the randomly selected field of one individual HeLa cell shown in panel b. The images are representative of 6 separate experiments.

2.2.7. New constructs to target HEL to various sub-cellular compartments

It is therefore clear that the constructs that I have used to target HEL either to the mitochondria, cytosol or nucleus do not lead to the correct localisation. This was not expected as these constructs were recently shown to correctly target HEL in transfected Sal/A^k cells (Qi et al., 2000) . Upon re-examination of the sequences contained in these plasmids, we observed that the HEL signal sequence was still present. It is therefore possible that this sequence may interfere with additional sub-cellular localisation sequence in HeLa cells.

Consequently, I designed new constructs lacking the HEL signal sequence to target HEL to either the mitochondria (mito-HEL(-SS) data not shown) or to the cytosol (cyto-HEL(-SS)).
These constructs were generated using PCR (**Materials and Methods**). Following restriction enzyme digestion (**Fig. 2.17.**) and sequencing cyto-HEL(-SS) construct was transiently transfected into HeLa cells.

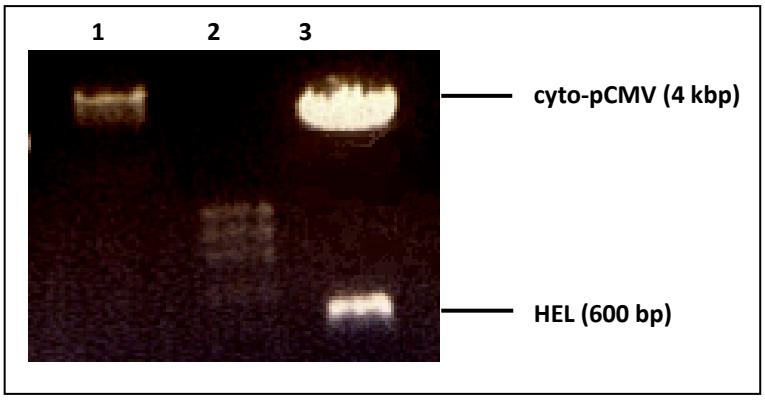

Fig. 2.17. DNA gel analysis (lane 1: λ–marker, lane 2. ϕX174NoeIII-size marker, lane 3 cyto-HEL). Digestion of 2μg cyto-HEL cloned to pShooter vector (cyto-pCMV) by *NcoI* and *NotI* restriction enzymes. This DNA gel analysis is representation of 1 experiment.

Transfectants were analysed by Western blotting. It can be clearly seen in both **Fig. 2.18.**, **panels a.** and **b.** that HEL expression was not observed in cells transfected with cyto-HEL(-SS) (lane 2), in contrast to previously tested cyto-HEL construct that apparently expresses HEL (lane 3) but with incorrect localisation.

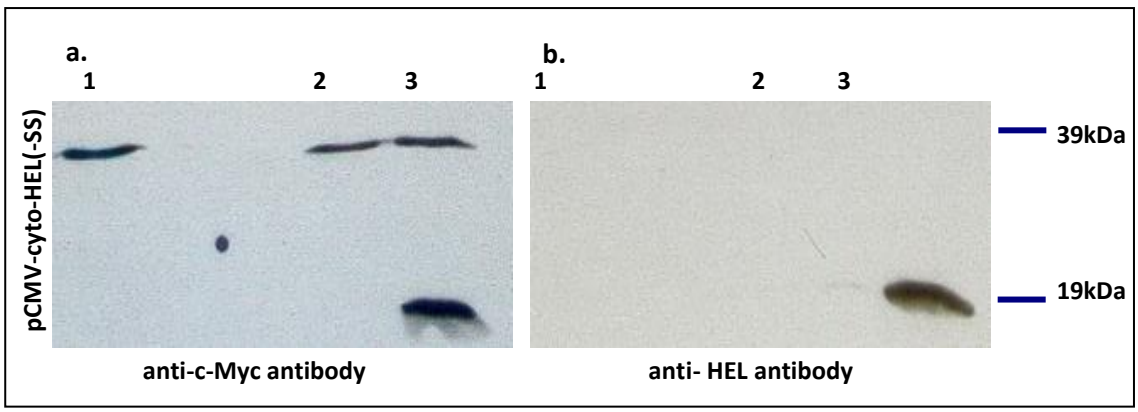

Fig. 2.18. Western blot analysis of transiently transfected (lane 1: lysates from untransfected HeLa cells, lane 2: lysates of new cyto-HEL(-SS), lane 3: lysates from cyto-HEL HeLa cells. Cell lysates from $0.8x10^5$ cells were separated on 14% gel and following transfer were stained with primary anti-cMyc (mouse 9E10) antibody and anti-mouse-HRP (a.), primary anti-HEL antibody and anti-rabbit-HRP (b.). Numbers to the right represent the migration of standard molecular weight markers (kDa) (ProSieve). The western blot analysis is representative of 1 separate experiment.

2.3. Discussion

In this chapter, I have attempted to express HEL in various sub-cellular compartments of HeLa cells to allow me to study the localisation of this model antigen following apoptotic-induced relocation. Western blotting analysis confirmed that the plasmid encoding mem-HEL produced protein of the correct molecular weight in HeLa cells (**Fig. 2.4.**). In addition, immunofluorescence analysis of non-permeabilized HeLa cells also revealed as expected that this protein was expressed on the cell surface (**Fig. 2.5**.).

Whilst using the pShooter-based constructs from Dr. S. Ostrand-Rosenberg to target HEL to the mitochondria (**Fig. 2.10**), nucleus (**Fig. 2.15.**) and cytosol (**Fig. 2.16., panel b.**), led to the expression of proteins of the correct molecular weight, the expected sub-cellular localisations were not observed. This was performed using both fluorescence microscopy and Western blotting. Furthermore, dual colour analysis of both mito-HEL and cyto-HEL transfectants demonstrated atypical localisation. Transfectants expressing the nuc-HEL construct showed a heterogeneous pattern that reflected both atypical, extra-nuclear staining as well as correct nuclear expression. This was not expected as these constructs were recently shown to correctly target HEL in transfected Sal/A^k cells (Qi et al., 2000). Upon re-examination of the sequences contained in these plasmids, we observed that the HEL signal sequence was still present. It is therefore possible that this sequence may interfere with additional sub-cellular localisation sequence in HeLa cells or may even have a dominant effect on the targeting sequence leading to mislocalisation that was observed. This moved me to design new HEL constructs without the signal sequence (**Fig. 2.17.**). Unfortunately, none of the new plasmids lacking the signal sequence (cyto-HEL(-SS) and mito-HEL(-SS)) led to HEL synthesis, even though restriction enzyme digestion, sequencing and PCR confirmed that cDNAs were correct. In addition, I fused HEL with a correctly targeted GFP positive control plasmid (mito-GFP-HEL) which resulted in only GFP expression in the mitochondria (**Fig. 2.12.**).

I speculate that the various sub-cellular conditions, to which I have attempted to target HEL, abrogate proper folding of this protein. This may be due to the presence of four disulphide bonds in the HEL secondary structure (**Fig. 2.2. panel a.**). These disulphide bridges form between the eight cysteine residues and are essential for HEL activity and contribute to its rigidity (Fischer et al., 1993). This fact may explain why the plasmid encoding the fusion protein (mito-GFP-HEL) was expressed only partially. Indeed, **Fig. 2.12.** demonstrates that GFP was synthesised but HEL was not. These findings indicated that posttranslational modification and redox potential of each compartment might abrogate HEL expression and need to be taken

into account when designing future experiments. Therefore, as an alternative to using the HEL antigen for B cell recognition and presentation, we decided to use different model antigen system that should not suffer from the same structural sensitivity as the disulphide bonds of HEL. This new model of antigen, used in further experiments, will be described in **Chapter 3**.

In conclusion:

HeLa cells transfected with a panel of plasmids were examined by Western blotting using anti-HEL or anti-c-Myc antibodies. I tested the transfectants expressed: mem-HEL, nuc-HEL, mito-HEL and cyto-HEL plasmids. In addition, the expression pattern of each plasmid was visualised using a combination of immunofluorescence and confocal microscopy. Plasmids expressing nuc-HEL, mito-HEL and cyto-HEL did not show correct co-localisation when compared to several standard markers (Hoechst and MitoTrackerRed) for each cellular compartment and only the mem-HEL plasmid led to the correct plasma membrane localisation of HEL.

I originally speculated that this atypical localisation of HEL may be caused by the presence of the HEL signal sequence (SS), in each pShooter constructs. For that reason, I generated three constructs that lacked the HEL signal sequence (-SS). Nevertheless, the deletion of the signal sequence from, mito-HEL(-SS), mito-GFP-HEL and cyto-HEL(-SS) plasmids, unexpectedly lead to complete inhibition of HEL expression. I envisage that the presence of a signal sequence allows limited disulphide bound formation within the ER and protein detection.

- 3. EGFP-TTCF as a model antigen -

3.1. Introduction

In the previous chapter, I chose to use hen egg lysozyme (HEL) as a model antigen. However, as documented, the correct intracellular localisation of HEL was problematic, probably resulting from incorrect folding of HEL. Therefore, I decided to use another model antigen tetanus toxin C fragment (TTCF). Our laboratory has previously generated TTCF-specific B cells (Antoniou et al., 2000). These cells will be used to detect the surface antigen expression and its presentation to TTCF-specific T cell hybridomas.

Importantly, TTCF has been well described as a model antigen to study the MHC class II-restricted antigen processing pathway and also frequently used to provide T help determinants in vaccine formulations (Manoury et al., 1998).

Furthermore, TTCF was N' terminal fused to enhanced green fluorescent protein EGFP allowing easy monitoring of EGFP-TTCF (E/T) model antigen. This E/T construct was previously successfully expressed in bacteria by Dr A. Knight (unpublished data). In **Fig. 3.1.**, this model antigen can be seen as a crystal structure of EGFP linked with TTCF. Using the E/T fusion protein as a model antigen has several advantages that will be discussed later in this section. Firstly, fusing EGFP to TTCF will allow the direct visualization of the fusion protein using fluorescence or confocal microscopy due to the natural autofluorescent properties of EGFP.

EGFP is a modified version of the Green Florescent Protein (GFP) originally generated from the jellyfish *Aequorea victoria* (Cormack et al., 1996). EGFP is a one of a series of GFP mutants, which has a shifted excitation peak of 490 nm. Changes in excitation spectra of EGFP result from the replacement of amino acids (64 phenylalanine to leucine and in position 65 is threonine instead of serine that is observed in the original GFP protein).

EGFP is a 27 kDa amino acid monomer which emits green light the maximum emission at 509 nm wavelength when excited by either blue light or UV. Importantly, the β-barrel of EGFP crystal structure is thought to be essential for preserving the chromophore for exposure of oxygen species damaging structure and consequently causing bleaching of EGFP fluorescence. It has been shown that EGFP is a stable fluorescent protein that is resistant to certain denaturating conditions. Surprisingly, Saeed has found that SDS, urea or heat, did not have any significant effect on the fluorescence of EGFP at pH 7.5 or 8.5 (Saeed and Ashraf, 2009). In addition there are many commercially available vectors which target GFP or EGFP to

various intracellular compartments (see control mito-GFP plasmid in **Fig. 2.9. panel a.**) demonstrating that GFP is not sensitive to intracellular variations in redox potential.

Therefore, fusing EGFP with TTCF (E/T) was predicted to allow simple monitoring of antigen relocation to the surface following apoptosis and extraction by readily available TTCF-specific B cells.

Due to EGFP presence as a reporter gene that naturally exhibits bright green fluorescence when exposed to blue light, assessing the expression of desired proteins, in this case TTCF, in microscopy was fast and relatively easy. Noteworthy, this fusion protein E/T was predicted not to suffer from the same structural sensitivity as the disulphide bonded HEL, initially used as a model antigen, as described in **Chapter 2**.

All these advantages suggest that E/T may be a useful model to study antigen extraction and presentation by B cells to specific CD4+ T cells. More importantly, this antigen may be a valuable tool in establishing an *in vitro* assay allowing the generation and monitoring of anti-tumour immunity by B cells.

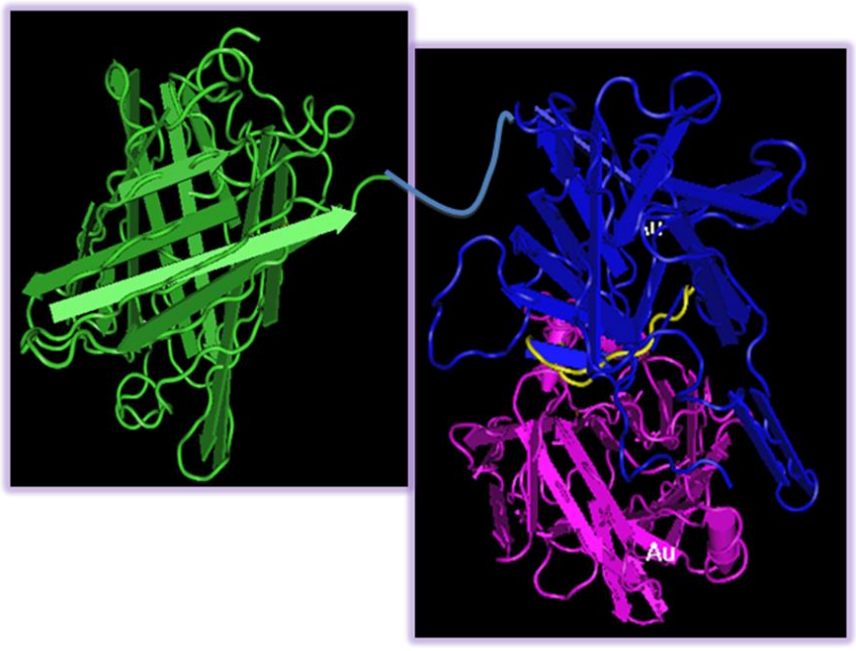

Fig.3.1. A schematic representation of the 3D structure of the fusion protein EGFP-TTCF (E/T). Green represents structure of EGFP fused with TTCF (illustrated by blue and purple colours reflecting two different domains of TTCF). Structure of E/T obtained and adapted from: www.pubmed.com.

3.2. Results

3.2.1. Construction of a model fusion antigen EGFP-TTCF (E/T) for the study of protein relocation from different intracellular compartments

In order to generate a panel of plasmids expressing a model antigen in the desired sub-cellular compartments the first step was to engineer the cDNA sequence of E/T flanked by 5'*PstI* site and 3'*NotI* site. These restriction sites consequently allowed easy cloning of E/T into the expression vector pCMV targeting E/T to different subcellular compartments.
Using 5'EGFP *PstI* as a forward external primer and 3'TTCF *NotI* as a reverse external primer (**Table 2.** blue primers), I analysed the E/T cDNA. This allowed me to generate a blunt-ended PCR product containing *PstI* and *NotI* restriction sites flanking the E/T cDNA.

Table 3. The sequences of primers which have been used to generate and sequencing E/T.

Name of primer	Sequence	Length
5'EGFP Pst1	5'-CTG CAG ATG GTG AGC AAG GGC GAG GAG -3'	27-mer
3'TTCF Not1	5'-GCG GCC GCG TCG TTG GTC CAA CCT TCA TC -3'	29-mer
EGFP Seq 3F 667	5'-CTG AGC ACC CAG TCC GCC CTG-3'	21-mer
TTCF Seq 4F 967	5'-TCT GAA GTT ATC GTG CAC AAG -3'	21-mer
TTCF Seq 5F 1267	5'-TGG GTT TTC ATC ACT ATC ACT -3'	21-mer
TTCF Seq 6F 1567	5'-ATC CCG GTA GCT TCT AGC TCT -3'	21-mer
TTCF Seq 7F 1867	5'-GCT CCG GGT ATC CCG CTG TAC -3'	21-mer

As a template for E/T amplification, I used a previously constructed plasmid pET-16b-EGFP-TTCF (Andrew Knight, unpublished data). This plasmid contains EGFP fused to the N'terminus of TTCF previously reported by Hewitt et al. (Hewitt et al., 1997). This plasmid also allowed bacterial expression and purification (using N-terminal His Tag sequence) of soluble E/T in *E.coli* cells. In **Chapters 4** and **5**, I will discuss further experiments analysing the soluble E/T protein. To amplify the E/T sequence from the pET-16b vector for mammalian expression, I used platinum PfX DNA polymerase to generate high-fidelity PCR application product. I then mixed the PCR product together with pCR-Blunt TOPO vector (**Fig. 3.2.**). Using this highly efficient cloning kit, I was able to generate *E.coli* colonies chemically transformed with the resulting plasmid.

As the pCR-Blunt vector contains the gene for kanamycin resistance, I selected *E.coli* cells on kanamycin supplemented LB.

Following plasmid isolation the DNA was bi-directionally sequenced using internal primers (**Table 2.** green primers). Colonies containing plasmids with the correct sequence were used to transfer this cDNA into vectors for mammalian expression and sub-cellular targeting. Following digestion with *PstI* and *NotI* restriction enzymes, the 2052 bp cDNA was ligated into the pShooter serious of vectors: pCMV-cyto, pCMV-mito and pCMV-ER. For cell surface E/T expression, a plasmid was modified from the pCMV-ER vector by inserting an H-2K^{b} trans-membrane domain (**Fig. 3.4.**). This domain was present in the previously described plasmid containing mem-HEL (**Chapter 2, Fig. 2.3**).

DNA was isolated from selected *E. coli* colonies. **Fig. 3.3**. shows an example of agarose gel electrophoresis following restriction enzyme digestion of pCMV-cyto-E/T plasmid DNA with *PstI* and *NotI*. The plasmid sequence can be seen as a band that migrates consistent with an expected size of 4 kbp. In addition, the E/T cDNA is also seen with an apparent molecular weight of 2 kbp. Identical procedures were used for the generation of plasmids targeting E/T to the mitochondria, ER and plasma membrane (data not shown).

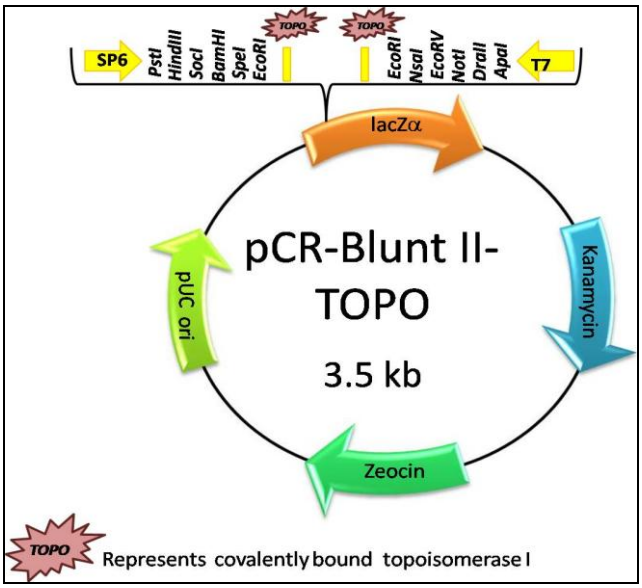

Fig. 3.2. A schematic representation of pCR-Blunt II TOPO (Invitrogen) plasmid. This plasmid was used to clone the E/T fusion protein with blunt ends previously amplified by PCR procedure. This map shows also the restriction sites, in particular *PstI* and *NotI* cleavage sites which were used to clone PCR product.

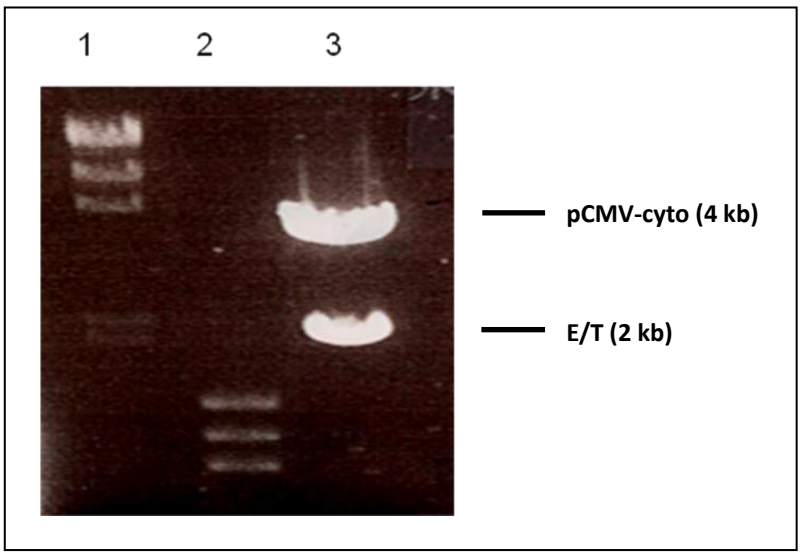

Fig. 3.3. Agarose electrophoresis of E/T cloned into the pShooter pCMV-cyto vector as one example of correct cloning of this model antigen. Lane 1: digestion of 2 μg EGFP- TTCF cloned to pShooter vector (cyto-pCMV) by *PstI* and *NotI* restriction enzymes, lane 2: ϕX174NoeIII-size marker, lane 3: λ–size marker. This DNA gel analysis is representation of 1 experiment. This experiment was done once.

The following pCMV plasmids were generated;

1. Cytosol-EGFP-TTCF (**cyto-E/T**). This construct does not contain any targeting sequences and is therefore expected to localise E/T in the cytosol. 75 kDa is its predicted molecular weight.

2. Endoplasmatic reticulum-EGFP-TTCF (**ER-E/T**). This construct contains a SEKDEL-ER retention signal that is expected to direct E/T expression in the ER. 76 kDa is its predicted molecular weight.

3. Mitochondria-EGFP-TTCF (**mito-E/T**). This construct contains a fragment of the cytochrome c oxidase subunit VIII that is expected to localise E/T within mitochondria. 76 kDa is its predicted molecular weight.

4. Membrane-EGFP-TTCF. I also generated a control plasmid (**mem-E /T**)). This construct encodes a membrane anchored variant of E/T using the trans-membrane and cytoplasmatic domains of the mouse MHC class I molecule, H-2K^{b}. 79 kDa is the predicted molecular weight.

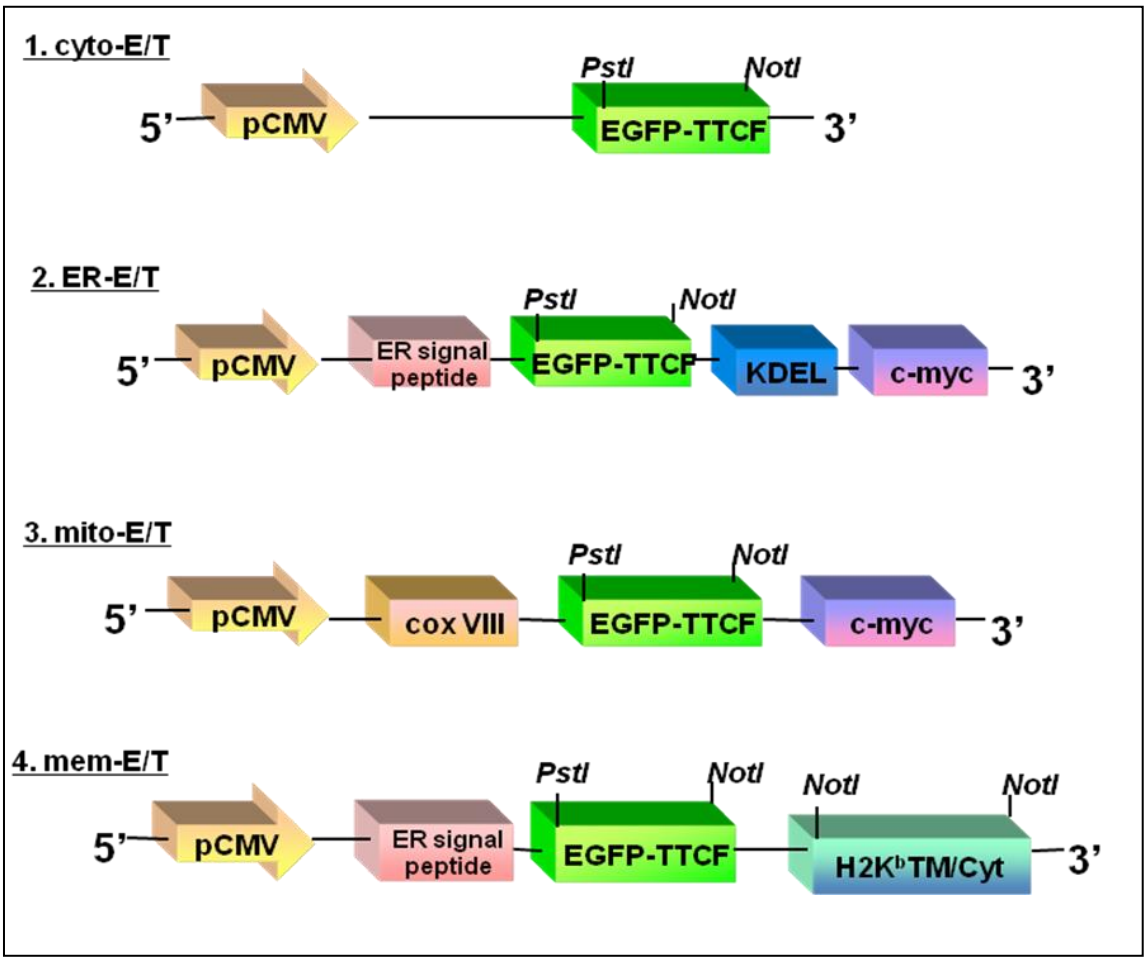

Fig. 3.4. Diagrammatic representation of the panel of E/T cDNA constructs used in this study.

3.2.2. Confirmation of E/T expression in HeLa cells by Western blotting

As previously described, I engineered a panel of plasmids, which were tested for expression and sub-cellular localisation. 24 h following transfection (using TurboFect with a transfection efficiency of 60-70%) these plasmids targeting E/T to the mitochondria, cytoplasm, ER or plasma membrane were validated using Western blotting. HeLa transfectant lysates were separated by SDS-PAGE and transferred to nitrocellulose where they were probed with either anti-TTCF or anti-GFP antibodies.

In **Fig. 3.5.**, it can be seen that anti-GFP antibodies recognises the various E/T fusion proteins (lanes 2-5) as well as GFP from a positive control plasmid pCMV-ER-GFP (lanes 7, 8). The bands represent the expected sizes for all the fusion proteins: cyto-E/T, mito-E/T, mem-E/T, ER-E/T (approximately 76 kDa) and also the positive control ER-GFP (30 kDa).

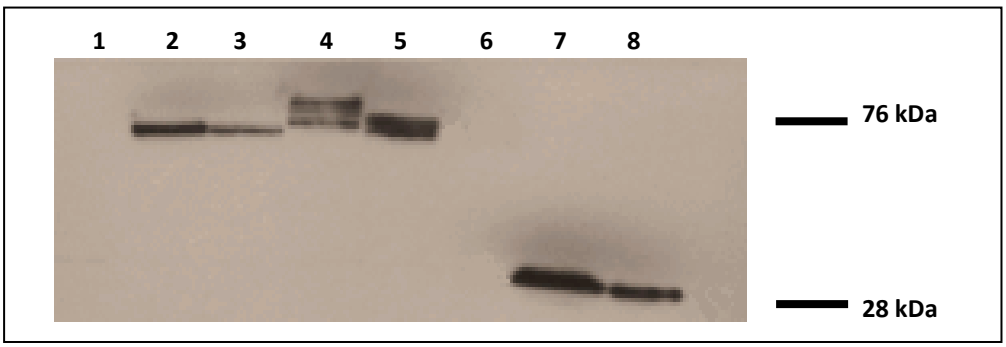

Fig. 3.5. Western blot analysis of HeLa cells transfected with different constructs. Cell lysates from lane 1: untransfected 0.8 x10^5 cells HeLa, lane 2: cyto-E/T , lane 3: mito-E/T, lane 4: mem-E/T, lane 5: ER-E/T, lane 6: empty, lane 7: ER-GFP (as a positive control), lane 8: ER-GFP (HeLa transfectants with less number of cells) were separated on 12 % gel and following transfer were stained with primary anti-GFP (rabbit) antibody and anti-rabbit-HRP. Numbers to the right represent the migration of standard molecular weight markers (kDa) (ProSieve). The western blot analysis is representative of 2 separate experiments.

3.2.3. Confirmation of E/T expression and localisation in HeLa cells by immunofluorescence microscopy and confocal

I then analysed the expression and localisation of the control mem-E/T construct. 24 h following transfection with TurboFect (**Material and Methods**), HeLa cells were fixed and analysed. Nuclei were visualised by incubation with Hoechst 33342. Finally, coverslips were mounted in anti-fading reagent and visualised using fluorescence and confocal microscopy. The expression pattern of mem-E/T plasmid can clearly be seen defining the edge of cell indicating correct surface expression of the fusion protein (**Fig. 3.6.**).

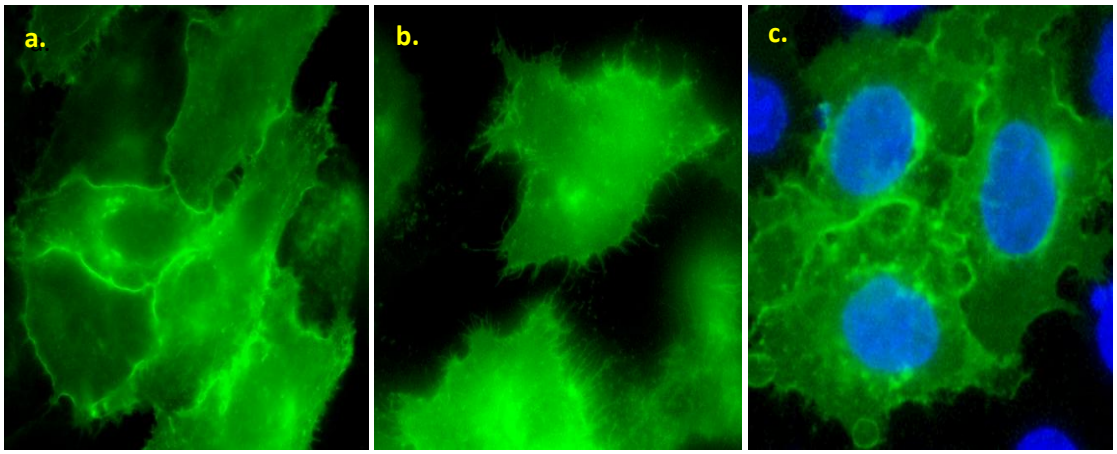

Fig. 3.6. Surface expression of mem-E/T construct in transiently transfected HeLa using fluorescence microscopy. After fixation cells were directly examined on microscopy (panel a. and b.) or additionally incubated with 5 µg/ml Hoechst 33342 dye (panel c.) to visualise nuclei. The images are representative of 6 separate experiments.

However, to confirm whether mem-E/T is exclusively expressed on the cell surface, I visualised mem-E/T HeLa transfectants additionally using confocal microscopy (**Fig. 3.7.**).

Confocal microscopy offers several advantages over conventional optical microscopy. The major attribute of confocal microscopy is the ability to collect serial optical sections from thick specimens. Therefore, a series of images taken at a controllable depth of field may allow localisation of the desired protein. Following transfection of HeLa cells with the mem-E/T construct, slides were examined by confocal microscopy. In **Fig. 3.7.**, the panel of serial images show EGFP fluorescence as green circles which are changing along the scanned cell depth. This is consistent with mem-E/T expression on the cell surface.

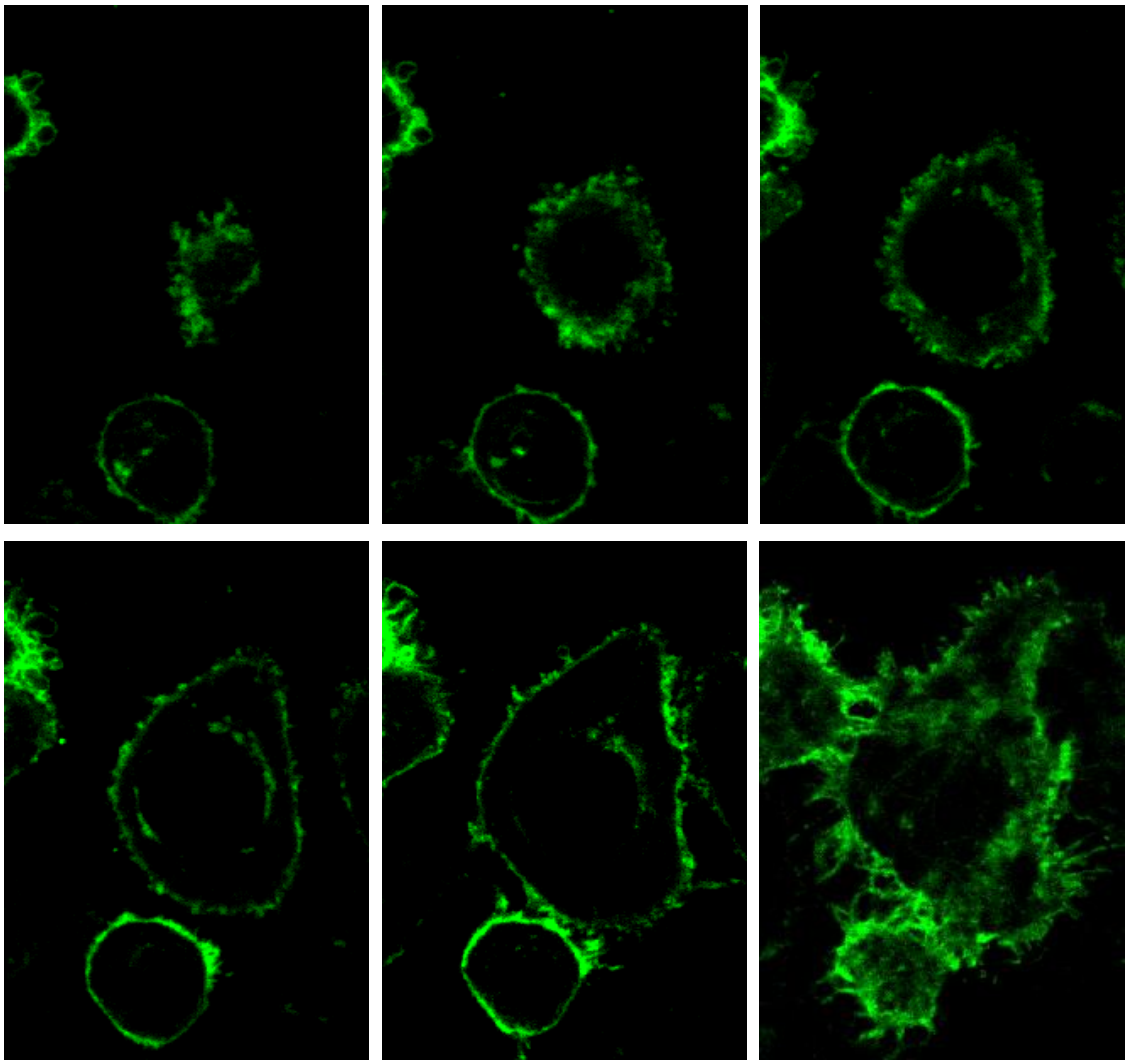

Fig. 3.7. Serial optical section of mem-E/T HeLa transfectants generated using confocal microscopy. HeLa cells were transfected with mem-E/T construct and 24 h later fixed. Following intensive washing, cells were placed to coverslips. Such prepared slides were then analysed on confocal microscopy using an objective lenses with a magnification of 60 times. The surface of entire cell was scanned six times from a different cell depth as indicated by the collection of 6 images of HeLa transfectants. The images are representative of 2 independent experiments.

Subsequently, I transfected HeLa cells with other constructs (mito-E/T, cyto-E/T, and ER-E/T) and visualised them using confocal microscopy (**Fig. 3.8**.). HeLa transfectants were also stained with Hoechst 3342 (for visualising nuclei) and wheat germ agglutinin (WGA) for visualisation of the plasma membrane. WGA is a carbohydrate-binding protein of approximately 36 kDa that selectively binds sialic acid and N-acetylglucosaminyl sugar residues which are predominantly found on the plasma membrane. The expression pattern of each construct suggests the correct targeting of E/T to the desired intracellular compartment. In particular, cells transfected with a cyto-E/T construct exhibit diffused cytosolic pattern, cells transfected with a mito-E/T show fluorescent small punctuate vesicles. Also, cells transfected with an ER-E/T construct show a typical expression pattern for ER as tubular elements surrounding the nuclei and cells expressing mem-E/T are visualised as a ring on the edge of the cell.

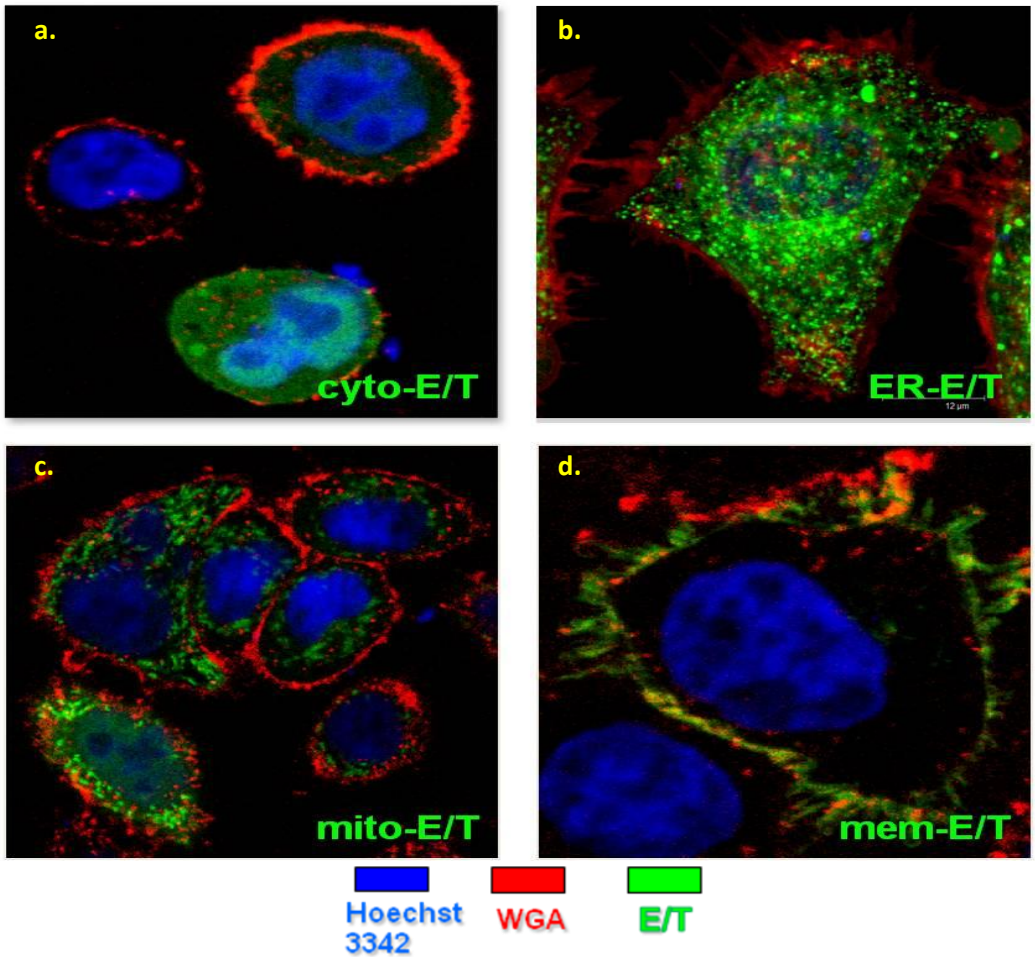

Fig. 3.8. Expression pattern of E/T constructs in transiently transfected HeLa cells. The images were captured using confocal microscopy and represent the expression of the green model antigen E/T) targeted to different subcellular compartments: cytosol (panel a.), ER (panel b.), mitochondria (panel c.), plasma cell membrane (panel d.). HeLa cells were transfected by cyto-E/T, ER-E/T, mito-E/T, mem-E/T plasmids respectively. Cells were stained with wheat germ agglutinin (WGA) (5 μg/ml) on red and nuclei were stained by Hoechst 33342 (5 μg/ml) (blue). The images are representative of 2 independent experiments.

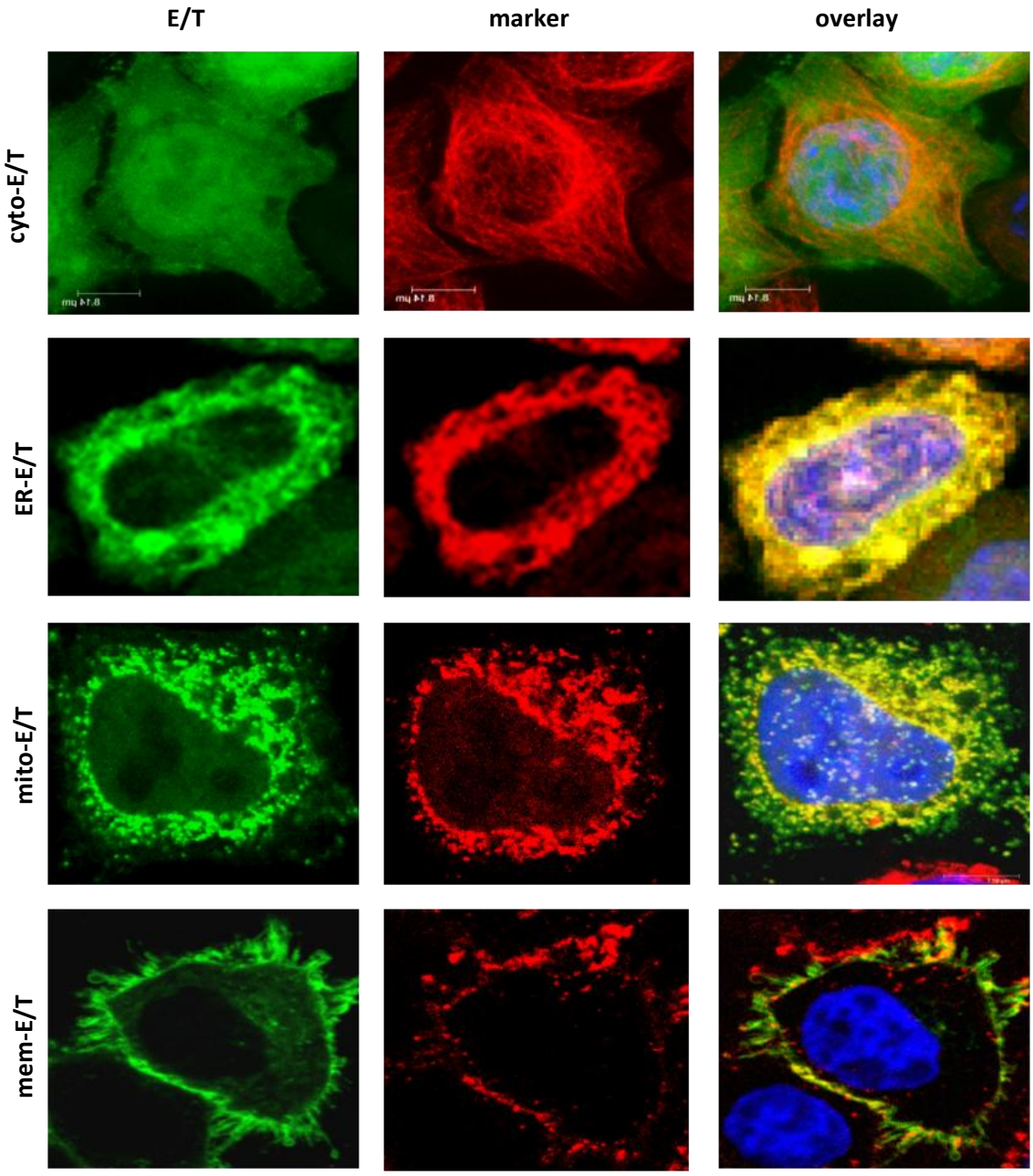

Fig. 3.9. Images captured from confocal microscopy representing transiently transfected HeLa cells. Fusion antigen targeted to different cellular compartments (green). Red represents markers for each compartment. The third column shows a merge between fusion protein and marker (yellow). Following fixation, cells were examined using confocal microscopy. The images are representative of 2 independent experiments.

Because these E/T constructs appear to demonstrate correct cellular localisation, I then performed a more detailed analysis by comparing their expression patterns to these of well characterised markers. To address that, I used markers determining cytosol, mitochondria and ER compartments: anti-β-tubulin antibody, MitoTracker Red dye and anti-IgG antibody respectively. In **Fig. 3.9.,** it can be clearly seen that all constructs overlap with the markers characterising particular cellular compartments. Furthermore, dual colour analysis chart (**Fig. 3.10.**) that converts the pixels on the axes from the overlying images of single HeLa transfectant seen in **Fig. 3.9.**, also confirmed colocalization.

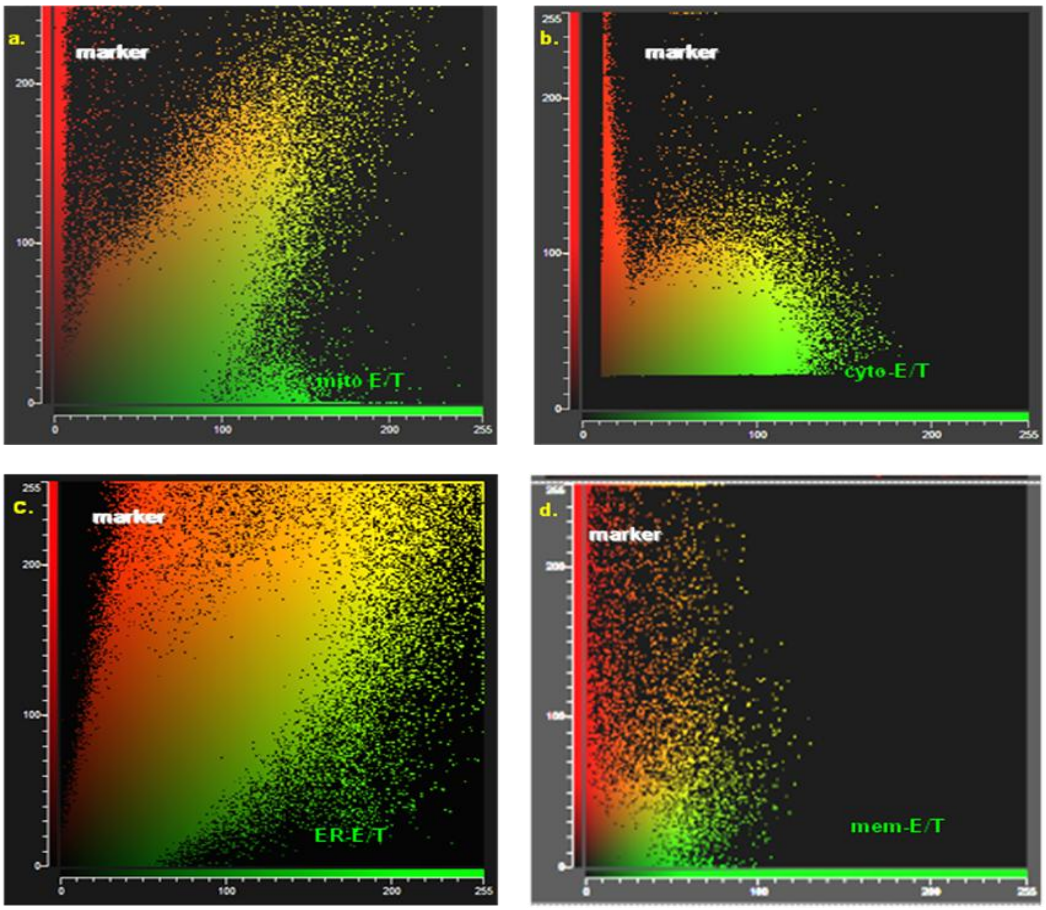

Fig. 3.10. Colocalization chart demonstrating the intensities of measured red (marker) and green (E/T) pixels (on the y and x axes respectively) corresponding to the randomly selected field of one individual HeLa cell shown in Fig. 3.9 (last column). E/T fusion antigen targeted to different cellular compartments: mitochondria (panel a.), cytoplasm (panel b.), ER (panel c.) or membrane (panel d.) of single HeLa cell (shown in Fig. 3.9., first column) was converted on green pixels on the y axe. Red pixels on the x axe illustrate markers of the each compartment: MitoTracker Red (panel a.) and anti-β-tubulin antibody directly conjugated with TRITC (panel b). Also in panel c. following co-transfection with plasmids expressing human heavy chain IgG and ER-E/T construct, the ER marker was determined. HeLa cells were stained primary with anti-human IgG antibody and secondary anti-rat TRITC conjugated antibody. In panel d., cells were stained with wheat germ agglutinin (WGA) for highly selective staining of the plasma membrane. Orange colours in the middle of the each chart indicate overlapping between fusion protein and marker. The images represent the experiment that was performed once.

3.3. Discussion

In this chapter, I have generated four constructs (mem-E/T, cyto-E/T, ER-E/T and mito-E/T) containing targeting sequences that localise the recombinant green protein E/T into various intracellular compartment. The reason why I decided to use E/T as a model antigen was because of the simplicity in visualisation of green recombinant protein in microscopy. Importantly, EGFP as auto-florescent protein is also resistant to apoptotic conditions.
Our laboratory has previously generated TTCF specific-B cells, which are able to recognise the relocated E/T antigen to the surface. Therefore, generating a panel of plasmids localising E/T in various sub-cellular compartments will find the ideal implementation in this project.

The first step of this experiment was to generate four constructs which will be expressed in certain sub-cellular compartments of HeLa cells. To address that, I performed the standard cloning procedure. Using pCR-Blunt TOPO cloning vectors, I inserted E/T previously amplified with certain primers. Followed transformation to chemically competent *E.coli* cells, I selected the colonies that expressed the desired plasmid and performed DNA isolation. The next step was to ligate pCMV expression vector previously dephosporylated with insert encoding E/T and to transform to chemically competent *E.coli* cells. 24 h after transformation, the isolated DNA was verified by sequencing, restriction enzymes digestion and the PCR technique. These selection procedures allowed me to generate four constructs that were checked in terms of open frame reading (sequencing), molecular weight (gel electrophoresis), occurrence restriction enzymes sites (restriction enzyme digestion) and matching template with primers (PCR amplification).
Relying on molecular techniques, which revealed positive results, I decided to examine E/T expression in HeLa cells by Western blotting and microscopy. Following optimisation of transfection conditions, HeLa cells were transfected by TurboFect and 24h later E/T expression was analysed. Transfected HeLa cells were lysed and proteins were extracted. Following SDS-PAGE, proteins transferred to a membrane where they were probed with an anti-GFP antibody. In **Fig. 3.5.** I show an image of a probed filter demonstrating the bands of the predicted size (78 kDa) of all the E/T construct. Additionally, HeLa transfectants were visualised using fluorescence and confocal microscopy. Approximately 70-80 % HeLa cells were transfected. Each construct exhibited the expression pattern that expected to be localised in the correct intra-cellular compartment. In order to determine whether the expression pattern of E/T is exclusive for a certain compartment, I also performed additional staining of HeLa transfectants with markers determining cellular compartments. In particular, I compared cyto-

E/T with β-tubulin, mito-E/T with MitoTrackerRed and ER-E/T with plasmid encoding human-heavy chain IgG in HeLa transfectants. Taken together, these results from Western blotting and confocal microscopy clearly indicate correct expression and correct localization of each E/T construct.

Having correctly expressed all four constructs in a transient transfection system, I also attempted to generate stable cell lines expressing each E/T construct. Unfortunately, I could not select a stable cell lines, even though I tried to use different cell lines (HeLa or LTK (mouse fibroblasts)) and various transfection reagents (calcium phosphate, Lipofectamine, TurboFect). Because of these problems in generation of stable cell lines, the levels of antigen expression in the HeLa transient transfectants were taken into account in the interpretation of further experiments. This will be discussed in more detail **Chapter 5**.

In conclusion:

I successfully generated a panel of plasmids expressing a fusion protein E/T in various intracellular compartments and on the plasma cell surface of HeLa cells. The correct sequence of E/T was confirmed by sequencing, enzymatic digestion and PCR procedure. Next, I moved from DNA to protein level to confirm the correct expression of E/T fusion protein. To address this, E/T expression was firstly tested using Western blotting. As expected, anti-GFP antibody recognised E/T protein transferred from lysates of HeLa transfectants.

Secondly, confocal microscopy confirmed the correct localisation of cyto-E/T, mito-E/T, ER-E/T and mem-E/T constructs in the cytosol, mitochondria, ER and on the plasma cell surface, respectively. Also, further experiments performed with markers characterising certain sub-cellular compartments, undoubtedly showed the co-localisation between marker and E/T expression. This observation clearly confirmed correct E/T localisation in four different cellular compartments.

- 4. Optimization of conditions for the induction of intracellular antigen relocation in E/T transfected HeLa cells -

4.1. Introduction

Classical inducers of apoptosis that target the ER (brefeldin, tunicamycin), the mitochondria (arsenite, C2 ceramide) or DNA (etoposide, mitomycin C) fail to induce immunogenic cell death. Treatment with anthracyclines including doxorubicin, idarubicin and mitoxantrone or with UVC exposure for example, has been shown to relocate the ER resident chaperone calreticulin (CRT) to the cell surface leading to a novel immunogenic form of cell death (Obeid et al., 2007b; Tufi et al., 2008; Zhang and Kaufman, 2008). Limited evidence also supports the concept that the induction of immunogenic cell death in various tumour cells leads to antigen relocation on the cell surface resulting in the induction of local anti-tumour immunity. The mechanism of intracellular antigen relocation is still unclear. McArthur et al. has shown that apoptosis induced by TNF-α in salivary gland cells also results in auto-antigen relocation to the cell surface. Using cell fractionation and immunofluorescence techniques they revealed the nuclear proteins SS-A (Ro) and SS-B (La) and the cytoplasmatic protein fodrin were relocated to the cell surface after TNF-α and cycloheximide treatment (McArthur et al., 2002).
Based on the above findings, I decided to test whether the anthracyclines doxorubicin (DX), mitoxantrone (MX) and UVC exposure were also capable of causing E/T relocation from the ER as well as from the cytosol and mitochondria to the cell surface. Furthermore, I compared the effect of staurosporine (STS), a well-defined agent causing non-immunogenic apoptotic cell death (Obeid et al., 2007b). This natural alkaloid inhibits the protein kinases through the prevention of ATP binding to the active centre of the kinase. Therefore, this chapter documents the effects of E/T HeLa transfectants treated with various doses of anthracyclines, UVC and STS with a particular emphasis on the alteration of E/T cellular location.

The biological effects of UVC exposure are multiple and include the release of soluble mediators, modification of the surface molecule expression, mitochondria alteration, cell shrinkage, surface membrane blebbing, chromatin condensation and DNA fragmentation. Takasawa et al., have described that in response to UVC exposure, cytochrome c is released from the mitochondrial inter-membrane space to the cytoplasm (Takasawa et al., 2005). In addition, the activation of death receptors CD95 on the cell surface induced by UVC and UVB

also triggered machinery apoptotic cell death (Kulms et al., 1999). These examples of UVC treatment have also been shown to induce immunogenic cell death by relocation of CRT from the ER to the cell surface.

4.2. Results

4.2.1. Morphological changes in HeLa cells induced by anthracyclines and staurosporine (STS) treatment

Firstly, I optimised the time and concentration of DX, MX and STS treatment of untreated HeLa cells based on a combination of morphological observations that were illustrated by light microscopy (**Fig. 4.1.**). Following drug treatment, HeLa cells start to exhibit morphological changes including cell detachment, cell shrinkage and the occurrence of apoptotic bodies.

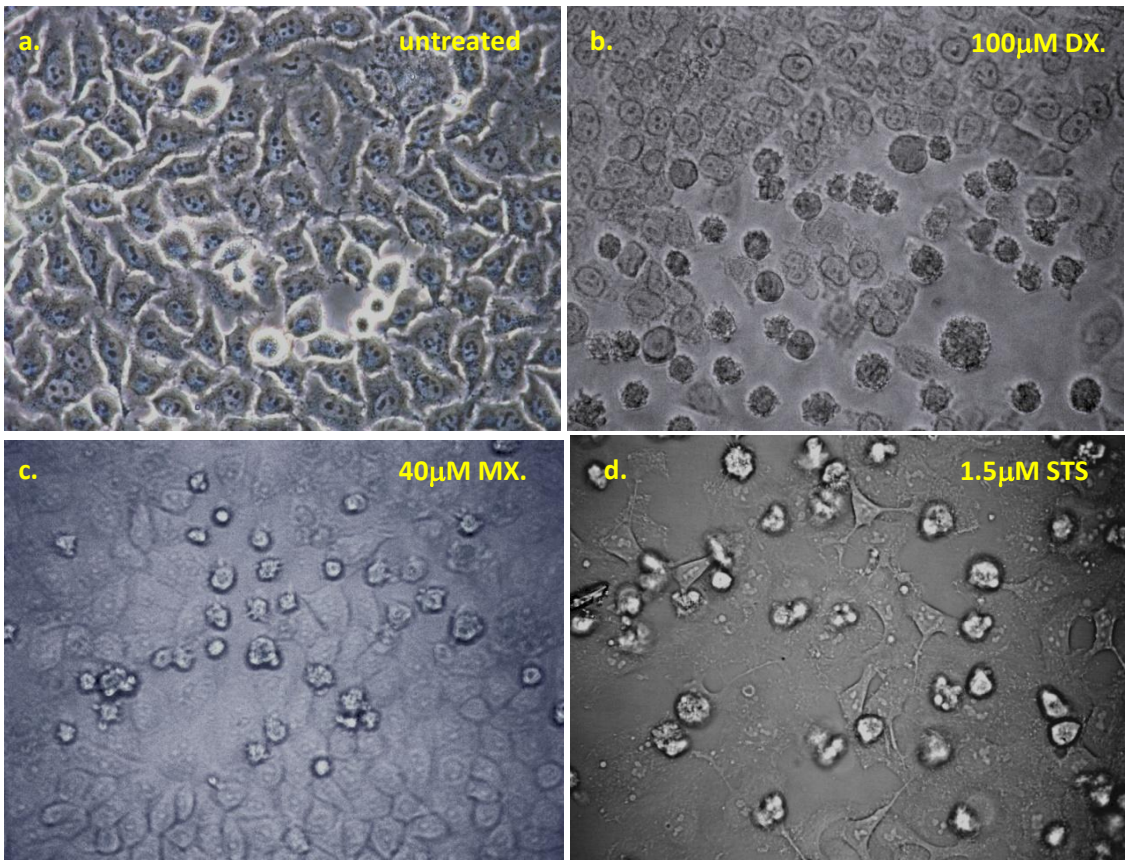

Fig. 4.1. Morphological changes of HeLa cells after drug treatment. Representative images from light microscopy using 40 times magnification of HeLa cells treated for 4 h with 100 μM DX (panel b.), 40 μM MX (panel c.) or 1.5 μM STS (panel d.). Panel a. shows untreated HeLa cells. The images are representative of 3 separate experiments.

In addition, I also performed the colorimetric MTT ((3-(4,5-Dimethylthiazol -2-yl)-2,5-diphenyltetrazolium bromide, a tetrazole) assay, as shown in **Fig. 4.2**. This assay measures cell viability through the colour density of the converted yellow MTT substrate to the purple product-formazan in the mitochondria of living cells. This reduction takes place only when mitochondrial reductase enzymes are active and therefore conversion of the substrate can be directly related to the number of viable cells. Expectedly, in each panel following drug treatment a dose dependent decrease in HeLa cell viability can be seen. In particular, after 1.5 μM STS or 200 μM DX treatment, HeLa cells were only 25 % viable. However, following 80 μM MX treatment, approximately 30% of HeLa cells died (**panel c.**). Nevertheless, the disadvantage of this test is that the MTT assay does not distinguish whether the observed cell death is apoptotic or necrotic.

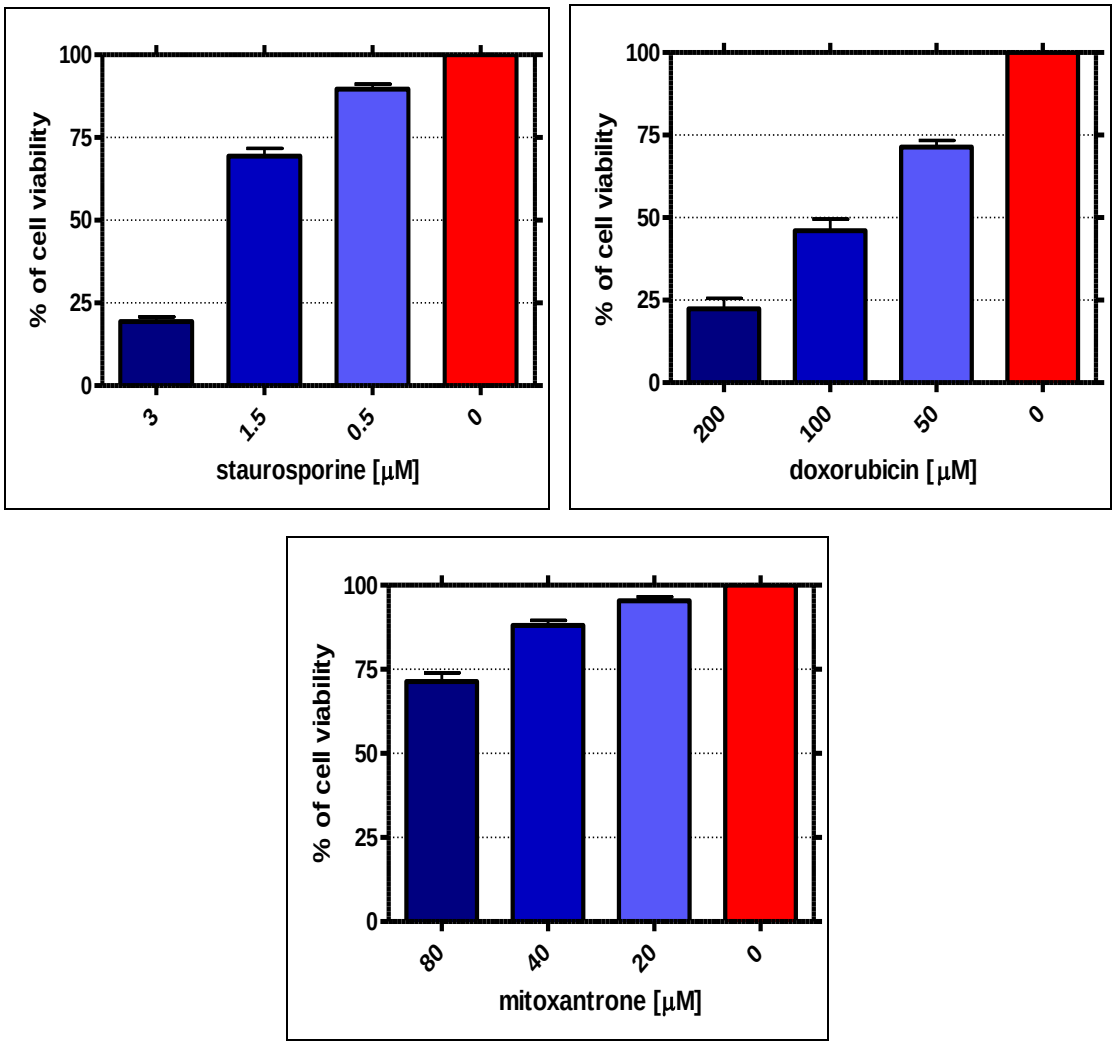

Fig. 4.2. Quantification of cell viability by MTT test. 4 h after addition of drugs treatment (panel a., b., c.) the activity of mitochondrial reductase enzymes was measured by production of formazan estimating cells viability. Treated cells (blue columns) were compared to vehicle treated cells (red columns) that were standardised to 100 % viability. Data is representative of three independent experiments where the mean optical density from triplicate wells was converted to % cell viability (using untreated cells as 100 %).

Therefore, I also performed the annexin V binding assay that characterises apoptotic cell death. One of the earlier features of apoptosis but not necrosis, is the translocation of phosphatidylserine (PS) from the internal to the external face of the plasma membrane. Annexin V is a 35.8 kDa, calcium-dependent phospholipid-binding protein with a high affinity for PS, which can be directly conjugated with desired fluorochrome. Therefore, annexin V binding to the cell surface is an indicator of the early stages of apoptosis.

In **Fig. 4.3. panel b.**, it can be seen that annexin V-Cy5 binds to the surface of apoptotic HeLa cells treated with STS. In **Fig. 4.3. panel d.**, the circle rings reflect the annexin V binding which overlay with the surface of dying HeLa cells captured by light image. This method of annexin V binding visualised using confocal microscopy was not significantly reproducible and I encountered many technical problems. In particular, the location of apoptotic cell plasma membrane stained with Cy5 proved technically difficult. This was due to the fact that annexin V-Cy5 was the only commercially available conjugate (annexin V-FITC could not be used) and this dye is excited at 649 nm in the far red part of the spectra. This means that Cy5 staining could only be visualised once images had been acquired. Therefore, I decided to use a different dye and another technique for detecting annexin V binding to apoptotic HeLa cells, which is described in **Section 4.3.3.**

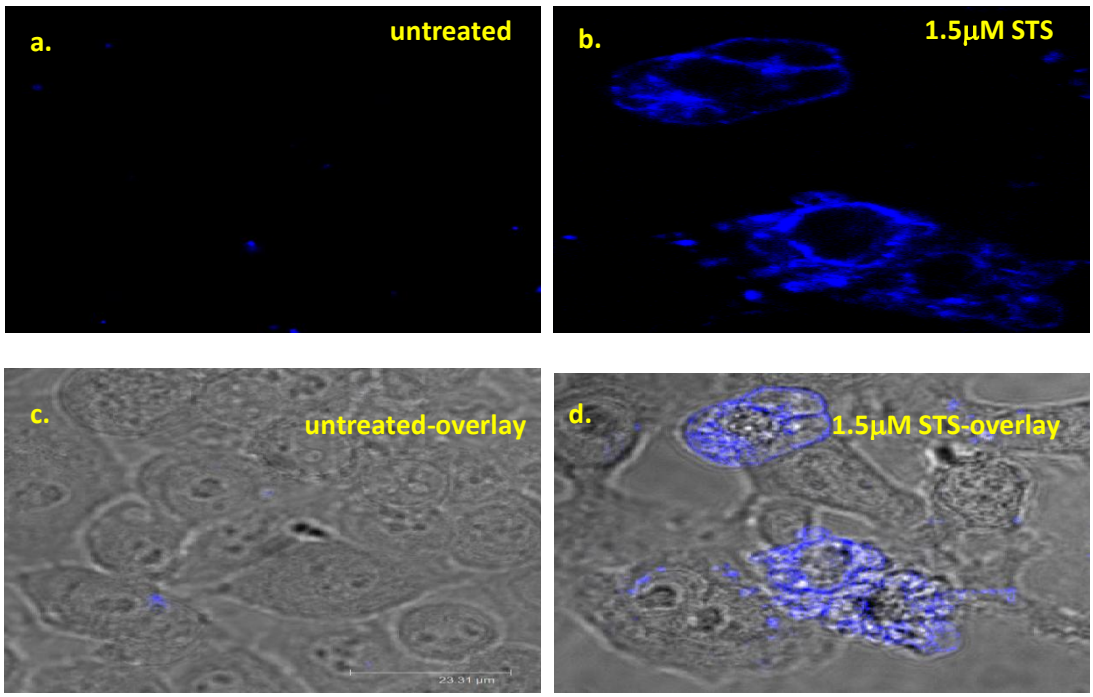

Fig. 4.3. Annexin V-Cy5 staining of apoptotic HeLa cells. Apoptosis was induced with 1.5 µM of STS (panel b.) for 4 h. After 4 h, cells were incubated for 20 min with 1 µg/ml of annexin V-Cy5 in binding buffer. Following fixation, HeLa cells were examined using confocal microscopy on the far-red fluorescence. Panel c. and d. represent overlay images from light microscopy reflecting cell morphology and confocal microscopy to visualise annexin-V-Cy5 staining. The images are representative of 4 independent experiments.

4.2.2. The effect of anthracyclines and STS on HeLa E/T transfectants

As the process of transfection itself leads to limited HeLa cytotoxicity, I established that this was minimal (with optimal protein expression) after 24 h using TurboFect, compared to that seen with Lipofectamine used in **Chapter 2**. In addition, I determined the concentration of DX, MX and STS (100 μM, 40 μM, 1.5 μM respectively) that induced apoptosis in HeLa cell transfectants at this time point while maintaining sufficient cell adherence for staining and microscopic analysis. I then examined the intracellular re-localisation of E/T expressed by the various plasmids following apoptosis induction in HeLa cells.

Fig. 4.4. shows HeLa cells transfected with the ER-E/T construct (**panels a.** to **c.**) and treated for 4 h with anthracyclines undergo apoptotic changes. These changes include the appearance of apoptotic bodies on the surface of cells. It can be also seen that these apoptotic bodies contain relocated E/T antigen following DX and MX treatment (**panel b.** and **c.**). The intracellular distribution of cyto-E/T also appears to change following drug treatment and fluorescent apoptotic bodies are observed (**panels e.** to **g.)**. HeLa cells transfected with mito-E/T constructs, however, do appear to show changes in intracellular localization but fluorescent apoptotic bodies are not seen (**panels i.** to **k.**). Treatment of all E/T expressing transfectants with STS does not lead to E/T relocation into apoptotic bodies but rather induces changes in the cytoskeleton causing cell elongation (**panel d., h.** and **l.**). This data is consistent with previously described reports demonstrating that only certain drugs including anthracyclines have the ability to induce immunogenic cell death as reflected by CRT surface relocation. In contrast, STS or mitomycin C induced canonical programmed cell death which did not lead to protein redistribution (Obeid, Tesniere et al. 2007).

Thus, this data showing relocation of E/T allowed me to test whether TTCF-specific B cells can acquire this antigen in a similar manner to that which has been reported for membrane tethered antigens.

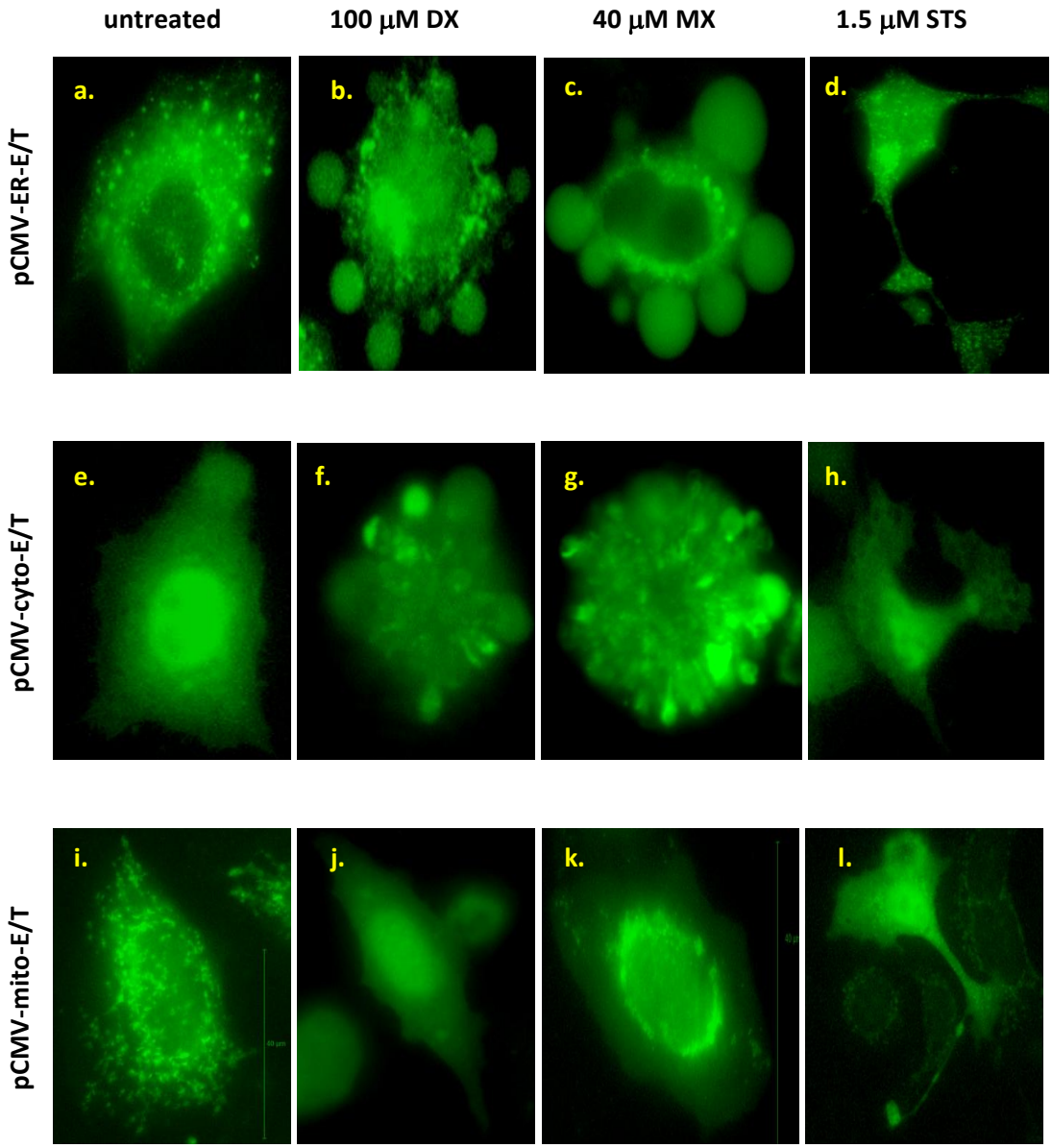

Fig. 4.4. The effect of drug treatment on transiently transfected HeLa cells. After 4 h incubation with 100 μM of DX (panel b., f., j.), 40 μM of MX (panel c., g., k.) or 1.5 μM of STS (panel d., h., l.) HeLa transfectants were fixed and directly examined on fluorescence microscopy. Panel a., e. and i. represent untreated E/T transfectants expressing ER-E/T, cyto-E/T, and mito-E/T respectively. The images are representative of 3 independent experiments.

Relying on the previously described observations using fluorescence microscopy and MTT tests, I decided to use the optimised concentration of 1.5 μM STS, 100 μM DX and 40 μM MX to induce apoptosis in HeLa ER-E/T transfectants. 4 h following treatment, transfectants were washed to remove excess drug and graded numbers were incubated for 24 h with TTCF-specific B and T cells. The generation of TTCF-specific B and T cells and a detailed description of the bio-assay will be described in **Chapter 5.**

Paradoxically, in **Fig. 4.5.** it can be observed that IL-2 production from the TTCF-specific T cells decreases when they were incubated with antigen-specific B cells and increased numbers of apoptotic transfectants. In control experiments when specific B and T cells were incubated with soluble TTCF antigen, IL-2 production was measured with increased concentration of soluble TTCF (**Fig 4.5. panel d**.). To establish if this cytotoxic effect was due to drug carryover of anthracycline-treated HeLa cells on either the TTCF-specific B or T cells, I performed MTT tests. Indeed, TTCF-specific B and T cells were incubated for 24 h with 50, 500 or even 5000 times less concentrated doses of MX (2 μM, 0.2 μM and 0.02 μM of MX) than that used in the bio-assay. As shown in **Fig. 4.6**. and **Fig. 4.7.**, B cell hybridomas were relatively insensitive to these low doses of anthracyclines and were therefore not likely to be affected following the extensive washing of the treated HeLa transfectants in the antigen presentation assay shown in **Fig. 4.5. panel a., b., c**. In contrast, however, **Fig. 4.6**. and **Fig. 4.7.** show that the T cell hybridomas appeared to be extremely sensitive to doses as low as 0.02 μM MX which represents 0.05% of the dose used in the antigen presentation assay.

Thus, this test indicated that the standard antigen presentation assay with T cell hybridomas, which were incubated for 24 h with anthracycline-treated (and extensively washed) HeLa transfectants, was not a viable assay for measuring antigen presentation.

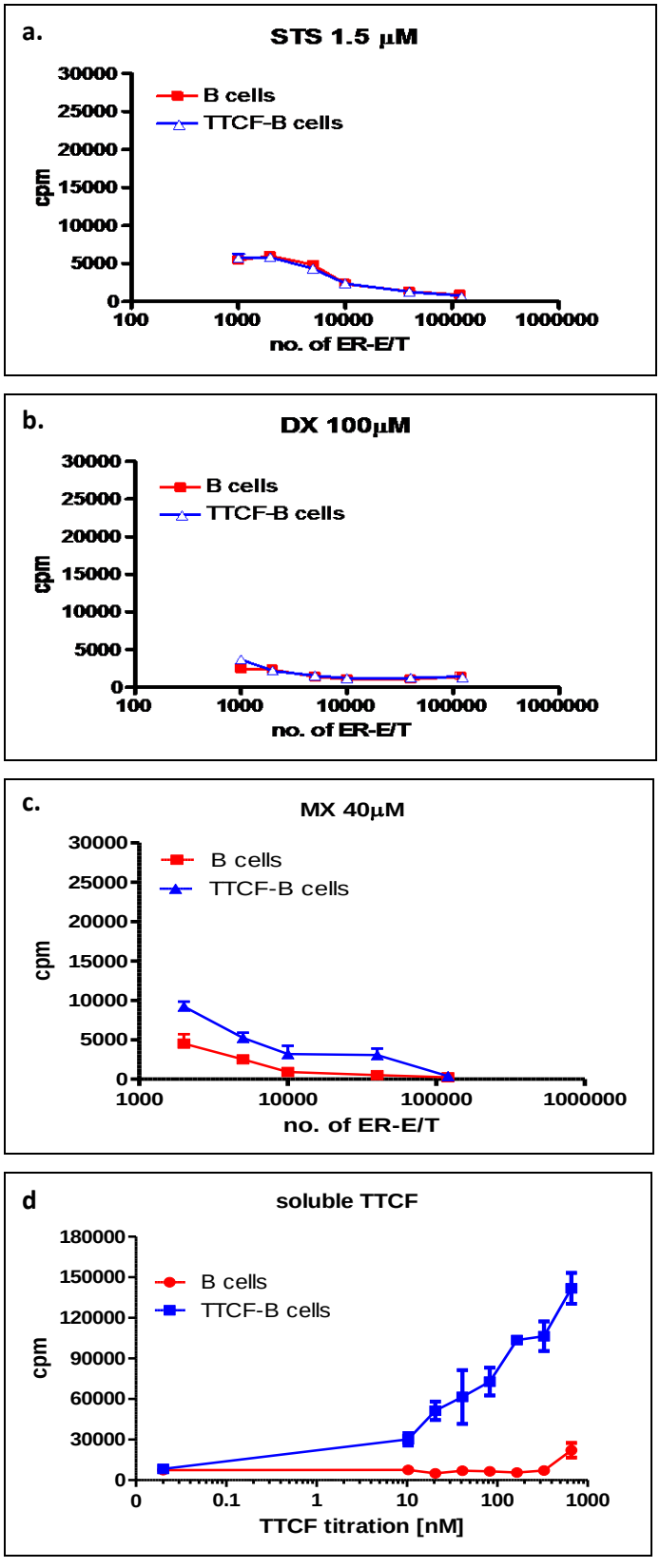

Fig. 4.5. B cell acquisition and presentation of relocated ER-E/T following apoptosis induction using standard assay. HeLa E/T transfectants were treated with STS (a.), MX (b.) or DX (c.) respectively and following washing incubated for 24 h with TTCF-specific B (blue line) or non-specific B cells (red line) and with TTCF-specific CD4+ T cells. Panel d. demonstrates presentation of soluble TTCF using TTCF-specific B and T cells. These proliferation assays are representative of 2 independent experiments.

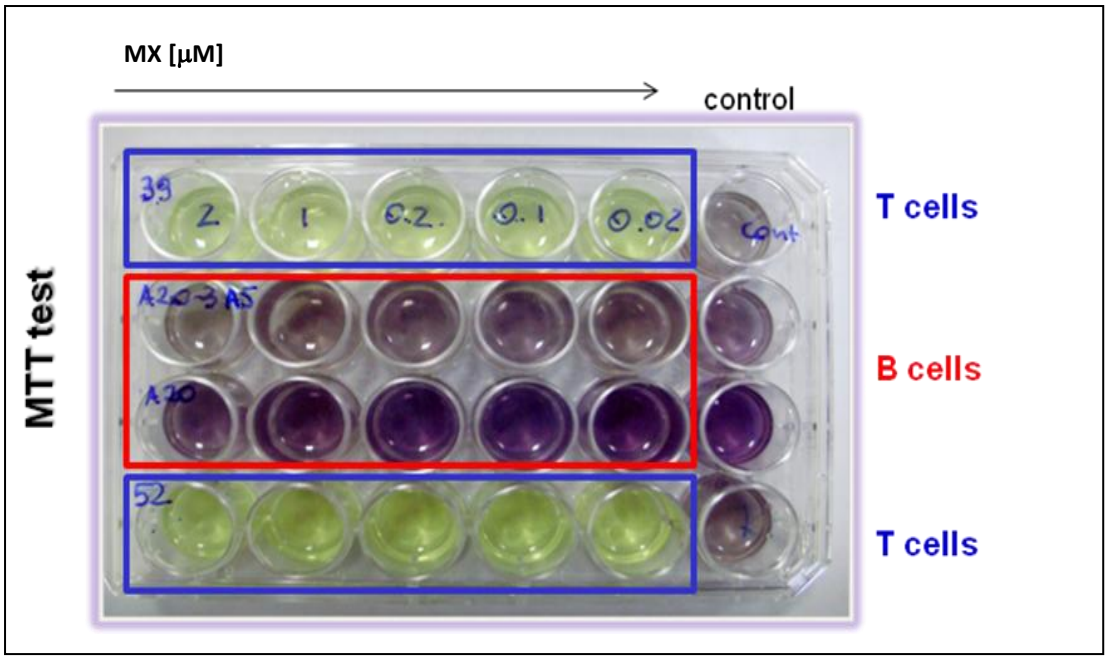

Fig.4.6. MTT test of B and T cell hybridomas treated with low doses of MX for 24 h. TTCF-specific CD4+ T cell hybridomas no. 39 and 52, TTCF-specific (A20-3A5) and non-specific (A20) B cells were treated with 2 µM, 1 µM, 0.2 µM, 0.1 µM and 0.02 µM MX for 24 h. This experiment was performed twice in independent experiments.

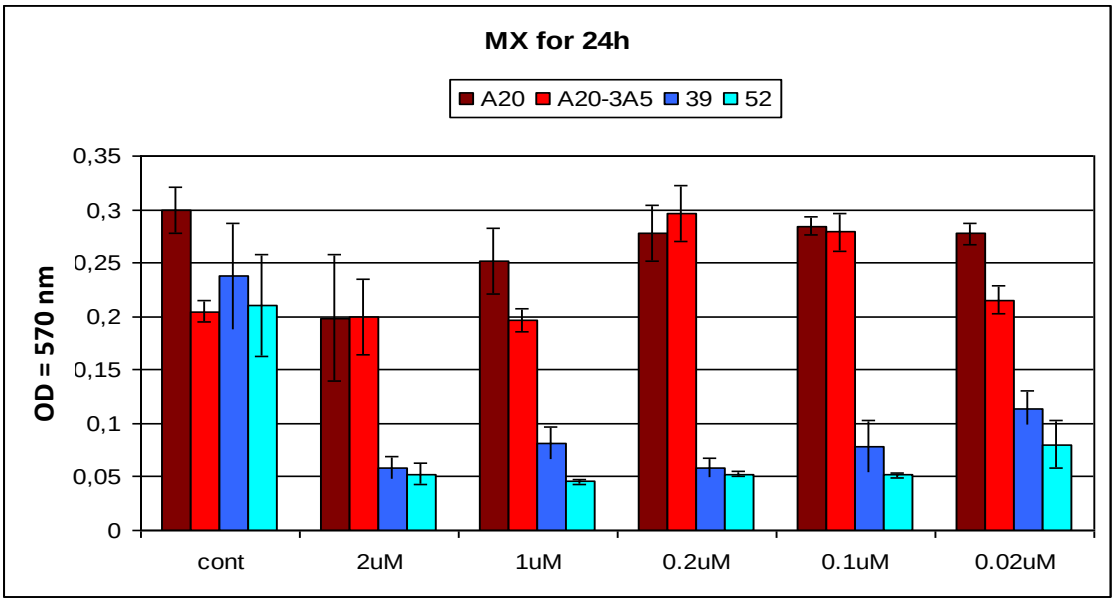

Fig. 4.7. Quantitative analysis of MTT test showing absolute values of OD 570 wavelength of B and T cell hybridomas treated with low doses of MX. Both T cell hybridomas no. 39 and 52 and B cells: A20 non-specific B cells and A20-3A5 TTCF-specific B cells were treated with different concentration of MX: 2 µM, 1 µM, 0.2 µM, 0.1 µM and 0.02 µM for 24 h. This experiment was performed twice in independent experiments.

4.2.3. Morphological changes in HeLa E/T transfectants following UVC exposure

As I have previously described, measuring relocated antigens using T cell hybridomas proved to be problematic due to the sensitivity of T cells to extremely low doses of anthracyclines, I therefore decided to analyse the effect of a different immunogenic apoptotic agent (UVC irradiation). The first step was to optimise the dose and time of UVC treatment for HeLa cells. HeLa cells were irradiated with a range of different doses of UVC: 100, 200 and 300 J/m^2, respectively. The optimal time which allowed me to monitor morphological changes in HeLa cells was established as 4 h. In **Fig. 4.8.**, it can be seen that UVC induces a dose dependent decrease in HeLa cell viability. In particular, 4 h after UVC exposure with 100, 200 and 300 J/m^2 the cell viability dropped to 90%, 80% and 65%, respectively.

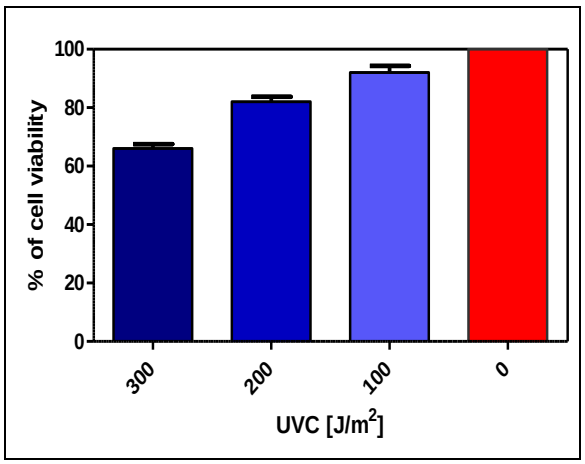

Fig. 4.8. Quantification of cell viability by MTT test. 4 h after UVC exposure the activity of mitochondrial reductase enzymes was measured by production of formazan estimating cells viability. Treated cells (blue columns) were compared to untreated cells that represented by 100 % cell viability (red columns). Data is representative of 3 independent experiments where the mean optical density from triplicate wells was converted to % cell viability (using untreated cells as 100 %).

This initial experiment testing HeLa cell sensitivity to UVC led to examination of the morphological changes in these cells. This type of cell death has been well documented and is characterised by typical apoptotic hallmarks including loss of membrane asymmetry and attachment, condensation of the cytoplasm and nucleus, and inter-nucleosomal cleavage of DNA (Nishigaki et al., 1998).

To test whether HeLa transfectants exhibit those morphological features in response to UVC treatment, I decided to visualise changes in cell morphology using microscopy.

Relying on my results from ER-E/T HeLa transfectants treated with anthracyclines (**Fig. 4.4. panel b.** and **c.**), I transfected HeLa with the ER-E/T plasmid. 24 h following transfection HeLa cells were exposed to 100, 200 and 300 J/m^2 of UVC respectively. 4 h later morphological changes were monitored using confocal microscopy.

In **Fig. 4.9. panel b.** it can be seen that typical apoptotic changes start to occur even following treatment with a 100 J/m^2 irradiation. These changes include DNA condensation and fragmentation reflected by blue nuclei, stained with Hoechst and punctuate expression of ER-E/T that differs from control non-irradiated HeLa ER-E/T transfectants. Expectedly, following 200 J/m^2 of UVC irradiation, the morphology of HeLa cells changed even further with fragmentation of ER-E/T expression, presumably as a consequence of cytoskeleton breakdown. Also nuclei content appears to be released from the cell to the extracellular matrix.

Maftoum-Cost et. al., described similar changes in HeLa cell morphology following photodynamic therapy (PDT). They showed that HeLa cells exposed to PDT undergo changes in the ER compartment. This ER damage causes ATP loss and membrane potential dissemination that consequently results in the formation of bleb-like structures (Maftoum-Costa et al., 2008).

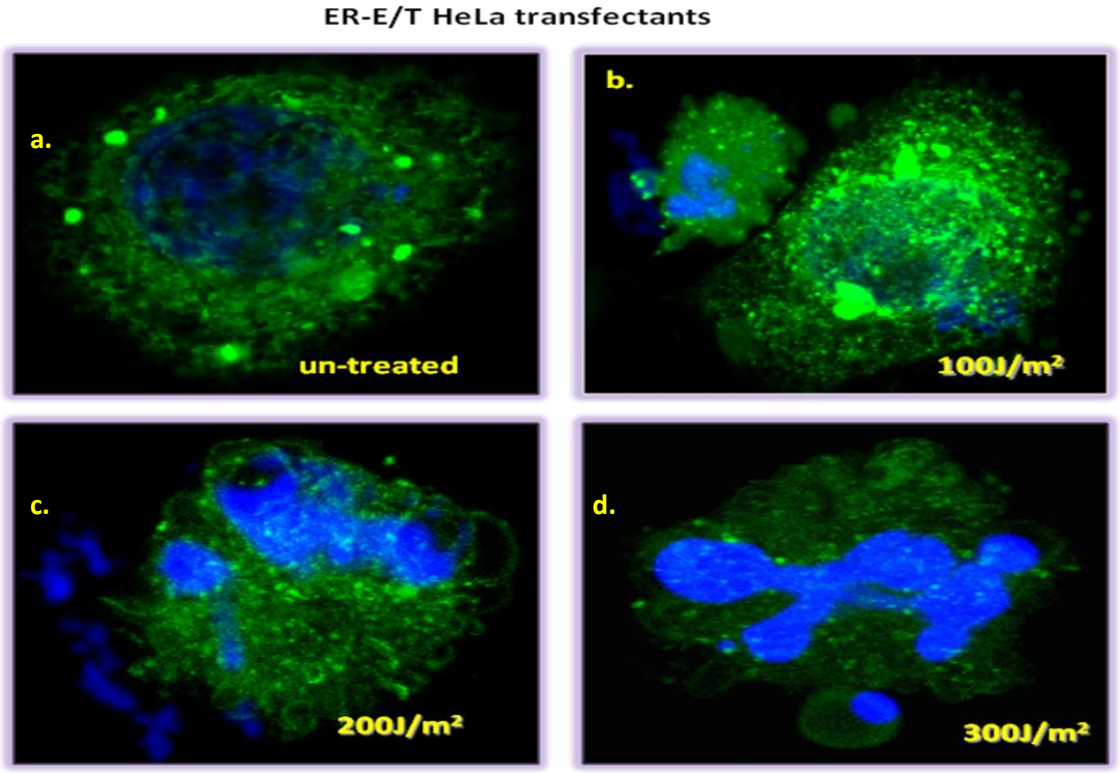

Fig. 4.9. Morphological changes in ER-E/T HeLa cells induced by different dose of UVC. Confocal microscopy of irradiated green transfectants by 100 J/m^2 (panel b.), 200 J/m^2 (panel c.), 300 J/m^2 (panel d.). Images reflect changes in the cellular morphology after 4 h from UVC irradiation. Panel a. represent untreated group of cells transfected with ER-E/T. Cells were also stained with Hoechst 33342 (5 μg/ml) (blue) to visualise nuclei. The images are representative of 2 independent experiments.

In accordance with the previously mentioned results, it can also be seen (**Fig. 4.9. panel c.**) that some ER-E/T-labelled apoptotic bodies contain Hoechst-stained DNA. Finally, the strongest dose of 300 J/m^2 UVC induced cell shrinkage, complete cytoskeleton damage and chromatin fragmentation. This fragmented DNA is also present in fully formed green apoptotic bodies containing E/T that originated from the ER.

These observations using confocal microscopy indicate that HeLa transfectants are undergoing apoptotic death. To confirm this treatment was inducing apoptosis, I stained HeLa cells treated with 300 J/m^2 of UVC with annexin V-FITC (for 40 min RT in Ca^{2+} containing binding buffer) and analysed annexin V binding using flow cytometry. As a positive control for apoptotic cell death, I also incubated HeLa cells with STS (1.5 μM) for 4 h and compared binding to non-treated HeLa cells. As illustrated in **Fig. 4.10.**, more than 80% cells treated with STS or UVC bind annexin V indicating that the vast majority of cells treated with both these reagents undergo programmed cell death.

Subsequently, I also visualised by confocal microscopy HeLa cells that were transfected with the other E/T constructs (cyto-E/T and mito-E/T) following exposure to 300 J/m^2 UVC. In **Fig. 4.11.**, it can be seen that following UVC exposure transfectants expressing the E/T constructs exhibited typical apoptotic changes similar to those previously described in ER-E/T transfectants. In particular, chromatin condensation, DNA fragmentation and cellular release, membrane disruption and bleb formation were visualised.

Furthermore, I also examined in more detail the morphological changes of HeLa E/T transfectants following UVC treatment. For this, I co-stained HeLa transfectants with WGA and Hoechst and compared intracellular compartments with organelles from untreated cells. In **Fig. 4.12.**, **4.13.** and **4.14.** E/T transfectants exhibited synchronized apoptotic changes. This included DNA fragmentation visualised by strong Hoechst staining. In addition, UVC treated E/T transfectants showed membrane asymmetry reflected by a diffused pattern of WGA staining. In contrast, untreated E/T transfectants showed well organised WGA circular staining representing typical cell surface membrane. As expected, the E/T antigen localisation was completely disrupted following UVC treatment. Indeed, in E/T transfectants expressing cyto-E/T (**Fig. 4.12.**) and ER-E/T (**Fig. 4.13.**) the blebs containing green fusion protein can be seen. This observation demonstrates that cyto-E/T and ER-E/T relocate from cytoplasm and ER, respectively to the cell surface. However, mito-E/T expression appears to be maintained in intracellular compartments with considerably less localisation at the cell surface.

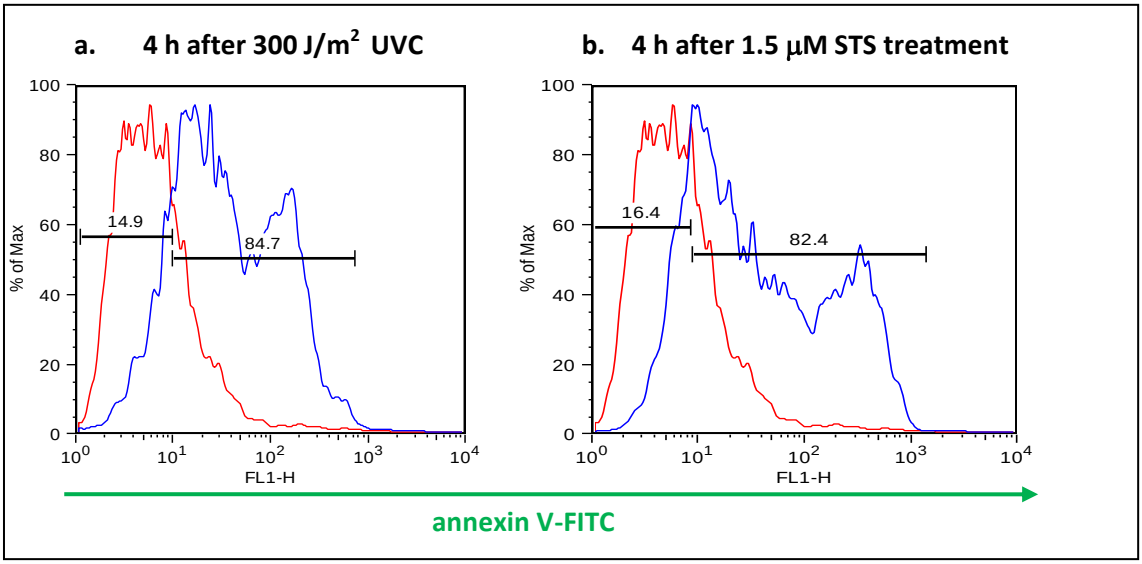

Fig.4.10. Determination of apoptotic cell death by annexin V staining in HeLa cells. 4 h after UVC irradiation, HeLa cells were stained with annexin V-FITC antibody and analysed by flow cytometry (panel a. blue histogram). As a positive control for surface binding of annexin V, HeLa cells were incubated for 4 h with staurosporine (1.5 µM) (panel b. blue histogram). Red histograms in both panels symbolise untreated HeLa cells. The images are representative of 2 independent experiments.

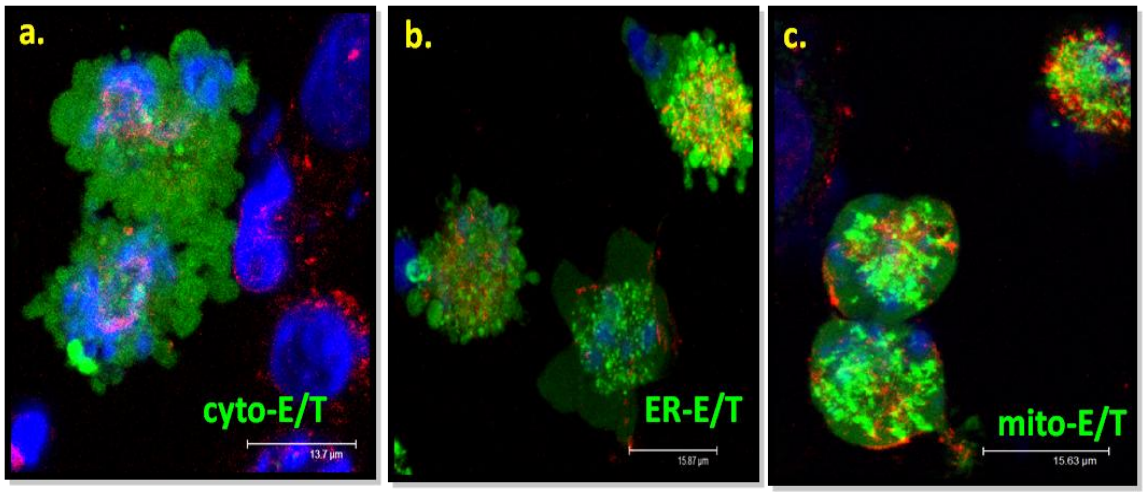

Fig. 4.11. Visualisation of altered expression of E/T model antigen following UVC-induced apoptosis. HeLa cells transfected with cyto-E/T, ER-E/T and mito-E/T panel a., b. and c. respectively, were fixed and analysed using confocal microscopy, 4 h following 300 J/m^2 UVC exposure. Green represents transfected E/T expression. In addition, to visualise plasma membrane and nuclei, HeLa cells were stained with WGA (5 µg/ml) and Hoechst (5 µg/ml) respectively. The images are representative of 3 independent experiments.

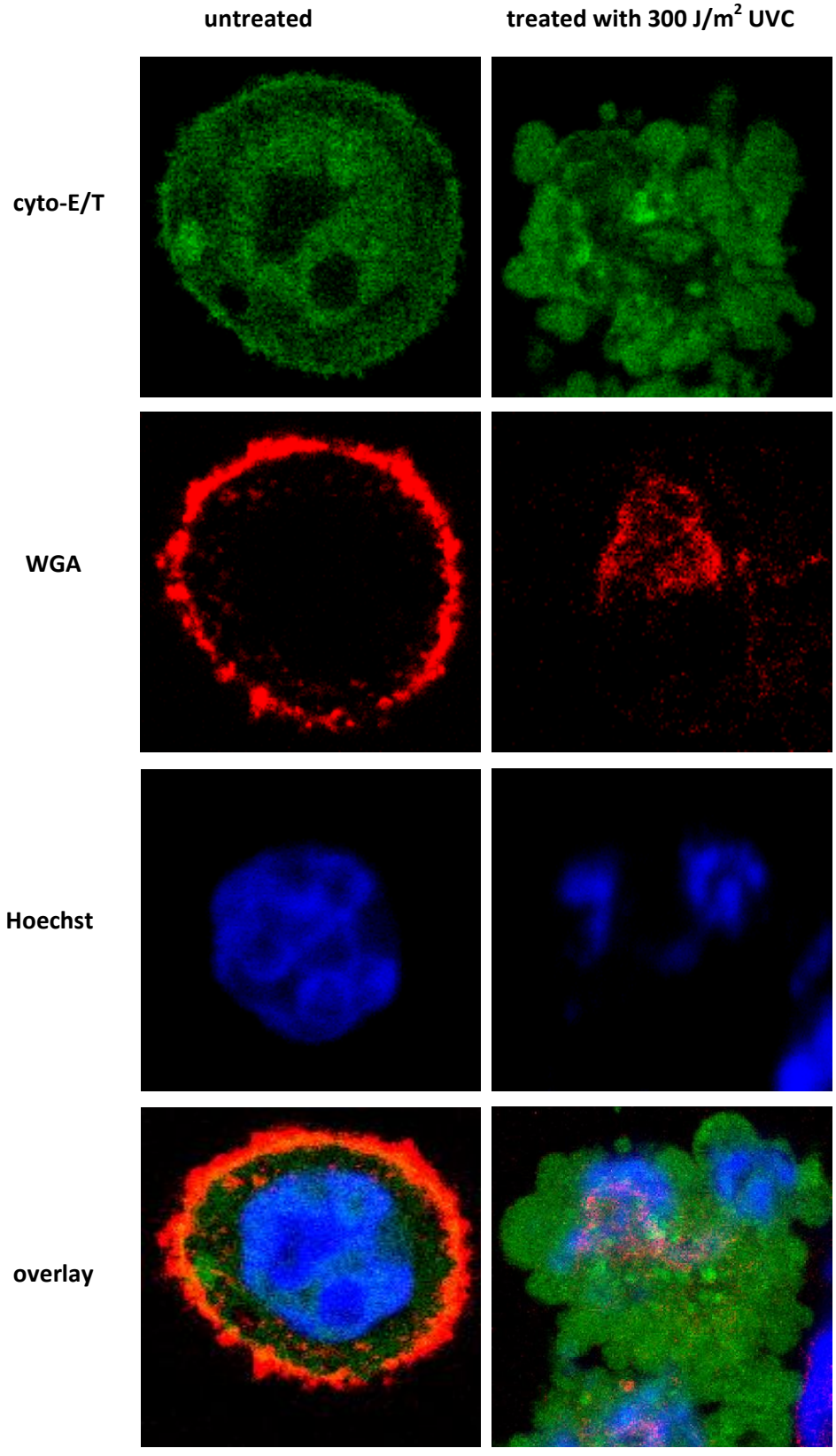

Fig. 4.12. Changes in the cellular morphology of cyto-E/T transfectants induced by UVC (300 J/m^2). 4 h after UVC irradiation HeLa cyto-E/T transfectants were fixed and directly examined using confocal microscopy. Green represents cyto-E/T, red shows WGA and blue demonstrates Hoechst, indicating the expression pattern of fusion protein, plasma membrane and nuclei respectively, of UVC treated HeLa cells (right column) or untreated transfectants (left column). The images are representative of 3 independent experiments.

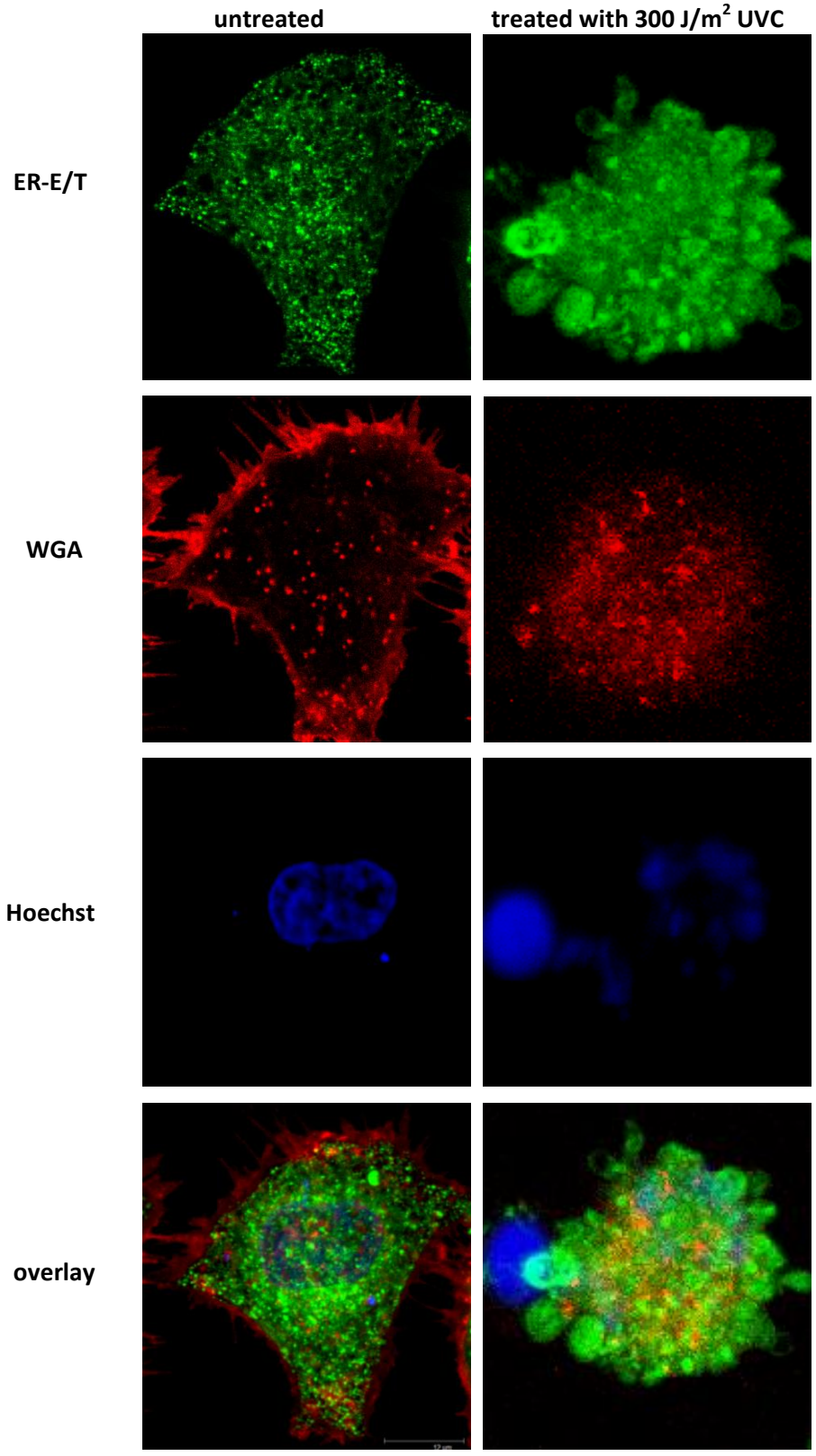

Fig. 4.13. Changes in the cellular morphology of ER-E/T transfectants induced by UVC (300 J/m^2). 4 h after UVC irradiation HeLa ER-E/T transfectants were fixed and directly examined using confocal microscopy. Green represents ER-E/T, red shows WGA and blue demonstrates Hoechst, indicating the expression pattern of fusion protein, plasma membrane and nuclei respectively, of UVC treated HeLa cells (right column) or untreated transfectants (left column). The images are representative of 3 independent experiments.

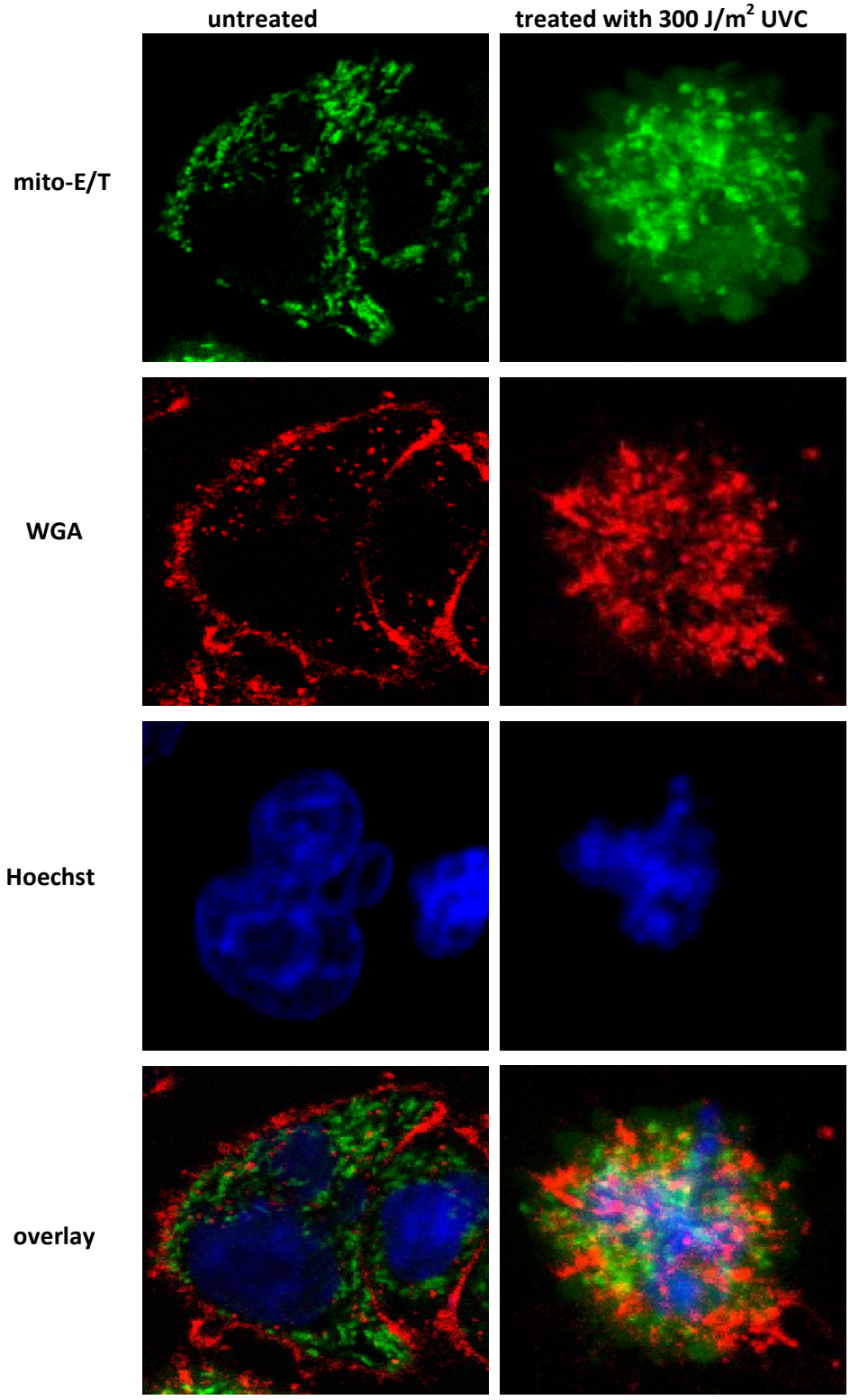

Fig. 4.14. Changes in the cellular morphology of mito-E/T transfectants induced by UVC (300 J/m^2). 4 h after UVC irradiation HeLa mito-E/T transfectants were fixed and directly examined using confocal microscopy. Green represents mito-E/T, red shows WGA and blue demonstrates Hoechst, indicating the expression pattern of fusion protein, plasma membrane and nuclei respectively, of UVC treated HeLa cells (right column) or untreated transfectants (left column). The images are representative of 3 independent experiments.

This was confirmed by further analysis of UVC treated ER-E/T transfectants. Data acquired from single ER-E/T transfectants was analysed both in vertical and horizontal planes to produce the images shown in **Fig. 4.15**. Indeed, the altered ER-E/T location can clearly be seen as a circle localised around the edge of apoptotic bodies. The redistributed ER-E/T expression present in the apoptotic body highlighted in **Fig. 4.15. panel b.** as a yellow arrow and is entirely overlaid with disrupted cell membrane as visualised by WGA staining. Thus, E/T was redistributed to the cell surface following UVC treatment.

a.

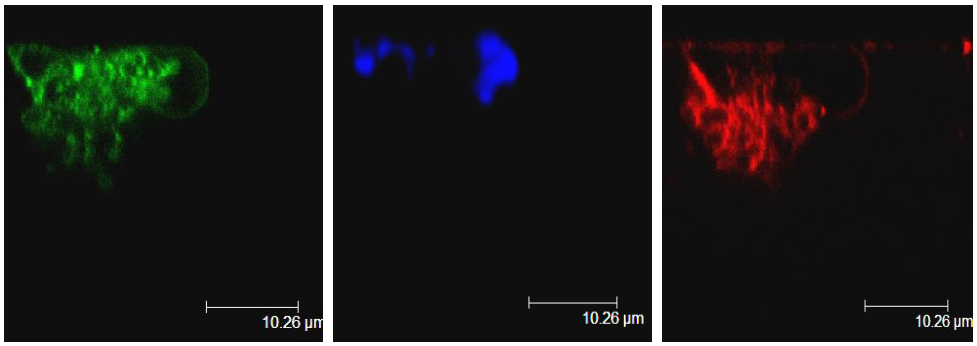

b.

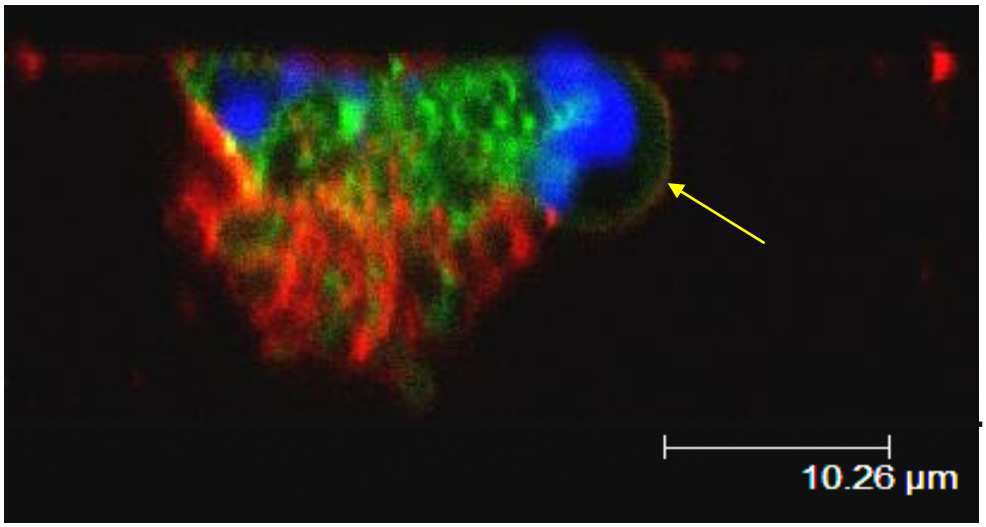

Fig. 4.15. Relocation of ER-E/T construct to the cell surface induced by UVC irradiation (300 J/m^2). Images captured using confocal microscopy showing a 3D projection of a single HeLa transfectant which was sectioned in a vertical and horizontal plane to directly visualise ER-E/T (green) relocated to the plasma membrane (red). Hoechst 3342 dye (blue) represents nuclei staining. The images are representative of 2 independent experiments.

4.3. Discussion

The ability to induce tumour cell apoptosis is an important property of a candidate anti-cancer drug (Frankfurt, Krishan 2003). Anthracyclines have recently been investigated as chemotherapeutic agents causing immunogenic cell death. However, previous work has documented the cytotoxic effect of doxorubicin as one of the most efficient drugs of cancer chemotherapy. In particular, this drug is generally related to its interaction with nuclear components, such as introduction of double strand breaks in DNA and topoisomerase II inhibition. According to Serafino et al. these changes in DNA structure correlate with apoptosis induction (Serafino et al., 1999). They observed that in melanoma cell line and erythroleukemia human cell line following doxorubicin treatment, both cell lines exhibited typical apoptotic morphological changes including condensation of nuclear chromatin, cell surface blebbing and cytoplasmic vacuolisation. Similar apoptotic characteristic such as the presence of membrane-bound apoptotic bodies and cell shrinkage can be seen in **Fig. 4.4.**, when HeLa cells were exposed to DX and MX for 4 h. The green apoptotic bodies might indicate that intracellular protein relocation to the cell surface occurs. Such relocated E/T might be then recognised by specific-B cells triggering immunogenicity and consequently leading to anti-tumour immunity.

Obeid described that MX has the ability to trigger apoptotic cell death but also to induce ERp57 and CRT (both ER chaperone proteins) relocation from ER to the cell surface in CT26 murine colon cancer cell lines (Obeid, 2008) (Obeid et al., 2007c). Such apoptotic cells were then better recognised by DC and tumour cells were rejected in those challenged mice. However, cells lacking ERp57 or with low expression of ERp57 could not be efficiently eliminated following MX treatment indicating that the activation of anti-tumour immunity was driven by surface expression of CRT or ERp57. This data clearly supports my observations that MX and DX treated HeLa transfectants relocated ER-E/T fusion protein to the surface of apoptotic bodies. In contrast, following STS treatment HeLa transfectants exhibited elongated morphology with no evidence of green apoptotic bodies' formation. In **Fig. 4.4.** it can be seen that E/T remained intracellular indicating that STS is an anti-cancer drug which causes non immunogenic cell lethality. This observation is also consistent with data provided by Obeid (Obeid et al., 2007b).

Anthracyclines also have strong effects on mitochondria activity. Tokarska-Schlattner et al. has observed numerous mechanisms for the inactivation of the mitochondrial respiratory chain by

anthracyclines (Tokarska-Schlattner et al., 2002). They proposed that these effects on mitochondria are mediated by the generation of free radicals, interaction with mitochondrial DNA, alteration of calcium exchange, lipid peroxidation inducing disturbance of mitochondrial membranes and consequently inactivating mitochondrial function. These results are consistent with our observations where HeLa cells treated with anthracyclines also decreased mitochondria activity. It has been confirmed by MTT test which quantified the metabolic dysfunction of mitochondrial reductase following anthracycline treatment (**Fig. 4.2.**). Inhibition of mitochondrial function was dose dependent in HeLa cells incubated with DX and MX. In particular, following 4 h incubation with 50 μM DX, the viability of HeLa cells was 70%, 50% when incubated with 100 μM DX and only 25% following 200 μM DX treatment. A similar pattern was seen following MX treatment. HeLa cells incubated with 20 μM MX for 4 h were in 90% viable, 40 μM MX caused 80% viability and only 70% cells were viable after treatment with 80 μM MX.

After optimizing apoptotic conditions, I decided to test whether relocated ER-E/T is acquired by TTCF-specific B cells and presented to CD4+ T cells. To this end, following 4 h treatment with anthracyclines, HeLa ER-E/T transfectants were incubated with specific B and T cells for 24 h. Before transferring the apoptotic ER-E/T HeLa cells into fresh well containing the TTCF-specific B and T cells, HeLa cells were extensively washed to exclude possible carryover of any remaining anthracycline. Despite this preventative step, I observed inhibition of antigen presentation following anthracycline treatment. It was likely, that HeLa cells treated with DX or MX accumulate intracellular anthracyclines (data not shown). **Fig. 4.5.** shows an inverse correlation between the number of apoptotic HeLa cells and IL-2 production by T cells. It is possible that 24 h after drug treatment, some HeLa cells undergo necrotic death and release their intracellular content including anthracyclines when the plasma membrane was ruptured resulting in T cell cytotoxicity.

This hypothesis is consistent with the studies performed by Ferraro et al. demonstrating that anthracyclines trigger apoptosis in both non-activated and phytohemagglutinin-activated human peripheral blood lymphocytes (Ferraro et al., 2000). In agreement with *in vitro* data, a single intraperitoneal injection of DX or MX in Balb/c mice also induced T cell depletion in lymph nodes, and in the thymus. These data indicate that anthracyclines may induce major peripheral T cell deletion, a property not shared by many cytotoxic agents and may explain why my proliferation assays failed.

To test whether anthracyclines have a strong cytotoxic effect on lymphocytes, I performed the MTT test measuring cell viability. This experiment clearly showed that similar to T lymphocytes (Ferraro et al., 2000), T cell hybridomas are extremely sensitive to anthracyclines as even 20 nM of MX induced cell death (**Fig. 4.7.**). Therefore, measurement of antigen redistribution following anthracycline treatment using T cell hybridomas was impractical. The solution to this problem was to test a different apoptotic-inducing agent which had previously been shown to trigger immunogenic cell death and would hopefully have limited effects on co-cultured T and B cell hybridomas. The use of UVC has been documented to induce immunogenic cell death, interacting with DNA to produce a range of mutations due to genomic instability. Also, UVC directly induces damage to intracellular organelles including ER or mitochondria that finally leads to cell death (Choi et al., 2000). I therefore optimised the dose of UVC irradiation required to induce cell death in HeLa cells using the MTT test. The highest HeLa lethality was observed after 300 J/m^2 irradiation. Therefore, I analysed the morphological changes seen in HeLa transfectants expressing cyto, mito and ER-E/T following 300 J/m^2 UVC using confocal microscopy. In **Fig. 4.11.** this can be observed as the appearance of apoptotic green blebs and chromatin condensation. Furthermore, to confirm that UVC irradiated HeLa cells are dying by apoptosis, I performed annexin V binding and analysis by flow cytometry. **Fig. 4.10.** demonstrates approximately 80% of HeLa cells bind annexin V – FITC either following STS treatment or 300 J/m^2 UVC treatment.

Finally the confocal microscopy analysis clearly showed that HeLa cells exposed to 300 J/m^2 UVC exhibited typical apoptotic morphological changes including chromatin condensation and fragmentation as indicated by strong Hoechst staining. Also membrane disruption, represented by asymmetries diffused pattern of WGA staining, was seen. Importantly, in cyto-E/T and ER-E/T transfectants, the formation of green apoptotic bodies was also observed (**Fig 4.12.** and **4.13.**). The E/T present in HeLa apoptotic bodies co-localised with the WGA membrane dye (indicated by the orange dots). Furthermore images, which were produced by sectioning in vertical and horizontal planes to directly visualise the magnified cell membrane, clearly demonstrated ER-E/T antigen redistribution to the plasma membrane by its co-staining with the WGA membrane dye (**Fig. 4.15.**).

All these observations show that UVC induces E/T relocation to the cell surface. As UVC-mediated intracellular protein relocation has previously been shown to trigger immunity, my observations may indicate that relocated E/T may be acquired by antigen-specific B cells for presentation to CD4+ T cells. This novel aspect of antigen relocation will be discussed in **Chapter 6**.

In conclusion:

Both DX and MX anthracyclines were shown to have cytotoxic effect on HeLa cells leading to apoptosis. This was observed using light and immunofluorescence microscopy as well as confocal microscopy (**Fig. 4.1.** and **Fig. 4.4.**). This form of cell death was characterised by cell shrinkage and the formation of apoptotic bodies that contained the green fusion protein E/T.

Nevertheless, in further experiments the ability of anthracycline-induced relocation to trigger B cell-mediated antigen acquisition and presentation to CD4+ T cells could not be tested, due to high sensitivity of T cell hybridomas to this drug. Therefore, I examined the consequences of UVC-treatment as an alternate means of inducing E/T relocation. Following optimisation of the dose and time of UVC exposure, HeLa cells were also examined for evidence of apoptosis. **Fig. 4.10.** demonstrates annexin V-FITC binding to surface PS in apoptotic cells and **Fig. 4.8.** shows the mitochondrial reductase inhibition as represented by a decreased number of cell viability in UVC treated HeLa cells using the MTT test. Also images obtained from confocal microscopy showed that following treatment with 300 J/m^2 UVC, HeLa transfectants exhibited typical apoptotic hallmarks including chromatin condensation, plasma membrane disruption and the relocation of intracellular E/T to the cell surface of apoptotic bodies (**Fig. 4.12.** and **4.13.**).

- 5. Generation of TTCF-specific T cell hybridomas -

5.1. Introduction

This study aimed to test the hypothesis that antigen expressed by apoptotic tumour cells can be recognised by antigen-specific B cells. This recognition, caused by apoptotic modification of normal protein localisation, can finally lead to the activation of tumour-specific T cells. To test this hypothesis in an *in vitro* system, **Chapters 2**, **3** and **4** have described model antigens that were targeted to the various subcellular compartments in HeLa cells. In particular, **Chapter 4** describes the relocation of E/T to the cell surface following either anthracycline or UVC treatment. In order to establish whether this relocated model antigen is able to induce B cell-mediated immunity, antigen-specific B and T cell hybridomas are required.
Our laboratory previously has generated TTCF-specific B cell lines (A20-TTCF). This chapter documents the generation of a novel TTCF-specific T cell hybridoma, which can be used to study the presentation of TTCF.

Since the original discovery of lymphocyte hybridization by Kohler & Milstein (1975), a number of investigators have used this technology to study T cell function. The first T cell hybrids were obtained by fusing activated T cells with EL 4 murine lymphoma (Taniguchi and Miller, 1978). However, the generated T cell hybridomas from EL 4 cells were very unstable. Since then, a major effort has been made to obtain stable populations of antigen-specific T cell hybridomas. Therefore, most of the fusions are currently performed with the TCR-/- BW 5147 mouse T cell line, because it is more likely to generate stable T cell hybridomas than EL4 cells (White et al., 2000).
BW 5147 cells have been characterised to have non-MHC-restricted, non-specific regulatory activities in mixed lymphocyte reactions. Therefore, fusion of BW 5147 with antigen-specific T cells isolated from immunized mice gives a great opportunity to measure antigen response in a long term experiments. In particular, assays detecting T cell hybridoma activation by the production of IL-2 production can be used as a very sensitive read out for the recognition of peptide/MHC complex formation by APC. There are a number of ways to detect IL-2 secreted by activated T cell hybrids. Our laboratory has previously used several of these and has selected to use the IL-2 dependent T cell line CTLL-2 based on high IL-2 sensitivity. Incubation of CTLL-2 in the presence of IL-2 causes rapid cell division which can be measured by the incorporation of radioactive thymidyne added to the culture media. As described in this

chapter, I generated and characterised TTCF-specific T cell hybridomas which allowed me to study the presentation of E/T following its relocation and acquisition by TTCF-specific B cells (**Fig. 5.1.**).

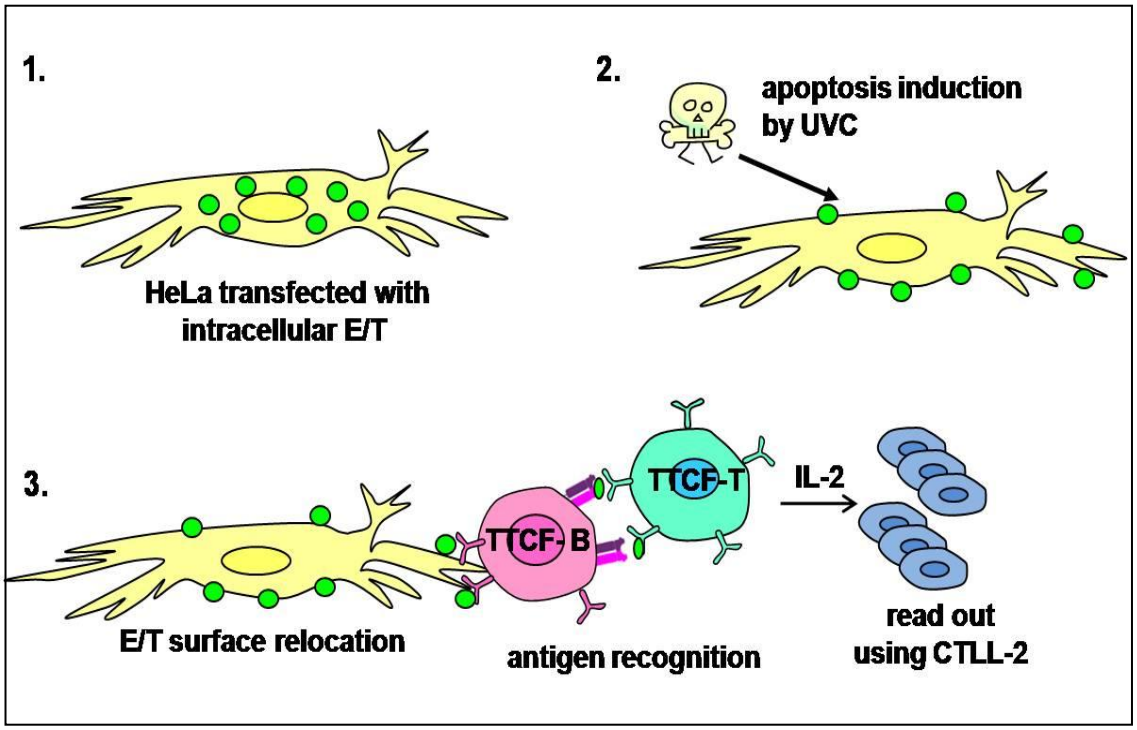

Fig. 5.1. A schematic representation of proliferation assay of relocated intracellular E/T (1.) following UVC treatment (2.) and recognised by TTCF-specific B cells (3.). Antigen acquisition by B cells leads to peptide/MHC complex formation that stimulates the activation of TTCF-specific CD4+ T cell hybridomas. Consequently, activated TTCF-specific T cell hybridomas produce IL-2 which can be measured by the proliferation of the IL-2 dependent T cell line CTLL-2.

5.2. Results

5.2.1. T cell hybrid generation

Balb/c mice were immunized sub-cutaneously in one hind leg with 50 μg of recombinant E/T emulsified with the adjuvant TitreMax. After 10 days, mice were killed and cells were isolated from the popliteal lymph nodes. Following *in vitro* re-stimulation with 50 μg/ml of E/T, blasts were fused with the TCR negative lymphoma fusion partner BW 5147 T cell lymphoma. The fusions were selected in hypoxantine-aminopterin-thymidyne (HAT) media.

Most mammalian cells have two pathways to synthesise DNA (Foung et al., 1982). The first one, *de novo* pathway, is dependent on folic acid as a coenzyme and the second salvage pathway relies on the enzyme hypoxanthine phosphoribosyltransferase (HPRT). BW 5147 T cell lymphoma has a mutation in the HPRT enzyme and is therefore entirely dependent on *de novo* pathway for its survival.

The conventional HAT selecting medium contains aminopterin, a drug which blocks *de novo* DNA synthesis leading to lethality of HPRT-deficient BW 5147 T cell lymphoma partners. Hence, un-fused BW 5147 cells will die as they cannot produce nucleotides by the *de novo* pathway. Furthermore, un-fused T cells will also die as they have a limited life span in culture. Thus, only fused T cell-lymphoma hybrids will survive in long-term cultures.

After approximately 2 weeks in HAT selecting medium, T cell hybridomas were then gradually moved to HT-containing medium. This medium does not contain aminopterin, only hypoxantine and thymidyne which help T cell hybridomas to growth. Finally, T cell hybridomas were transferred to complete RPMI. Following a 4 week selection process, approximately 50 HAT resistant hybrids were screened for TTCF specificity using standard antigen presentation assays. The murine macrophage cell line (J774) was used as APC. For these assays, $5x10^4$ of each candidate hybridomas were co-cultured with two concentrations of recombinant TTCF and $5x10^4$ J774 for 24 h in 96 well plates. As a positive control for T cell stimulation, I used concanavalin A (ConA) at a concentration of 5 μg/ml.

Antigen specific IL-2 production by hybridomas was measured by transferring the supernatant from these assays into fresh wells containing $3x10^4$ of the IL-2 dependent line CTLL-2. To determine whether any of the hybrids were specific to EGFP, I also incubated each hybrid with two concentrations of recombinant soluble E/T. In **Fig. 5.2.**, the IL-2 dependent proliferation

(measured by ^{3}H-thymidine DNA incorporation) of CTLL-2 cells is shown for 12 representative hybrids. The vast majority of hybrids show no evidence of TTCF or E/T specificity and also no significant response to ConA (for example hybrids 1-8, **Fig. 5.2. a.**). However, three hybrids (no. 38, 39, 52) clearly showed TTCF specific proliferation. In particular, hybridomas no. 39 and 52 respond the strongest to both soluble TTCF and E/T antigens as indicated by the grey and blue column respectively (**Fig. 5.2. b.**). Thus, I further characterised these two hybridomas.

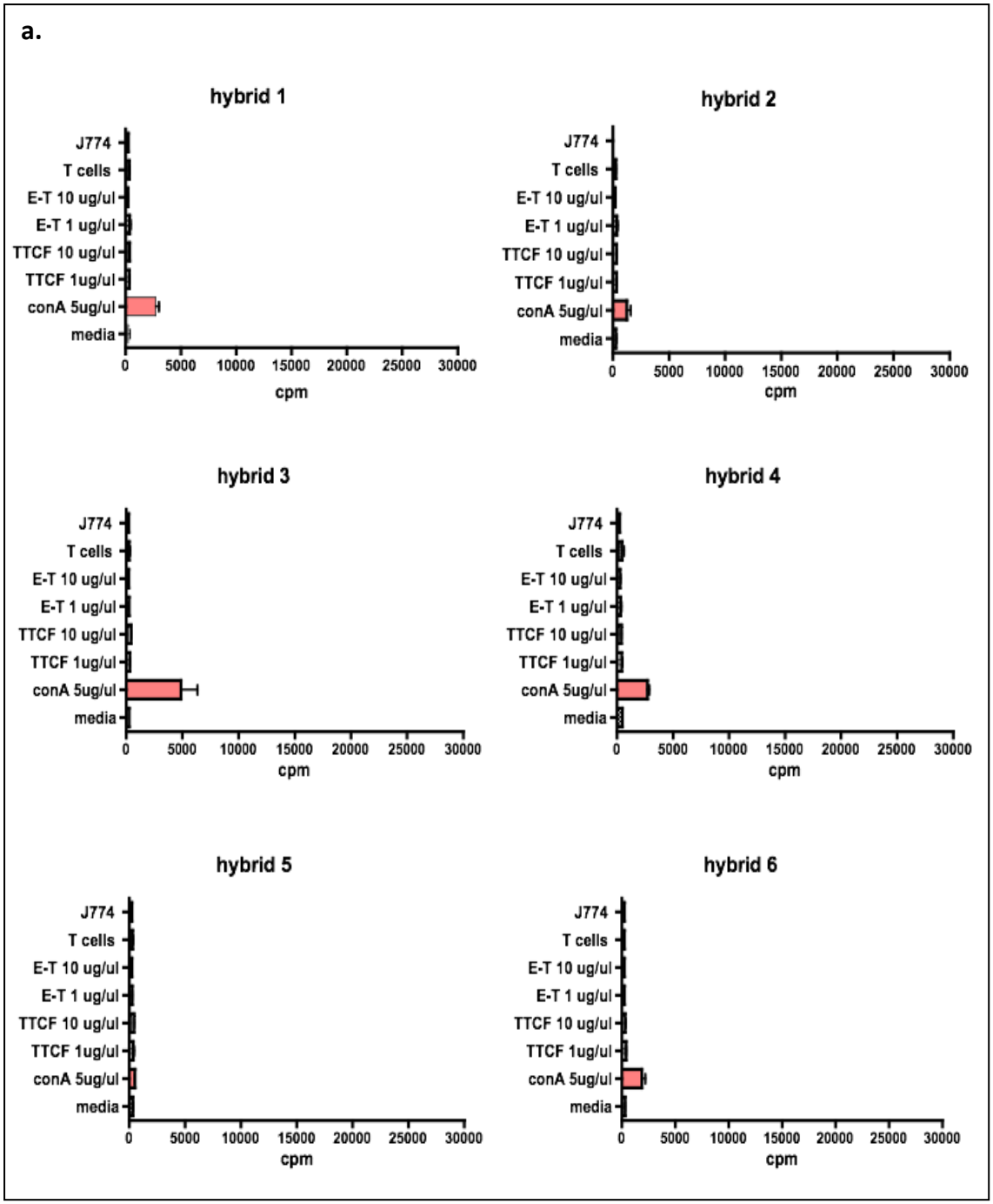

Fig. 5.2. a. A screening of T cells hybridomas specific for TTCF using two concentrations of soluble TTCF (1 μg/ml and 10 μg/ml) and E/T (1 μg/ml and 10 μg/ml. Shown are 6 representative hybrids (1-6). Proliferation assays screening T cell hybridomas were performed once.

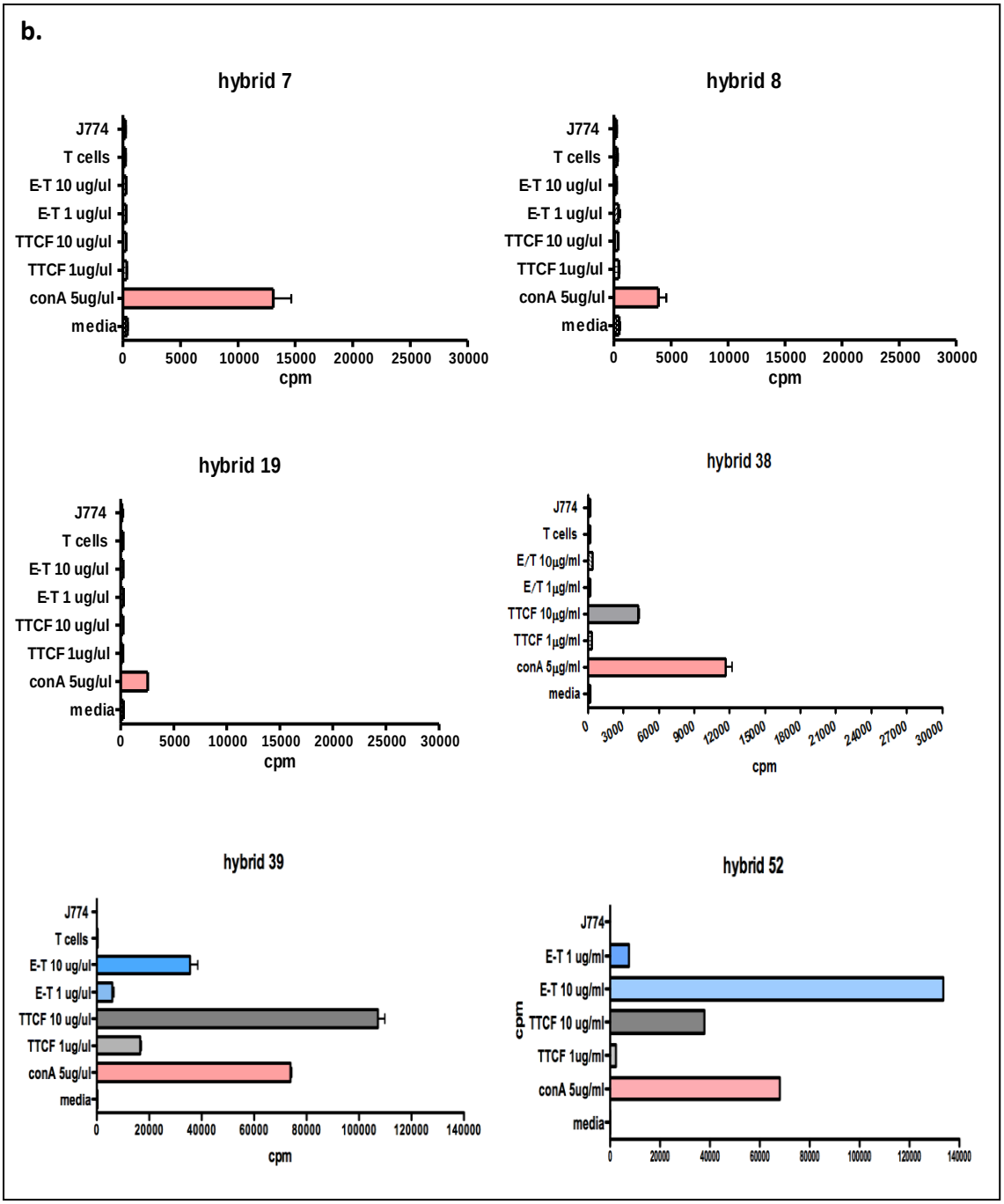

Fig. 5.2. b. A screening of T cells hybridomas specific for TTCF using two concentrations of soluble TTCF (1 µg/ml and 10 µg/ml) and E/T (1 µg/ml and 10 µg/ml. Shown are 6 representative hybrids (7, 8, 19, 38, 39, 52). Proliferation assays screening T cell hybridomas were performed once.

Following initial selection of two the best responding T cell hybridomas (no. 39 and 52), I re-tested them again using graded concentrations of TTCF and TTCF-specific B cells as APC (blue line in **Fig. 5.3. panel a.** and **b.**). In addition, presentation by non-specific B cells (A20) (red line in **Fig. 5.3. panel a., b.**) and macrophages cell lines J774 (purple and green line in **Fig. 5.3. panel c**) were used for comparison. When the TTCF-specific B cells were used as APC, presentation was significantly increased, compared to that seen with either J774 or non-specific B cells with T cell responses being detected at significantly lower concentrations of TTCF. This is consistent with other studies using antigen-specific B cell (Ferrari et al., 1997; Knight et al., 1997; Lanzavecchia and Bove, 1985).

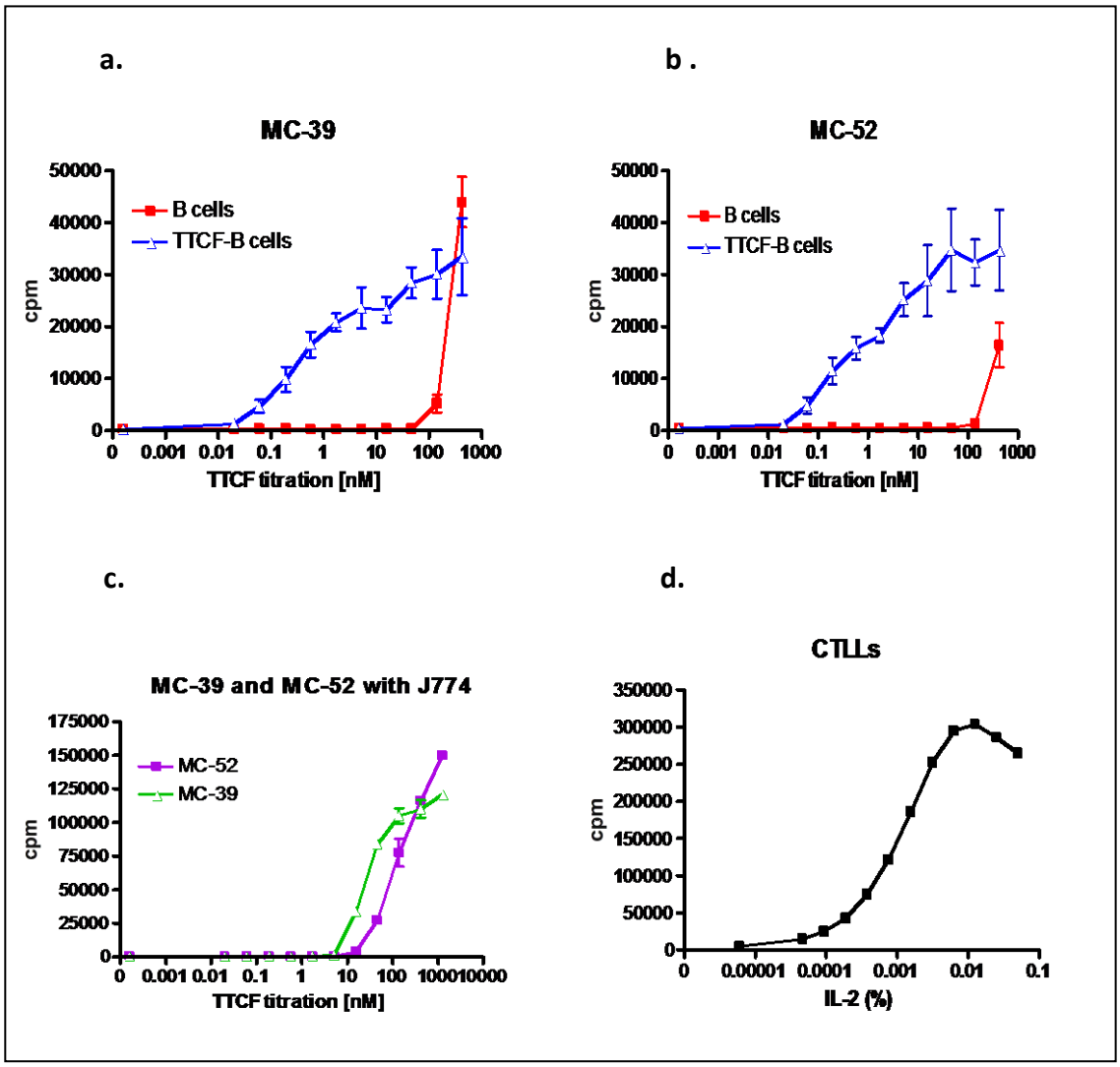

Fig. 5.3. Proliferation assays of the generated hybrids MC-39 and MC-52 against various doses of soluble TTCF. Three types of APC cells were used in this experiment: TTCF-specific B cells A20-3A5, non-specific B cells A20 (panel a. and b.) and J774 microphage cell line (panel c.). Panel d. shows control proliferation of CTLL-2 lines responding for titration of recombinant IL-2.

5.2.2. Characterisation of surface marker and TCR repertoire in MC-39 and MC-52 T cell hybridomas

Newly generated hybrids MC-39 and MC-52 were also characterized for expression of T cell markers using flow cytometry. **Fig. 5.4.** (**panel** from **a** to **d.**), represents the histograms for CD8, CD4 and TCR staining. Histograms illustrated that both CD4 and TCR were expressed by both generated T cell hybridomas MC-39 and MC-52. Control staining were performed using murine thymocytes for specificity of anti-TCR, CD4, CD8 antibodies (**Fig. 5.4., panel e.**).

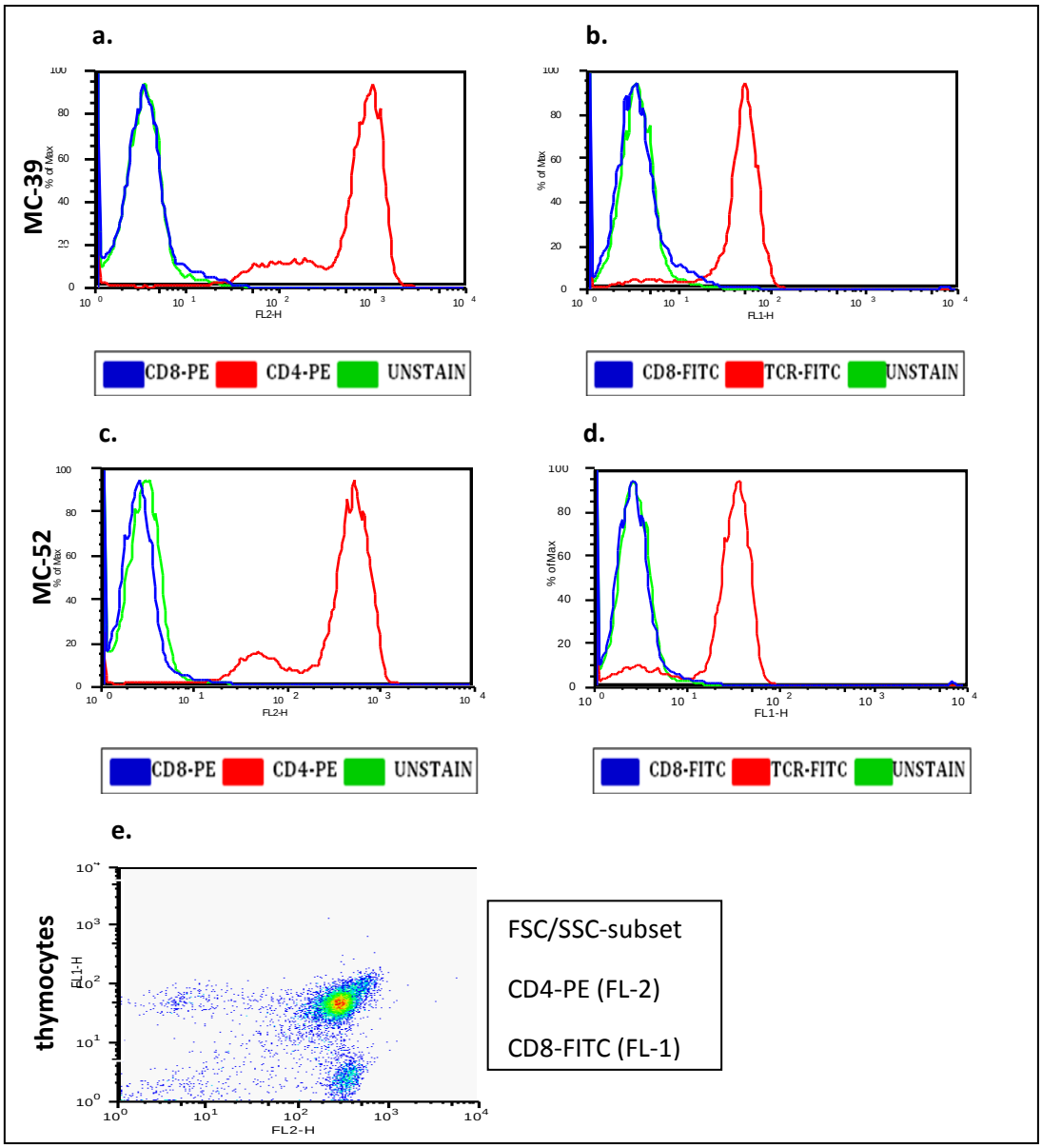

Fig. 5.4. Flow cytometry analysis of the generated T cell hybrids. The expression of TCR, CD4 and CD8 markers was measured on the cell surface. Histograms overlays show the differential expression of TCR, CD4 and CD8 in hybrid no. 39 (panel a. and b.) and 52 (panel c. and d.). Green represents unstained cells. Panel e. represents staining of murine thymocytes as a positive control for the anti-CD4 and anti-CD8 antibodies used in this experiment.

In addition, the TCR Vβ gene usage of MC-52 T cell hybrids was also tested. To this end, I used a screening panel of 15 specific monoclonal antibodies against different Vβ TCR chains directly conjugated with FITC. Following incubation with this panel of antibodies, MC-52 T cell hybridomas were analysed by flow cytometry. In **Fig. 5.5.**, it can be seen that MC-52 T cells incubated with an anti-Vβ2 antibody gave one log shift (red line) highlighted by a green arrow in antibody staining. In contrast, the rest of the 14 antibodies (specific for various other TCR Vβ chains) showed negligible binding compared to the auto-fluorescence seen with unstained cells.

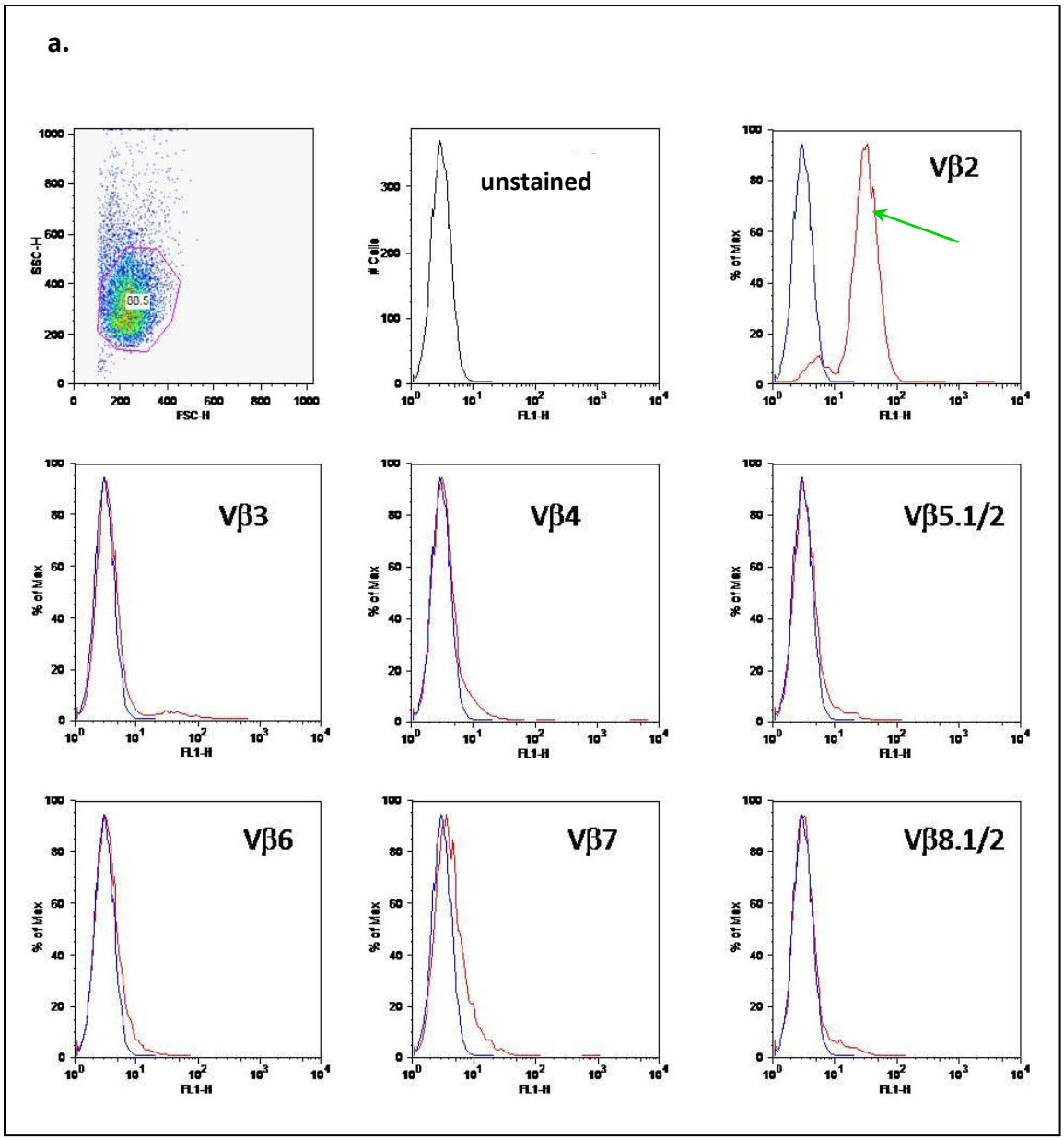

Fig. 5.5. a. Characterization of the TCR structure of MC-52 hybridomas using mouse Vβ TCR screening panel. Flow cytometry analysis of MC-52 hybridomas stained with FITC-conjugated monoclonal antibodies which recognise mouse Vβ2, 3, 4, 5.2, 6, 7, 8.1 and 8.2 T cell receptor (red histogram) respectively. Blue histograms represent unstained MC-52 T cells. Antibody reacting with the Vβ2 exclusively binds to TCR receptor of MC-52 hybridomas.

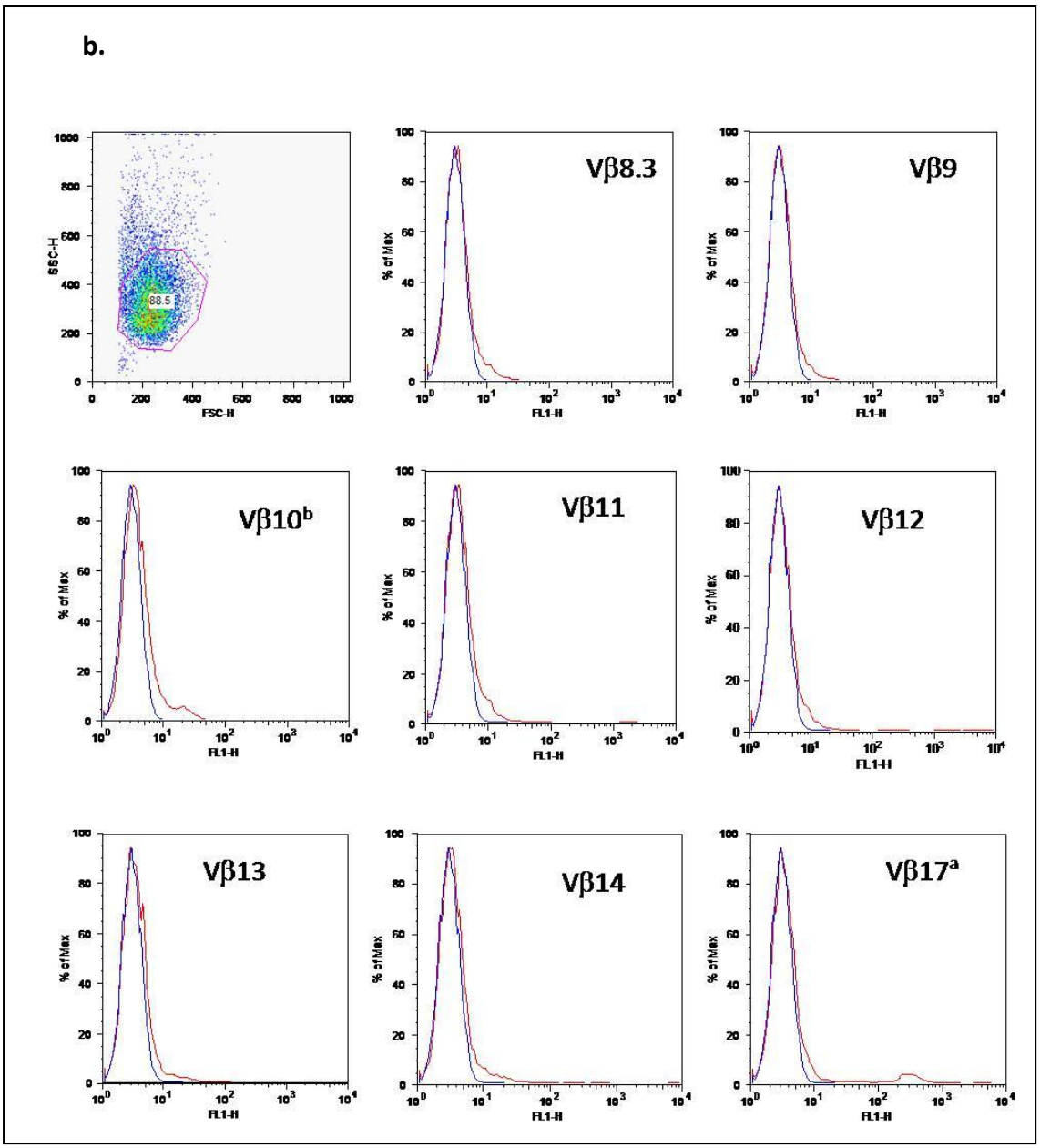

Fig. 5.5. b. Characterization of the TCR structure of MC-52 hybridomas using mouse Vβ TCR screening panel. Flow cytometry analysis of MC-52 hybridomas stained with FITC-conjugated monoclonal antibodies which recognise mouse Vβ 8.3, 9, 10^{b}, 11, 12, 13, 14 and 17^{a} T cell receptor (red histogram) respectively. Blue histograms represent unstained MC-52 T cells. Antibody reacting with the Vβ2 exclusively binds to TCR receptor of MC-52 hybridomas.

This indicated that MC-52 T cell hybridomas are a homogeneous population of CD4+ T cell hybridomas expressing the TCR Vβ2 chain.

5.2.3. Identification of epitope specificity in MC-52 T cell hybrids

In order to characterise the epitope of TTCF recognised by MC-52 hybridomas, I incubated these cells with APC and a panel of overlapping peptides that span the entire sequence of TTCF (kind gift from Colin Watts, Dundee University (Antoniou and Watts, 2002)). These 88, 17-mer peptides were originally supplied as 22 pools (A to V), each containing 4 individual peptides (**Fig. 5.6. panel a.**). To this end, I measured the response of MC-52 T cells hybridomas when incubated with each of these 22 pools. In this experiment, TTCF-specific B cells were used as APC. This initial test allowed me to identify pools containing peptides which span the epitope recognised by MC-52. In **Fig. 5.6. panel b.**, it can clearly be seen that MC-52 responded to the peptides present in pool M (purple column) as indicated by a strong response of approximately 60 000 cpm.

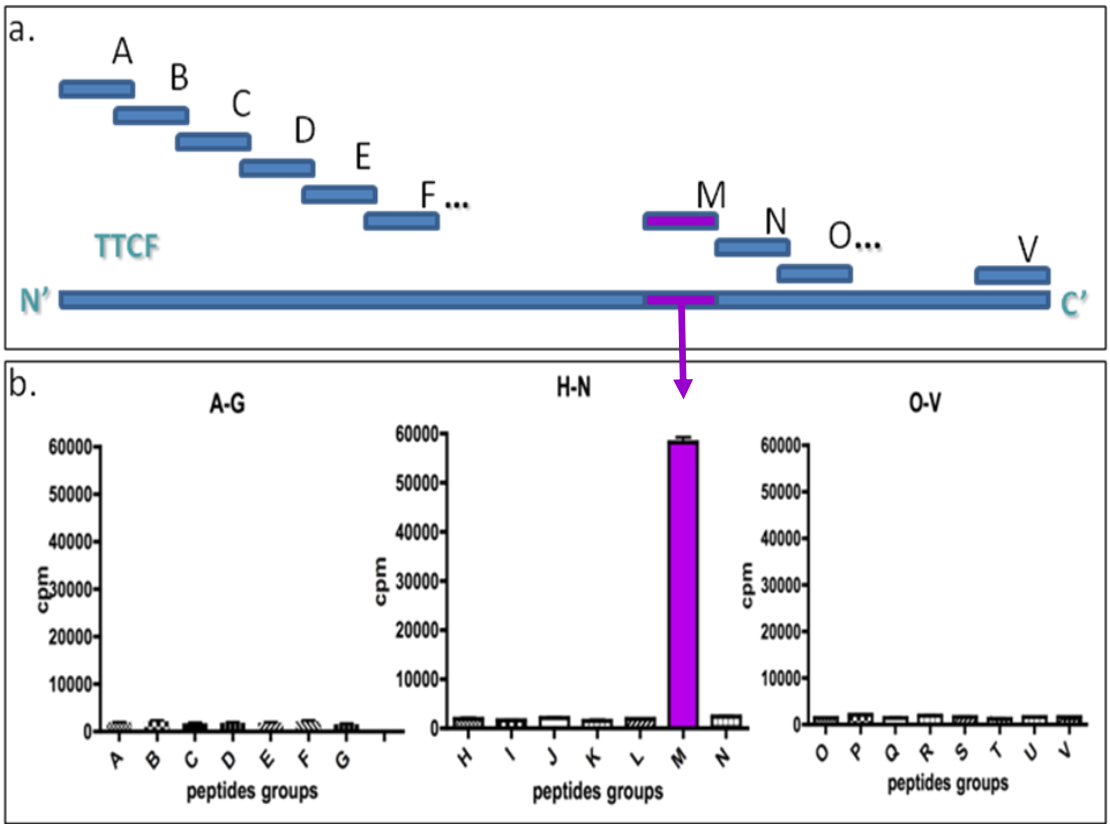

Fig. 5.6. Determination of MC-52 fine specificity using a panel of overlapping peptides. Panel a. shows schematic representation of overlapping 17-mer peptides pooled into groups (from A to V) that span the entire TTCF fragment protein. Panel b. represents proliferation assays of MC-52 hybrids responded for above groups of 17-mer peptides (2 μg/ml each). TTCF-specific B cells were used as APC in this experiment.

Consequently, I measured the response of MC-52 to the individual peptides contained in group M. As a positive control, pool M was re-used and a negative control was represented by pool A. As shown in **Fig. 5.7.**, MC-52 T cells recognised only one 17-mer peptide (52) as indicated by a strong response reaching approximately 110 000 cpm (pink column).

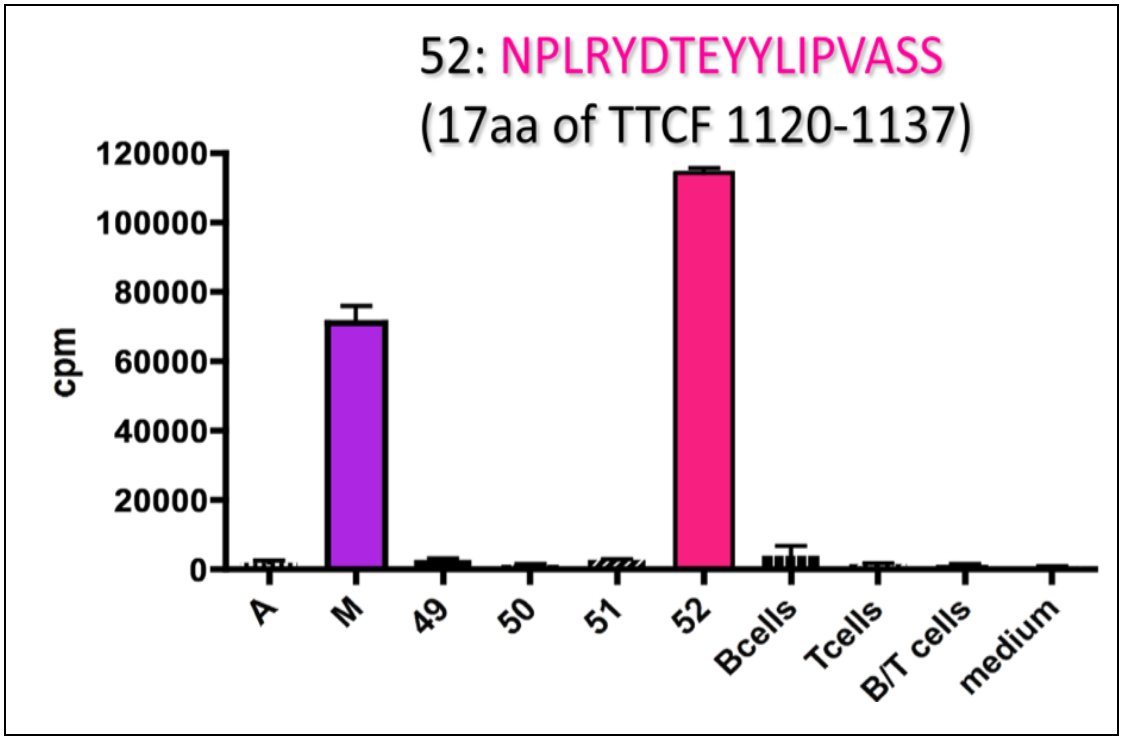

Fig. 5.7. Determination of MC-52 fine specificity using a panel of overlapping peptides. Proliferation assays of MC-52 hybrids significantly responded only for peptide 52 (red column) previously pooled in group M together with 49, 50 and 51 peptides (2 μg/ml each). As negative controls, peptides from group A, B and T cells without antigen or medium only were used in this experiment. As a positive control pool M were added to the assay (purple column). TTCF-specific B cells were used as APC in this experiment.

The 3D structure of TTCF and the localisation of the 17-mer peptide 52 are illustrated in **Fig. 5.8**.

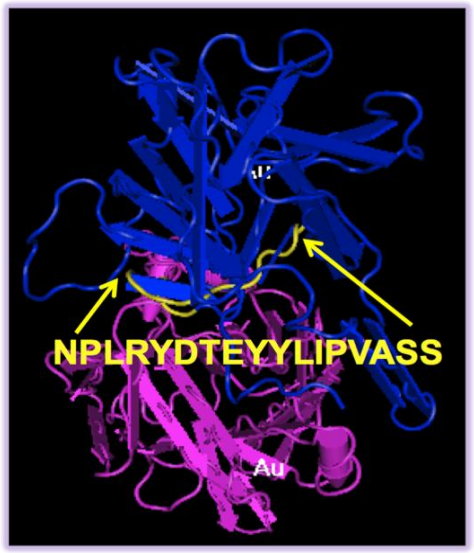

Fig. 5.8. The 3D structure of TTCF including 17-mer sequence of peptide 52 indicated by a yellow line.

I have previously shown that TTCF-specific B cells present TTCF protein more efficiently than that seen by non-specific B cells (**Fig. 4.5.**). This is demonstrated in antigen presentation assays where TTCF-specific B cells require considerably less antigen than non-specific B cells to induce a similar magnitude of response in MC-52. This is consistent with other studies showing that processing of TTCF is enhanced by its binding and internalization as part of the TTCF-specific BCR complex (Knight et al., 1997). To confirm that peptide 52 was the natural processing product recognised by MC-52, I compared the presentation of either peptide 52 or soluble TTCF protein by both TTCF-specific and non-specific B cells. As expected, **Fig. 5.9. panel a.** demonstrates that TTCF-specific B cells are more efficient in processing and presentation of TTCF to MC-52 T cells. When I incubated B cells with T cells in the presence of TTCF protein BCR-mediated processing was evident with 10 μM of TTCF only inducing a response when TTCF-specific B cells were used. In contrast, when both B cells were incubated with peptide 52 an identical response was observed (**Fig. 5.9. panel b.**).

This experiment clearly demonstrated that MC-52 clones are specific for peptide 52 which could be presented by specific and non specific APC equally. However, when T cell hybridomas were incubated with soluble protein, TTCF specific-B cell were required for efficient antigen

recognition (via specific BCR) and processing of TTCF with peptide/MHC complexes required by MC-52 T cell hybridomas.

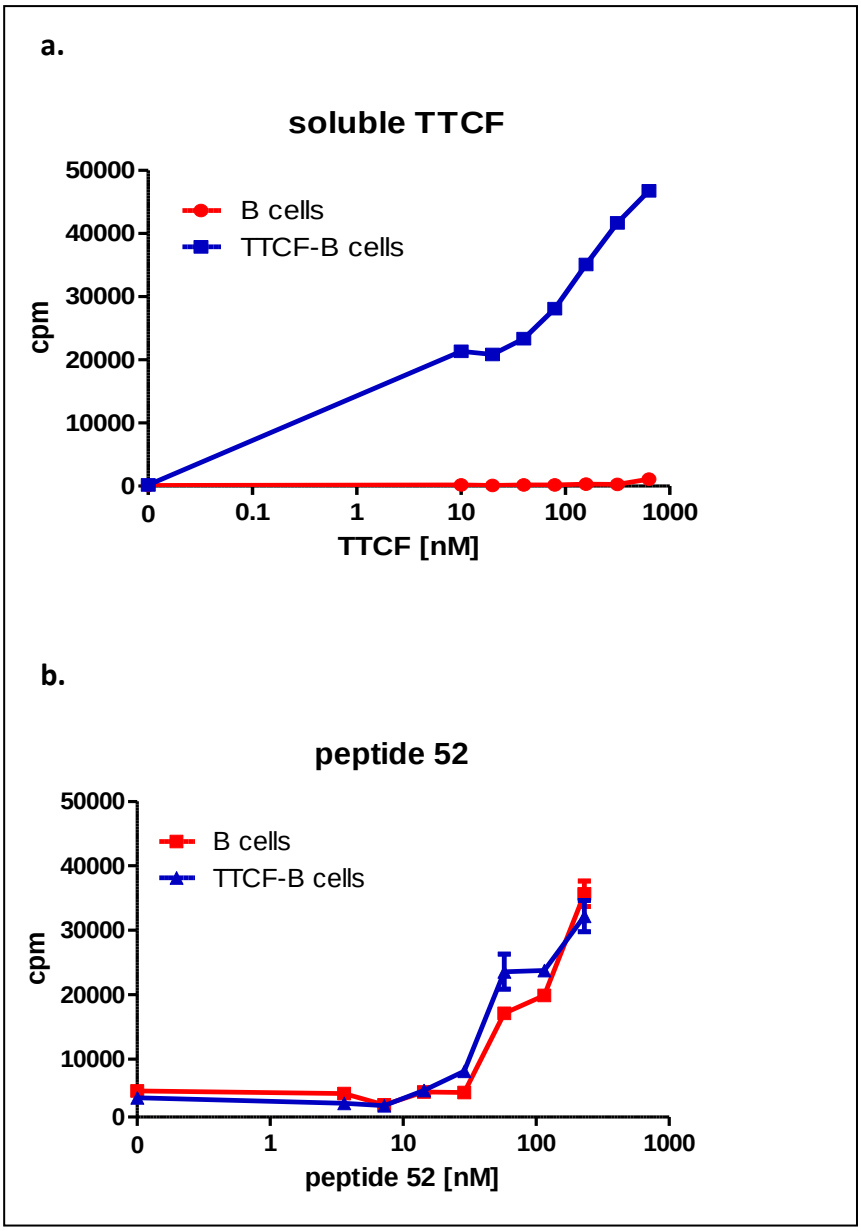

Fig. 5.9. Determination of MC-52 fine specificity. Proliferation assays of MC-52 T cell hybridomas responded for titrated dose of soluble TTCF presented only by TTCF-specific B cells (panel a. blue line) but not non-specific B cells (panel a. red line). Panel b. shows pooled peptides from group M containing peptide 52 (panel b.) presented similarly either by TTCF-specific (blue line) or non-specific B cells (red line) in MHC class II pathway to MC-52 T cell hybridomas.

5.2.4. Characterisation of the MHC restriction of MC-52 T cell hybridomas

To establish the H-2d class II molecule involved in the presentation of peptide 52 to MC-52, I incubated MC-52 T cell hybridomas with murine fibroblasts (gifts from John Robinson), which either express H-2A^d or H-2E^d class II molecules. To avoid any deficiency of antigen processing which may be present in these cells, I performed these experiments with pre-processed peptide 52. Following titration of peptide 52, both H-2A^d and H-2E^d expressing fibroblasts were plated with MC-52 into 96 well plates. 24 h later supernatants were transferred into a new plate containing both radioactive thymidyne and IL-2 deprived CTLL cells. Subsequently, IL-2 production was measured as previously described. In **Fig. 5.10.**, it can be seen that peptide 52 was exclusively presented by the fibroblasts expressing H-2A^d molecules and consequently recognised by MC-52 T cell hybridomas (blue line). In contrast, fibroblasts expressing H-2E^d molecules did not present peptide 52 (pink line). This experiment clearly demonstrates that MC-52 T cell hybridomas are H-2A^d restricted.

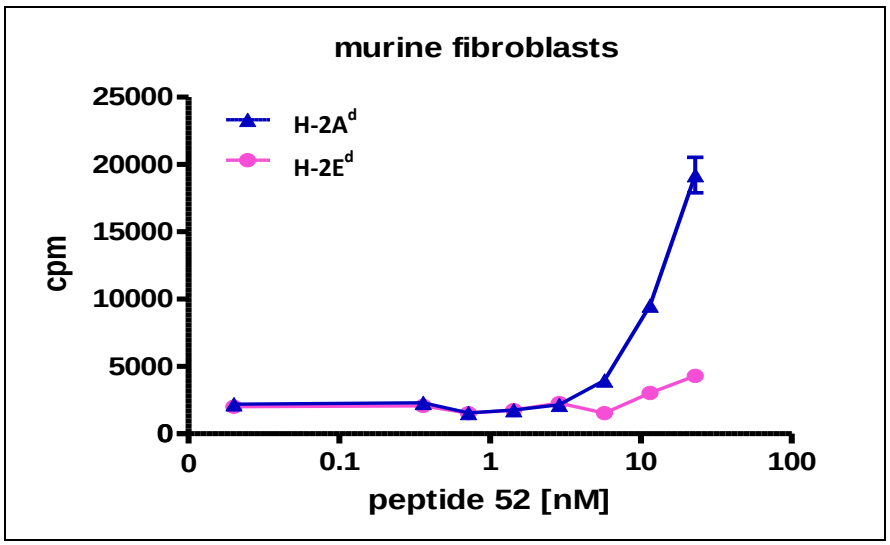

Fig. 5.10. Proliferation assay of mouse fibroblasts as a antigen presenting cells for MC-52 T cell hybridomas. Murine fibroblasts transfected with H-2A^d (blue line) or H-2E^d (pink line) MHC class II molecules were incubated with graded dose of peptide 52 and TTCF-specific T cell hybridomas MC-52 for 24 h. IL-2 production was measured as described previously.

5.2.5. Detection of surface E/T using antigen-specific B and T cells

To determine whether TTCF-specific B cells are capable of presenting TTCF acquired from mem-E/T transiently transfected HeLa cells (as opposed to soluble recombinant TTCF), I performed pilot proliferation assays. HeLa cells were transfected with the mem-E/T construct and one day later they were harvested and titrated into 96 well plates containing either non (A20) or TTCF-specific B cells (A20-3A5) and MC-52 T cell hybrids. As an additional control replicate wells containing HeLa cells transfected with the ER-E/T construct were also included. The inclusion of these control transfectants allowed me to exclude the possibility that specific B cells may acquire and present E/T released from the slightly increased number of cells naturally dying in culture following transfection. As can be seen in **Fig. 5.11. panel a.**, when HeLa cells transfected with ER-E/T were mixed with various APC (including TTCF-specific B cells), MC-52 did not produce IL-2. This indicates that ER-E/T remained intracellular and any antigen released was insufficient for acquisition and presentation by antigen-specific B cells. In contrast, when HeLa cells expressing mem-E/T were incubated with various APC only antigen-specific B cells (A20-3A5) were capable of extracting and presenting antigen to MC-52 hybrids (**Fig. 5.11.**, **panel b.**). Thus, membrane located E/T can be recognised, extracted and presented to TTCF-specific T cell hybrids by B cells expressing a TTCF-specific BCR. This pilot experiment forms the basis of further experiments which I described in more detail in **Chapter 6**.

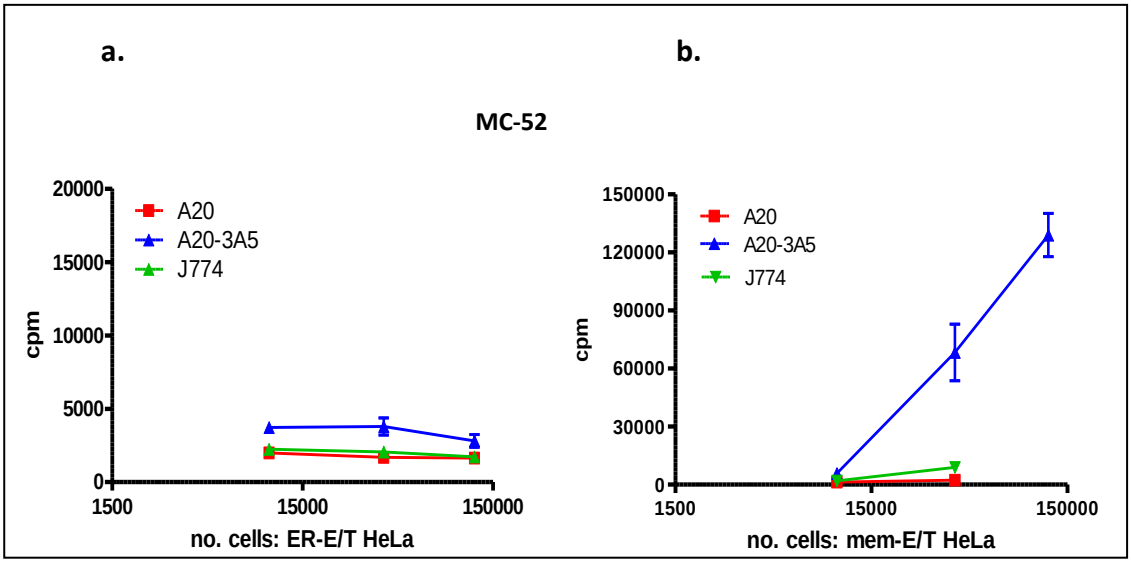

Fig. 5.11. Antigen presentation assays using newly generated T cell hybrid MC-52 incubated with various APC (non-specific B cells (red line), TTCF-specific B cells (blue line) or J774 macrophages (green line)) and graded number of HeLa ER-E/T (a.) or mem-E/T (b.) transfectants.

5.3. Discussion

In this chapter I described the generation of two TTCF-specific T cell hybrids: MC-39 and MC-52 according to standard protocols. Balb/c mice were immunized with E/T antigen and 2 weeks later antigen specific T cells were isolated from lymph nodes. Subsequently, T cells were fused with the BW 5147 lymphoma partner and selected on medium containing HAT in order to generate antigen-specific T cell hybridomas. Approximately 50 HAT-resistant hybridomas were screened for TTCF specificity. Two hybridomas MC-39 and MC-52 significantly recognised TTCFF and E/T antigens (**Fig. 5.2.**, **b.**). Therefore, I further characterised MC-39 and MC-52 T cell hybridomas with respect to expression of several surface marker and responses to titrated antigen concentrations.

As the MC-52 cells responded to antigen more significantly than MC-39, I decided to focus further studies on MC-52 T cell hybridomas. These experiments included the identification of the TCR Vβ gene usage, characterisation of TCR epitope specificity and identification of the MHC epitope restriction of the MC-52. Following the characterisation of MC-52, I decided to perform a series of pilot experiments testing whether TTCF-specific B cells are able to extract and present surface tethered E/T to MC-52. **Fig. 5.11.** demonstrates that TTCF-B cells were capable of extracting and presenting mem-E/T to MC-52. This figure also shows that this antigen presentation is dose dependent as an increase in MC-52 IL-2 production was seen following incubation with a fixed number of TTCF-specific B cells with graded numbers of HeLa transfectants. In contrast, non-specific B cells and J774 murine macrophages cell lines did not acquire and present antigen indicating that surface antigen extraction is BCR-dependent. Also HeLa cells transfected with the ER-E/T construct did not allow TTCF-specific B cells extraction and presentation confirming the lack of sufficient release following transfectant death.

In conclusion:

In this chapter, I successfully generated and characterised the MC-52 T cell hybridomas. These cells appeared to be a homogeneous population derived from the single clone and have been characterised as CD4+, TCR+, Vβ2+. In addition, using a panel of overlapping peptides, I determined the epitope specificity of MC-52 which was recognised in the context of H-2A^{d}.

Using HeLa transfectants, I have also established an assay demonstrating extraction and presentation of a plasma membrane-anchored antigen by antigen-specific B cells. These findings raise the distinct possibility that antigen specific B cells may be able to extract and present only those intracellular ‘neo’ antigens which relocate to the plasma cell surface following apoptotic cell death.

- 6. Antigen-specific B cells acquire and present E/T that has relocated to the cell surface following the induction of apoptosis -

6.1. Introduction

There is a growing body of evidence supporting the beneficial role of radiotherapy as an adjuvant enhancing the activation of anti-tumour immunity. In particular, it has been reported that both γ-irradiation and UVC induce immunogenic tumour cell death in colon and breast carcinomas (Obeid et al., 2007a) (Tesniere et al., 2009). As previously described, one of the principal characteristics of immunogenic cell death is the relocation of the intracellular antigens to the cell surface. Indeed, I have shown in **Chapter 4** that the model antigen E/T is relocated from the ER, cytoplasm and mitochondria following anthracycline or UVC treatment. This relocation was shown to lead to E/T expression in the apoptotic blebs in cells transfected with cyto and ER-E/T.

It has been previously reported, that B cells are able to recognise antigens in different forms: either in solution (Kim et al., 2006) or tethered to the surface of various cell types (Carrasco and Batista, 2007) (Allen and Cyster, 2008). Also in **Chapter 5**, I presented preliminary data that HeLa surface tethered E/T can be acquired and presented to CD4+ T cells by antigen-specific B cells. Following BCR-mediated antigen internalization, a series of proteolytic and other enzymatic events lead to the generation of antigen/MHC class II complexes which activate CD4+ T cells.

In this chapter, I have used the reagents and assays that I have previously generated and characterised to test the hypothesis that, following UVC induced relocation, intracellular E/T can be acquired and presented to CD4+ T cells by TTCF-specific B cells. In particular, I have first designed and used a novel assay where TTCF-specific B cells are monitored using flow cytometry that has allowed me to analyse the kinetics of E/T acquisition following incubation with various HeLa transfectants. Based on the results from this novel assay, I have also modified the standard antigen presenting assays previously described, again to give further insight into the biological consequences of E/T acquisition by antigen-specific B cells. Importantly, these modified antigen presentation assays allowed the ability to control the time of interaction between B cells and HeLa cells expressing E/T prior to their incubation with CD4+ T cells. In addition, I have also investigated the physical parameters of E/T acquisition by TTCF-specific B cells.

6.2. Results

6.2.1. Detection of BCR-mediated E/T acquisition by flow cytometry

In **Chapter 4**, I have demonstrated that mem-E/T is detected on the surface of transfected HeLa cells. In order to establish whether the TTCF component of this chimeric protein is also available for B cell acquisition, I stained mem-E/T transfectants with an anti-TTCF monoclonal antibody (10G5) (Antoniou and Watts, 2002). Following a 1 h incubation (4^{o}C) with 10G5 antibodies, HeLa cells were washed and incubated with PerCP conjugated anti-mouse secondary antibodies and examined using flow cytometry. **Fig. 6.1.** shows that 10G5 antibodies bound to surface of mem-E/T HeLa transfectants. In addition, it can also be seen that there is a direct correlation between the 10G5 staining and the EGFP fluorescence, covering a range of expression levels that would be expected in a transient expression system.

Thus, this confirms that full length E/T chimeric protein is expressed on the surface of HeLa cells and future experiments using TTCF-specific B cells will be possible.

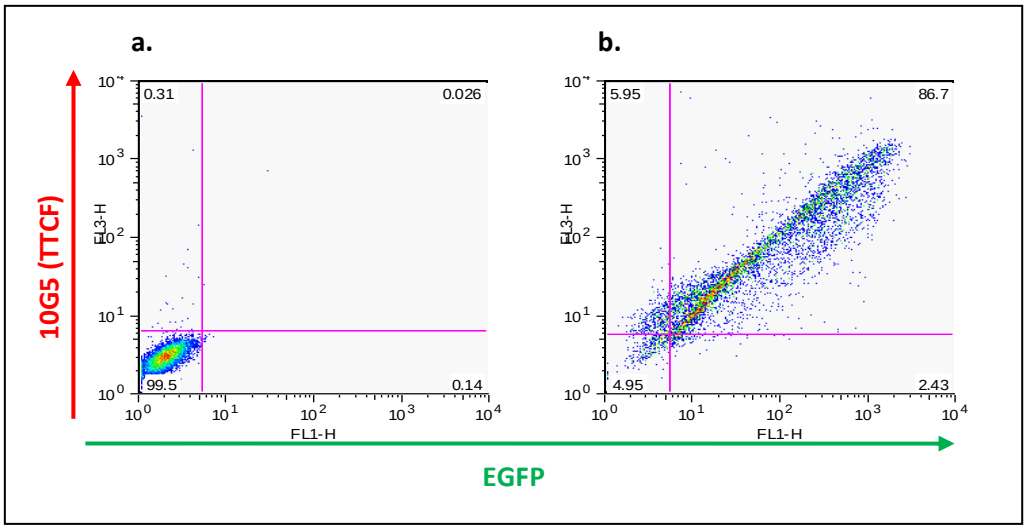

Fig. 6.1. Surface binding of 10G5 antibody recognizing TTCF epitopes in HeLa mem-E/T transfectants. Following 1 h incubation with 2 μg/ml of 10G5 antibody recognising TTCF, mem-E/T HeLa cells were stained with anti-mouse-PerCP secondary antibody and analysed using flow cytometry. Dot blots (b.) represent co-localization between HeLa mem-E/T transfectants (FL-1) and 10G5 antibody (FL-3). Panel a. demonstrates untransfected mem-E/T transfectants stained with 10G5 antibody.

As the 10G5 monoclonal antibody was capable of detecting mem-E/T, I decided to perform flow cytometry analysis to determine whether TTCF-specific-B cells incubated with HeLa E/T transfectants could be labelled by the acquisition of the chimeric fluorescent antigen. Prior to that, I tested whether flow cytometry would allow detection of soluble E/T binding to TTCF-specific B cells after incubation for various time periods (1 min, 1 h, and 3 h). TTCF-specific B cells were incubated with 2.5 μg/ml of soluble E/T at 4°C. Following washing, B cells were then stained with a mouse anti-B220 antibody directly conjugated with PerCP fluorochrome and analysed by flow cytometry. As the anti-B220 antibodies exclusively recognise the CD45R antigen expressed by the B cell lineage, this allowed a gate to be drawn on B cell population. In **Fig. 6.2.**, it can be seen that following incubation with soluble E/T for 1 or 3 h, more than 60% of the B220 positive cells were also positive for EGFP acquisition and with a significant increase in mean fluorescence intensity (MFI) during this time course (from 5.35 following 1h to 5.82 after 3 h incubation). Interestingly, it can also be seen that incubation with soluble E/T for time points as short as 1 min was also sufficient for E/T acquisition (**Fig. 6.2. bottom left panel**) with more than 60% of double positive cells but with lower MFI=4.97.

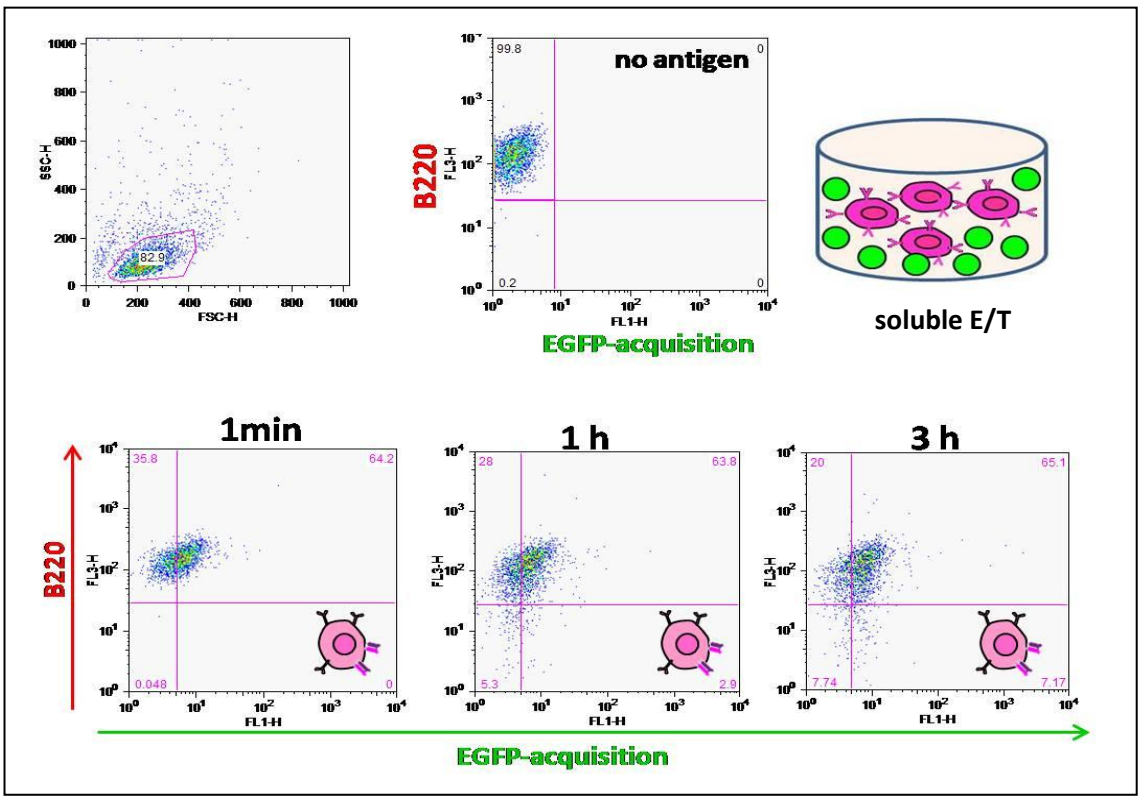

Fig. 6.2. Soluble E/T acquisition by TTCF-specific B cells. Flow cytometry analysis of TTCF-specific B cells that bind green fluorescent E/T antigen to the cell surface via specific BCR. Fallowing incubation with soluble E/T (2.5 μg/ml) in a various time periods (1 min, 1 h, 3 h), TTCF-specific B cells were washed and incubated with B220-PerCP. After final wash 10 000 events were collected using a FACScan Calibur (BD). As a control, TTCF-specific B cells were incubated in medium without any antigen (upper dot plot). This flow cytometry analysis is representative of 2 independent experiments.

Having established a relatively simple assay for an the acquisition of soluble E/T by TTCF-specific B cells, I then progressed to determine if this assay would allow the detection of acquired mem-E/T by these B cells. As previously described for soluble E/T, TTCF specific-B cells were incubated at 37°C with mem-E/T HeLa transfectants for the same time points (1 min, 1 h and 3 h) and following staining with B220 antibody, I quantified B cells fluorescence using flow cytometry. **Fig. 6.3.** demonstrates that, similar to that seen with soluble E/T, incubation with TTCF-specific B cells with mem-E/T transfectants for periods of 1 or 3 h resulted in 51% and 55% B220/EGFP double positive cells (MFI=3.78 and MFI=3.96 respectively). In contrast, when these cells were incubated with untransfected HeLa cells there is no co-staining (**Fig. 6.3. upper right panel**). In addition, a 1 min incubation with mem-E/T transfectants was sufficient for more than 20% of TTCF-specific B cells to acquire E/T (MFI=2.39).

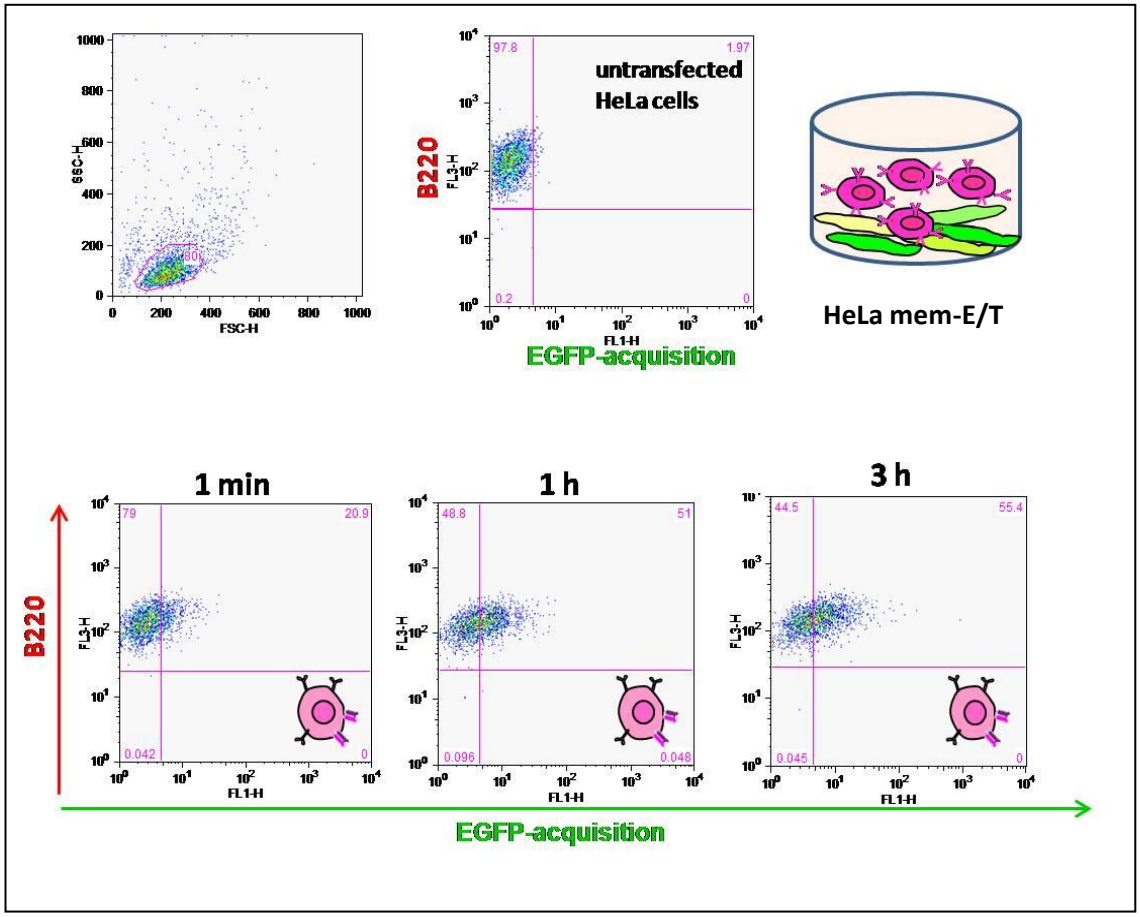

Fig. 6.3. Surface-tethered mem-E/T acquisition by TTCF-specific B cells. Flow cytometry analysis of TTCF-specific B cells that bind via specific BCR green fluorescent E/T antigen expressed on the plasma cell membrane of HeLa transfectants. Antigen acquisition increases with the time course (lower dot plots). Fallowing incubation with mem-E/T HeLa transfectants, TTCF-specific B cells were washed and incubated with B220-PerCP. After final wash 10 000 events were collected using a FACScan Calibur (BD). As a control, TTCF-specific B cells were incubated in medium without any antigen (upper dot plot). This flow cytometry analysis is representative of 2 independent experiments.

To test whether either soluble or mem-E/T acquisition was BCR-mediated, I also performed these experiments using non-specific B cells. **Fig. 6.4.** indicates that non-specific B cells failed to acquire both soluble E/T or mem-E/T from HeLa surface following incubation periods as long as 1 h. In can be seen that 0.35% of non-specific B cells incubated with soluble E/T for 1 h were double positive, compared to 64% seen in **Fig. 6.2.** using TTCF-specific B cells. Similarly, 3.7% of non-specific B cells incubated with mem-E/T transfectant were double positive, compared to 54% seen in **Fig. 6.3**. Finally as a control for E/T release and its acquisition by TTCF-specific B cells, I also incubated TTCF-specific B cells for 3 h with HeLa cells transfected with ER-E/T. **Fig. 6.4.** (right panel) shows that only 3.7% of TTCF-specific B cells acquire intracellular antigen which is similar to the acquisition of mem-E/T by non-specific B cells and significantly less than that acquired by TTCF-specific B cells following incubation with mem-E/T transfectants. This low level of background acquisition probably reflects the number of naturally dying HeLa cells releasing small quantity of E/T into the media. This experiment shows that antigen extraction is BCR-mediated and occurs only when E/T antigen is on the cell surface.

In order to quantify the E/T acquisition by TTCF-specific B cells, the median fluorescence intensity (MFI) of E/T fluorescence following B cell incubation with various E/T targets was examined statistically. **Fig. 6.4. panels b.**, **d.** and **f.** shows a summary of the data obtained from several replicates of these novel experiments. It can be seen (**Fig. 6.5. panel. b.**) that there is a significant increase in the acquisition of soluble E/T by TTCF-specific versus non-specific B cells. Likewise, **panel d.** shows a similar significant increase in the acquisition of mem-E/T by TTCF-specific B cells. **Panel f**. shows that acquisition of E/T by TTCF-specific B cells is dependent on expression of E/T at the cells surface as there is a significant difference in the acquisition of mem-E/T versus ER-E/T.

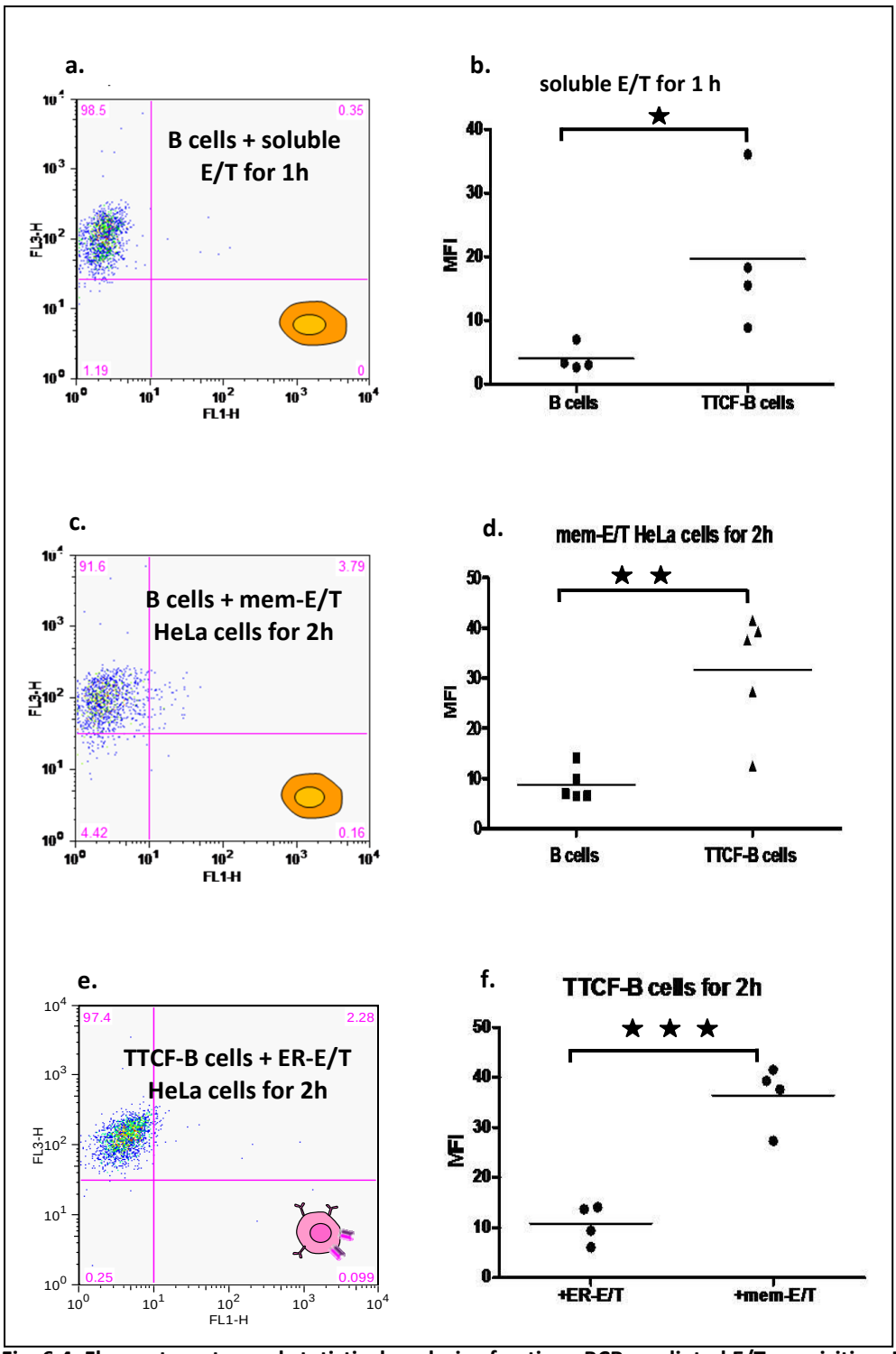

Fig. 6.4. Flow cytometry and statistical analysis of antigen BCR-mediated E/T acquisition. The dot plots shows the non-specific B cells incubated for 1 h with soluble E/T (2.5 μg/ml) (panel a.) or for 2 h with mem-E/T HeLa transfectants (panel c.). Panel e. demonstrates TTCF- B cells incubated for 3 h with ER-E/T HeLa transfectants. Statistical analysis significantly quantifies the differences in the E/T acquisition between TTCF-specific and non-specific B cells from solution (panel b.) or cell surface of mem-E/T HeLa cells. (panel d.) In addition, panel f. demonstrates the differences in antigen acquisition from ER-E/T or mem-E/T HeLa transfectants by TTCF-B cells.

★ indicates p< 0.05 ★★ indicates p<0.01 ★★★ indicate p<0.001

Thus the use of flow cytometry represents a reliable assay for the measurement of the acquisition of E/T by antigen-specific B cells. I have previously demonstrated in **Chapter 4** that intracellular E/T relocates to the cell surface following UVC and anthracycline treatment. Therefore, in the next series of experiments I tested whether this flow cytometry-based assay would allow me to detect acquisition of relocated E/T by TTCF-specific B cells. To address this HeLa cyto-E/T transfectants were exposed to 300 J/m^2 of UVC light or left un-treated. After 4 h TTCF-specific B cells (or non-specific B cells) were added to the transfectants for a period of 2 h. Following this time the non-adherent B cells were removed, washed, stained with anti-B220 antibodies and analysed by flow cytometry. **Fig. 6.5.** summarises this series of experiments and shows that when TTCF-specific B cells were incubated with UVC treated cyto-E/T transfectant a significant number (14.8%) acquired E/T fluorescence as visualised by the number of double positive (B220+, E/T+) cells. Importantly, this number of double positive cells was significantly reduced when TTCF-specific B cells were incubated with either un-treated cyto-E/T transfectants (0.7%) or non-transfected HeLa cells (0.18%). It can also be seen that non-specific B cells incubated with all transfectants did not show significant E/T acquisition. Surprisingly, when TTCF-specific B cells were co-cultured with UVC treated HeLa cells expressing ER-E/T, I failed to observe relocated antigen acquisition (**Fig. 6.6. panel b.**).

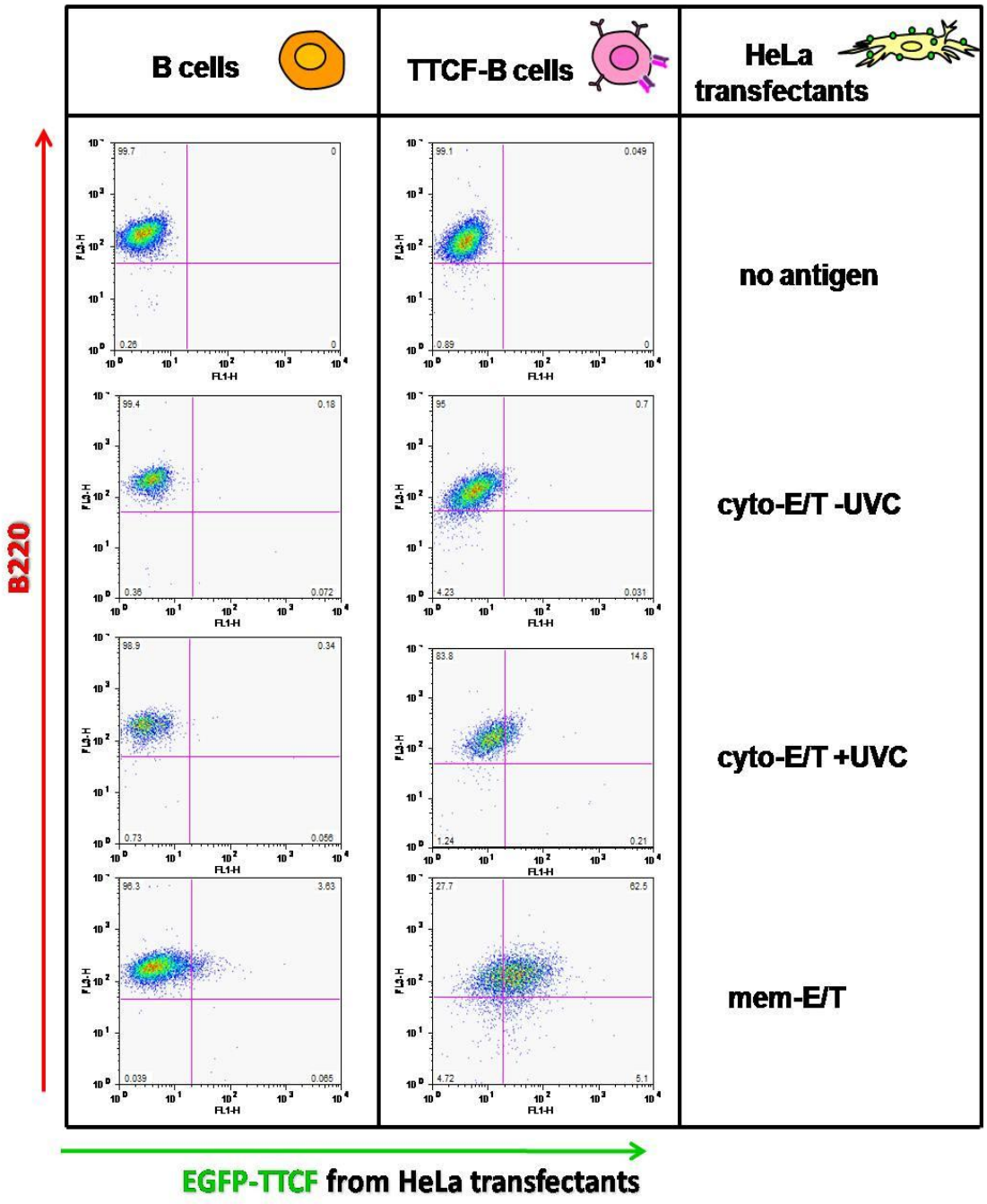

Fig. 6.5. Relocated E/T antigen extraction by TTCF-specific B cells from cyto-E/T HeLa transfectants following UVC treatment. Flow cytometry analysis of TTCF-specific B cell acquisition of relocated intracellular antigen from surface of HeLa transfectants via specific BCR. TTCF-specific B cells following incubation with cyto-E/T or mem-E/T HeLa transfectants were removed, washed and stained with B220-PerCP. Control experiments in which B cells were incubated with untransfected (no antigen) HeLa cells (upper dot plot) were also included. This flow cytometry analysis is representative of 2 independent experiments.

In order to quantitate E/T acquisition following incubation of TTCF-specific B cells with apoptotic cyto-E/T HeLa transfectants, the E/T MFI of E/T+, B220+ B cells was calculated from three independent experiments and these are shown in **Fig. 6.6**.

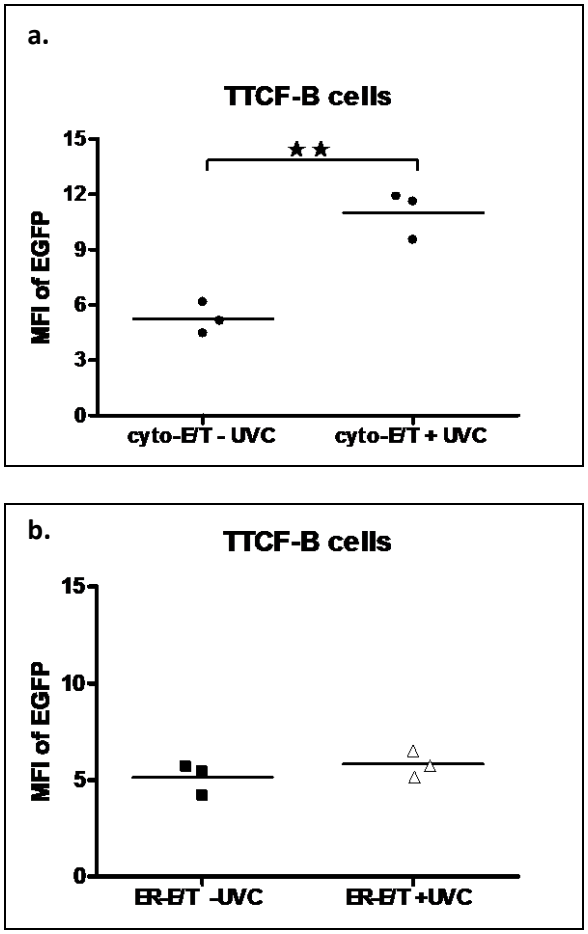

Fig. 6.6. Statistical analysis of the three independent experiments performed by flow cytometry demonstrating MFI EGFP acquisition by TTCF-B cells from cyto-E/T (panel a.) and ER-E/T (panel b.) HeLa transfectants. B220+ TTCF-specific B cells incubated either with untreated transfectants or with transfectants following UVC (300 J/m^2) treatment acquire E/T antigen represented as MFI of EGFP.

★★ indicates p< 0.01

Thus, these experiments demonstrate for the first time, that intracellular cyto-E/T (but not ER-E/T) is relocated following UVC treatment and can be acquired by TTCF-specific B cells.

6.2.2. Detection of E/T presentation by antigen-specific B cells using a novel antigen presentation assay

In the previous section, I have demonstrated that TTCF specific B cells were able to extract both surface antigens and those relocated from intracellular compartments (cytoplasm), as a consequence of immunogenic cell death using flow cytometry. In this section, I have addressed whether antigen acquired in this manner is a suitable substrate for BCR-mediated internalization and intracellular processing that leads to the generation of peptide/MHC complexes that are recognisable by CD4+ T cells. Initially, to test this I performed standard antigen presentation assays where various numbers of mem-E/T HeLa transfectants were incubated with TTCF-specific (or non-specific) B cells and MC-52 TTCF specific-T cells (described in **Chapter 5**) for 24 h. **Fig. 6.7. panel a.** extends the analysis of mem-E/T acquisition and presentation by TTCF-specific B cells earlier shown in **Fig. 5.10**. As shown before, **Fig. 6.7**. shows that only TTCF-specific B cells can efficiently acquire and present mem-E/T to MC-52 T cells. Maximal T cell stimulation was observed with approximately 6 000 mem-E/T transfectants. Paradoxically, when the number of transfectants in each well was increased above this number, T cell stimulation was reduced. This may indicate that these standard assays may be limited by large number of cells present in each well. This is confirmed by control experiments performed simultaneously with soluble TTCF that show significantly more MC-52 activation following presentation by TTCF-specific B cells (**Fig. 6.7. panel b**.).

Furthermore, I examined whether mem-E/T acquisition is contact dependent. To test this, I repeated these assays in the presence of 0.4 μm diameter blocking filters. This size of pore would be expected to allow free diffusion of soluble antigen, but would introduce a barrier between the adherent mem-E/T HeLa transfectants and the co-cultured B cells. **Fig. 6.8.** demonstrates that antigen presentation again was only observed when mem-E/T HeLa cells were incubated with specific TTCF-B and T cells. In those wells (**panel a. arrow**) that contained filters, it can be seen that mem-E/T presentation was inhibited. In contrast and as expected blocking filters had no effect on the presentation of soluble TTCF by TTCF-specific B cells (**panel b. arrow**).

This experiment shows that TTCF-specific B cells require direct contact with the surface of mem-E/T transfected HeLa cells for E/T acquisition and presentation to MC-52 T cells. This is in agreement with previous experiments performed by Batista where immobilized HEL antigen was also extracted in a contact dependent manner by HEL-specific B cells (Batista et al., 2001).

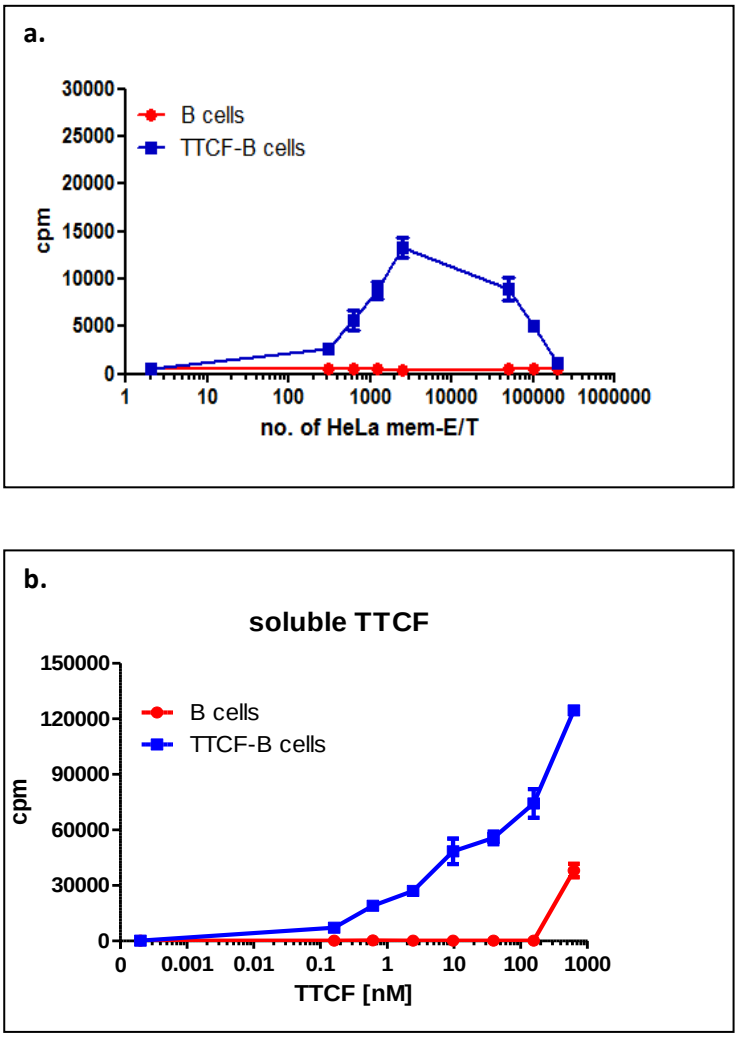

Fig. 6.7. Antigen recognition from the cell surface or solution and presentation to MC-52 T cell hybridomas by specific or not specific B cells using proliferation bio-assay. Both panels demonstrate the standard procedure of proliferation bio-assay where B and T cell hybridomas were incubated for 24 h with mem-E/T HeLa cells (panel a.) or with soluble TTCF (panel b.) and IL-2 was measured. This proliferation assay is representative of 6 independent experiments.

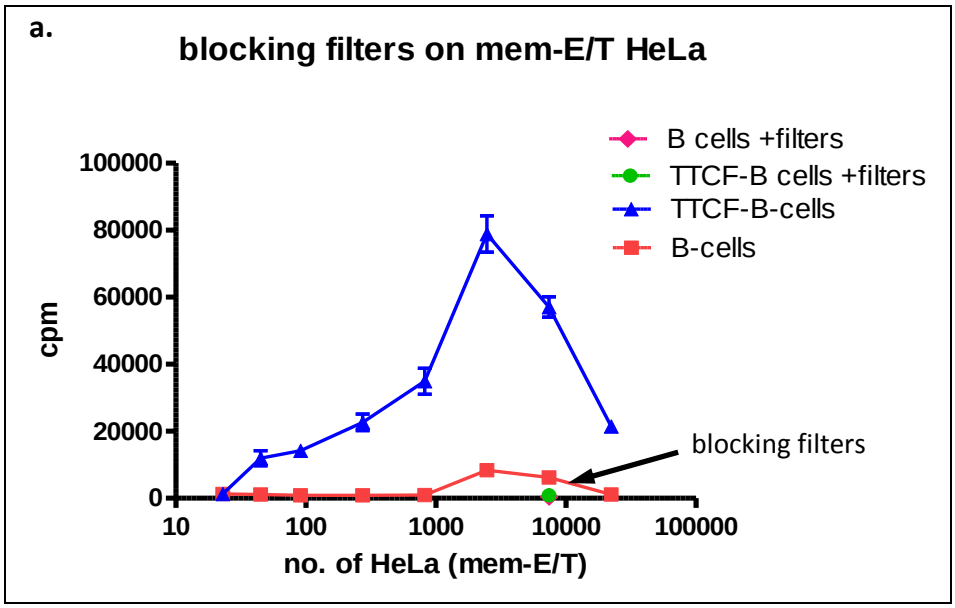

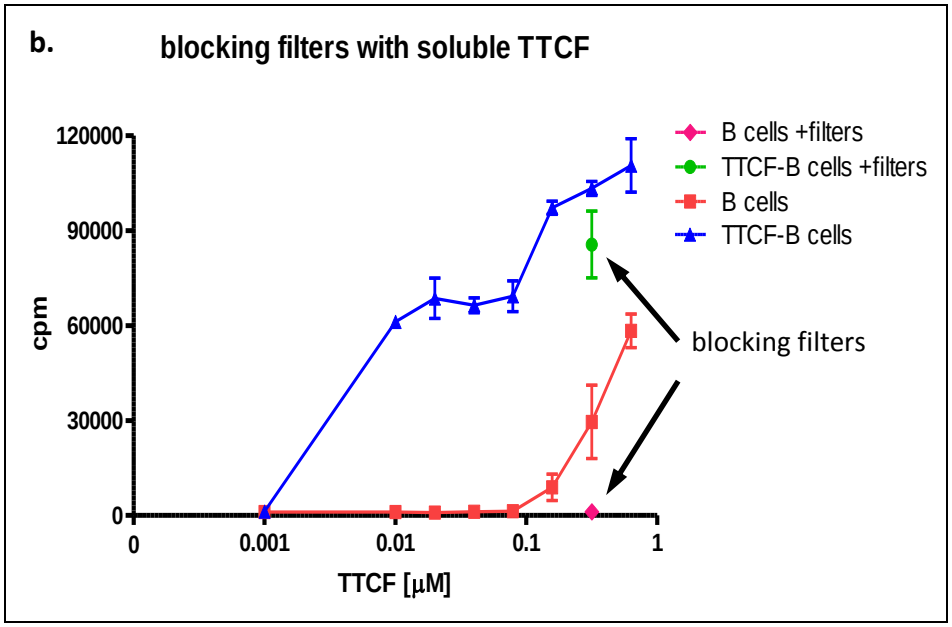

Fig. 6.8. Proliferation bio-assays of TTCF-B cells (blue line) or non specific B cells (red line) co-cultured with graded numbers of mem-E/T HeLa cells (panel a.) or graded doses of soluble TTCF (panel b.) and MC-52 T cells hybridomas. Green and pink circles represent additional wells containing blocking filters separating the HeLa E/T transfectants from the T and B cells. This proliferation assay analysis is representative of 4 independent experiments.

As these standard antigen presentation assays may be limited by cell number and do not allow the process of antigen acquisition and presentation to be physically separated from subsequent production of T cell derived IL-2, I decided to establish a novel assay measuring antigen recognition by MC-52 T cells. This improved assay was designed to allow B cell antigen acquisition over various time points. Following this, B cells were then removed from the target cells and re-plated with MC-52 T cells in absence of any further antigen for 24 h to allow IL-2 production to be detected. Thus, only antigen acquired during the various times of the first incubation would be processed by TTCF-specific B cells. **Fig. 6.9. panel a.**, demonstrates that when TTCF-specific B cells were incubated with mem-E/T transfectants for periods of 1, 2, 4 and 6 h and graded numbers transferred to fresh wells containing MC-52, IL-2 production was observed. Interestingly, the IL-2 produced by MC-52 following incubation with TTCF-specific B cells that had been co-cultured with the HeLa transfectants for 1 or 6 h was similar. Furthermore, when MC-52 T cells were co-cultured with TTCF-specific B cells that had been incubated with HeLa transfectants for time periods as short as 1 min, levels of IL-2 production were also similar (**panel b.**). Thus, it appears that TTCF-specific B cells acquire sufficient E/T following incubation periods as short as 1 min that subsequently leads to maximal MC-52 stimulation. To exclude the possibility that sufficient mem-E/T was released into the media, I also transferred HeLa transfectants supernatant (following the various time points) into fresh wells containing MC-52 and TTCF-specific B cells in the absence of any additional antigen. **Panel c.** shows these supernatants were insufficient to stimulate MC-52 IL-2 production.

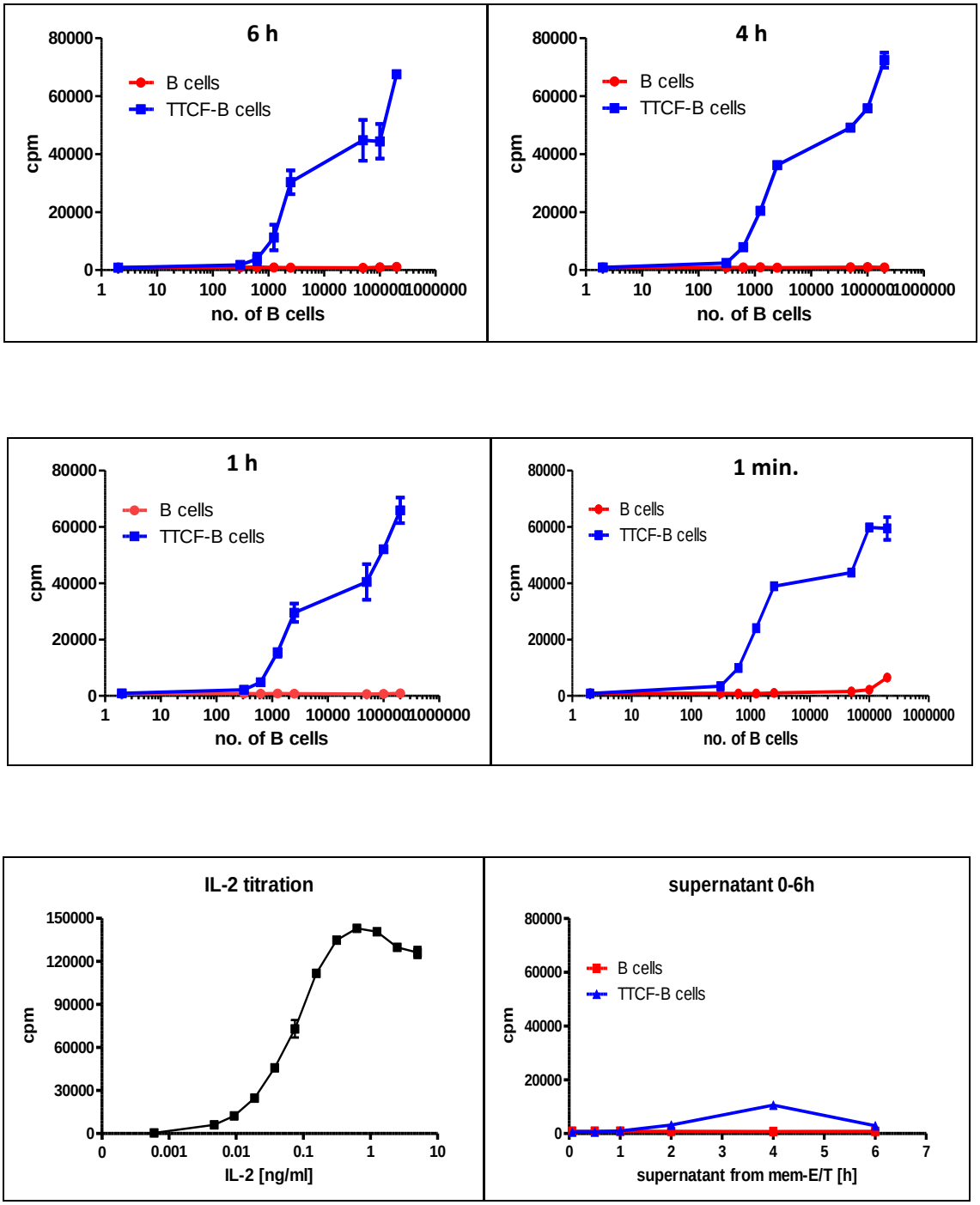

Fig. 6.9. The kinetics of antigen extraction by B cells and presentation to T cell hybridomas from HeLa transfectants. Proliferation assay of MC-52 hybridomas responded for E/T antigen presented by specific TTCF-specific B cells (blue line) and non-specific B cells (red line). Both B cells (specific and non-specific) were previously incubated with mem-E/T HeLa transfectants for a various time points (from 1 min to 6 h) before co-culture with T cell hybridomas. In addition, the supernatant from HeLa transfectants was examined whether may stimulate B cells to recognition of de-attached antigen. This proliferation assay analysis is representative of 2 independent experiments.

6.2.3. Detection of intracellular E/T presentation by antigen-specific B cells following UVC treatment

Finally to investigate whether intracellular E/T, that has previously been shown that relocate to the cell surface after UVC-treatment of HeLa transfectants (**Fig. 4.12, 4.14.**) was acquired by TTCF-specific B cells, I performed the following experiments. Using the previously described antigen presentation assay, I exposed HeLa transfectants expressing ER, cyto and mito-E/T to 300 J/m^2 UVC light. 4 h later these transfectants (or non-treated) were incubated with specific- or non-specific B cells for 2 h. Based on the experiment shown in **Fig. 6.5.**, this time was predicted to be sufficient to allow relocated E/T to be extracted by antigen-specific B cells. Subsequently, B cells were removed and graded numbers were then transferred to new wells containing a constant number of MC-52 T cells for a further 24 h (**Fig. 6.10.**). **Panel a.** demonstrates that when TTCF-specific B cells were incubated with UVC treated ER-E/T transfectants they acquired sufficient relocated E/T for the activation of MC-52 T cells Similarly, when TTCF-specific B cells were co-cultured with UVC treated cyto-E/T HeLa transfectants (**panel b.**), relocated E/T antigen from the cytoplasm was sufficient to be acquired by TTCF-specific B cells and presented to MC-52 T cell hybridomas. Importantly, in both these series of experiments presentation was not seen when either non-specific B cells were used (data not shown) or when TTCF-specific B cells were incubated with un-treated transfectants (red line). The results from this experiment differ to that seen in **Fig. 6.6.** where statistical analysis of three independent experiments performed by flow cytometry showed that TTCF-specific B cells acquired relocated cyto-E/T from UVC treated HeLa cells but did not extract relocated antigen from ER compartment. The discrepancy in ER-E/T acquisition by TTCF-B cells may be caused by the lower sensitivity of flow cytometry than the bio-assay measuring MC-52 activation. It was possible that ER relocated antigen was extracted by TTCF-specific B cells, despite the levels being insufficient to be detected by flow cytometry. However, these levels were clearly sufficient to activate MC-52 T cells to produce IL-2.

In panel c. it can be seen that only limited presentation occurred following incubation of TTCF-specific B cells with UVC treated mito-E/T transfectants. This is consistent with data shown in **Fig. 4. 13**. **panel b.** where immunogenic apoptosis did not lead to significant surface expression of mito-E/T.

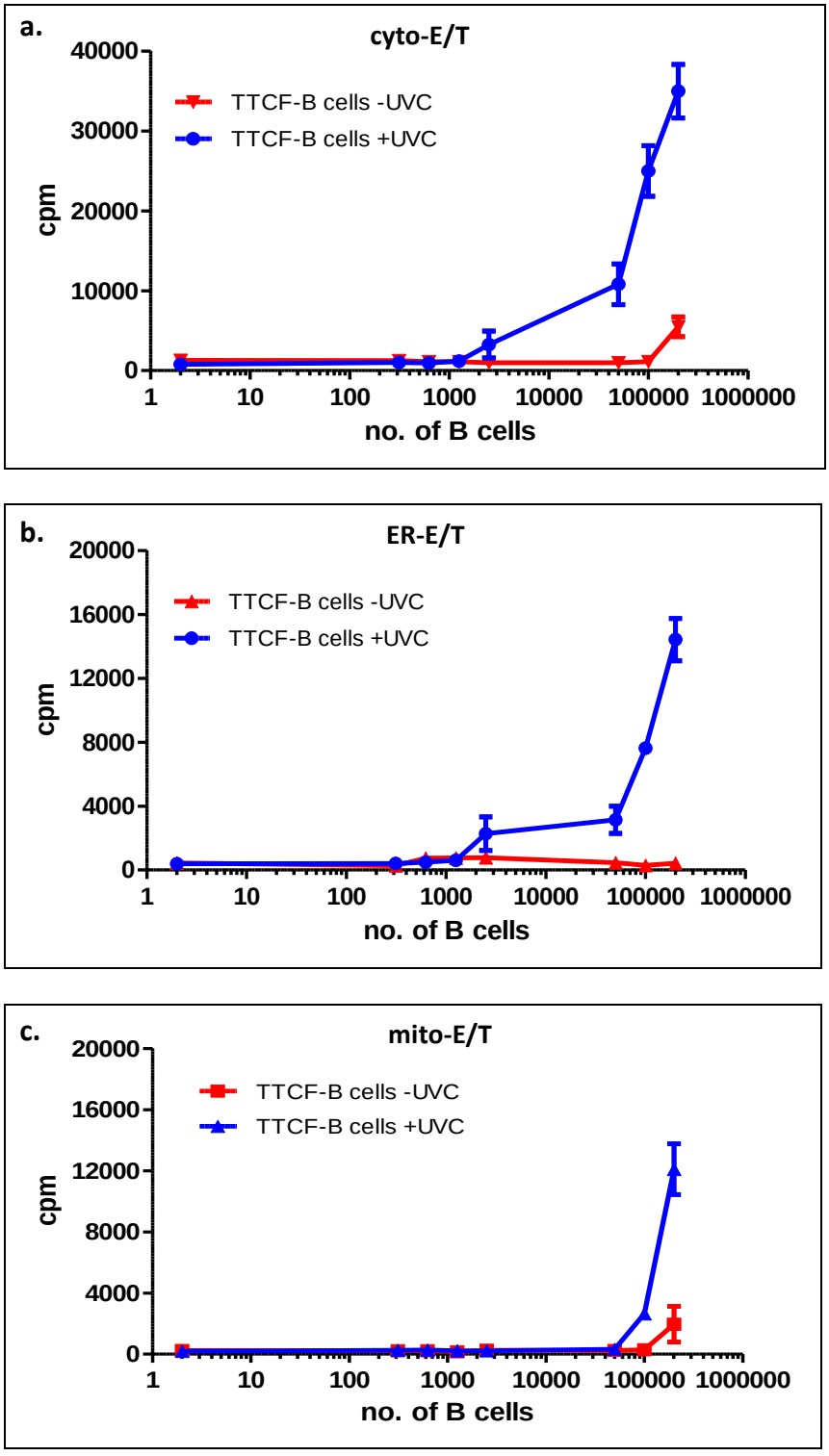

Fig. 6.10. TTCF-specific B cells acquired apoptosis-induced relocated E/T. TTCF-specific B cells following 2 h incubation with UVC treated or untreated cyto-E/T (panel a.), ER-E/T (panel b.) or mito-E/T (panel c.) HeLa transfectants, were harvested and washed. Subsequently, the different numbers of such stimulated TTCF-specific B cells (blue line) were added to $5*10^4$ MC-52 T cell hybridomas for 24 h. As a control, I used TTCF-specific B cells incubated with untreated HeLa transfectants (red line). 24 h later the supernatant were added to IL-2 deprived CTLL-2 cells and IL-2 production was measured indirectly by 3H-thymidyne incorporation to proliferating CTLL-2 cells. This proliferation assay analysis is representative of 5 independent experiments.

These findings were confirmed by statistical analysis of several independent sets of experiments that are shown in **Fig. 6.11**. It can be seen that while TTCF-specific B cells significantly acquired relocated ER (**panel a.**) and cyto-E/T (**panel b.**), acquisition of mito-E/T was not statistically significant above background levels (data not shown).

Thus, these findings demonstrate that following the induction of immunogenic apoptosis using UVC, intracellular ER and cyto-E/T antigen in HeLa cells is relocated to the cell surface and acquired by antigen-specific B cells. This antigen acquisition consequently leads to presentation to MC-52 T cell hybridomas.

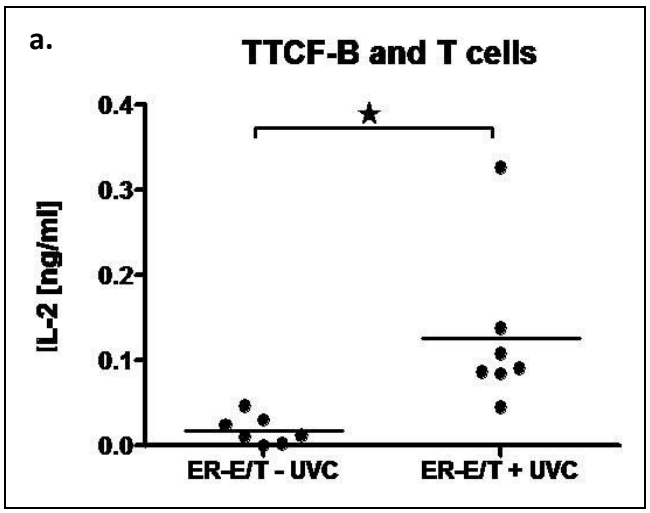

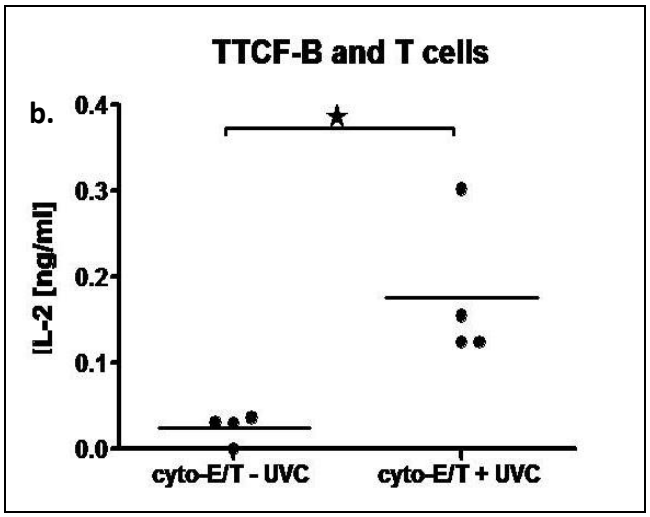

Fig 6.11. Statistical analysis of the seven (panel a.) and four (panel b.) independent experiments from proliferation assays. Statistical significance between antigen recognition from untreated or UVC treated HeLa transfectants by TTCF-specific B cells resulted in IL-2 production by MC-52 hybridomas and consequently the proliferation of CTLL-2 IL-2 dependent cell line, was calculated using the Student's t-test for unpaired samples.
★ indicates $p < 0.05$

6.3. Discussion

Although many studies have shown that B cells recognise soluble antigens *in vitro*, it is likely that *in vivo*, a proportion of antigens encountered by B cells are membrane–bound. It is well documented that FDC that retain native antigens are able to act as target cells for B cells, in particularly in specialised areas knows as germinal centres. In these regions, B cells acquire tethered antigens and following processing, present peptides fragments to cognate CD4+ T cells (MacLennan, 2007).

Furthermore, evidence also shows that macrophages are able to present intact antigens to B cells in the follicle-subcapsular sinus (SCS) boundary of the lymph node (Carrasco and Batista, 2007). In addition, Wykes et al. showed that DC pulsed with soluble antigen can prime naive B cells both in *in vivo* and in *in vitro* models (Wykes et al., 1998). Importantly, direct contact between live DC and B cells was required to initiate antigen recognition and subsequent presentation to T cells. However, lysed DC were ineffective as an antigen source suggesting that DC play an active role in antigen priming. Antigen acquisition in an *in vitro* model by B cells was observed during the initial phases before specific antibody production appear. Other findings from Batista et. al. surprisingly demonstrated that antigen-specific B cells were also able to extract membrane bound antigens from other cells including transfected fibroblasts (Batista et al., 2001).

These described examples of tethered antigen extraction from a variety of different cell types led me to establish an *in vitro* model where the parameters of B cell dependent antigen extraction could be studied. Using mem-E/T HeLa transfectants, I performed flow cytometry analysis that demonstrated that the anti-TTCF antibody (10G5) was capable of recognising chimeric E/T antigen present on the HeLa cell surface. This experiment confirmed that the full length fusion protein was expressed on the HeLa cell surface, as the antibody staining entirely overlapped with EGFP auto-fluorescence (**Fig. 6.1.**). I then showed that soluble E/T acquisition by TTCF-specific B cells could be detected using flow cytometry. Consequently, I established the kinetics of mem-E/T acquisition from HeLa transfectants by TTCF-specific B cells also using flow cytometry. **Fig. 6.2.** and **6.3.**, demonstrate that TTCF-specific B cells acquired E/T from solution or tethered to the surface of HeLa cells very rapidly, in time periods as short as 1 min. Incubating TTCF-specific B cells with mem-E/T transfectants for longer time periods led to an increase in the percentage of TTCF-B cells that acquired fluorescent antigen (approximately 64% from solution and 20% from the membrane of HeLa cells). This experiment was repeated several times and the EGFP MFI acquired in the various experiments were compared using a

Student 't' test. **Fig. 6.4. panels b.**, **d.** and **f.** shows a statistical significance ($p<0.05$, $p<0.01$ and $p<0.001$, respectively for each panel) in the MFI intensity between non-specific and TTCF-specific B cells incubated with soluble or membrane bound antigen. Furthermore, in these experiments (see **Fig. 6.2., 6.3.**) the population of cells which were shown to be double positive for both B220 and EGFP were contained within the parameters of a forward scatter (FSC) and side scatter (SSC) gate which was set on B cells incubated with untransfected HeLa cells (**Fig. 6.3. top left panel**). Therefore, this strongly indicates that the EGFP positive population of cells are single B cells and not B-HeLa cell conjugates. The demonstration that the B220/EGFP double positive population does not contain B-HeLa cell conjugates is of particular importance in subsequent experiments where this population of cells is transferred to fresh well containing MC-52 T cell hybridomas in the absence of antigen (**Fig. 6.10.**). I also performed experiments, where TTCF-B cells were incubated with HeLa cells transfected with intracellular antigen ER-E/T. This test allowed me to exclude that TTCF-B cells might recognise released intracellular antigen. Expectedly, the representative dot plot (**Fig. 6.4. panel e.**) and statistical analysis from four independent experiments (**Fig. 6.4. panel f.**) demonstrate that TTCF-B cells were able to extract only surface tethered E/T antigen. This experiment was consistent with Batista data showing that only HEL-specific B cells formed synapse with target cell expressing membrane-bound HEL and were able to extract the antigen, in contrast to non specific B cells which failed to do so (Batista et al., 2001) .

Having optimised the parameters of surface antigen uptake, I decided to examine whether flow cytometry analysis was able to detect and quantify the acquisition of relocated antigen by TTCF-specific B cells from intracellular compartments following UVC treatment. Based on previous reports showing that UVC induces immunogenic cell death in cancer cell lines by displaying intracellular CRT protein on the cells surface (Obeid et al., 2007a) and my current experiments (**Fig. 4.12.** and **Fig. 4.13.**), I decided to use UVC treatment on cyto-E/T HeLa transfectants. Therefore, UVC treated HeLa transfectants were co-cultured with both TTCF-specific and non-specific B cells for 2 h. **Fig. 6.5.** demonstrates that only TTCF-B cells were able to acquire E/T expressed by UVC treated cyto-E/T HeLa cells. In contrast to untreated HeLa transfectants, E/T was retained in the cytoplasm and antigen acquisition was not observed. In these experiments, I also used non-specific B cells which failed to acquire E/T antigen from both UVC-treated or control HeLa transfectants. The statistical difference in the MFI of acquired E/T between TTCF-B cells incubated with UVC treated cyto-E/T HeLa transfectants or untreated cells was assessed using the Student 't' test (**Fig. 6.6.**).

In **Chapter 5**, I performed pilot experiments indicating that E/T fusion protein expressed on the surface of HeLa cells was extracted by TTCF specific-B cells and presented to specific CD4+ T cells as shown using an IL-2 dependent proliferation bio-assay (**Fig. 5.10.**). Therefore, I decided to investigate in more detail, whether intracellular antigen relocated to the surface following immunogenic apoptosis-induction is acquired by TTCF-specific B cells and presented to CD4+ T cells. For these experiments, I established a novel antigen presentation assay that allowed me to control the time of B /target cell interaction. B cells were firstly incubated with HeLa transfectants previously exposure to UVC light. Subsequently, these B cells were removed and incubated with specific CD4+ T cells, in the absence of any additional antigen (see previous discussion for exclusion of B/HeLa cell conjugates).

This novel bio-assay allowed me to confirm that TTCF-specific B cells are indeed able to extract membrane tethered E/T antigen in time periods as short as 1 min and to present processed peptide to TTCF-specific T cells (**Fig. 6.9.**). Furthermore, I tested whether direct physical contact between target cells and B cells was essential in the process of antigen extraction. HeLa cells expressing mem-E/T were co-cultured with TTCF-specific B and T cells in the presence of 0.4 μm blocking filter. This size of pores was able to inhibit the movement of lymphocytes, but not the diffusion of soluble TTCF. **Fig. 6.8. panel a.** shows that the presence of blocking filter completely abrogated mem-E/T recognition by TTCF-specific B cells. In contrast, when specific B and T cells were incubated with soluble TTCF for 24 h the presence of blocking filters did not affect antigen recognition and presentation (green dot in **Fig. 6.8. panel b.**). This experiment clearly indicates that physical contact between the E/T expressing target cell and TTCF-specific B cell was necessary required for antigen extraction from the plasma membrane. This is in agreement with data presented by Batista et al. showing the inhibition of membrane-anchored HEL extraction by HEL-specific B cells. Again, insertion a mesh separating target cells expressing mem-HEL from HEL-specific B cells, prevented antigen extraction, but not soluble HEL recognition (Batista et al., 2001). I then examined whether relocated intracellular E/T expression by HeLa transfectants can be extracted by TTCF-specific B cells and presented to antigen-specific CD4+ T cells using a novel bio-assay, where the process of antigen acquisition was physically separated from the process of antigen induced IL-2 production. **Fig. 6.10.** shows that HeLa cells transfected with plasmid targeting E/T either to the cytoplasm or to the ER were able to provide relocated E/T for TTCF-specific B cell acquisition following UVC treatment, compared to non-specific B cells. This experiment was repeated several times and the statistical significance of BCR-mediated surface E/T acquisition was verified using the Student 't' test. Thus, the proliferation assay to measure acquisition of

relocated antigen by B cells seems to be more sensitive than flow cytometry analysis which failed to demonstrate ER-E/T acquisition from UVC treated HeLa transfectants (**Fig. 6.6 panel b.**).

HeLa cells transfected with mito-E/T construct were not examined statistically because I did not performed enough experiments allowing me to introduce statistical analysis.

In conclusion:

In this chapter, I have shown that B cells can extract surface-tethered antigen from target cells very rapidly, in time period as short as short as 1 min. This extraction was BCR-mediated in a contact dependent manner.

Flow cytometry analysis for the first time allowed me to demonstrate that relocated intracellular antigen, as a consequence of immunogenic cell death is extracted by antigen-specific B cells. Statistical analysis of this data was robust. Furthermore, in this chapter I developed a novel bio-assay allowing the detection and quantification of relocated antigen by specific B and T cells. This assay indicated that relocated antigen originating from either the cytoplasm or the ER, but not from mitochondria was recognised by TTCF-specific B cells and presented to cognate CD4+ T cells. Statistical analysis of this data confirmed that UVC treated cyto-E/T and ER-E/T HeLa transfectants were able to stimulate MC-52 T cell hybridomas via BCR-mediated, B cell antigen presentation.

- 7. Discussion -

The immune response to cancer is a dynamic process in which uncontrolled growth of cancer cells is countered by various protective mechanisms. The complexity of anti-cancer treatment recently has been focused on a positive interaction between conventional therapeutic modalities, including chemotherapeutic drugs or radiotherapy inducing the direct death of cancer cells and the activation of the host immune system eliciting anti-tumour immunity. Therefore, understanding the mechanisms leading to a more efficient collaboration and implantation of both these approaches in the clinic, will allow cancer patients to inhibit the progression of disease.

Since the discovery of the first tumour associated antigen TAA, against which T cell immunity can be directed, many others still need to be identified. However, one of the main reasons why tumours are able to progress and expand is their ability to escape immune recognition. The inability to induce tumour anti-immunity is a consequence of down-regulation of many signals, including decrease in MHC molecules expression, which are required for antigen presentation. Additionally, the induction of regulatory T cells, the alteration of the APC properties of DC and macrophages lead to long-term tumour tolerance. This raises the question whether alternate B cells may efficiently present TAA. Therefore, there is a great need to perform further studies which will clarify the role of B cells as APC of tumour antigens that consequently induce anti-tumour immunity. The aim of this project was to test this hypothesis.

Although many previous studies have demonstrated that apoptosis appears to be tolerogenic rather than immunogenic, recent evidence suggests that following treatment with reagents such as UVC irradiation or anthracyclines, apoptotic tumour cells elicit immune responses. In particular, DC that engulf these 'immunogenic' apoptotic tumour cells are able to cross-present antigens and prime cytotoxic CD8 T cells extremely vigorously. It has been shown that immuno-competent mice, challenged with anthracycline treated EL4, CT26 colon cancer or MCA205 fibrosarcoma, inhibited tumour progression more effectively, when compared to athymic immune-deficient animals (Apetoh et al., 2007a). Also, locally irradiated immuno-competent mice rejected tumour tissue, in contrast to immuno-deficient mice which died as a consequence of tumour progression. Another study performed by Perez et. al. showed similar results; local irradiation of cancer cells can enhance host anti-tumour immune responses *in*

vivo (Perez et al., 2009). They used B16F0 melanoma cell line, as a model to monitor lung metastasis. Irradiation of cutaneous melanomas prior to their implementation resulted in more than a 20-fold reduction in lung metastases after systemic challenge with untreated melanoma cells compared to control mice receiving untreated melanoma cells. This clearly demonstrates a positive correlation between chemotherapy and radiotherapy on the host immune system as a vaccination strategy eliciting a more effective anti-tumour response. Importantly, these independent studies link the findings that CRT is redistributed to the cell surface and stimulate maturation of DC and antigen cross-presentation to CD8+ T cells. Many studies describe the great potential of tumour antigen recognition by CD8+ T cells, but overall such immune responses are generally weak and transient (Wang, 2001). One of the possible explanations for a transient effect of CD8+T cell-mediated anti-tumour immunity is the lack of CD4 T cell help (Corthay et al., 2005; Hung et al., 1998; Savelyeva et al., 2005). This implies that to fully achieve an effective anti-tumour response, well organised and cooperative networking between each subset of T cells is required. Therefore, a better understanding of the CD4+ T cell function that consequently initiates and maintains the memory response, might be essential in long-term clinical treatment against cancer.

Although T cells are the major component of the mononuclear cells infiltrating many solid tumours, B cells and plasma cells are also present in the tumour microenvironment. In particular, Hansen et al. demonstrated that an increase number of B cells, penetrating MCB cancer tissue correlates with a better survival prognosis for patients. This was related to an induction of apoptosis in MCB cells by granzyme B released from CTL. Such dying MCB cells were shown to expose actin on their cell surface, permitting recognition by the TIB and resulting in oligoclonal expansion of B cells. This suggests that a major function of TIB was not antibody production but rather acting as a professional APC that prime CD4+ T cells (Hansen et al., 2001). Furthermore, Yasuda et. al. investigated the functional significance of TIB in tumour sites. They showed that patients with lung cancer have a population of TIB, constituting 4-16 % of the total number of infiltrating cells in seven tested lung cancers. These TIB showed up-regulated expression of molecules involved in antigen presentation inducing CD40, CD80 and MHC class II compared with that seen in peripheral blood B cells (Yasuda et al., 2002). However, the broader cohort of different clinical stages, histopathology and immune status are necessary for a complete clarification of the importance of B cells in anti-tumour immunity.

Based on previously described reports documenting novel forms of immunogenic cancer cell death and the unclear role of B cells in anti-tumour immunity, I have decided to explore the possibility that B cells are able to extract and present to cognate CD4+ T cells tumour antigens relocated to the plasma membrane of dying cancer cells. Understanding this process would lead to a better understanding of the different components of anti-tumour immunity and mutual cooperation and may result in the induction of more effective and persistent anti-tumour responses. I believe that this might strongly contribute to the future of clinical practice for cancer patients.

7.1. Generation of a model antigen

The first step of this project involved generation targeting of a model antigen hen egg lysozyme (HEL) to various cellular compartments. This would allow me to monitor protein relocation following apoptosis.

The structure of HEL and a number of different anti-HEL antibodies is well characterised (Gerwing and Thompson, 1968; Smith-Gill et al., 1984). One of these antibodies, HyHEL10, was used to detect HEL expression using immunofluorescence techniques. Additionally, our laboratory possesses B cells expressing this antibody as a membrane bound BCR and also has a panel of HEL-specific T cell hybridomas (Adorini et al., 1988). Unfortunately, none of the plasmids that I generated (cyto-HEL, mito-HEL, nuc-HEL) led to HEL localisation in the correct intracellular compartment. Despite additional re-cloning of HEL into GFP-containing plasmids resulted in partial GFP expression, the synthesis of the expected fusion protein in HeLa cells did not occur. It was likely that the disulphide bonds present in the HEL structure negatively affected folding and consequently inhibited expression. Therefore, we decided to use another model antigen, EGFP-TTCF (E/T). The N' terminal region of the E/T fusion protein - EGFP has a natural ability to emit green light when excited by blue light. For this reason, visualisation of E/T antigen using fluorescence microscopy when expressed in HeLa cells would be relatively straightforward. Furthermore, having previously generated and tested TTCF-specific B cells it was even more encouraging to choose E/T as a model antigen.

To this end, I generated four different E/T constructs targeting the fusion protein into the cytoplasm, mitochondria, ER or to the plasma membrane, respectively and tested their expression pattern in HeLa cells. The sub-cellular localization of each construct was detected by Western blotting and was also confirmed by immunofluorescence. The microscopic images

shown in **Chapter 3** demonstrate the correct co-localisation with introduced markers characterising particular compartments and the individual E/T expressing constructs. Each co-localisation chart clearly revealed the correct localisation of E/T antigen in the desired sub-cellular compartments of HeLa cells.

7.2. Establishing the apoptotic parameters required for intracellular antigen relocation

Apoptosis is an evolutionarily conserved form of programmed cell death during which dying cells acquire a series of morphological and biochemical alterations. These changes include cytoplasmic shrinkage, membrane blebbing, chromatin condensation and nuclear DNA fragmentation (Wyllie et al., 1980). Importantly, this fundamental biological process is involved not only in the maintenance of tissue homeostasis, but also plays a pivotal role in the prevention and elimination of cancer cells (Kerr et al., 1994).

Most cytotoxic drugs kill cancer cells by the induction apoptosis through the p53 pathway and by activating effector caspases such as caspases-3 (Kim et al., 2002). Anthracyclines (including doxorubicin and mitoxantron), along with oxaliplatine, are a new generation of chemotherapeutics which not only induce cancer cell death via inhibition of DNA and RNA synthesis, but also activate the immune system to destroy cancer cells. In particular, it has been shown in *in vivo* models, following anthracycline treatment of CT26 colon cancer cells, that DC which penetrate the tumour tissue have increased expression of maturation markers (CD80, CD83, CD86) and also secrete increased amounts of pro-inflammatory cytokines (Apetoh et al., 2008) (Zitvogel et al., 2008). The induction of molecules involved in antigen presentation by DC was due to the intracellular relocation of CRT from the ER of dying CT26 cells to the plasma membrane. Such surface displayed CRT induced DC maturation which led to enhanced cross-presentation to CTL and therefore a better anti-tumour response was elicited.

Based on these findings, I decided to test whether B cells are able to extract relocated antigens from an anthracycline treated cancer cell line resulting in CD4+ T cell activation.

Before studying E/T relocation, I optimised the kinetics of apoptosis in HeLa cells following incubation with several anthracyclines. This was performed using the viability MTT test and annexin V binding. Based on these results, I subsequently treated HeLa cells for 4 h with optimised concentration of drugs (STS, DX and MX respectively). Subsequently, I tested

whether the E/T was able to relocate in HeLa transfectants following drug treatment. The results from fluorescence microscopy clearly showed that ER-E/T relocated to apoptotic bodies of dying cells incubated with DX or MX but not if treated with the non-immunogenic drug STS. For this reason, it was possible that ER-E/T expressed in HeLa cells would be a good candidate for B cell recognition following apoptosis induction by anthracyclines. Unexpectedly, the pilot experiments carried out with anthracycline treated ER-E/T HeLa cells and co-cultured with specific-B and T cells did not show the recognition and presentation of relocated E/T antigen. Paradoxically, proliferation bio-assays demonstrated a reverse correlation between the numbers of drug treated HeLa transfectants and T cell stimulation. Surprisingly, the MTT test showed that T cells were extremely sensitive to anthracyclines following incubation with extensively washed HeLa transfectants treated with DX or MX. The sensitivity of T cells following anthracycline administration is well documented (Kim et al., 2009a).

Obeid and others showed that local radiotherapy in mice bearing breast cancer was more efficient in immune-competent mice then in immune-deficient animals. They showed that following UVC treatment, apoptotic tumour cells were engulfed more vigorously by DC leading to TAA cross-presentation by MHC class I molecules to CD8+ T cells (Obeid et al., 2007b). Also, UVC-treated breast cancer cells released inflammatory mediators including HMGB1, DAMPs that induced the upregulation of costimulatory signals on DC. Thus DC were able to act more efficiently as APC in CTL-mediated anti-tumour immunity (Green et al., 2009b). Based on these observations, I optimised the dose and time required for monitoring the apoptotic changes in UVC-treated HeLa cells. Following 100, 200 and 300 J/m^2 UVC exposure, I measured HeLa viability using the MTT test and visualised using fluorescence and confocal microscopy, how ER-E/T intracellular localization was effected. Optimal UVC-induced apoptosis resulted in 40% cell death following treatment with 300 J/m^2. Additionally, annexin V staining revealed that at this dose of UVC more than 80% cells were undergoing apoptosis. This dose was therefore used for rest of this study. Subsequently, I monitored changes in cellular morphology following 300 J/m^2 treatment in HeLa transfectants expressing E/T in various subcellular compartments. In particular, I focused on changes in the structure of the nuclei, plasma cell membrane and intracellular E/T localisation in HeLa transfectants, exposed to 300 J/m^2 UVC. UVC-treated HeLa cells exhibited typical apoptotic changes such as DNA condensation and fragmentation indicated by strong Hoechst 33342 staining and plasma membrane asymmetry visualised by WGA dye. Importantly, the expression patterns of cyto-E/T and ER-E/T constructs in UVC-treated HeLa cells were completely changed. The occurrence of green apoptotic bodies was observed. Similar observations have been seen by Maftoum-Cost et. al., in HeLa cells exposed

to photodynamic therapy (PDT). They showed that dying PDT-treated HeLa cells underwent changes in the ER compartment that tead to formation of bleb-like structures as a consequence of ATP loss and membrane potential dissemination (Maftoum-Costa et al., 2008). Furthermore, Fuller et al., also observed morphological changes following light exposure during PDT in lymphoma cells (Furre et al., 2006). The images from fluorescence microscopy demonstrated that PDT treated Jurkat cells exhibited typical apoptotic features such as cell shrinkage, chromatin condensation and importantly apoptotic body formation.

The molecular mechanism of bleb-like structure formation was investigated by the Lane group (Lane et al., 2005). They showed the pathway of apoptotic body formation was attenuated if actin (LutrunculinA), myosin II (Blebbistatin), or caspace-6 activity (zVEID.fmk) inhibitors were added to dying HeLa cells following anisomycin treatment. They presented images of apoptotic bodies in HeLa cells that contained ER structures (indicated by strong staining of anti-calnexin antibody in membrane layer) and also condensed fragments of chromatin visualised by DAPI staining. Prior to apoptosis induction, the pre-incubation of HeLa cells with each inhibitor individually reduced the occurrence of apoptotic bodies. They suggested that microtubule motors and caspase-6 activity are required for remodelling of chromatin and ER structure that is encapsulated by the plasma membrane consequently leading to formation of apoptotic bodies. These observations are consistent with my data obtained by confocal microscopy, where the condensed chromatin and ER in UVC treated HeLa ER-E/T transfectants were shown to undergo inclusion within large plasma membrane blebs. However, in my study, the occurrence of green bleb-like structures not only confirms that HeLa transfectants died by apoptosis, but more importantly, that the intracellular E/T antigen surface remodelling might now be accessible for B cell extraction. This observation was essential for further experiments requiring specific-B cells.

7.3. Implications for anti-tumour immunity of understanding the molecular mechanisms involved in intracellular antigen relocation

Apart from CRT and a few other proteins currently reported to relocate following chemo or radiotherapy (**Chapter 1**), there is a great need to perform more advanced studies identifying and classifying novel tumour antigens originally derived from intracellular compartments. In particular, understanding the molecular mechanisms of intracellular tumour antigen relocation will allow better control and consequently the elimination of growing tumours. Currently, Kepp et al. showed that CRT surface exposition following anthracycline or oxaliplatine treatment was due to eukaryotic initiation factor 2α (eIF2α) phosphorylation by eIF2α kinase PERK and inhibition of eIF2α phosphatase (composed of the catalytic subunit (PPI) and the regulatory subunit (GADD34)) (Kepp et al., 2009). Using a commercially synthesised peptide disrupting of PPI/GADD34 complex, they demonstrated that following anthracyclines treatment HeLa cells had both reduced enzymatic activity of the PPI subunit and significantly had increased phosphorylation of eIF2α that consequently led to CRT surface exposition. Surprisingly, they showed that a disruption PPI/GADD34 complex peptide could also stimulate CRT exposure without chemotherapeutic inducer. Therefore, these *in vitro* findings indicate that using a protein inhibiting eIF2α phosphatase, CRT-mediated tumour immunogenicity might be elicited without cytotoxic side effect and eventually could be beneficial for patients. However, future studies which will focus on role of B cells as APC recognising CRT or other relocated tumour antigens need to be addressed. Based on the many examples described in **Chapters 1**, it is possible that B cells may prove to be an alter population of APC recognising relocated tumour antigens. Furthermore, studies performed by Tesniere et al. demonstrate that colon cancer patients who lack functional TLR4 (receptor expressed by DC that mediates the recognition of relocated tumour antigen) had a reduced survival rate compare to patients with functional TLR4. Therefore, in such situations it is important to look at the role of B cells as an alternative population of APC recognising tumour antigen differently (BCR-mediated) rather than via non-specific TLR4 binding (Tesniere et al.).

Results obtained during this project represent only an initial analysis of the possible role of B cells as APC that need to be explored further. Therefore, in the future, it may be worthwhile to generate panel of CRT or TAA-specific B cells recognising relevant antigens and to test it in *in vivo* models of B cell-mediated immunity following UVC or anthracycline treatment.

7.4. The physiological consequences of antigen recognition by specific-B cells from the surface of target cells

To investigate the immunogenic potential of apoptotic cells monitored by antigen-specific B cells, I established several *in vitro* models. Firstly, I examined whether E/T derived from apoptotic HeLa cells will be acquired by antigen-specific B cells and visualised using flow cytometry.

Based on my previous observations using confocal microscopy, that following UVC treatment, intracellular E/T expressed by HeLa transfectants relocated to cell surface, I speculated that relocated E/T antigen would be acquired by TTCF-specific B cells. Therefore, the detection of extracted E/T antigen by specific B cells should be visible using flow cytometry. Indeed, when experiments gating on B220 +ve cells were performed, I demonstrated that specific B cells (but not non-specific B cells) incubated with apoptotic E/T HeLa transfectants, selectively acquired green fluorescence. Such experiments, to my best knowledge, are the first ones to demonstrate the acquisition of UVC-induced relocated intracellular antigen by B cells using fluorescence cytometry. In addition, to test whether relocated E/T acquired by TTCF-specific B cells was subsequently processed and complexed with MHC class II molecules, I performed a functional bio-assay measuring TTCF-specific T cell stimulation. This required a generation of new H-2d restricted TTCF-specific T cell hybridomas. Therefore, I fused *ex-vivo* T cells (isolated from lymph nodes from E/T immunised mice) with the BW 5417 T cell lymphoma fusion partner. Using this new reagent allowed me to establish a novel antigen presentation assay that tested the biological consequences of E/T acquisition from apoptotic HeLa cells by B cells. In particular, I quantified the IL-2 production by antigen-specific CD4+ T cells following incubation with B cells that had been pre-incubated with mem-E/T HeLa transfectants for various time periods.

Somewhat surprisingly, I showed using both techniques (flow cytometry and antigen presentation assay) that membrane-tethered antigen acquisition can occur very rapidly. In particular, incubation for time periods as short as 1 min was sufficient to detect BCR-mediated E/T acquisition by TTCF-specific B cells. Additionally, this level of antigen acquisition was sufficient for maximum CD4+ T cell stimulation.

These findings are consistent with, and extend observations from different groups demonstrating BCR-mediated antigen acquisition is very rapid. For example, Batista et al.,

using confocal microscopy was able to visualise synapse formation between HEL-specific B cells and various HEL expressing target cells in times of approximately 10 min. Furthermore, serial optical sections of fixed and permeabilized B cells removed from the target cells, indicated that HEL-specific B cells internalized extracted HEL antigen (Batista et al., 2001). Flow cytometry analysis of these B cells also showed upregulation of CD86 as a result of antigen acquisition. However, these studies did not test the physiological aspect of surface tethered antigen extraction. This has been successfully demonstrated in this project, that specific-T cell hybridomas are able to respond to antigen attached to the surface of other cells – target cell. Furthermore, by introducing 0.4 μM blocking filters, I confirmed BCR-mediated E/T acquisition is a contact-dependent process. In contrast, soluble antigen can be recognised and presented by TTCF-B cells to specific CD4+ T cells with or without blocking filters equally, as the soluble TTCF is able to penetrate across the 0.4 μm blocking filters. These findings extend those of the Batista laboratory showing that the incubation of target cells expressing mem-HEL and separated by a mesh from HEL-specific B and T cells, abrogated antigen recognition, but not if soluble HEL was added to the those B and T cells (Batista et al., 2001). Importantly, Batista's studies did not examine B cell acquisition of antigens relocated from intracellular compartments. Therefore, this project demonstrates for the first time that following the induction of the previously described immunogenic apoptosis, HeLa transfectants relocate intracellular antigens onto the cell surface as integral part of apoptotic bodies. Importantly, I have also demonstrated that this form of tethered antigen can be extracted by immuno-specific B cells and presented to cognate CD4+ T cells.

The majority of current studies examining the consequences of apoptotic cell death focus on a role for DC or macrophages engulfing apoptotic cells leading to cross-presentation and CTL-mediated immunity (Gregory and Devitt, 2004). However, this project for the first time demonstrate that B cells act as APC and stimulate CD4+ T cell-mediated response for antigens derived from apoptotic target cells. Therefore, these studies reveal a previously un-described aspect of B cell biology. In particular, the ability of B cells to initiate CD4+ T cell responses against antigens expressed in intracellular compartments of tumour cells. Furthermore, understanding the mechanism of how TIB penetrate tumour sites needs to be clarified. As previously described in **Chapter 1** (**Section 1.2.2.**), it is possible for DC to convert (in a tumour microenvironment) to become tolerogenic leading to a state of tumour immunosuppression. Therefore, identification of the key feature which allows better activation and recruitment of tumour-specific B cells before homing at the tumour site may improve tumour antigen recognition and consequently may cause more effective anti-tumour immunity.

Studies performed by Pages et al. representing a large cohort of patients with colorectal tumours (approximately 1000 patients) showed that a high frequency of tumour infiltrating T cells had cytotoxic and memory phenotypes, They also showed that the presence of TIB was significantly predictive of a favourable clinical outcome (Pages et al.). In particular, they demonstrated that tumour infiltration by B and T cells was strongly correlated with DC expressing high level of lysosomal-associated membrane protein (Lamp). They suggested that Lamp+ DC are involved in tumour antigen presentation by recruitment naive B and T cells in adjacent tertiary lymphoid organs (such as GALT, MALT or BALT) as primary sites of tumour-initiated immune reaction.

Based on the above mentioned findings and results presented in **Chapter 6**, it may be likely, that following UVC treatment, TIB might be activated in adjacent tertiary lymphoid organs by DC resulting in the activation of the adaptive anti-tumour immunity. Therefore, the explanation of the role of B cells in recognising relocated tumour antigens may be a very promising approach to anti-tumour therapy and requires further investigation.

7.5. Summary

The underlying concept behind this project was to examine the possible role of B cells as APC in the induction of anti-tumour immunity. In particular, I have examined the ability of B cells to recognise intracellular antigens that have relocated following the induction of the apoptosis by anthracyclines and UVC. I have shown that these relocated antigens are acquired by antigen-specific B cells for processing and presentation that consequently can elicit anti-tumour CD4 T cell-mediated immunity.

This was performed by the establishment of several novel *in vitro* systems. The first was engineering a panel of plasmids expressing a model antigen in various sub-cellular compartments of HeLa cells. Subsequently, optimisation of the apoptotic conditions inducing the intracellular protein relocation to the cell surface was achieved. Finally, using antigen-specific B and T cells, I was able to demonstrate CD4+ T cell activation following recognition of relocated intracellular antigen.

In conclusion, the *in vitro* studies described in this thesis demonstrate a 'proof of principle' that B cells are capable of acting as effective APC leading to a generation of anti-tumour immunity. Therefore, better understanding of the molecular mechanisms inducing surface antigen relocation may find potential implantation in the clinic. In particular, characterisation of the signaling pathways that drive intracellular E/T relocation to the surface needs to be understood. Further studies involving organelle fractionation and co-immunoprecipitation to allow the identification of proteins essential in the process of E/T relocation should be performed. Based on the previous studies by Kepp et al., 2009 (discussed in **Chapter 7.3.)** comparing whether such proteins e.g. ERp57 that co-locate with CRT relocations or eIF2a that initiates CRT relocation, also participate in intracellular E/T relocation should be performed. In addition, further characterisation of stimuli inducing immunogenic apoptosis with reduced harmful side effects needs to be carried out.

Following these *in vitro* studies, the next step to understand the role of B cell-mediated anti-tumour immunity could involve the development of a more physiological *in vivo* model. Indeed, during the final stages of my studies, a report has shown a requirement for B cells in the induction in anti-tumour immunity in a mouse model (Dilillo et al.). In this study, B cell depleted mice challenged with B16 melanoma were shown to have enhanced tumour growth and metastasis compared to control mice. Furthermore, the number of CD4+ memory and CD8+ effector T cells were both shown to be reduced in tumour challenged B cell depleted

mice. These studies imply that B cells are directly required for cellular response against B16 melanoma *in vivo*. However, this study did not address the role of B cell APC-function. This role could be addressed in B cell deficient mice challenged with B16 melanoma cells expressing the model antigen (E/T) used in my study for example. This would involve analysing E/T specific T cell populations from such animals and therefore may provide additional evidence for role of B cells as APC in anti-tumour immunity.

Thus, I envisage that following the induction the immunogenic apoptosis B cell-mediated immunotherapy may have an enhanced effect on tumour elimination and consequently may improve the quality of life and extend the survival rate of cancer patients in the future.

- 8. Materials and methods -

8.1. Materials

8.1.1. Antibodies

The following antibodies were used for both Western blotting (WB), immunofluorescence (IF) and flow cytometry (FACS):

Table 8.1. Primary antibodies.

Antigen	Antibody name	Source	Dilution and application
hen egg lysozyme (HEL)	HyHEL10 (mouse) 1mg/ml	Knight lab	1/100: IF
HEL	α–HEL (rabbit)	Sigma	1/5000: WB
c-Myc	9E10 (mouse) supernatant	Knight lab	1/10: WB
green fluorescent protein (GFP)	α-GFP (rabbit)	Sigma	1/2000: WB
B220	directly labelled α-B220-PerCP (rat)	BD Pharmingen	1/100: FACS
CD4,	directly labelled α–CD4–FITC and PE (rat)	BD Pharmingen	1/100: FACS
CD8	directly labelled α-CD8-FITC and PE (rat)	BD Pharmingen	1/100: FACS
TCR	directly labelled α-TCR-FITC (rat)	BD Pharmingen	1/200: FACS
TCR Vβ type 2-17	directly labelled (FITC) antibodies from different species	BD Pharmingen	TCR Vβ taping : FACS

HRP-conjugated secondary antibodies were from Sigma (anti-rabbit 1/5000) and BD Pharmingen (anti-mouse 1/2000, anti-human1/2000) and fluorescently conjugated antibodies (FITC or TRITC) were from Molecular Probes, Sigma Aldrich, and ImmunoResearch (1/100 dilution).

8.1.2. Oligonucleotides

PCR primers were designed based on known nucleotide specific sequences of HEL or EGFP-TTCF. Oligonucleotides were synthesised by MWG Biotech and HPLC purified. Some of the primers contain the appropriate restriction enzyme recognition sites (underlined). The forward primers specific for the sense DNA strand are donated 'F' and reverse primers, specific for anti-sense DNA strand are donated 'R'.

Table 8.2. Primers for recloning HEL and TTCF including the various restriction sites.

Primer	Sequence
5'Nco1-HEL(cyto)	5'-CCA TGG GGA AAG TCT TTG GAC GAT GT-3'
5'Pst1-HEL(mito)	5'-CTG CAG AAA GTC TTT GGA CGA TGT-3'
5'Not1-HEL(mitoGFP)	5'-GCG GCC GCA AAA GTC TTT GGA CGA TGT GAG-3'
3'Not1-HEL	5'-GCG GCC GCC AGC CGG CAG CCT CTG ATC CA-3"
5'EGFP Pst1	5'-CTG CAG ATG GTG AGC AAG GGC GAG GAG -3'
3'TTCF Not1	5'-GCG GCC GCG TCG TTG GTC CAA CCT TCA TC -3'
EGFP Seq 3F 667	5'-CTG AGC ACC CAG TCC GCC CTG-3'
TTCF Seq 4F 967	5'-TCT GAA GTT ATC GTG CAC AAG -3'
TTCF Seq 5F 1267	5'-TGG GTT TTC ATC ACT ATC ACT -3'
TTCF Seq 6F 1567	5'-ATC CCG GTA GCT TCT AGC TCT -3'
TTCF Seq 7F 1867	5'-GCT CCG GGT ATC CCG CTG TAC -3'

8.1.3. Bacterial strains

E. coli strain	Application	Source
TOPO10 One Shout	50 μl	Invitrogen

The Invitrogen One Shot® TOP10 chemically competent *E.coli* (genotype F- mcrA Δ(mrr-hsdRMS-mcrBC) ϕ80lacZΔM15 ΔlacX74 recA1 araD139 Δ (ara-leu)7697 galU galK rpsL (StrR) endA1 nupG)) were used for cloning and propagating DNA. The chemically competent, ampicilin resistant cells were used to amplify the DNA of each generated plasmids. TOPO10 One Shout *E.coli* cells used to clone blunt ends (Invitrogen) were kanamycin resistant.

8.1.4. Plasmid constructs used for HEL and EGFP-TTCF (E/T) sub-cellular compartment expression

The following constructs were used:

Table 8.3. Constructs used in this study.

Construct	Source
pCMV-cyto-HEL	Gift from S. Ostrand-Rosenberg
pCMV-mito-HEL	Gift from S. Ostrand-Rosenberg
pCMV-nuc-HEL	Gift from S. Ostrand-Rosenberg
β–globulin–mem-HEL	Gift from F. Batista
pCMV-mito (-SS)-HEL	This study
pCMV-mito-GFP-HEL	This study
pCMV-cyto-(-SS)-HEL	This study
pCMV-mito-GFP	Invitrogen
pCMV-cyto-EGFP	Clontech
pCMV-cyto-E/T	This study
pCMV-ER-E/T	This study
pCMV-mito-E/T	This study
β–globulin–mem-E/T	This study

Plasmids no. 1, 2 and 3 were kindly received from S. Ostrand-Rosenberg and no. 4 from F. Batista. Constructs no. 5 and 6 were re-cloned from the original vector pCMV-mito-GFP (no. 8 (Invitogen)) by insertion or replacement the GFP part to HEL, thereby I received pCMV-mito-GFP-HEL or pCMV-mito-HEL. Plasmid pCMV-cyto-HEL (no.7), was generated by replacement the EGFP part from cyto-EGFP plasmid (no. 9 (Clontech)) for HEL sequence. Plasmids no. 10.-cyto-E/T, 11.- ER-E/T, and 12.-mito-E/T, were engineered from the original pShoover plasmids (Invitrogen): pCMV-cyto, pCMV-ER and pCMV-mito by introduction into the cloning side (N'Pst1 and C'Not1') the E/T sequence. Constructs no. 13 was made from the commercial pCMV-ER (Invitrogen) by inserting E/T sequence and fragment of DNA encoding the transmembrane and cytoplasmatic domains of the mouse MHC class I molecule, H-2Kb.

8.1.5. Cell lines

Cell lines	Name	Characteristic	Reference:
B cell lines	A20 - non-specific B cells	mouse IgG2a, B220+, H-2d B cell lymphoma	(Kim et al., 1979)
	A20-TTCF -TTCF-specific B cells	mouse IgG2a, B220+, H-2d B cell lymphoma expressing TTCF-specific BCR	Andrew Knight
T cell lines	MC-52 TTCF-specific T cells	mouse CD4+, CD8-, H-2d restricted, recognizing 17-mer peptide of TTCF in position 1120-1137 T cell lymphoma expressing TTCF- specific Vβ2 TCR	This study
	CTLL-2	mouse IL-2 dependent T cell hybridomas	(Gillis and Smith, 1977)
Others	HeLa	human epithelial carcinoma cells line	George Otto Gey
	J774	mouse peritoneal macrophage cell line	(Ralph and Nakoinz, 1975)

8.1.6. Proteins and peptides

A panel of 88 overlapping peptides spanning the TTCF sequence was used to characterize the antigen-specific T cell hybridomas MC-52. These 17-mer peptides were a kind gift from Colin Watts (Dundee University).

Recombinant EGFP-TTCF (E/T) protein were isolated by Andrew Knight from transformated *E.coli* K-12 derivative, Origami^{TM} (DE3) pLysS (Novabiotech) with previously generated bacterial expression plasmid encoding EGFP-TTCF sequence and flanked on N' terminal end by 10 histydyne residues.

8.1.7. Apoptotic regiments

Doxorubicin (DX) - doxorubicin/adriamycin hydrochloride was parched from Fluka.

Mitoxantron (MX) - mitoxantrone dichydrochloride was parched from Sigma-Aldrich.

Staurosporin (STS) - from Streptomyces sp. was parched from Sigma-Aldrich.

In order to induce UVC light – the special lamp was built in the purpose of this project. The lamp was calibrated to delivery 0.2 mJ of UVC /cm^2/s.

8.2. Methods

8.2.1. DNA manipulation

8.2.1.1. Preparation of plasmid DNA

Plasmid purification on a small or large scale was performed with the Qiagen Miniprep or Maxiprep kit, respectively. Bacteria were grown over night at 37^{o}C in 2.5 ml or 250 ml cultures containing the appropriate selection antibiotic. After centrifugation, plasmid DNA was prepared as per manufactures instruction. DNA concentrations/purity were quantified in a spectrophotometer at a wavelength of 260/280 nm after dilution in H_20.

8.2.1.2. Polymerase Chain Reaction (PCR)

PCR reactions were carried out in 50 µl reactions containing 100 ng template cDNA, 2 nM dNTPs, forward and reverse primers (5 µg/ml) and 1 unit *Taq* or *PFX* polymerase using the following cycles using Thermocycler 'Alpha Unit Block Assembly for PTC DNA' (Bio-Rad, Model PTC-200) machine:

1 cycle	Initial denaturation	94 C, 2min	
	Denaturation	94 C, 15 sec	30 cycles
	Annealing	55 C, 30 sec	
	Extension	68 C, 1 min	
1 cycle	Final extension	68 C, 10 min	

8.2.1.3. Restriction digestion

Restriction digests were carried out in 20 µl reactions containing a minimum of 1 µg DNA, 5 units restriction enzyme (New England Biolabs), 2 µl 10x restriction buffer supplied and 100 µg/ml BSA. Samples were incubated at 37^{o}C for 1-4 h before the reaction was stopped by adding 4x sample buffer (Bromophenol blue in 50% glycine, 1 mM EDTA pH 8.0).

8.2.1.4. DNA agarose gel electrophoresis

Both restriction digests and PCR products were analysed by agarose gel electrophoresis.
1.2 % agarose was dissolved in TAE buffer (Tris-HCl pH 8.0, 20 mM acetic acid, 1 mM EDTA). Ethidium bromide (5 μg/ml) was added to a final concentration 0.5 μg/ml. Samples were mixed with 4x sample buffer and separated in TAE at 110 Volts (V) constant.

8.2.1.5. Gel purification of DNA fragments

DNA fragments were cut from agarose and the DNA isolated and purified from the gel slice using the QIAquick gel extraction kit (Qiagen) according to manufacturing protocols.

8.2.1.6. Ligation

Gel purified cDNA and vectors were mixed at a molar ratio of approximately 5:1. Before ligation, vectors were dephosphorylated using calf intestinal phosphatase (CIP) (New England Biolabs). Ligation was carried out with T4 ligase (New England Biolabs) in 14 μl reactions for either 2 hours at room temperature or overnight at 16^{o}C. 1 μl or 3 μl ligation was transformed into *E. coli* (TOPO10 Invitrigen).

8.2.1.7. Bacterial transformation

Cells were transformed chemically, based on manufacturer's recommended protocols. Briefly, after thawing 50 μl aliquots of competent TOPO10 cells were mixed with either 3 μl or 1 μl ligation product or 10 ng plasmid and incubated on ice for 15 min. Cells were transformed by heat-shock at 42^{o}C for 60 seconds. The 200 μl of pre-warmed (to 42^{o}C) SOC medium was added and the reaction was incubated at 37^{o}C for a further 1 hour. Bacteria were plated out on LB agar plates containing either kanamycin (50 μg/ml) or ampicilin (50 μg/ml) antibiotics and incubated overnight at 37^{o}C to allow colonies to form.

8.2.1.8. Screening and expansion of bacterial colonies

Single bacterial colonies were expanded in order to isolate sufficient. A sterile tip was used to inoculation individual bacterial colonies for analysis. Inoculated colony with 5 ml of LB containing appropriate selective antibiotics were cultured overnight at 37^{o}C with shaking for expansion. On the next day 0.5 ml of culture was used to inoculate 250 ml of new LB medium and 18 h later the plasmid DNA was isolated using MaxiPrep (Qiagen). Following DNA isolation the correctly replicated plasmid was identified by PCR amplification and restriction digestion and bi-directionally sequencing (Lark) prior to use.

8.2.2. Cell culture

8.2.2.1. Maintenance of mammalian cells

HeLa cells were grown in RPMI 1640 supplemented with 10% foetal calf serum (FCS), 100 g/ml kanamycin and 2mM glutamine, 1mM sodium pyruvate (Invitrogen), non-essential amino acids (Invitrogen), and 50 μM β-mercaptoethanol (Sigma-Aldrich), at 37^{o}C in an atmosphere of 5% CO_2. For passaging cells were washed once with fresh RPMI and incubated at 37^{o}C in 5% CO_2 in 0.05% trypsin (Invitrogen) until cells detached from the plastic. They were then either split into new flask or seeded into plates at the desired cell number.

8.2.2.2. Transient transfection

Transient transfection of HeLa cells expressing HEL was carried out using Lipofectamine 2000 (Invitrogen) according to manufactures instruction. Approximately 0.8x10^5 or 2.5x10^5 cells were seeded in either 24 or 6-wells plates respectively containing glass coverslips (for IF). Growth medium was changed to growth medium lacking antibiotics one hour before transfection. The next day transfectants were either lysed (for WB) or analysed for IF.

As Lipofectamine 2000 demonstrated high cytotoxic effects of on HeLa transfectants when using HEL plasmids, I decided use a different lipolityc cationic polymer Turbofect^{TM} (Fremantes) which showed less cell death for the TTCF constructs used subsequently. This polymer forms complexes with negatively charged DNA. The transfection efficiency using 2 μl of Turbofect from 1 μg of DNA on 1x10^5 HeLa cells was routinely more than 80%. The detailed steps of transfection were performed according to manufacturer's protocols.

8.2.2.3. Stable transfection

In order to generate stable cells lines $0.8x10^5$ HeLa or J774 cell lines were transfected by different constructs expressing HEL or E/T constructs with also curry gene of neomycin (G418) resistance. One week later, the single clones' dilution was made and such single cells were then plated out in 96-well plates. Such single cells were cultivated for the next 2weeks in RPMI supplemented with G418 1mg/ml allowing selection only the clones, which expressed desired construct. Two weeks later selected survived colonies were picked up and divided on the two groups: one group which was analysed on microscopy in order to visualised E/T expression and second one was expanded and kept as a backup.

8.2.3. Analysis of protein expression and sub-cellular localization

8.2.3.1. Indirect immunofluorescence

Following fixation with PFA 3% for 20 min at room temperature, HeLa cells were rinsed three times with PBS and incubated for 15 min in 50 mM NH_4Cl to neutralize PFA. PBS-washed cells were then permeabilized in 0.1%-TX-100/PBS for 4 min at room temperature and washed again. Coverslips containing cells were then inverted onto 50 μl drops of primary antibody (mouse anti-HEL: HyHEL 10; diluted in PBS/2% FCS) and incubated at room temperature for 1 h. Cells were washed three times and the antibodies were visualised with anti-mouse FITC or TRITCI secondary antibodies (ImmunoResearch, Sigma) after incubation at room temperature for an additional 1 h. Finally, the cover slips were inverted onto slides containing a drop of the mounting/anti-fade medium CitiFluor (Agar Scientific) and analysed using either a Leica Microsystems (Heidelberg GmbH) confocal or fluorescence microscope. Three emission spectra were used for different dyes: TRITC or MitoTracker Red-excitation 543nm, emission 580 nm; FITC-excitation 488 nm, emission 510-535nm; Hoechst 33342-excitation 343 nm, emission 483 nm, Alexa Fluor 594-excited 594 nm, emission 617 nm. Combined maximum intensity of fluorescence was measured by Leica TCS SP2 UV confocal laser scanning microscope (LSM) Leica Microsystem using a MCX Plan Apo. Na. software. The 0.85x40 or x60 magnification lenses were used and images were analysed by LCS 2.61 software with help and assistance of Trevor Booth.

The images from fluorescence microscopy were generated using Laica Microscope Type 020-919.509 LB 100 TB. and SPOT Advanced Software by permission of Dr. Mark Birch.

8.2.3.2. MitoTracker Red labeling

To visualise mitochondria MitoTracker Red (Molecular Probe, 200 nM) was used. This red fluorescent dye (tetramethylrhodamine) is selectively concentrated by active mitochondria due to its positive charge. Viable cells that have active mitochondria with considerable membrane potential will pick up and concentrate the dye in the mitochondria. MitoTracker is well-retained even after fixing and permeabilization. MitoTracker Red was added to HeLa cells for 20 min at 37^{o}C and cells were then washed extensively with cRPMI and before fixation with 3% paraformaldehyde (PFA) in phosphate buffer saline (PBS) for 20 min at room temperature and performed as previously described to visualise slides on microscopy.

8.2.3.3. Hoechst and WGA staining

After staining with antibodies cells were treated with 5 μg/ml of the DNA dye Bisbenzimide H 33342 (Hoechst 33342; Sigma). Hoechst 33342 is a cell membrane-permeable dye that intercalates in the A-T regions of DNA and produces a blue fluorescence under a UV filter. Additionally, in order to distinguish plasma membrane structures in HeLa cells, the red-fluorescent Alexa Fluor 594 wheat germ agglutinin (WGA) was used. Not-permeabilized HeLa cells following 10 min incubation with 5 μl/ml of WGA, incorporated dye, which binds selectively to N-acetylneuraminic (sialic) acid residues of cell membrane.

8.2.3.4. Preparation of cell lysates and SDS-polyacrylamide gel electrohoreisis

Approximately 1x10^{5} HeLa cells were remove from plates by incubating in 5 mM EDTA/PBS for 5 min at 37^{o}C. Detached cells were spun down for 5 min at 8000 rcf and lysed for 30 min at 4^{o}C in 1% Triton X-100, 1x TBS, plus protease inhibitor cocktail (Sigma P-8340). Nuclei acids and insoluble debris was removed from lysates by re-spinning 25 min, 16 000 rcf. Protein concentration was determined based on initial number of cells. Samples were mixed with 4x SDS-sample buffer (12.5 ml 1M Tris-HCl pH 6.8, 30 ml 20% SDS, 20 g glycerol, 2 ml 1% Bromophenol Blue) and 100 mM dTT. Before loading, samples were boiled for 5 min. Equal amounts of protein based on the number of cells were loaded per lane and separated on 14% SDS-PAGE gels using 100 V constant for 15 min, then 120 V until the dye front reached the bottom of the gel.

8.2.3.5. Western blot immunodetection

After SDS polyacrylamide gel electrophoresis, proteins were transferred onto nitrocellulose (Hybond, Amersham Pharmacia Biotech) at 0.35 Amperes (A) for 90 min. Gel and nitrocellulose membranes were embedded in a sandwich of 3 sheets 3mm Whatman paper and two pads on each side. The membrane was then blocked in 0.2% Tween 20 in 1x PBS containing 5% dried milk for 1 hour and probed with appropriate primary antibodies. Following extensive washing (3x10 min., PBS/0.02% Tween), HRP-conjugated antibodies were added and SuperSignal West Pico Chemiluminescent were used to detect primary antibodies (**Table 8.1.**)

8.2.4. Determination of cell death

8.2.4.2. Annexin V staining

Annexin V-FITC is a sensitive probe for identifying apoptotic cells, binding to negatively charged phospholipid surfaces with high affinity for phosphatidyl-serine (PS). Annexin V binding is calcium dependent and defined calcium and salt concentrations are required for optimal staining. This reagent was to identify apoptotic cell by:

- **microscopy**

Approximately $1x10^5$ treated HeLa cells were grown on a round cover glass of 13mm diameter (VWR International) in 24-well plates. Following three times washes in 1X binding buffer (10x binding buffer: 0.1 M Hepes/NaOH (pH 7.4) (Invitrogen), 1.4 M NaCl (Sigma-Aldrich), 25 mM $CaCl_2$ (Sigma-Aldrich)) and sterilized by 0.2 μm filterers, the cover slips with HeLa cells were placed onto laboratory film (Parafilm M) containing 5 μl drop of Annexin V-Cy5 (BD Pharmingen). Following 20 min incubation at RT in dark cover slips were mounted in anti-fadent solution (CitiFluor) and analysed on confocal microscopy using filters for Cy5 fluorochrome.

- **flow cytometry**

Following various treatments, HeLa cells intensively washed in cold PBS and approximately $1x10^6$ /ml of HeLa cells were re-suspended in 1X binding buffer (as above). Then, 100 μl of solution ($1x10^5$ of cells) were transferred to round-bottomed 96-wells plate with 5 μl of

annexin V-FITC (BD Pharmingen). Following incubation at RT in the dark for 15 min, 400 ml of 1X binding buffer was added and 10 000 cells collected by flow cytometry.

8.2.4.1. MTT test

MTT test is laboratory standard colorimetric assay for measuring cell viability, based on reduction of yellow MTT substrate to purple formazan in the mitochondria of living cells.

Drug or UVC-treated HeLa were cells cultivated on 24 well plates. Cell viability was ascertained by adding to dying HeLa cells 30 µl of MTT stock solution (25 mg MTT [3-(4,5-dimethyldiazol-2-yl)-2,5 diphenyl Tetrazolium Bromid] (Sigma Aldrich), 5 ml PBS (pH 7.4) and sterile filtered) diluted in 270 µl of fresh RPMI. Followed 2h incubation in 5% aspirated CO_2 incubator, the equal volume lysis solution (50% DMF [N,N-dimetyloformamid] (Sigma-Aldrich), 2.5% acetic acid (Fisher Scientific), 2.5% HCl (Fisher Scientific), 20% SDS (Sigma-Aldrich)) was added to every well. Followed 4h incubation the 100ml of supernatant containing lysed cells was transferred into the new 96-well plate in the triplicate wells for each sample. Using spectrophotometer at 570 nm wavelength the absorbance of coloured solution was measured and quantified in respect un-treated (100% live) HeLa cells.

8.2.5. Immunological techniques

8.2.5.1. FASC analysis

Lymphocytes ware harvested from the culture and plated out at 1-5x10^5/ml to round-bottomed 96-well plates and wash twice in cold FACS buffer (PBS supplemented with 2% FCS) by centrifugation at 400 x g for 1 min. Subsequently, 100ml of appropriately pre-diluted antibody was added and incubated for 1 h in dark at 4^{o}C. The cells were washed five times and, if necessarily, stained with secondary antibody. Following final washing, the pellet of cells was re-suspended in 100 µl of FACS buffer and transferred to FACS tubes containing 400 ml of FACS buffer. Samples were then analysed using a FACScalibur flow cytometer and CellQuest software (Becton Dickinson, Mountain View, CA, USA). 10 000 events were collected. The data analysis was carried out using FlowJo software (TreeStar Inc.).

8.2.5.2. T cell hybridomas generation and characterisation

In collaboration with Prof. J. Robinson, and using existing bacterially expressed and purified recombinant E/T, Rob Steward immunized mice to generate a panel of new antigen specific T cell hybridomas that recognise EGFP or TTCF. The Balb/c mice were maintained in pathogen free environment of Medical School of Newcastle University facilities. The 9 week–old female were injected sub-cutaneously in the one leg with 50 μm of TTCF emulsified in TiterMax (Sigma-Aldrich). 7days later a single cell suspension from pooled draining lymph nodes was incubated in 24-well plates (Grainger) at $2x10^6$ cell/ml with 50 μg/ml TTCF. After 3 days cells were purified using density gradient and re-plated at $0.7\text{-}1.5x10^5$ cell/ml were re-spun with an equal number of similarly washed with serum-free Hanks' balanced salt solution (Sigma-Aldrich) over the a period of 90 s with continuous gentle agitation. The cells were diluted into 20ml of warm Hanks balanced salt solution over 5 min with continues shaking before re-spanning and re-suspending in 30 ml growth media. Cells were then plated out in 96-well flat bottomed plates (Grainger) at various dilutions. 24h later the media was supplemented with hypoxanthine, aminopterin, thymidyne (HAT) from Sigma-Aldrich. Two weeks later the selective media was removed and 60 surviving clones were tested for TTCF reactivity using standard proliferation bio-assay. $0.5x10^5$ of each hybridoma was mixed with $1x10^5$ macrophage cell lines J774 as APCs and 1 or 10 μg/ml of TTCF. The IL-2 produced by TTCF-depended hybridomas was measured by transferring the supernatant into the fresh wells containing $3x10^4$ CTLL-2 cells Those IL-2 dependent CTLL-2 T cell line was 24h prior cultivated in the absence of IL-2. CTLL-2 proliferation was quantified by 0.02MBq ^{3}H-thymidyne (GE Healthcare) incorporation for 24h at 37^{o}C. Plates were harvested on to printed filters mats fro 1450 Micro Beta (Wallac Oy, Tutuku) using Harvester 96 (Tomtec).

Only one clone of T cell hybridomas (MC-52) was selected and curried our further the analysis. Using a panel of 88 overlapping 17-mer peptides (from Colin Watts's lab) the characterisation of epitope specificity MC-52 hybridomas was able. This experiment shows that MC-52 recognising the 1120-1137 (NPLRYDTEYYLIPVASS) amino acid sequence of TTCF. Also using murine fibroblast expressing either H-2A^d or H-2E^d as APC in standard proliferation assay showed that MC-52 T cell hybridomas are H-2A^d restricted.

8.2.5.3. Proliferation bio-assays

In the initials experiments the triplicate wells were set up in order to perform the grade dose of antigen (TTCF) or different number of HeLa cells which were mixed with B and T cells. In some experiments additionally, the blocking filters were introduced between lymphocytes and HeLa cells.

The vast majority of proliferation assays focusing on antigen extraction or relocated antigen recognition were performed using modified version of bio-assay. Firstly, $1x10^5$ of B cells were stimulated by $1x10^5$ HeLa transfectants growing in 24-well plates. Followed certain period of time ranging from 1 min to 6 h, B cells were removed and transferred into new 96-well plate containing $0.5x10^5$ of T cells. Assay were then incubated at 37°C for the next 24 h in the presence of 5% of $C0_2$ and frozen. T cell stimulation was measured as IL-2 release by incubating 50 μl of defrosted supernatant with $5x10^3$ IL-2 dependent CTLL-2 cells, prior starved in medium lacking IL-2, for 24h in incubator at 37°C. The proliferation of CTLL-2 cells was assessed by 0.02 MBq ^{3}H-thymidyne incorporation during 24 h (for details see above).

8.2.6. Statistical analysis

Data analysis was performed using Prisim5 for Mac OS X Version 5.0b (GraphPad Software Inc.).

Values are expressed as +/- SEM. To evaluate the difference in means between two groups, the Student't' test was used for parametric date. Significance was defined as P value less than 0.05.

9. References -

Adorini, L., Appella, E., Doria, G., and Nagy, Z.A. (1988). Mechanisms influencing the immunodominance of T cell determinants. J Exp Med *168*, 2091-2104.

Adorini, L., Guery, J.C., Fuchs, S., Ortiz-Navarrete, V., Hammerling, G.J., and Momburg, F. (1993). Processing of endogenously synthesized hen egg-white lysozyme retained in the endoplasmic reticulum or in secretory form gives rise to a similar but not identical set of epitopes recognized by class II-restricted T cells. J Immunol *151*, 3576-3586.

Allen, C.D., and Cyster, J.G. (2008). Follicular dendritic cell networks of primary follicles and germinal centers: phenotype and function. Semin Immunol *20*, 14-25.

Ames, E., Hallett, W.H., and Murphy, W.J. (2009). Sensitization of human breast cancer cells to natural killer cell-mediated cytotoxicity by proteasome inhibition. Clin Exp Immunol *155*, 504-513.

Andersen, M.H., and thor, S.P. (2002). Survivin--a universal tumor antigen. Histol Histopathol *17*, 669-675.

Antoniou, A.N., Blackwood, S.L., Mazzeo, D., and Watts, C. (2000). Control of antigen presentation by a single protease cleavage site. Immunity *12*, 391-398.

Antoniou, A.N., and Watts, C. (2002). Antibody modulation of antigen presentation: positive and negative effects on presentation of the tetanus toxin antigen via the murine B cell isoform of FcgammaRII. Eur J Immunol *32*, 530-540.

Antony, P.A., Piccirillo, C.A., Akpinarli, A., Finkelstein, S.E., Speiss, P.J., Surman, D.R., Palmer, D.C., Chan, C.C., Klebanoff, C.A., Overwijk, W.W.*, et al.* (2005). CD8+ T cell immunity against a tumor/self-antigen is augmented by CD4+ T helper cells and hindered by naturally occurring T regulatory cells. J Immunol *174*, 2591-2601.

Apetoh, L., Ghiringhelli, F., Tesniere, A., Obeid, M., Ortiz, C., Criollo, A., Mignot, G., Maiuri, M.C., Ullrich, E., Saulnier, P.*, et al.* (2007a). Toll-like receptor 4-dependent contribution of the immune system to anticancer chemotherapy and radiotherapy. Nat Med *13*, 1050-1059.

Apetoh, L., Mignot, G., Panaretakis, T., Kroemer, G., and Zitvogel, L. (2008). Immunogenicity of anthracyclines: moving towards more personalized medicine. Trends Mol Med *14*, 141-151.

Apetoh, L., Obeid, M., Tesniere, A., Ghiringhelli, F., Fimia, G.M., Piacentini, M., Kroemer, G., and Zitvogel, L. (2007b). Immunogenic chemotherapy: discovery of a critical protein through proteomic analyses of tumor cells. Cancer Genomics Proteomics *4*, 65-70.

Arana, E., Vehlow, A., Harwood, N.E., Vigorito, E., Henderson, R., Turner, M., Tybulewicz, V.L., and Batista, F.D. (2008). Activation of the small GTPase Rac2 via the B cell receptor regulates B cell adhesion and immunological-synapse formation. Immunity *28*, 88-99.

Ashkenazi, A. (2008). Targeting the extrinsic apoptosis pathway in cancer. Cytokine Growth Factor Rev *19*, 325-331.

Barbera-Guillem, E., May, K.F., Jr., Nyhus, J.K., and Nelson, M.B. (1999). Promotion of tumor invasion by cooperation of granulocytes and macrophages activated by anti-tumor antibodies. Neoplasia *1*, 453-460.

Batista, F.D., and Harwood, N.E. (2009). The who, how and where of antigen presentation to B cells. Nat Rev Immunol *9*, 15-27.

Batista, F.D., Iber, D., and Neuberger, M.S. (2001). B cells acquire antigen from target cells after synapse formation. Nature *411*, 489-494.

Batista, F.D., and Neuberger, M.S. (2000). B cells extract and present immobilized antigen: implications for affinity discrimination. EMBO J *19*, 513-520.

Battaglia, A., Buzzonetti, A., Baranello, C., Ferrandina, G., Martinelli, E., Fanfani, F., Scambia, G., and Fattorossi, A. (2009). Metastatic tumour cells favour the generation of a tolerogenic milieu in tumour draining lymph node in patients with early cervical cancer. Cancer Immunol Immunother *58*, 1363-1373.

Bergmann, C., Strauss, L., Zeidler, R., Lang, S., and Whiteside, T.L. (2007). Expansion and characteristics of human T regulatory type 1 cells in co-cultures simulating tumor microenvironment. Cancer Immunol Immunother *56*, 1429-1442.

Bergtold, A., Desai, D.D., Gavhane, A., and Clynes, R. (2005). Cell surface recycling of internalized antigen permits dendritic cell priming of B cells. Immunity *23*, 503-514.

Bevan, M.J. (1976). Minor H antigens introduced on H-2 different stimulating cells cross-react at the cytotoxic T cell level during in vivo priming. J Immunol *117*, 2233-2238.

Beyer, M., and Schultze, J.L. (2009). Regulatory T cells: major players in the tumor microenvironment. Curr Pharm Des *15*, 1879-1892.

Bonehill, A., Heirman, C., and Thielemans, K. (2005). Genetic approaches for the induction of a CD4+ T cell response in cancer immunotherapy. J Gene Med *7*, 686-695.

Borghaei, H., Smith, M.R., and Campbell, K.S. (2009). Immunotherapy of cancer. Eur J Pharmacol.

Broers, J.L., and Ramaekers, F.C. (2004). Dynamics of nuclear lamina assembly and disassembly. Symp Soc Exp Biol, 177-192.

Brusa, D., Garetto, S., Chiorino, G., Scatolini, M., Migliore, E., Camussi, G., and Matera, L. (2008). Post-apoptotic tumors are more palatable to dendritic cells and enhance their antigen cross-presentation activity. Vaccine *26*, 6422-6432.

Brusa, D., Migliore, E., Garetto, S., Simone, M., and Matera, L. (2009). Immunogenicity of 56 degrees C and UVC-treated prostate cancer is associated with release of HSP70 and HMGB1 from necrotic cells. Prostate *69*, 1343-1352.

Burz, C., Berindan-Neagoe, I., Balacescu, O., and Irimie, A. (2009). Apoptosis in cancer: key molecular signaling pathways and therapy targets. Acta Oncol *48*, 811-821.

Carrasco, Y.R., and Batista, F.D. (2006a). B-cell activation by membrane-bound antigens is facilitated by the interaction of VLA-4 with VCAM-1. Embo J *25*, 889-899.

Carrasco, Y.R., and Batista, F.D. (2006b). B cell recognition of membrane-bound antigen: an exquisite way of sensing ligands. Curr Opin Immunol *18*, 286-291.

Carrasco, Y.R., and Batista, F.D. (2007). B cells acquire particulate antigen in a macrophage-rich area at the boundary between the follicle and the subcapsular sinus of the lymph node. Immunity *27*, 160-171.

Casares, N., Pequignot, M.O., Tesniere, A., Ghiringhelli, F., Roux, S., Chaput, N., Schmitt, E., Hamai, A., Hervas-Stubbs, S., Obeid, M.*, et al.* (2005). Caspase-dependent immunogenicity of doxorubicin-induced tumor cell death. J Exp Med *202*, 1691-1701.

Chan, C.W., and Housseau, F. (2008). The 'kiss of death' by dendritic cells to cancer cells. Cell Death Differ *15*, 58-69.

Chathoth, S., Thayyullathil, F., Hago, A., Shahin, A., Patel, M., and Galadari, S. (2009). UVC-induced apoptosis in Dubca cells is independent of JNK activation and p53(Ser-15) phosphorylation. Biochem Biophys Res Commun *383*, 426-432.

Chaux, P., Favre, N., Martin, M., and Martin, F. (1997). Tumor-infiltrating dendritic cells are defective in their antigen-presenting function and inducible B7 expression in rats. Int J Cancer *72*, 619-624.

Choi, K.H., Hama-Inaba, H., Wang, B., Haginoya, K., Odaka, T., Yamada, T., Hayata, I., and Ohyama, H. (2000). UVC-induced apoptosis in human epithelial tumor A431 cells: sequence of apoptotic changes and involvement of caspase (-8 and -3) cascade. J Radiat Res (Tokyo) *41*, 243-258.

Clark, M.R., Massenburg, D., Zhang, M., and Siemasko, K. (2003). Molecular mechanisms of B cell antigen receptor trafficking. Ann N Y Acad Sci *987*, 26-37.

Cohen, P.A., Peng, L., Kjaergaard, J., Plautz, G.E., Finke, J.H., Koski, G.K., Czerniecki, B.J., and Shu, S. (2001). T-cell adoptive therapy of tumors: mechanisms of improved therapeutic performance. Crit Rev Immunol *21*, 215-248.

Cools, N., Ponsaerts, P., Van Tendeloo, V.F., and Berneman, Z.N. (2007). Balancing between immunity and tolerance: an interplay between dendritic cells, regulatory T cells, and effector T cells. J Leukoc Biol *82*, 1365-1374.

Cormack, B.P., Valdivia, R.H., and Falkow, S. (1996). FACS-optimized mutants of the green fluorescent protein (GFP). Gene *173*, 33-38.

Coronella-Wood, J.A., and Hersh, E.M. (2003). Naturally occurring B-cell responses to breast cancer. Cancer Immunol Immunother *52*, 715-738.

Corthay, A., Skovseth, D.K., Lundin, K.U., Rosjo, E., Omholt, H., Hofgaard, P.O., Haraldsen, G., and Bogen, B. (2005). Primary antitumor immune response mediated by CD4+ T cells. Immunity *22*, 371-383.

Coughlin, C.M., Vance, B.A., Grupp, S.A., and Vonderheide, R.H. (2004). RNA-transfected CD40-activated B cells induce functional T-cell responses against viral and tumor antigen targets: implications for pediatric immunotherapy. Blood *103*, 2046-2054.

Crawford, A., Macleod, M., Schumacher, T., Corlett, L., and Gray, D. (2006). Primary T cell expansion and differentiation in vivo requires antigen presentation by B cells. J Immunol *176*, 3498-3506.

Croft, D.R., Coleman, M.L., Li, S., Robertson, D., Sullivan, T., Stewart, C.L., and Olson, M.F. (2005). Actin-myosin-based contraction is responsible for apoptotic nuclear disintegration. J Cell Biol *168*, 245-255.

de Visser, K.E., and Coussens, L.M. (2006). The inflammatory tumor microenvironment and its impact on cancer development. Contrib Microbiol *13*, 118-137.

De Wever, O., and Mareel, M. (2003). Role of tissue stroma in cancer cell invasion. J Pathol *200*, 429-447.

Debatin, K.M., and Krammer, P.H. (2004). Death receptors in chemotherapy and cancer. Oncogene *23*, 2950-2966.

Degrate, L., Nobili, C., Franciosi, C., Caprotti, R., Brivio, F., Romano, F., Leone, B.E., Trezzi, R., and Uggeri, F. (2009). Interleukin-2 immunotherapy action on innate immunity cells in peripheral blood and tumoral tissue of pancreatic adenocarcinoma patients. Langenbecks Arch Surg *394*, 115-121.

Derre, L., Corvaisier, M., Charreau, B., Moreau, A., Godefroy, E., Moreau-Aubry, A., Jotereau, F., and Gervois, N. (2006). Expression and release of HLA-E by melanoma cells and melanocytes: potential impact on the response of cytotoxic effector cells. J Immunol *177*, 3100-3107.

Dilillo, D.J., Yanaba, K., and Tedder, T.F. B Cells Are Required for Optimal CD4+ and CD8+ T Cell Tumor Immunity: Therapeutic B Cell Depletion Enhances B16 Melanoma Growth in Mice. J Immunol *184*, 4006-4016.

Douvdevani, A., Huleihel, M., Segal, S., and Apte, R.N. (1991). Aberrations in interleukin-1 expression in oncogene-transformed fibrosarcoma lines: constitutive interleukin-1 alpha transcription and manifestation of biological activity. Eur Cytokine Netw *2*, 257-264.

Dudley, M.E., Wunderlich, J.R., Yang, J.C., Sherry, R.M., Topalian, S.L., Restifo, N.P., Royal, R.E., Kammula, U., White, D.E., Mavroukakis, S.A.*, et al.* (2005). Adoptive cell transfer therapy following non-myeloablative but lymphodepleting chemotherapy for the treatment of patients with refractory metastatic melanoma. J Clin Oncol *23*, 2346-2357.

Dudley, M.E., Yang, J.C., Sherry, R., Hughes, M.S., Royal, R., Kammula, U., Robbins, P.F., Huang, J., Citrin, D.E., Leitman, S.F., *et al.* (2008). Adoptive cell therapy for patients with metastatic melanoma: evaluation of intensive myeloablative chemoradiation preparative regimens. J Clin Oncol *26*, 5233-5239.

Dudziak, D., Kamphorst, A.O., Heidkamp, G.F., Buchholz, V.R., Trumpfheller, C., Yamazaki, S., Cheong, C., Liu, K., Lee, H.W., Park, C.G., *et al.* (2007). Differential antigen processing by dendritic cell subsets in vivo. Science *315*, 107-111.

Duiker, E.W., van der Zee, A.G., de Graeff, P., Boersma-van Ek, W., Hollema, H., de Bock, G.H., de Jong, S., and de Vries, E.G. The extrinsic apoptosis pathway and its prognostic impact in ovarian cancer. Gynecol Oncol *116*, 549-555.

Dumitriu, I.E., Bianchi, M.E., Bacci, M., Manfredi, A.A., and Rovere-Querini, P. (2007). The secretion of HMGB1 is required for the migration of maturing dendritic cells. J Leukoc Biol *81*, 84-91.

Eriksen, K.W., Sondergaard, H., Woetmann, A., Krejsgaard, T., Skak, K., Geisler, C., Wasik, M.A., and Odum, N. (2009). The combination of IL-21 and IFN-alpha boosts STAT3 activation, cytotoxicity and experimental tumor therapy. Mol Immunol *46*, 812-820.

Esche, C., Shurin, G.V., Kirkwood, J.M., Wang, G.Q., Rabinowich, H., Pirtskhalaishvili, G., and Shurin, M.R. (2001). Tumor necrosis factor-alpha-promoted expression of Bcl-2 and inhibition of mitochondrial cytochrome c release mediate resistance of mature dendritic cells to melanoma-induced apoptosis. Clin Cancer Res *7*, 974s-979s.

Ferrari, G., Knight, A.M., Watts, C., and Pieters, J. (1997). Distinct intracellular compartments involved in invariant chain degradation and antigenic peptide loading of major histocompatibility complex (MHC) class II molecules. The Journal of cell biology *139*, 1433-1446.

Ferraro, C., Quemeneur, L., Prigent, A.F., Taverne, C., Revillard, J.P., and Bonnefoy-Berard, N. (2000). Anthracyclines trigger apoptosis of both G0-G1 and cycling peripheral blood lymphocytes and induce massive deletion of mature T and B cells. Cancer Res *60*, 1901-1907.

Ferre, F., Martin, P., Begue, A., Ghysdael, J., Saule, S., and Stehelin, D. (1986). [Preparation and characterization of specific antisera directed against different polypeptide domains encoded by the c-myc oncogene for studying the expression of this gene introduced into quail or rat cells]. C R Acad Sci III *303*, 633-636.

Ferri, K.F., and Kroemer, G. (2001a). Mitochondria--the suicide organelles. Bioessays *23*, 111-115.

Ferri, K.F., and Kroemer, G. (2001b). Organelle-specific initiation of cell death pathways. Nat Cell Biol *3*, E255-263.

Fionda, C., Soriani, A., Malgarini, G., Iannitto, M.L., Santoni, A., and Cippitelli, M. (2009). Heat shock protein-90 inhibitors increase MHC class I-related chain A and B ligand expression on multiple myeloma cells and their ability to trigger NK cell degranulation. J Immunol *183*, 4385-4394.

Fischer, B., Perry, B., Phillips, G., Sumner, I., and Goodenough, P. (1993). Physiological consequence of expression of soluble and active hen egg white lysozyme in Escherichia coli. Appl Microbiol Biotechnol *39*, 537-540.

Foung, S.K., Sasaki, D.T., Grumet, F.C., and Engleman, E.G. (1982). Production of functional human T-T hybridomas in selection medium lacking aminopterin and thymidine. Proc Natl Acad Sci U S A *79*, 7484-7488.

Fournel, S., Aguerre-Girr, M., Huc, X., Lenfant, F., Alam, A., Toubert, A., Bensussan, A., and Le Bouteiller, P. (2000). Cutting edge: soluble HLA-G1 triggers CD95/CD95 ligand-mediated apoptosis in activated CD8+ cells by interacting with CD8. J Immunol *164*, 6100-6104.

Franz, S., Herrmann, K., Fuhrnrohr, B., Sheriff, A., Frey, B., Gaipl, U.S., Voll, R.E., Kalden, J.R., Jack, H.M., and Herrmann, M. (2007). After shrinkage apoptotic cells expose internal membrane-derived epitopes on their plasma membranes. Cell Death Differ *14*, 733-742.

Fratta, E., Sigalotti, L., Colizzi, F., Covre, A., Nicolay, H.J., Danielli, R., Fonsatti, E., Altomonte, M., Calabro, L., Coral, S., and Maio, M. Epigenetically regulated clonal heritability of CTA expression profiles in human melanoma. J Cell Physiol *223*, 352-358.

Fricke, I., and Gabrilovich, D.I. (2006). Dendritic cells and tumor microenvironment: a dangerous liaison. Immunol Invest *35*, 459-483.

Frumento, G., Piazza, T., Di Carlo, E., and Ferrini, S. (2006). Targeting tumor-related immunosuppression for cancer immunotherapy. Endocr Metab Immune Disord Drug Targets *6*, 233-237.

Furre, I.E., Moller, M.T., Shahzidi, S., Nesland, J.M., and Peng, Q. (2006). Involvement of both caspase-dependent and -independent pathways in apoptotic induction by hexaminolevulinate-mediated photodynamic therapy in human lymphoma cells. Apoptosis *11*, 2031-2042.

Gattinoni, L., Finkelstein, S.E., Klebanoff, C.A., Antony, P.A., Palmer, D.C., Spiess, P.J., Hwang, L.N., Yu, Z., Wrzesinski, C., Heimann, D.M.*, et al.* (2005). Removal of homeostatic cytokine sinks by lymphodepletion enhances the efficacy of adoptively transferred tumor-specific CD8+ T cells. J Exp Med *202*, 907-912.

Ge, N., Ye, S., Liu, Y., and Tang, Z. (2002). [Immunoprotective effect of IL-2 and B7-1 gene co-transfected liver cancer vaccines on hepatocarcinogenesis in mice]. Zhonghua Gan Zang Bing Za Zhi *10*, 417-420.

Gerwing, J., and Thompson, K. (1968). Studies on the antigenic properties of egg-white lysozyme. I. Isolation and characterization of a tryptic peptide from reduced and alkylated lysozyme exhibiting haptenic activity. Biochemistry *7*, 3888-3892.

Gillis, S., and Smith, K.A. (1977). Long term culture of tumour-specific cytotoxic T cells. Nature *268*, 154-156.

Gozuacik, D., and Kimchi, A. (2004). Autophagy as a cell death and tumor suppressor mechanism. Oncogene *23*, 2891-2906.

Granville, D.J., Cassidy, B.A., Ruehlmann, D.O., Choy, J.C., Brenner, C., Kroemer, G., van Breemen, C., Margaron, P., Hunt, D.W., and McManus, B.M. (2001). Mitochondrial release of apoptosis-inducing factor and cytochrome c during smooth muscle cell apoptosis. Am J Pathol *159*, 305-311.

Green, C.E., Liu, T., Montel, V., Hsiao, G., Lester, R.D., Subramaniam, S., Gonias, S.L., and Klemke, R.L. (2009a). Chemoattractant signaling between tumor cells and macrophages regulates cancer cell migration, metastasis and neovascularization. PLoS One *4*, e6713.

Green, D.R., Ferguson, T., Zitvogel, L., and Kroemer, G. (2009b). Immunogenic and tolerogenic cell death. Nat Rev Immunol *9*, 353-363.

Green, S.K., Karlsson, M.C., Ravetch, J.V., and Kerbel, R.S. (2002). Disruption of cell-cell adhesion enhances antibody-dependent cellular cytotoxicity: implications for antibody-based therapeutics of cancer. Cancer Res *62*, 6891-6900.

Gregory, C.D., and Devitt, A. (2004). The macrophage and the apoptotic cell: an innate immune interaction viewed simplistically? Immunology *113*, 1-14.

Groh, V., Li, Y.Q., Cioca, D., Hunder, N.N., Wang, W., Riddell, S.R., Yee, C., and Spies, T. (2005). Efficient cross-priming of tumor antigen-specific T cells by dendritic cells sensitized with diverse anti-MICA opsonized tumor cells. Proc Natl Acad Sci U S A *102*, 6461-6466.

Hansen, M.H., Nielsen, H., and Ditzel, H.J. (2001). The tumor-infiltrating B cell response in medullary breast cancer is oligoclonal and directed against the autoantigen actin exposed on the surface of apoptotic cancer cells. Proc Natl Acad Sci U S A *98*, 12659-12664.

Hansen, M.H., Nielsen, H.V., and Ditzel, H.J. (2002). Translocation of an intracellular antigen to the surface of medullary breast cancer cells early in apoptosis allows for an antigen-driven antibody response elicited by tumor-infiltrating B cells. J Immunol *169*, 2701-2711.

Hawkins, M.J. (1993). Interleukin-2 antitumor and effector cell responses. Semin Oncol *20*, 52-59.

Hewitt, E.W., Treumann, A., Morrice, N., Tatnell, P.J., Kay, J., and Watts, C. (1997). Natural processing sites for human cathepsin E and cathepsin D in tetanus toxin: implications for T cell epitope generation. J Immunol *159*, 4693-4699.

Hirohashi, Y., Torigoe, T., Hirai, I., Tamura, Y., Nakatsugawa, M., Inoue, Y., Kanaseki, T., Kamiguchi, K., Ikeda, H., Sasaki, A.*, et al.* (2009). Establishment of shared antigen reactive cytotoxic T lymphocyte using co-stimulatory molecule introduced autologous cancer cells. Exp Mol Pathol.

Ho, W.Y., Yee, C., and Greenberg, P.D. (2002). Adoptive therapy with CD8(+) T cells: it may get by with a little help from its friends. J Clin Invest *110*, 1415-1417.

Honda, K., Yamada, T., Endo, R., Ino, Y., Gotoh, M., Tsuda, H., Yamada, Y., Chiba, H., and Hirohashi, S. (1998). Actinin-4, a novel actin-bundling protein associated with cell motility and cancer invasion. J Cell Biol *140*, 1383-1393.

Hou, P., Araujo, E., Zhao, T., Zhang, M., Massenburg, D., Veselits, M., Doyle, C., Dinner, A.R., and Clark, M.R. (2006). B cell antigen receptor signaling and internalization are mutually exclusive events. PLoS Biol *4*, e200.

Howell, W.M., and Rose-Zerilli, M.J. (2006). Interleukin-10 polymorphisms, cancer susceptibility and prognosis. Fam Cancer *5*, 143-149.

Hung, K., Hayashi, R., Lafond-Walker, A., Lowenstein, C., Pardoll, D., and Levitsky, H. (1998). The central role of CD4(+) T cells in the antitumor immune response. J Exp Med *188*, 2357-2368.

Iannello, A., and Ahmad, A. (2005). Role of antibody-dependent cell-mediated cytotoxicity in the efficacy of therapeutic anti-cancer monoclonal antibodies. Cancer Metastasis Rev *24*, 487-499.
Ibrahim, E.C., Guerra, N., Lacombe, M.J., Angevin, E., Chouaib, S., Carosella, E.D., Caignard, A., and Paul, P. (2001). Tumor-specific up-regulation of the nonclassical class I HLA-G antigen expression in renal carcinoma. Cancer Res *61*, 6838-6845.

Itoh, M., Takahashi, T., Sakaguchi, N., Kuniyasu, Y., Shimizu, J., Otsuka, F., and Sakaguchi, S. (1999). Thymus and autoimmunity: production of CD25+CD4+ naturally anergic and suppressive T cells as a key function of the thymus in maintaining immunologic self-tolerance. J Immunol *162*, 5317-5326.

Jacobs, J.F., Grauer, O.M., Brasseur, F., Hoogerbrugge, P.M., Wesseling, P., Gidding, C.E., van de Rakt, M.W., Figdor, C.G., Coulie, P.G., de Vries, I.J., and Adema, G.J. (2008). Selective cancer-germline gene expression in pediatric brain tumors. J Neurooncol *88*, 273-280.

Jazirehi, A.R., and Bonavida, B. (2005). Cellular and molecular signal transduction pathways modulated by rituximab (rituxan, anti-CD20 mAb) in non-Hodgkin's lymphoma: implications in chemosensitization and therapeutic intervention. Oncogene *24*, 2121-2143.

Jones, D.E., Palmer, J.M., Bennett, K., Robe, A.J., Yeaman, S.J., Robertson, H., Bassendine, M.F., Burt, A.D., and Kirby, J.A. (2002). Investigation of a mechanism for accelerated breakdown of immune tolerance to the primary biliary cirrhosis-associated autoantigen, pyruvate dehydrogenase complex. Lab Invest *82*, 211-219.

Junt, T., Moseman, E.A., Iannacone, M., Massberg, S., Lang, P.A., Boes, M., Fink, K., Henrickson, S.E., Shayakhmetov, D.M., Di Paolo, N.C.*, et al.* (2007). Subcapsular sinus macrophages in lymph nodes clear lymph-borne viruses and present them to antiviral B cells. Nature *450*, 110-114.

Kaplan, D.H., Shankaran, V., Dighe, A.S., Stockert, E., Aguet, M., Old, L.J., and Schreiber, R.D. (1998). Demonstration of an interferon gamma-dependent tumor surveillance system in immunocompetent mice. Proc Natl Acad Sci U S A *95*, 7556-7561.

Kemp, T.J., Moore, J.M., and Griffith, T.S. (2004). Human B cells express functional TRAIL/Apo-2 ligand after CpG-containing oligodeoxynucleotide stimulation. J Immunol *173*, 892-899.

Kepp, O., Galluzzi, L., Giordanetto, F., Tesniere, A., Vitale, I., Martins, I., Schlemmer, F., Adjemian, S., Zitvogel, L., and Kroemer, G. (2009). Disruption of the PP1/GADD34 complex induces calreticulin exposure. Cell Cycle *8*, 3971-3977.

Kerr, J.F., Winterford, C.M., and Harmon, B.V. (1994). Apoptosis. Its significance in cancer and cancer therapy. Cancer *73*, 2013-2026.

Kiessling, A., Fussel, S., Wehner, R., Bachmann, M., Wirth, M.P., Rieber, E.P., and Schmitz, M. (2008). Advances in specific immunotherapy for prostate cancer. Eur Urol *53*, 694-708.

Kim, H.S., Lee, Y.S., and Kim, D.K. (2009a). Doxorubicin exerts cytotoxic effects through cell cycle arrest and Fas-mediated cell death. Pharmacology *84*, 300-309.

Kim, H.S., Lee, Y.S., and Kim, D.K. (2009b). Doxorubicin Exerts Cytotoxic Effects through Cell Cycle Arrest and Fas-Mediated Cell Death. Pharmacology *84*, 300-309.

Kim, K.J., Kanellopoulos-Langevin, C., Merwin, R.M., Sachs, D.H., and Asofsky, R. (1979). Establishment and characterization of BALB/c lymphoma lines with B cell properties. J Immunol *122*, 549-554.

Kim, R., Tanabe, K., Uchida, Y., Emi, M., Inoue, H., and Toge, T. (2002). Current status of the molecular mechanisms of anticancer drug-induced apoptosis. The contribution of molecular-level analysis to cancer chemotherapy. Cancer Chemother Pharmacol *50*, 343-352.

Kim, S., Fridlender, Z.G., Dunn, R., Kehry, M.R., Kapoor, V., Blouin, A., Kaiser, L.R., and Albelda, S.M. (2008a). B-cell depletion using an anti-CD20 antibody augments antitumor immune responses and immunotherapy in nonhematopoetic murine tumor models. J Immunother *31*, 446-457.

Kim, S.C., Park, S.S., and Lee, Y.J. (2008b). Effect of UV irradiation on colorectal cancer cells with acquired TRAIL resistance. J Cell Biochem *104*, 1172-1180.

Kim, S.H., Lee, S., Lee, C.H., Lee, M.K., Kim, Y.D., Shin, D.H., Choi, K.U., Kim, J.Y., Park do, Y., and Sol, M.Y. (2009c). Expression of cancer-testis antigens MAGE-A3/6 and NY-ESO-1 in non-small-cell lung carcinomas and their relationship with immune cell infiltration. Lung *187*, 401-411.

Kim, Y.M., Pan, J.Y., Korbel, G.A., Peperzak, V., Boes, M., and Ploegh, H.L. (2006). Monovalent ligation of the B cell receptor induces receptor activation but fails to promote antigen presentation. Proc Natl Acad Sci U S A *103*, 3327-3332.

Kimura, S., Warabi, E., Yanagawa, T., Ma, D., Itoh, K., Ishii, Y., Kawachi, Y., and Ishii, T. (2009). Essential role of Nrf2 in keratinocyte protection from UVA by quercetin. Biochem Biophys Res Commun *387*, 109-114.

Kirkwood, J. (2002). Cancer immunotherapy: the interferon-alpha experience. Semin Oncol *29*, 18-26.

Kirkwood, J.M., Ibrahim, J.G., Sosman, J.A., Sondak, V.K., Agarwala, S.S., Ernstoff, M.S., and Rao, U. (2001). High-dose interferon alfa-2b significantly prolongs relapse-free and overall survival compared with the GM2-KLH/QS-21 vaccine in patients with resected stage IIB-III melanoma: results of intergroup trial E1694/S9512/C509801. J Clin Oncol *19*, 2370-2380.

Knight, A.M., Lucocq, J.M., Prescott, A.R., Ponnambalam, S., and Watts, C. (1997). Antigen endocytosis and presentation mediated by human membrane IgG1 in the absence of the Ig(alpha)/Ig(beta) dimer. EMBO J *16*, 3842-3850.

Knutson, K.L., and Disis, M.L. (2005). Tumor antigen-specific T helper cells in cancer immunity and immunotherapy. Cancer Immunol Immunother *54*, 721-728.

Kohler, B., Anguissola, S., Concannon, C.G., Rehm, M., Kogel, D., and Prehn, J.H. (2008). Bid participates in genotoxic drug-induced apoptosis of HeLa cells and is essential for death receptor ligands' apoptotic and synergistic effects. PLoS One *3*, e2844.

Kokhaei, P., Rezvany, M.R., Virving, L., Choudhury, A., Rabbani, H., Osterborg, A., and Mellstedt, H. (2003). Dendritic cells loaded with apoptotic tumour cells induce a stronger T-cell response than dendritic cell-tumour hybrids in B-CLL. Leukemia *17*, 894-899.

Koopman, G., Keehnen, R.M., Lindhout, E., Newman, W., Shimizu, Y., van Seventer, G.A., de Groot, C., and Pals, S.T. (1994). Adhesion through the LFA-1 (CD11a/CD18)-ICAM-1 (CD54) and the VLA-4 (CD49d)-VCAM-1 (CD106) pathways prevents apoptosis of germinal center B cells. J Immunol *152*, 3760-3767.

Kotlan, B., Simsa, P., Teillaud, J.L., Fridman, W.H., Toth, J., McKnight, M., and Glassy, M.C. (2005). Novel ganglioside antigen identified by B cells in human medullary breast carcinomas: the proof of principle concerning the tumor-infiltrating B lymphocytes. J Immunol *175*, 2278-2285.

Kubota, T., Niwa, R., Satoh, M., Akinaga, S., Shitara, K., and Hanai, N. (2009). Engineered therapeutic antibodies with improved effector functions. Cancer Sci *100*, 1566-1572.

Kulms, D., Poppelmann, B., Yarosh, D., Luger, T.A., Krutmann, J., and Schwarz, T. (1999). Nuclear and cell membrane effects contribute independently to the induction of apoptosis in human cells exposed to UVB radiation. Proc Natl Acad Sci U S A *96*, 7974-7979.

Kute, T.E., Savage, L., Stehle, J.R., Jr., Kim-Shapiro, J.W., Blanks, M.J., Wood, J., and Vaughn, J.P. (2009). Breast tumor cells isolated from in vitro resistance to trastuzumab remain sensitive to trastuzumab anti-tumor effects in vivo and to ADCC killing. Cancer Immunol Immunother *58*, 1887-1896.

Labrada, M., Clavell, M., Bebelagua, Y., Leon, J., Alonso, D.F., Gabri, M.R., Veloso, R.C., Verez, V., and Fernandez, L.E. Direct validation of NGcGM3 ganglioside as a new target for cancer immunotherapy. Expert Opin Biol Ther *10*, 153-162.

Lamkanfi, M., Festjens, N., Declercq, W., Vanden Berghe, T., and Vandenabeele, P. (2007). Caspases in cell survival, proliferation and differentiation. Cell Death Differ *14*, 44-55.

Lane, J.D., Allan, V.J., and Woodman, P.G. (2005). Active relocation of chromatin and endoplasmic reticulum into blebs in late apoptotic cells. Journal of cell science *118*, 4059-4071.

Lanzavecchia, A. (1985). Antigen-specific interaction between T and B cells. Nature *314*, 537-539.

Lanzavecchia, A., and Bove, S. (1985). Specific B lymphocytes efficiently pick up, process and present antigen to T cells. Behring Inst Mitt, 82-87.

Lapointe, R., Bellemare-Pelletier, A., Housseau, F., Thibodeau, J., and Hwu, P. (2003). CD40-stimulated B lymphocytes pulsed with tumor antigens are effective antigen-presenting cells that can generate specific T cells. Cancer Res *63*, 2836-2843.

Lebrecht, D., Kirschner, J., Geist, A., Haberstroh, J., and Walker, U.A. (2009). Respiratory chain deficiency precedes the disrupted calcium homeostasis in chronic doxorubicin cardiomyopathy. Cardiovasc Pathol.

Leist, M., and Jaattela, M. (2002). Burning up TNF toxicity for cancer therapy. Nat Med *8*, 667-668.

Li, G., Andreansky, S., Helguera, G., Sepassi, M., Janikashvili, N., Cantrell, J., Lacasse, C.L., Larmonier, N., Penichet, M.L., and Katsanis, E. (2008). A chaperone protein-enriched tumor cell lysate vaccine generates protective humoral immunity in a mouse breast cancer model. Mol Cancer Ther *7*, 721-729.

Li, Q., Li, L., Shi, W., Jiang, X., Xu, Y., Gong, F., Zhou, M., Edwards, C.K., 3rd, and Li, Z. (2006). Mechanism of action differences in the antitumor effects of transmembrane and secretory tumor necrosis factor-alpha in vitro and in vivo. Cancer Immunol Immunother *55*, 1470-1479.

Linton, P.J., Harbertson, J., and Bradley, L.M. (2000). A critical role for B cells in the development of memory CD4 cells. J Immunol *165*, 5558-5565.

Liu, L.L., Smith, M.J., Sun, B.S., Wang, G.J., Redmond, H.P., and Wang, J.H. (2009). Combined IFN-gamma-endostatin gene therapy and radiotherapy attenuates primary breast tumor growth and lung metastases via enhanced CTL and NK cell activation and attenuated tumor angiogenesis in a murine model. Ann Surg Oncol *16*, 1403-1411.

Lou, Y., Basha, G., Seipp, R.P., Cai, B., Chen, S.S., Moise, A.R., Jeffries, A.P., Gopaul, R.S., Vitalis, T.Z., and Jefferies, W.A. (2008). Combining the antigen processing components TAP and Tapasin elicits enhanced tumor-free survival. Clin Cancer Res *14*, 1494-1501.

MacLennan, I. (2007). Holding antigen where B cells can find it. Nat Immunol *8*, 909-910.

Maftoum-Costa, M., Naves, K.T., Oliveira, A.L., Tedesco, A.C., da Silva, N.S., and Pacheco-Soares, C. (2008). Mitochondria, endoplasmic reticulum and actin filament behavior after PDT with chloroaluminum phthalocyanine liposomal in HeLa cells. Cell Biol Int *32*, 1024-1028.

Mami-Chouaib, F., Echchakir, H., Dorothee, G., Vergnon, I., and Chouaib, S. (2002). Antitumor cytotoxic T-lymphocyte response in human lung carcinoma: identification of a tumor-associated antigen. Immunol Rev *188*, 114-121.

Manoury, B., Hewitt, E.W., Morrice, N., Dando, P.M., Barrett, A.J., and Watts, C. (1998). An asparaginyl endopeptidase processes a microbial antigen for class II MHC presentation. Nature *396*, 695-699.

Mata-Espinosa, D.A., and Hernandez-Pando, R. (2008). [Gamma interferon: basics aspects, clinic significance and terapeutic uses]. Rev Invest Clin *60*, 421-431.

McArthur, C., Wang, Y., Veno, P., Zhang, J., and Fiorella, R. (2002). Intracellular trafficking and surface expression of SS-A (Ro), SS-B (La), poly(ADP-ribose) polymerase and alpha-fodrin autoantigens during apoptosis in human salivary gland cells induced by tumour necrosis factor-alpha. Archives of oral biology *47*, 443-448.

McCune, C.S., and Marquis, D.M. (1990). Interleukin 1 as an adjuvant for active specific immunotherapy in a murine tumor model. Cancer Res *50*, 1212-1215.

Melief, C.J. (2008). Cancer immunotherapy by dendritic cells. Immunity *29*, 372-383.

Mellor, A.L., and Munn, D.H. (2004). IDO expression by dendritic cells: tolerance and tryptophan catabolism. Nat Rev Immunol *4*, 762-774.

Micalizzi, D.S., and Ford, H.L. (2009). Epithelial-mesenchymal transition in development and cancer. Future Oncol *5*, 1129-1143.

Miller, M.J., Hejazi, A.S., Wei, S.H., Cahalan, M.D., and Parker, I. (2004). T cell repertoire scanning is promoted by dynamic dendritic cell behavior and random T cell motility in the lymph node. Proc Natl Acad Sci U S A *101*, 998-1003.

Mitchell, D.A., and Sampson, J.H. (2009). Toward effective immunotherapy for the treatment of malignant brain tumors. Neurotherapeutics *6*, 527-538.

Mizutani, H. (2007). [Mechanism of DNA damage and apoptosis induced by anticancer drugs through generation of reactive oxygen species]. Yakugaku Zasshi *127*, 1837-1842.

Motoyoshi, Y., Kaminoda, K., Saitoh, O., Hamasaki, K., Nakao, K., Ishii, N., Nagayama, Y., and Eguchi, K. (2006). Different mechanisms for anti-tumor effects of low- and high-dose cyclophosphamide. Oncol Rep *16*, 141-146.

Muranski, P., and Restifo, N.P. (2009). Adoptive immunotherapy of cancer using CD4(+) T cells. Curr Opin Immunol *21*, 200-208.

Nakagawa, T., Zhu, H., Morishima, N., Li, E., Xu, J., Yankner, B.A., and Yuan, J. (2000). Caspase-12 mediates endoplasmic-reticulum-specific apoptosis and cytotoxicity by amyloid-beta. Nature *403*, 98-103.

Nguyen, T., Thomas, W., Zhang, X.D., Gray, C., and Hersey, P. (2000). Immunologically-mediated tumour cell apoptosis: the role of TRAIL in T cell and cytokine-mediated responses to melanoma. Forum (Genova) *10*, 243-252.

Nishigaki, R., Mitani, H., and Shima, A. (1998). Evasion of UVC-induced apoptosis by photorepair of cyclobutane pyrimidine dimers. Exp Cell Res *244*, 43-53.

O'Neill, S.K., Cao, Y., Hamel, K.M., Doodes, P.D., Hutas, G., and Finnegan, A. (2007). Expression of CD80/86 on B cells is essential for autoreactive T cell activation and the development of arthritis. J Immunol *179*, 5109-5116.

Obeid, M. (2008). ERP57 membrane translocation dictates the immunogenicity of tumor cell death by controlling the membrane translocation of calreticulin. J Immunol *181*, 2533-2543.

Obeid, M., Panaretakis, T., Joza, N., Tufi, R., Tesniere, A., van Endert, P., Zitvogel, L., and Kroemer, G. (2007a). Calreticulin exposure is required for the immunogenicity of gamma-irradiation and UVC light-induced apoptosis. Cell Death Differ *14*, 1848-1850.

Obeid, M., Tesniere, A., Ghiringhelli, F., Fimia, G.M., Apetoh, L., Perfettini, J.L., Castedo, M., Mignot, G., Panaretakis, T., Casares, N.*, et al.* (2007b). Calreticulin exposure dictates the immunogenicity of cancer cell death. Nature medicine *13*, 54-61.

Obeid, M., Tesniere, A., Panaretakis, T., Tufi, R., Joza, N., van Endert, P., Ghiringhelli, F., Apetoh, L., Chaput, N., Flament, C.*, et al.* (2007c). Ecto-calreticulin in immunogenic chemotherapy. Immunol Rev *220*, 22-34.

Ogino, T., Moriai, S., Ishida, Y., Ishii, H., Katayama, A., Miyokawa, N., Harabuchi, Y., and Ferrone, S. (2007). Association of immunoescape mechanisms with Epstein-Barr virus infection in nasopharyngeal carcinoma. Int J Cancer *120*, 2401-2410.

Oh, S.T., Kim, C.H., Park, M.Y., Won, E.H., Sohn, H.J., Cho, H.I., Kang, W.K., Hong, Y.K., and Kim, T.G. (2006). Dendritic cells transduced with recombinant adenoviruses induce more efficient anti-tumor immunity than dendritic cells pulsed with peptide. Vaccine *24*, 2860-2868.

Osinsky, S., Zavelevich, M., and Vaupel, P. (2009). Tumor hypoxia and malignant progression. Exp Oncol *31*, 80-86.

Pages, F., Galon, J., Dieu-Nosjean, M.C., Tartour, E., Sautes-Fridman, C., and Fridman, W.H. Immune infiltration in human tumors: a prognostic factor that should not be ignored. Oncogene *29*, 1093-1102.

Palamara, F., Meindl, S., Holcmann, M., Luhrs, P., Stingl, G., and Sibilia, M. (2004). Identification and characterization of pDC-like cells in normal mouse skin and melanomas treated with imiquimod. J Immunol *173*, 3051-3061.

Panaretakis, T., Joza, N., Modjtahedi, N., Tesniere, A., Vitale, I., Durchschlag, M., Fimia, G.M., Kepp, O., Piacentini, M., Froehlich, K.U., *et al.* (2008). The co-translocation of ERp57 and calreticulin determines the immunogenicity of cell death. Cell death and differentiation.

Panaretakis, T., Kepp, O., Brockmeier, U., Tesniere, A., Bjorklund, A.C., Chapman, D.C., Durchschlag, M., Joza, N., Pierron, G., van Endert, P., *et al.* (2009). Mechanisms of pre-apoptotic calreticulin exposure in immunogenic cell death. EMBO J *28*, 578-590.

Patel, M.P., Masood, A., Patel, P.S., and Chanan-Khan, A.A. (2009). Targeting the Bcl-2. Curr Opin Oncol *21*, 516-523.

Pavoni, E., Monteriu, G., Santapaola, D., Petronzelli, F., Anastasi, A.M., Pelliccia, A., D'Alessio, V., De Santis, R., and Minenkova, O. (2007). Tumor-infiltrating B lymphocytes as an efficient source of highly specific immunoglobulins recognizing tumor cells. BMC Biotechnol *7*, 70.

Perez, C.A., Fu, A., Onishko, H., Hallahan, D.E., and Geng, L. (2009). Radiation induces an antitumour immune response to mouse melanoma. Int J Radiat Biol *85*, 1126-1136.
Pettit, S.J., Seymour, K., O'Flaherty, E., and Kirby, J.A. (2000). Immune selection in neoplasia: towards a microevolutionary model of cancer development. Br J Cancer *82*, 1900-1906.

Priestman, T.J. (1979). Interferon: an anti-cancer agent? Cancer Treat Rev *6*, 223-237.

Putcha, G.V., Harris, C.A., Moulder, K.L., Easton, R.M., Thompson, C.B., and Johnson, E.M., Jr. (2002). Intrinsic and extrinsic pathway signaling during neuronal apoptosis: lessons from the analysis of mutant mice. J Cell Biol *157*, 441-453.

Qi, L., Rojas, J.M., and Ostrand-Rosenberg, S. (2000). Tumor cells present MHC class II-restricted nuclear and mitochondrial antigens and are the predominant antigen presenting cells in vivo. J Immunol *165*, 5451-5461.

Ralph, P., and Nakoinz, I. (1975). Phagocytosis and cytolysis by a macrophage tumour and its cloned cell line. Nature *257*, 393-394.

Rees, R.C., and Mian, S. (1999). Selective MHC expression in tumours modulates adaptive and innate antitumour responses. Cancer Immunol Immunother *48*, 374-381.

Reich, A., Schwudke, D., Meurer, M., Lehmann, B., and Shevchenko, A. (2009). Lipidome of narrow-band ultraviolet B irradiated keratinocytes shows apoptotic hallmarks. Exp Dermatol.

Rivera, A., Chen, C.C., Ron, N., Dougherty, J.P., and Ron, Y. (2001). Role of B cells as antigen-presenting cells in vivo revisited: antigen-specific B cells are essential for T cell expansion in lymph nodes and for systemic T cell responses to low antigen concentrations. Int Immunol *13*, 1583-1593.

Robe, A.J., Kirby, J.A., Jones, D.E., and Palmer, J.M. (2005). A key role for autoreactive B cells in the breakdown of T-cell tolerance to pyruvate dehydrogenase complex in the mouse. Hepatology *41*, 1106-1112.

Rosenberg, S.A. (2001). Progress in human tumour immunology and immunotherapy. Nature *411*, 380-384.

Ruchaud, S., Korfali, N., Villa, P., Kottke, T.J., Dingwall, C., Kaufmann, S.H., and Earnshaw, W.C. (2002). Caspase-6 gene disruption reveals a requirement for lamin A cleavage in apoptotic chromatin condensation. Embo J *21*, 1967-1977.

Ryan, K.R., and Evavold, B.D. (1998). Persistence of peptide-induced CD4+ T cell anergy in vitro. J Exp Med *187*, 89-96.

Saeed, I.A., and Ashraf, S.S. (2009). Denaturation studies reveal significant differences between GFP and blue fluorescent protein. Int J Biol Macromol *45*, 236-241.

Sakamoto, T., Saito, H., Tatebe, S., Tsujitani, S., Ozaki, M., Ito, H., and Ikeguchi, M. (2006). Interleukin-10 expression significantly correlates with minor CD8+ T-cell infiltration and high microvessel density in patients with gastric cancer. Int J Cancer *118*, 1909-1914.

Santin, A.D., Bellone, S., Underwood, L.J., O'Brien, T.J., Ravaggi, A., Pecorelli, S., and Cannon, M.J. (2002). Novel immunotherapeutic strategies in gynecologic oncology. Dendritic cell-based immunotherapy for ovarian cancer. Minerva Ginecol *54*, 133-144.

Santini, S.M., Lapenta, C., Santodonato, L., D'Agostino, G., Belardelli, F., and Ferrantini, M. (2009). IFN-alpha in the generation of dendritic cells for cancer immunotherapy. Handb Exp Pharmacol, 295-317.

Savelyeva, N., King, C.A., Vitetta, E.S., and Stevenson, F.K. (2005). Inhibition of a vaccine-induced anti-tumor B cell response by soluble protein antigen in the absence of continuing T cell help. Proc Natl Acad Sci U S A *102*, 10987-10992.

Savill, J., Gregory, C., and Haslett, C. (2003). Cell biology. Eat me or die. Science *302*, 1516-1517.

Scherer, W.F., Syverton, J.T., and Gey, G.O. (1953). Studies on the propagation in vitro of poliomyelitis viruses. IV. Viral multiplication in a stable strain of human malignant epithelial cells (strain HeLa) derived from an epidermoid carcinoma of the cervix. J Exp Med *97*, 695-710.

Schnizlein, C.T., Szakal, A.K., and Tew, J.G. (1984). Follicular dendritic cells in the regulation and maintenance of immune responses. Immunobiology *168*, 391-402.

Schultze, J.L., Michalak, S., Seamon, M.J., Dranoff, G., Jung, K., Daley, J., Delgado, J.C., Gribben, J.G., and Nadler, L.M. (1997). CD40-activated human B cells: an alternative source of highly efficient antigen presenting cells to generate autologous antigen-specific T cells for adoptive immunotherapy. J Clin Invest *100*, 2757-2765.

Seliger, B., Abken, H., and Ferrone, S. (2003a). HLA-G and MIC expression in tumors and their role in anti-tumor immunity. Trends Immunol *24*, 82-87.

Seliger, B., Atkins, D., Bock, M., Ritz, U., Ferrone, S., Huber, C., and Storkel, S. (2003b). Characterization of human lymphocyte antigen class I antigen-processing machinery defects in renal cell carcinoma lesions with special emphasis on transporter-associated with antigen-processing down-regulation. Clin Cancer Res *9*, 1721-1727.

Serafino, A., Sinibaldi-Vallebona, P., Pierimarchi, P., Bernard, P., Gaudiano, G., Massa, C., Rasi, G., and Ranagnan, G. (1999). Induction of apoptosis in neoplastic cells by anthracycline antitumor drugs: nuclear and cytoplasmic triggering? Anticancer Res *19*, 1909-1918.

Seymour, K., Pettit, S., O'Flaherty, E., Charnley, R.M., and Kirby, J.A. (1999). Selection of metastatic tumour phenotypes by host immune systems. Lancet *354*, 1989-1991.

Shah, S., Divekar, A.A., Hilchey, S.P., Cho, H.M., Newman, C.L., Shin, S.U., Nechustan, H., Challita-Eid, P.M., Segal, B.M., Yi, K.H., and Rosenblatt, J.D. (2005). Increased rejection of primary tumors in mice lacking B cells: inhibition of anti-tumor CTL and TH1 cytokine responses by B cells. Int J Cancer *117*, 574-586.

Shigematsu, Y., Hanagiri, T., Kuroda, K., Baba, T., Mizukami, M., Ichiki, Y., Yasuda, M., Takenoyama, M., Sugio, K., and Yasumoto, K. (2009). Malignant mesothelioma-associated antigens recognized by tumor-infiltrating B cells and the clinical significance of the antibody titers. Cancer Sci *100*, 1326-1334.

Shlomchik, M.J. (2009). Activating systemic autoimmunity: B's, T's, and tolls. Curr Opin Immunol *21*, 626-633.

Sica, A., Rubino, L., Mancino, A., Larghi, P., Porta, C., Rimoldi, M., Solinas, G., Locati, M., Allavena, P., and Mantovani, A. (2007). Targeting tumour-associated macrophages. Expert Opin Ther Targets *11*, 1219-1229.

Smith-Gill, S.J., Lavoie, T.B., and Mainhart, C.R. (1984). Antigenic regions defined by monoclonal antibodies correspond to structural domains of avian lysozyme. J Immunol *133*, 384-393.

Steitz, J., Bruck, J., Lenz, J., Knop, J., and Tuting, T. (2001). Depletion of CD25(+) CD4(+) T cells and treatment with tyrosinase-related protein 2-transduced dendritic cells enhance the interferon alpha-induced, CD8(+) T-cell-dependent immune defense of B16 melanoma. Cancer Res *61*, 8643-8646.

Szakal, A.K., Kapasi, Z.F., Masuda, A., and Tew, J.G. (1992). Follicular dendritic cells in the alternative antigen transport pathway: microenvironment, cellular events, age and retrovirus related alterations. Semin Immunol *4*, 257-265.

Szakal, A.K., and Tew, J.G. (1992). Follicular dendritic cells: B-cell proliferation and maturation. Cancer Res *52*, 5554s-5556s.

Takasawa, R., Nakamura, H., Mori, T., and Tanuma, S. (2005). Differential apoptotic pathways in human keratinocyte HaCaT cells exposed to UVB and UVC. Apoptosis *10*, 1121-1130.

Tan, T.T., and Coussens, L.M. (2007). Humoral immunity, inflammation and cancer. Curr Opin Immunol *19*, 209-216.

Tanaka, H., Tanaka, J., Kjaergaard, J., and Shu, S. (2002). Depletion of CD4+ CD25+ regulatory cells augments the generation of specific immune T cells in tumor-draining lymph nodes. J Immunother *25*, 207-217.

Taniguchi, M., and Miller, J.F. (1978). Specific suppressive factors produced by hybridomas derived from the fusion of enriched suppressor T cells and a T lymphoma cell line. J Exp Med *148*, 373-382.

Tesniere, A., Schlemmer, F., Boige, V., Kepp, O., Martins, I., Ghiringhelli, F., Aymeric, L., Michaud, M., Apetoh, L., Barault, L.*, et al.* Immunogenic death of colon cancer cells treated with oxaliplatin. Oncogene *29*, 482-491.

Tesniere, A., Schlemmer, F., Boige, V., Kepp, O., Martins, I., Ghiringhelli, F., Aymeric, L., Michaud, M., Apetoh, L., Barault, L.*, et al.* (2009). Immunogenic death of colon cancer cells treated with oxaliplatin. Oncogene.

Therrien, J.P., Drouin, R., Baril, C., and Drobetsky, E.A. (1999). Human cells compromised for p53 function exhibit defective global and transcription-coupled nucleotide excision repair, whereas cells compromised for pRb function are defective only in global repair. Proc Natl Acad Sci U S A *96*, 15038-15043.

Tobar, N., Caceres, M., Santibanez, J.F., Smith, P.C., and Martinez, J. (2008). RAC1 activity and intracellular ROS modulate the migratory potential of MCF-7 cells through a NADPH oxidase and NFkappaB-dependent mechanism. Cancer Lett *267*, 125-132.

Tokarska-Schlattner, M., Wallimann, T., and Schlattner, U. (2002). Multiple interference of anthracyclines with mitochondrial creatine kinases: preferential damage of the cardiac isoenzyme and its implications for drug cardiotoxicity. Mol Pharmacol *61*, 516-523.

Tomlinson, I., Sasieni, P., and Bodmer, W. (2002). How many mutations in a cancer? Am J Pathol *160*, 755-758.

Treanor, B., Depoil, D., Gonzalez-Granja, A., Barral, P., Weber, M., Dushek, O., Bruckbauer, A., and Batista, F.D. The Membrane Skeleton Controls Diffusion Dynamics and Signaling through the B Cell Receptor. Immunity *32*, 187-199.

Tufi, R., Panaretakis, T., Bianchi, K., Criollo, A., Fazi, B., Di Sano, F., Tesniere, A., Kepp, O., Paterlini-Brechot, P., Zitvogel, L.*, et al.* (2008). Reduction of endoplasmic reticulum Ca2+ levels favors plasma membrane surface exposure of calreticulin. Cell death and differentiation *15*, 274-282.

van Zijl, F., Mair, M., Csiszar, A., Schneller, D., Zulehner, G., Huber, H., Eferl, R., Beug, H., Dolznig, H., and Mikulits, W. (2009). Hepatic tumor-stroma crosstalk guides epithelial to mesenchymal transition at the tumor edge. Oncogene.

Viret, C., and Lindemann, A. (1997). Tumor immunotherapy by vaccination with cytokine gene transfected cells. Int Rev Immunol *14*, 193-212.

Wang, J.C., and Livingstone, A.M. (2003). Cutting edge: CD4+ T cell help can be essential for primary CD8+ T cell responses in vivo. J Immunol *171*, 6339-6343.

Wang, R.F. (2001). The role of MHC class II-restricted tumor antigens and CD4+ T cells in antitumor immunity. Trends Immunol *22*, 269-276.

Ward, J.F. (1994). The complexity of DNA damage: relevance to biological consequences. Int J Radiat Biol *66*, 427-432.

Weiner, L.M., Dhodapkar, M.V., and Ferrone, S. (2009). Monoclonal antibodies for cancer immunotherapy. Lancet *373*, 1033-1040.

Weitzman, J., Betancur, M., Boissel, L., Rabinowitz, A.P., Klein, A., and Klingemann, H. (2009). Variable Contribution of Monoclonal Antibodies to ADCC in patients with chronic lymphocytic leukemia. Leuk Lymphoma, 1-8.

White, J., Kappler, J., and Marrack, P. (2000). Production and characterization of T cell hybridomas. Methods Mol Biol *134*, 185-193.

Whitmire, J.K., Asano, M.S., Kaech, S.M., Sarkar, S., Hannum, L.G., Shlomchik, M.J., and Ahmed, R. (2009). Requirement of B cells for generating CD4+ T cell memory. J Immunol *182*, 1868-1876.

Wu, D.Y., Segal, N.H., Sidobre, S., Kronenberg, M., and Chapman, P.B. (2003). Cross-presentation of disialoganglioside GD3 to natural killer T cells. J Exp Med *198*, 173-181.

Wykes, M., Pombo, A., Jenkins, C., and MacPherson, G.G. (1998). Dendritic cells interact directly with naive B lymphocytes to transfer antigen and initiate class switching in a primary T-dependent response. J Immunol *161*, 1313-1319.

Wyllie, A.H., Kerr, J.F., and Currie, A.R. (1980). Cell death: the significance of apoptosis. Int Rev Cytol *68*, 251-306.

Yan, Q., Cheung, Y.K., Cheng, S.C., Wang, X.H., Shi, M., Hu, M.H., and Yong, X. (2007). A DNA vaccine constructed with human papillomavirus type 16 (HPV16) E7 and E6 genes induced specific immune responses. Gynecol Oncol *104*, 199-206.

Yang, D., Chen, Q., Yang, H., Tracey, K.J., Bustin, M., and Oppenheim, J.J. (2007). High mobility group box-1 protein induces the migration and activation of human dendritic cells and acts as an alarmin. J Leukoc Biol *81*, 59-66.

Yasuda, M., Takenoyama, M., Obata, Y., Sugaya, M., So, T., Hanagiri, T., Sugio, K., and Yasumoto, K. (2002). Tumor-infiltrating B lymphocytes as a potential source of identifying tumor antigen in human lung cancer. Cancer Res *62*, 1751-1756.

Zhang, C., Wang, Y., Zhou, Z., Zhang, J., and Tian, Z. (2009a). Sodium butyrate upregulates expression of NKG2D ligand MICA/B in HeLa and HepG2 cell lines and increases their susceptibility to NK lysis. Cancer Immunol Immunother *58*, 1275-1285.

Zhang, K., and Kaufman, R.J. (2008). From endoplasmic-reticulum stress to the inflammatory response. Nature *454*, 455-462.

Zhang, T., and Herlyn, D. (2009). Combination of active specific immunotherapy or adoptive antibody or lymphocyte immunotherapy with chemotherapy in the treatment of cancer. Cancer Immunol Immunother *58*, 475-492.

Zhang, Z., Neiva, K.G., Lingen, M.W., Ellis, L.M., and Nor, J.E. (2009b). VEGF-dependent tumor angiogenesis requires inverse and reciprocal regulation of VEGFR1 and VEGFR2. Cell Death Differ.

Zitvogel, L., Apetoh, L., Ghiringhelli, F., and Kroemer, G. (2008). Immunological aspects of cancer chemotherapy. Nat Rev Immunol *8*, 59-73.

Zwirner, N.W., Fuertes, M.B., Girart, M.V., Domaica, C.I., and Rossi, L.E. (2007). Cytokine-driven regulation of NK cell functions in tumor immunity: role of the MICA-NKG2D system. Cytokine Growth Factor Rev *18*, 159-170.